

**University of Alberta**

**Stratigraphy, Petrography and Geochemistry of the Bad Heart  
Formation, Northwestern Alberta**

by

**Basant Kafle**

A thesis submitted to the Faculty of Graduate Studies and Research  
in partial fulfillment of the requirements for the degree of

**Master of Science**

Department of Earth and Atmospheric Sciences

©Basant Kafle

Spring 2011

Edmonton, Alberta

Permission is hereby granted to the University of Alberta Libraries to reproduce single copies of this thesis and to lend or sell such copies for private, scholarly or scientific research purposes only. Where the thesis is converted to, or otherwise made available in digital form, the University of Alberta will advise potential users of the thesis of these terms.

The author reserves all other publication and other rights in association with the copyright in the thesis and, except as herein before provided, neither the thesis nor any substantial portion thereof may be printed or otherwise reproduced in any material form whatsoever without the author's prior written permission.

## **Examining Committee**

Octavian Catuneanu, Department of Earth and Atmospheric Sciences

Jack Lerbekmo, Department of Earth and Atmospheric Sciences

Pamela R Willoughby, Department of Anthropology

## **ABSTRACT**

Bad Heart Formation oolitic ironstone is the largest resources of iron in western Canada. During this study, 45 new sections from outcrop, trench and drill holes were mapped, and 325 samples were collected for petrographic and geochemical analysis. The objective of the first paper is to refine the previously published stratigraphic model based on the new data. The second paper deals with geochemistry and discuss genesis of ooids and source of iron in oolitic ironstone.

The textures of the Bad Heart Formation ironstone suggest the ooids formed in-place in a relatively shallow, wave-agitated, oxygenated marine environment with repetitive growth of the ooids in water column. There are two possible source of iron in the ooids. Some geochemical data indicate it is continental sedimentary, but it is also possible that the iron sourced from sub-sea hydrothermal or meteoric vents, similar to recent iron deposits at Paint Pots in Kootenay National Park.

## **ACKNOWLEDGEMENTS**

I would express sincere gratitude to my supervisor Prof. Octavian Catuneanu for his support, advice and encouragement throughout my degree. I am indebted to Dr. Reg Olson (formerly from the Alberta Geological Survey) who introduced me to the subject matter and also helped me during the fieldwork and editing the thesis. I would also like to extend my thanks to the Alberta Geological Survey for providing me an employment opportunity in their project during a part of my degree. Special thanks go to Dr. Art Sweet (GSC, Calgary) for the analysis and interpretation of the palynology samples. I would also like to thank Clear Hills Iron Ltd and specially Mr. Tom Sneddon for access to logging and sampling the core from their recent drilling.

## TABLE OF CONTENTS

### CHAPTER 1: INTRODUCTION

Introduction	1
References	7

### CHAPTER 2: STRATIGRAPHY AND PETROGRAPHY OF THE BAD HEART FORMATION IN THE CLEAR HILLS AND THE SMOKY RIVER AREAS, ALBERTA

Introduction	10
Study area	11
Scope of research	11
Geological Background	12
Methodology	16
Stratigraphy of the Bad Heart Formation	17
Petrography	24
Discussion	28
Conclusions	33
References	55

### CHAPTER 3: GEOCHEMISTRY OF OOLITIC IRONSTONE, BAD HEART FORMATION, NORTHWESTERN ALBERTA

Introduction	61
Database	63
Previous work	63
Geological setting	64
Methodology	65
Results	66
Discussion	72
Conclusions	78

References	94
<b>CHAPTER 4: CONCLUSIONS</b>	<b>102</b>

## **APPENDIX**

Appendix I Stratigraphic sections	106
Appendix II Analytical results for selected rock samples	135
Appendix III Comparative results from duplicate samples	147
Appendix IV Comparative results for Canmet Standard samples	150

## LIST OF TABLES

Table 1.1- Correlation of Bad Heart Formation by previous researcher and in the present study	6
Table 2.1- Summary of facies observed within the Bad Heart Formation as modified by this study	35
Table 2.2 - Summary of formation picks criteria in selected oil and gas wells in the Clear Hills region	36
Table 3.1A – Concentrations of major, trace and rare earth elements and oxides in intensely oolitic ironstones (IOIS) from the selected sections within the Bad Heart Formation	80
Table 3.1B – Concentrations of major, trace and rare earth elements and oxides in moderately oolitic ironstones (MOIS) from the selected sections within the Bad Heart Formation	81
Table 3.1C - Concentrations of major, trace and rare earth elements and oxides in weakly oolitic ironstones (WOIS) from the selected sections within the Bad Heart Formation	82
Table 3.1D - Summary results of major, trace and rare earth elements and oxides in oolitic ironstones (including all three types) from the selected section within the Bad Heart Formation	83
Table 3.2 - Summary of the elements and their underlying geochemical distribution	84
Table 3.3 - Summary of major oxide and trace element averages and maximum contents in the Bad Heart Ironstones	85
Table 3.4 - Summary of average and maximum Rare Earth Element contents in the Bad Heart Ironstones	86

## **LIST OF FIGURES**

Figure 1.1: Location map of the study area	7
Figure 2.1 - Location of the Clear Hills and Smoky River study areas	37
Figure 2.2 - Location of mapped outcrops, diamond drill hole core and excavated trench sections; (a) Clear Hills region (b) Smoky River region	38
Figure 2.3 - Simplified stratigraphy of Late Cretaceous formations in the northwest Alberta Plains (modified from Alberta Energy and Utilities Board, 2002)	39
Figure 2.4 - Major structural features in the Clear Hills to Smoky River region	40
Figure 2.5 - Available well logs in the Clear Hills region and the two cross sections (A-A' & B-B') that were constructed from 23 selected wells	41
Figure 2.6 - Complete Bad Heart Formation sequence near the original type section of McLearn (1919) along the Smoky River just south of the intersection with the Bad Heart River	42
Figure 2.7 - Northwest to southeast cross section of measured sections in the Smoky River region	43
Figure 2.8 - Two east- west Bad Heart Formation cross sections in the Clear Hills Rambling Creek area	44
Figure 2.9 - Bad Heart Formation Erosional surfaces ES2 and ES1 seen at section ASR9A in the cliff along central Smoky River	45
Figure 2.10 - Well-log cross-section along line A-A' in the Clear Hills region. The Base of Fish Scales (BFSC) marker is used as a datum	46
Figure 2.11 - Well-log cross-section along line B-B'. The Base of Fish Scales (BFSC) is used as datum	47
Figure 2.12 - Measured stratigraphic section with selected palynology samples at (a) diamond drill core DDH0203, and (b) section ASR3	48

Figure 2.13 - Pisoids from Bad Heart Formation at section ARR3 along Rambling Creek	49
Figure 2.14 (A)- Thin section view of ooids in plane polarized light; (B) SEM view of Iron ooids broken into two halves, both with a nucleus and cortex	49
Figure 2.15 - Internal morphology of ooids under SEM	50
Figure 2.16 - Post-depositional cracks in the ooids (Under SEM)	50
Figure 2.17 - SEM photographs of Bad Heart Type 1 iron ooids	51
Figure 2.18 - SEM photographs of Type 2 ooids	52
Figure 2.19 - The extent of Bad Heart Formation defined from the work of Donaldson (1999), Collom (2001) and the present study	53
Figure 2.20 - Schematic correlation diagram of Bad Heart Formation between the sections from the Smoky River and Clear Hills regions	54
Figure 3.1 - Location map of the study area	87
Figure 3.2 - Variation in oxides and selected trace element along a Bad Heart section ASR9A in the Smoky River region	88
Figure 3.3 - Variation in oxides and selected trace element along a Bad Heart section ARR3 near Rambling Creek in the Clear Hills region	89
Figure 3.4 - Correlation diagram of various oxides from Bad Heart oolitic Ironstone	90
Figure 3.5 - Comparison of chondrite normalized pattern of REE for Bad heart ooids with other oolitic ironstones from around the world	91

Figure 3.6 - Comparison of NASC normalized pattern of REE for Bad heart  
ooids with other oolitic ironstones from around the world 91

Figure 3.7 - Comparison of chondrite normalized REE pattern for Bad Heart  
ooids with Cretaceous bentonite from northern Alberta 92

Figure 3.8 - Ratio of TiO<sub>2</sub>-Al<sub>2</sub>O<sub>3</sub> for iron ooids from different parts of the world 93

## CHAPTER 1: INTRODUCTION

The Upper Cretaceous (Coniacian) Bad Heart Formation is a unique unit within the Western Canada Sedimentary Basin (WCSB) due to the extensive, potentially important oolitic ironstones that exist within it, plus its ubiquitous shallow marine macro- and ichnofossil assemblages whereas it is underlain and overlain by deeper water shale assemblages. It is exposed in northwestern Alberta in the southern and southeastern parts of the Clear Hills, and to the south along the Smoky River and in the Blueberry Mountains to the Birch Hills areas (Figure 1.1). The term Bad Heart Formation is used in this thesis because of its traditional use of the term, even though the studied unit does not confirm *sensu stricto* to the definition of a lithostratigraphic unit because it includes the upper thick sandstone and lower thick mudstone (Table 1.1) Plint et al. (1990) redefined the original stratigraphic definition of the Bad Heart Formation along with Muskiki and Marshybank Formation. In the present study the Bad Heart Formation includes the lower mudstone, middle sandstone and oolitic ironstone and also the upper sandstone and oolitic ironstone. Although Plint et al (1990) did not include the latter in the Bad Heart Formation, but Collom (2001) included the upper sandstone and oolitic ironstone within the Bad Heart. The boundaries of Bad Heart Formation as defined by previous workers and in the present study are presented in Table 1.1.

The Bad Heart Formation oolitic ironstone comprises oolitic iron- and silica-rich facies that in places reach a thickness of up to 10 m and occur in a relatively thin sandstone-siltstone unit that generally has an average thickness of about 10 to 15 m.

Although oolitic ironstone is common within the WCSB (Leckie and Singh, 1991; Taylor et al., 2002), the Bad Heart Formation is the thickest and most regionally extensive deposit of oolitic ironstone in the WCSB. In the southeastern Clear Hills, the Bad Heart Formation is estimated to contain about 1.1 billion tonnes of iron resources with an average grade of 34% iron (Hamilton, 1982).

Mclearn (1919) was the first to name the Bad Heart as a clearly identifiable unit within the Smoky Group, describing it as “10 to 25 ft [ 3.0 m to 7.6 m] of coarse sandstone weathering reddish brown” at its type locality at the Smoky River near the intersection with the Bad Heart River. Initially, the Bad Heart was assigned as a member of the then Smoky Formation, but later when this formation was elevated to Group status, the Bad Heart was upgraded and named the Bad Heart Formation (Mclearn and Henderson, 1944).

The lithostratigraphy and, to a lesser extent, the sequence stratigraphy of the Bad Heart Formation has been relatively well studied in the surface, especially along the Smoky River, and subsurface by Donaldson (1997). As well, Collom (2001) studied the macrofossil biostratigraphy at selected sections along the Smoky River. In their respective thesis studies, Donaldson (1997; also Donaldson et al., 1998, 1999) and Collom (2001) provided detailed lithostratigraphy and biostratigraphy of selected sections in the Smoky River region and made some inferences with respect to correlation with the Bad Heart sections exposed to the north in both the Spirit River – Birch Hills and Clear Hills regions. However, their correlations were severely hampered because the stratigraphy of the Bad Heart Formation within the Clear Hills region is not well understood as a result of the poor exposures and the relatively few prior stratigraphic studies, other than what is available from scantily described logs from some exploratory drilling carried out by mineral exploration companies, especially during the 1950s and 1960s. As a result, debate is still ongoing regarding (1) the correlative stratigraphy of the Bad Heart Formation between the Smoky River and Clear Hills regions, (2) the paleo-depositional environment of the formation, particularly as it pertains to the locally present, potentially economically important, oolitic ironstones, and (3) the genetic origin of the ironstones, especially the source of the iron.

Prior work has indicated the oolitic ironstones occur at more than one stratigraphic level within the Bad Heart Formation. For example, Donaldson (1997) showed two oolitic

ironstone units in the Smoky River region: (1) a lower thick ironstone occurs in his allomember 1, which he postulated had its top truncated by an erosional surface (named ES1), and (2) an upper thinner ironstone unit exists near the top of his allomember 2. Donaldson (1997) interpreted the lower oolitic ironstone to be within the Bad Heart Formation, but he suggested that the upper thinner oolitic ironstone may be in the lowermost part of the overlying Puskawaskau Formation. In contrast, Collom (2001) argued in his biostratigraphic study that the lower thick ironstone bed at the Smoky River lies within the uppermost Kaskapau Formation (which he named the Birch Hills member), whereas the upper oolitic ironstone is entirely within the Bad Heart Formation. It is clear, therefore, that differing interpretations exist, and as a result the current litho- and sequence-stratigraphic correlations of the Bad Heart Formation from the Smoky River, to the Spirit River-Birch Hills and north to the Clear Hills are uncertain. Olson et al. (1999) conducted a preliminary study of the potential co-product trace elements within oolitic ironstone of the Bad Heart Formation from a set of selected samples from the Clear Hills region and concluded the oolitic ironstones were enriched in a few elements, other than iron and silica, including As, Mn, V, Sb and Zn.

Oolitic ironstones have distinct mineral compositions, typically being composed of one or more of berthierine (an iron-rich serpentine), nontronite (an iron-rich montmorillonite clay), chamosite (an iron-rich chlorite), siderite (an iron carbonate), goethite and hematite (both are iron oxides). Further, a mineralogical comparison of the different oolitic ironstones from around the world shows that the Proterozoic ooids<sup>1</sup> typically have hematite as the dominant iron oxide, whereas, in contrast, the Mesozoic and Paleozoic ooids have goethite as the principal iron oxide (Kimberley, 1989)

In general, there is consensus (Donaldson et al., 1999, Collom, 2001) that the Bad Heart Formation oolitic ironstone was deposited in a wave-agitated shallow marine environment, but the exact source of the high concentrations of iron and silica in the late

---

<sup>1</sup> The term 'loid' as written in this thesis has been simplified from the proper spelling 'ooid' (Bucher, 1918) for convenience.

Coniacian sea water is less certain. In general, there are two different hypotheses regarding the source of the iron in oolitic ironstones: (1) one hypothesis suggests the iron-enrichment can occur from normal sedimentary processes, such as the weathering and transporting of iron by rivers and streams to a shallow marine environment (Van Houten and Arthur, 1989; Young, 1989; Burkhalter, 1995; Macquaker et al., 1996), (2) whereas, the other proposes that the iron-enriched sea water results from hydrothermal and/or volcanic activity, and oolitic banks were deposited in a shallow marine environment (Kimberley, 1979; Sturesson et al., 2000).

With respect to the Bad Heart Formation, Donaldson (1999) seemed to favour the first model, because he proposed that the genesis of the oolitic ironstone in the Bad Heart Formation was related to a sea-level rise, upon which a localized tectonic effect was superimposed. Whereas, in contrast, Olson et al. (1994) and Collom et al. (2001) favoured the second model. Olson et al. (1994) speculated that the source of the iron and silica in Bad Heart ironstone is from "igneous fumarolic activity or to fumarolic deep-circulating hydrothermal basin fluids".

The objective of this thesis is to refine the previously published stratigraphic models of the Bad Heart Formation based on the new data collected during this study and also to find out which of the two hypothesis provides a more likely explanation of provenance of the iron during deposition of the Bad Heart Formation oolitic ironstone; that is, is the iron purely sedimentary and from a continental provenance, or is the iron largely from sub-sea vents and thus of 'hydrothermal' origin, or is the iron from some combination of the above two processes.

During this study, detailed geological section mapping of all available outcrops, excavated trenches and diamond drill cores was done, and systematic samples for geochemical, palynological and petrographic studies were also collected. The objectives behind the palynology study were (1) to ascertain the stratigraphic relationship of the

oolitic ironstone between the Smoky River and Clear Hills regions, (2) to determine the relative ages of the strata immediately below and above the oolitic ironstone.

The thesis is presented in two papers: one deals with the stratigraphy, petrography and palynology, whereas the second deals with the geochemistry of the Bad Heart Formation. The purpose of the first paper (in Chapter 2) is to present the new data, e.g. detailed stratigraphic sections and results from the palynology and petrography samples, that were collected during detailed mapping and sampling of the outcrop and excavated bedrock exposures and available diamond drill cores. The new data presented in this study help refine the previously published stratigraphic models of the Bad Heart Formation.

The second paper (in chapter 3) deals with the geochemistry and possible genesis of the oolitic ironstone. In the second paper, new geochemical data from systematically collected samples from the Bad Heart Formation, the majority of which are from oolitic ironstone horizons, are presented. Finally, the second paper concludes by discussing the most likely provenance for the iron in the oolitic ironstone based on its composition of major, trace and rare earth elements, and also by comparing the Bad Heart oolitic ironstones with other oolitic ironstone deposits from around the world.

The first paper has been submitted to the Bulletin of Canadian Society of Petroleum Geologists, and the second paper has been submitted to Exploration and Mining Geology Journal.

Table 1.1 Correlation of Bad Heart Formation by previous researcher and in the present study

Lithology	McLaren (1919)	McLaren & Henderson (1949)	Stott (1967)		Plint et.al. (1990)	Donaldson (1997)	Collom (2001)	Present Study
	Smoky River Formation	Smoky Group	Upper Shale Member	Upper Shale Formation	Puskawaskau Formation	Puskawaskau Formation	Puskawaskau Formation	Puskawaskau Formation
			Bad Heart sandstone Member	Bad Heart sandstone Formation	Bad Heart Formation	Bad Heart Formation	Bad Heart Formation	Bad Heart 'Formation'
			Lower Shale Member	Kaskapau Formation	Muskiki Formation	Muskiki Formation	Muskiki Formation	Muskiki Formation

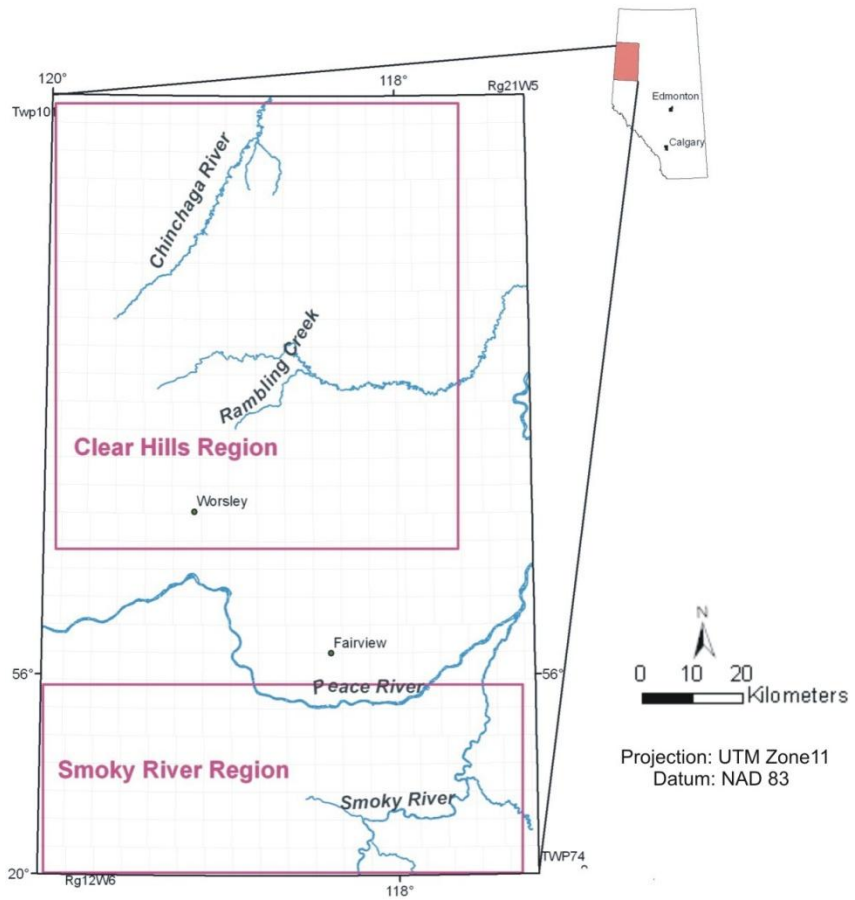


Figure 1.1: Location map of the study area

## REFERENCES

- Bucher,H., 1918, On Oolites and Spherulites.The Journal of Geology, v. 26, p 593-609
- Burkhalter, R. M., 1995, Oolitic ironstones and ferruginous microbialites; origin and relation to sequence stratigraphy (Aalenian and Bajocian, Swiss Jura Mountains).  
Sedimentology, vol. 42, no. 1, p. 57-74.
- Collom, C. J. 2001. Systematic paleontology, biostratigraphy, and paleoenvironmental analysis of the Wapiabi Formation and equivalents (upper cretaceous), Alberta and

British Columbia, Western Canada .Unpublished Ph.D. thesis, University of Calgary, Calgary, 817p.

Collom, C. J., P. A. Johnston, and Anonymous, 2001, Oolitic ironstones; products of exhalative paleoenvironments in shallow epeiric seas; Earth system processes; programmes with abstracts, Geological Society of America and Geological Society of London.

Donaldson, W. S. 1997. The sedimentology, stratigraphy and diagenesis of the Upper Cretaceous Bad Heart Formation, NW Alberta. Ph.D. thesis, University of Western Ontario, London, Canada, 492p.

Donaldson, W. S., Plint, A. G. and Longstaffe, F. J. 1998. Basement tectonic control on distribution of the shallow marine Bad Heart Formation: Peace River Arch area, Northwest Alberta. Bulletin of Canadian Petroleum Geology, v. 46, p. 576-598.

Donaldson, W. S., Plint, A. G. and Longstaffe, F. J. 1999. Tectonic and eustatic control on deposition and preservation of Upper Cretaceous oolitic ironstone and associated facies: Peace River Arch area, NW Alberta, Canada. Sedimentology, v. 46, p. 1159-1182.

Hamilton, W. N. 1980. Clear Hills iron deposit geology, mineralogy and ore reserves. Alberta Research Council, Open File Report 1982-13, 43 p.

Kimberley, M. M., 1979, Origin of oolitic iron formations, Journal of Sedimentary Petrology, vol. 49, no. 1, p. 111-131.

Kimberley, M. M., 1989, Exhalative origins of iron formations, Ore Geology Reviews, vol. 5, no. 1-2, p. 13-145.

Leckie, D. A. and Singh, C. 1991. Estuarine deposits of the Albian Paddy Member (Peace River Formation) and lowermost Shaftesbury Formation, Alberta, Canada. Journal of Sedimentary Research, v. 61, p. 825-849.

Macquaker, J. H. S., K. G. Taylor, T. P. Young, and C. D. Curtis, 1996, Sedimentological and geochemical controls on oolitic ironstone and "bone-bed" formation and some comments on their sequence-stratigraphical significance; Sequence stratigraphy in British geology, Geological Society Special Publications, vol. 103, p. 97-107.

McLearn, F. H. 1919. Cretaceous, lower Smoky River, Alberta. Geological Survey of Canada, Summary Report, p. 1-7.

McLearn, F. H. and J. F. Henderson, 1944, Geology and oil prospects of Lone Mountain area, British Columbia, Geological Survey of Canada, Paper, 44-2.

Olson, R.A., M.B. Dufresne, M.E. Freeman, R.J.H. Richardson, and D.R. Eccles, 1994, Regional Metallogenetic Evaluation of Alberta. Alberta Energy and Utilities Board/Alberta Geological Survey, Open File Report 1994-08, 158 p.

Olson, R.A., D.R. Eccles, and C.J. Collom, 1999, A Study of Potential Co-Product Trace Elements Within the Clear Hills Iron Deposits, Northwestern Alberta; Alberta Energy and Utilities Board/Alberta Geological Survey Special Report 08, 87 p.

Plint, A. G., Norris, B. and Donaldson, W. S. 1990. Revised definitions for the Upper Cretaceous Bad Heart Formation and associated units in the foothills and plains of Alberta and British Columbia. Bulletin of Canadian Petroleum Geology, v. 38, p. 78-88.

Sturesson, U., J. M. Heikoop, and M. J. Risk, 2000, Modern and Palaeozoic iron ooids; a similar volcanic origin, Sedimentary Geology, vol. 136, no. 1-2, p. 137-146.

Taylor, K. G., Simo, J. A., Yocum, D. and Leckie, D. A. 2002. Stratigraphic significance of oolitic ironstones from the Cretaceous Western Interior Seaway: the Peace River Formation, Alberta, Canada, and the Castlegate Sandstone, Utah, U.S.A. Journal of Sedimentary Research, v. 72, p. 316-327.

Van Houten, F. B. and M. A. Arthur, 1989, Temporal patterns among Phanerozoic oolitic ironstones and oceanic anoxia; Phanerozoic ironstones, Geological Society Special Publications, vol. 46, p. 33-49.

Young, T. P., 1989, Phanerozoic ironstones: an introduction and review; in Young, T.P. and Taylor, W.E.G. (Eds.), Phanerozoic Ironstones; published by The Geological Society of London as Special Publication No. 46, p. iv-xxv.

## **CHAPTER 2: STRATIGRAPHY AND PETROGRAPHY OF THE BAD HEART FORMATION IN THE CLEAR HILLS AND THE SMOKY RIVER AREAS, ALBERTA**

### **INTRODUCTION**

The Late Cretaceous (Coniacian) Bad Heart Formation in northwest Alberta is a relatively thin, typically less than about 10 to 15 m, clastic unit (largely sandstone, siltstone and locally present oolitic ironstone) that hosts the largest, potentially economic, deposit of iron in western Canada (Hamilton, 1980). Although oolitic ironstone is common within the Western Canada Sedimentary Basin (WCSB) (Leckie and Singh, 1991; Taylor et al., 2002), the Bad Heart Formation contains the thickest and most regionally extensive deposit of oolitic ironstone in the entire WCSB. Oolitic ironstones typically have a distinctive mineralogical composition that includes iron silicates (berthierine, chamosite and nontronite), carbonate (siderite), and oxides (goethite and hematite) (Young, 1989). In addition to their distinct mineralogy, their oolitic texture is believed to have formed by wave agitation in relatively shallow, iron-enriched sea waters, although it has also been suggested that oolitic textures can form as a result of the diagenesis of iron hydroxides and clay minerals, derived either from soil material (Taylor and Curtis, 1995) or by volcanic processes (Kimberley, 1979; Sturesson et al., 2000). The oolitic ironstones are condensed deposits that accumulated in iron-enriched, but clastic depleted waters during a transitional stage that developed either at the end of a regional regression (Hallam and Bradshaw, 1979; Bhattacharyya, 1989; Burkhalter, 1995; Macquaker et al., 1996) or at the beginning of transgression above an initial flooding surface (Kimberley, 1979; Burkhalter, 1995; Donaldson et al, 1999).

The purpose of this paper is to present new detailed stratigraphic sections and palynology and petrography data for the Bad Heart Formation in the Clear Hills and Smoky River regions based on detailed mapping and sampling of outcrop and excavated bedrock exposures from 2006 to 2007, and available diamond drill cores.

## **STUDY AREA**

The study area is in the plains (Smoky River region south of the Peace River) and local highlands (Clear Hills region north of the Peace River) of northwestern Alberta, Canada (Figure 2.1). In the Clear Hills region, the Bad Heart Formation is well exposed in outcrops along Rambling Creek, but very few outcrops exist elsewhere in the southern Clear Hills; as well, two diamond drill cores are available west of Rambling Creek that intersect a complete section of the Bad Heart Formation. In the Smoky River region, the Bad Heart Formation is exposed locally in road cuts along the Spirit River ridge and in the Birch Hills Mountain area, and to the southeast along the Smoky River, it is exposed semi-continuously between confluences with the Puskwaskau River and the Little Smoky River.

## **SCOPE OF RESEARCH**

The following separates the current study of the Bad Heart Formation from prior work done by Donaldson (1997, 1998, 1999) and Collom (2001): (1) in both the Clear Hills and Smoky River regions several selected very poorly exposed outcrop or road-cut exposures were mechanically trenched and excavated to facilitate the mapping and sampling across all or most of the entire formation (e.g., at the BBM, SPRV and WH sections at the Smoky River region, and Worsley Pit, KC14, LVH, KC17 and some other sections at the Clear Hills region) (Figure 2.2); (2) the Bad Heart Formation along the Smoky River was systematically mapped by rappelling down the face of the exposures and cleaning the section to facilitate detailed geological section mapping and sampling; and (3) samples were obtained through access to diamond drill cores (e.g., drill holes DDH0202 and DDH0203) (Figure 2.2a) from drilling done by industry in late 2006. In particular, in 2006 and 2007 the author did detailed geological mapping of sections and systematic rock chip sampling at 45 natural outcrops and backhoe dug trenches, and also logged the drill cores. As a result, the additional insights afforded by the new data presented in this study help refine the previously published stratigraphic models of the Bad Heart Formation.

## **GEOLOGICAL BACKGROUND**

### **PREVIOUS WORK**

The Bad Heart was first named by McLearn (1919) as a clearly identifiable unit within the Smoky Group at its type locality near the intersection of the Smoky River with the Bad Heart River (Figure 2.2). Initially, the Bad Heart was deemed to be a member of the Smoky Formation, but later when the Smoky Formation was elevated to Group status, the Bad Heart unit was upgraded to Formation status (Mclearn and Henderson,, 1944).

The Alberta Research Council subsequently conducted regional geological mapping at 1:500,000 scale of the Clear Hills area (Green and Mellon, 1962; Mellon, 1962).

Donaldson (1997) and Donaldson et al. (1998, 1999) made an extensive study of the Bad Heart Formation stratigraphy and depositional history along the Smoky River and at Rambling Creek in the eastern Clear Hills region. Collom (2001) made a significant contribution to the macro-paleontology of the Bad Heart Formation. Olson et al. (2006) conducted preliminary detailed stratigraphic mapping and sampling of the Bad Heart Formation during 2004 and 2005, and compiled a digital dataset from all publicly available data from maps, diamond-drill holes, water wells, and coal, oil and gas exploration wells from the Bad Heart Formation within the Clear Hills and Smoky River regions.

## **REGIONAL STRATIGRAPHY**

The Clear Hills and Smoky River regions are underlain by nearly flat-lying to shallowly dipping sandstone and shale formations of the Late Cretaceous age (Figure 2.3) that are covered in most places by unconsolidated glacial deposits of variable thickness (Green and Mellon, 1962). The Cretaceous rocks range in age from Cenomanian to Campanian (~99 to 71.3 Ma) and form a sequence of alternating marine and non-marine sandstone and shale. However, only the Smoky Group is briefly summarized below; this group comprises, from base to top, the Kaskapau, Cardium, Muskiki, Bad Heart and

Puskwaskau formations, and was deposited from the latest Cenomanian (~94 Ma) to the early to mid- Campanian (~80+ Ma).

#### *Kaskapau Formation*

The Kaskapau Formation (late Cenomanian to late Turonian) consists of a series of three shallow-marine sandstone bodies encased in marine mudstone (Wallace-Dudley and Leckie, 1993). Locally, the Kaskapau Formation comprises a sequence of dark grey to black mudstone with rusty-weathering sideritic concretions, and the mudstone is intercalated between the predominant sandstones of the underlying Dunvegan and overlying Cardium and Bad Heart formations.

#### *Muskiki Formation*

The Muskiki Formation (early to mid- Coniacian) consists of non-calcareous, dark marine shale that commonly contains fossiliferous siderite concretions. These marine facies have been interpreted as a transgressive systems tract, characterized by a retrogradational parasequence stacking pattern that culminates in a thin condensed section (Bhattacharya and Walker, 1991).

#### *Bad Heart Formation*

The Bad Heart Formation (late Coniacian) is a thin, mappable, sandy to oolitic ironstone unit between the thick shales of the underlying Kaskapau/Muskiki and overlying Puskwaskau formations. The Bad Heart Formation was deposited in a shallow-marine environment and consists of sandstone and siltstone with locally thick and extensive oolitic ironstone. It comprises at least two upward-shoaling facies successions bounded by regionally-mappable erosional-surfaces.

The Bad Heart Formation is in the central to upper part of the Late Cretaceous Smoky Group (Figure 2.3) and is equivalent to at least part of the Alberta Group in the south

(Stott, 1967). McLarn (1919) was the first to recognize and initially define the Bad Heart Formation. Stott (1967) subsequently defined it as a sandstone unit that occurs above the Cardium Formation in the Foothills and the Alberta Plains north of the Smoky River. Plint et al. (1990), however, differentiated this unit into two formations: the Bad Heart Formation *sensu stricto* in the northwestern Plains near the original type section of McLarn (1919) along the Smoky River, and in the Foothills they redefined the stratigraphically equivalent unit as the Marshybank Formation. Donaldson (1997) suggested these two units are separated by a regional unconformity with a chert-pebble horizon in the outcrop and core that is easily recognizable in well logs. Further, Donaldson (1997) suggested that along the Smoky River the Bad Heart Formation consists of two upward-shoaling allomembers with a basal erosion surface (BES) below allomember 1, an erosion surface (ES1) that separates the two allomembers, and an upper erosion surface (ES2) at the top. Collom (2001), on the other hand, disagreed, siding with Stott (1967), and considered the Bad Heart and Marshybank formations to be coeval. Further, Collom (2001) assigned the lower allomember, which contains a relatively thick oolitic ironstone, to the Kaskapau Formation.

#### *Puskwaskau Formation*

The Puskwaskau Formation (Santonian to middle Campanian) consists of dark grey marine shale. This formation underlies the upper slopes of the northwestern highland terrains, particularly the northeastern part of the Chinchaga Hills, which are north of the Clear Hills, and also occurs in the upper part of the sections along the Smoky River. Basal Puskwaskau shale crops out above the Bad Heart Formation oolitic ironstone north of Worsley and at Rambling Creek in the Clear Hills region, and along the Smoky River in the Smoky River region.

## TECTONIC SETTING

The main structural element active during the Paleozoic in the study area is the Peace River Arch (PRA). The PRA is perhaps the longest lasting structural feature in northern Alberta, being active from the mid to late Precambrian to perhaps the Present (O'Connell et al., 1990). The PRA is an easterly plunging, east-northeast trending asymmetrical basement high that extends from the British Columbia-Alberta border, east-northeast to at least the fourth meridian in Alberta. The evolution of the PRA, especially reactivation of some of the ancient basement faults, has had a profound influence on the patterns of Phanerozoic sedimentation, accumulation of hydrocarbon and enrichment of minerals in the PRA region. The main importance of the PRA to the depositional environment of the Bad Heart Formation is during the third stage of the post-Jurassic subsidence (O'Connell et al., 1990); that is, during the development of the Jurassic and Cretaceous foreland basin, localized subsidence occurred in the Peace River region, and older underlying structures, particularly the Early Carboniferous graben system, appear to have influenced the Cretaceous basin configuration and facies distribution.

According to Donaldson et al. (1998), four Late Cretaceous faults were active during the Bad Heart Formation deposition in the Smoky River region; these faults trend northwest-southeast and three of them, labelled 1 to 3 (fault 4 is outside the present study area), are shown by the blue dashes in Figure 2.4. Donaldson et al. (1998) suggested these four faults are re-activated Paleozoic faults that, in turn, are a subtle extension of the low-angle shear zones in the Precambrian basement.

## AGE AND CORRELATION

The Bad Heart Formation lies within the ammonite zone *Scaphites depressus* and this suggests the unit is Late Coniacian (Cobban, 1993). The Bad Heart oolitic ironstone unit in the Clear Hills region typically has been correlated with the type section at the Smoky River on the basis of identical fossil assemblages of *Inoceramus pontoni* and *Inoceramus Coulthardi* (McLearn, 1926) from within the Bad Heart sandstone at Smoky River and at

the base of the oolitic ironstone in the Rambling Creek section at the Clear Hills (Mellon, 1962).

At the Smoky River, the Bad Heart Formation is underlain by the early Coniacian Muskiki Formation. In contrast, the foraminiferal assemblage from the shale immediately below the oolitic ironstone in the Rambling Creek area indicates a considerably older age for this shale, equivalent to the Kaskapau Formation (Lentz, 1956). These diachronous ages in the underlying shale between the Clear Hills and Smoky River regions suggest differential erosion at the base of the Bad Heart Formation, with the Muskiki and upper Kaskapau shales being regionally eroded to the north (Donaldson et al., 1999). With respect to the shale overlying the Bad Heart Formation in both the Clear Hills and Smoky River regions, the foraminiferal assemblage present is characteristic of the Puskawaskau Formation in both regions (Green and Mellon, 1962).

#### METHODOLOGY

Systematic detailed section measurement was done, and samples were collected for palynology, geochemistry and petrography at 39 natural outcrops, 6 shallow trenches which exposed the Bad Heart Formation bedrock (dug mechanically to a depth of about 4 m), and 2 diamond drill cores; 28 of these mapped sections are presented in Appendix I. Palynology samples were collected from within, above and below the Bad Heart Formation, and prepared at the Geological Survey of Canada (GSC) laboratory in Calgary. The dinoflagellate, angiosperms and spores were identified by Dr. Art Sweet and Ms K. Boyce of GSC Calgary, under contract to the Alberta Geological Survey (Boyce and Sweet, 2006, 2007; Sweet, 2009); their contribution to the understanding of the palynology cannot be overstated.

Publicly available geophysical well logs were used to construct two regional cross-sections for the Clear Hills region. Few pertinent well logs are available because most well logs do not transect the Bad Heart Formation, and, as a result, geophysical data typically start only below this unit. Nonetheless, there are sufficient well logs to prepare

the two east-west cross sections, A-A' and B-B', the locations of which are shown in Figure 2.5.

Thin sections were prepared for 73 selected Bad Heart Formation samples to study the ironstone ooids and associated detrital grain mineralogy. These sections were first examined under petrographic microscope; then selected sections from oolitic ironstone were coated with chromium in order to study them under a Scanning Electron Microscope (SEM). Finally, ooid grains from selected samples were handpicked under a binocular microscope, and the selected ooids were split into halves by using a sharp blade and then coated with gold to study the inner morphology and texture of the nucleus and cortex of the ooids under JEOL 35 SEM. The SEM study was done at the University of Alberta SEM laboratory.

#### **STRATIGRAPHY OF THE BAD HEART FORMATION**

Donaldson et al. (1999) suggested that at the Smoky River, the Bad Heart Formation consists of two upward coarsening facies successions of mudstone, siltstone and sandstone bounded by three erosional surfaces: (1) the Basal Erosion Surface (BES) exists at the base of the Bad Heart Formation and is a regional unconformity; (2) Erosion Surface 1 (ES1) is at the top of the lower Bad Heart facies succession, and (3) Erosion Surface 2 (ES2) lies at the top of the upper Bad Heart facies succession (Figure 2.6). The maximum thickness of the Bad Heart Formation in the outcrop is 18.5 m along the western part of the Smoky River belt of the Bad Heart outcrops (Section ASR3 in Figure 2.7; note that section ASR3 is about 400 m south of the comparative section shown in Figure 2.6).

#### **FACIES**

The Bad Heart Formation is divided into 7 different facies, as initially proposed by Donaldson (1997) and Donaldson et al. (1999), which are summarized in Table 2.1.

Following are comments about each facies based on the field observations from this study.

#### FACIES SUCCESSIONS

##### *Bad Heart facies succession 1*

The lower facies succession 1 of the Bad Heart Formation commonly has a coarse chert and phosphate pebble (facies A) at its base (existing above the BES), and is upward coarsening from mudstone (facies B) to siltstone to siltstone-sandstone (facies C), bioturbated sandstone (facies D) and eventually to the clastic-starved facies E oolitic ironstone. At the Smoky River, facies E is overlain by erosional surface ES 1, which locally has a thin, chert-pebble conglomerate (facies A) above the veneered ES1 erosion surface (e.g., at sections ASR5 to ASR8 and ASR9B to ASR10, Figure 2.7). This idealized facies sequence from A to E in lower the Bad Heart Formation is exemplified by the succession in sections ASR10 and ASR10A at the central Smoky River (Figure 2.7). To the east and west of this locale, however, some facies are missing, especially facies D and E. The variation in facies succession laterally is possibly due to syndepositional tectonic activity in the Clear Hills to Smoky River area during the Bad Heart time (Donaldson et al. 1999).

The pebble-veneered (facies A) unit marking the basal part of the lower facies succession at Smoky River comprises a chert pebble and phosphatic intraclasts horizon of varying thickness, ranging from 8 cm up to 1.1 m, that can be traced across the entire Smoky River region except at a few outcrops, such as sections ASR9A, ASR14C and ASR12 at the eastern Smoky River (Figures 2.2b, 2.7). In section ASR14C (Figures 2.2b, 2.7) at the eastern Smoky River, the BES surface is marked by a sharp change upward in the color of the shale from black to grey, and also by an abrupt change in the palynology (see below). The lack of pebbles marking the BES surface in the easternmost sections at the Smoky River suggests this locale was more distal to the paleo-shoreline. As well, the rapid change in thickness of the facies A conglomerate which marks the BES occurs over very short distances; e.g., over about 1.3 km between sections ASR7 and ASR8 and also

over 2.2 km from sections ASR6 to ASR5 (Figure 2.7). These rapid changes in facies A thickness over relatively short distances indicate the deposition of thicker conglomerate occurred in subtle lows in the paleo-topography (such as that between sections ASR5 to ASR8 as illustrated in Figure 2.7). Finally, the facies A and the BES are not readily obvious in the Spirit River road cut (SPRV) (Figures 2.2b, 2.7) or Blue Berry Mountain (BBM) trenched exposures, which are west of the Smoky River. However, the trenched sections at these two locales might not have been deep enough to find either facies A or the BES.

Facies A is overlain by laminated mudstone of facies B. In general, facies B blankets the whole area of the Smoky River region and is much thicker in the eastern and western Smoky River outcrops, whereas in the central outcrops, it is relatively thinner, typically less than 1 m thick.

The laminated mudstone of facies B is overlain by facies C bioturbated siltstone, siltstone-sandstone and sandstone. In general, facies C also occurs across the entire Smoky River region (Figure 2.7).

Facies D, oolitic sandstone, and facies E, oolitic ironstone, occur only in the central portion of the Smoky River region between sections ASR5 and ASR10A (Figures 2.2b, 2.7). In this study the oolitic lithologies have been defined as follows: (1) oolitic sandstone contains from 1 volume per cent (%) to <10% ooids, (2) weakly oolitic ironstone (WOIS) contains from 10% to 30% ooids, (3) moderately oolitic ironstone (MOIS) contains 30% to 70% ooids, and (4) intensely oolitic ironstone (IOIS) contains >70% ooids and often >90% ooids. In the eastern and western Smoky River outcrops, the facies D and E successions above facies C were removed by erosion along the ES1 surface. The cause of this erosion is uncertain, but may be linked to local tectonism related to the down-dropped block bounded by faults 2 and 3 between sections ASR6 and ASR10A (Donaldson et al, 1999). The Facies D present in the central Smoky River outcrops is extensively burrowed by *Thalassinoides* and scattered oolitic ironstone beds are locally present. These indicate less clastic influx and a shallower oxygenated environment

beginning in the facies D time. These conditions, plus the iron-enrichment of the waters, must have continued in an enhanced way to cause the deposition of the intensely oolitic ironstone that constitutes facies E.

In the Clear Hills region, the lack of well exposed outcrops makes it difficult to document a complete facies succession in the lower Bad Heart Formation from facies A to E. However, an incomplete facies succession does exist, for example, (1) at the LVH section, where facies A, C, D and E are present, and (2) in the core from drill hole DDH0203, where facies B, C, D and E are present(Figs 2.2a, 2.8)

As at the Smoky River, facies E in the Clear Hills is truncated by erosion surface ES1. Thus, this extensive regional erosion surface occurs both in the Clear Hills region (Figure 2.8) and the central part of the Smoky River region (Figure 2.7). However, the thin chert pebble conglomerate that commonly overlies and marks the ES1 erosion surface is not continuous across all the measured outcrops.

#### *Bad Heart facies succession 2*

The second facies succession of the Bad Heart Formation is bounded at its base by the ES1 erosion surface and at its top by the ES2 erosion surface (Figures 2.7, 2.9). In the Bad Heart facies succession 2 the lower part commonly is marked by a facies A thin chert pebble and phosphatic intraclasts conglomerate unit, or the intraclasts unit is absent, and facies C directly overlies the ES1 surface (e.g., in section ASR9I at the central Smoky River, Figure 2.7). At the SPRV section, the placement of both the ES1 and ES2 erosion surfaces is uncertain; however, the ES1 surface is postulated to be within the facies B laminated mudstone, and Donaldson (1999) suggested the ES2 surface is at the base of the first oolitic sandstone (Figure 2.7). The fine sandstone of facies F commonly overlies facies C in most of the Smoky River Region sections where the Bad Heart facies succession 2 is present. Facies F is locally horizontally laminated and commonly has mud-filled *Skolithos* trace fossils. Facies F is absent west of the Wanham (WH) section and east of section ASR10A (Figures 2.2b, 2.7), with the latter

section being just west of fault 3 in the Smoky River region. The Bad Heart facies succession 2 is truncated by erosion surface ES2 in the Smoky River region (Figures 2.7, 2.9).

In the Clear Hills sections (Figure 2.8), the facies succession between the ES1 and ES2 erosion surfaces either is (1) completely absent or (2) may exist at a few sections, including the Worsley Pit, drill hole DDH0203 and ARR3 (Figures 2.2a, 2.8) at Rambling Creek. In the Worsley Pit section above the postulated ES1 surface, facies A intraclasts conglomerate, a very thin sandstone bed, another thin facies A intraclasts conglomerate, facies E oolitic ironstone and finally oolitic sandstone are observed. In contrast, in all the other Clear Hills sections, mainly facies C exists above the ES1 surface.

#### *Bad Heart facies succession 3*

In the Smoky River region, the ES2 surface commonly is overlain by oolitic ironstone to non-oolitic muddy sandstone of facies G, which exists as a continuous unit in almost all the exposed outcrops in the Smoky River region (Figure 2.7). In a few places (e.g., sections ASR3, ASR14C and ASR12), a thin conglomeratic unit exists above the ES2 surface. In most places, facies G above the ES2 surface grades rapidly upwards from oolitic sandstone, to sandstone, sandstone-siltstone, and siltstone over a meter or less into the black shale of the Puskwaskau Formation. A possible exception is the Spirit River section where facies G is overlain by the oolitic ironstone of facies E.

In general, the relatively thin, typically less than about 1.0 m to 2.0 m, facies G oolitic sandstone with locally oolitic ironstone and the overlying sandstone to siltstone layers above the ES2 surface in the Blueberry Mountain, Spirit River and Smoky River sections (Figure 2.7) are lithologically very similar to the facies in the underlying Bad Heart succession 1 (i.e., between BES and ES1) and succession 2 (i.e., between ES1 and ES2). As a result, it is proposed here that the thin oolitic and clastic succession above the ES2 surface should be considered as a third facies succession of the Bad Heart Formation, rather than being assigned to the overlying Puskwaskau Formation.

## **WELL-LOG CROSS SECTIONS**

Two east-west trending regional cross-sections, A-A' and B-B', were constructed for the Clear Hills region from 23 oil and gas wells, using the Base of Fish Scale (BFSC) marker as datum (Figures 2.5, 2.10, 2.11). Above the BFSC, five formations, the BFSC, Shaftesbury, Dunvegan, Kaskapau and Bad Heart top, were picked by the criteria listed in Table 2.2.

The well-log study shows that it is relatively easy to pick the top of the Bad Heart Formation in the Clear Hills data, but difficult to pick the lower contact with the Muskiki/Kaskapau formations. Nonetheless, the gamma log signature for the Bad Heart Formation observed along section A-A' (Figure 2.10) in the Clear Hills region shows two to three coarsening up packages with a total thickness ranging from 10 m to 12 m. These total thickness and thickening up sandstone packages are similar to the Bad Heart Formation observed in the outcrops along the Smoky River, but are not as obvious in the Bad Heart Formation outcrops in Clear Hills and diamond drill hole data. Further, in both the Clear Hills well data and the Smoky River mapped sections, the upper sandstone package is more pronounced than the lower. In the south part of the Clear Hills along line B-B' (Figure 2.11), the two coarsening up packages coalesce towards the east into a single package of 5 to 8 m thickness; this thinning of the Bad Heart Formation to the southeast in the well data is similar to that seen in the measured outcrops (Figure 2.8). The two coarsening upward cycles in the Bad Heart Formation in the Clear Hills well data are similar to those in the two Bad Heart Formation facies successions at the Smoky River outcrops.

## **PALYNOLOGY**

Dinoflagellates, miospores and pollen are useful to determine if there are any identifiable time gaps within the Bad Heart Formation and in the sequences immediately contiguous. Among the dinoflagellates, the range base of *Chatangiella* sp. cf. *C. spectabilis* has

biostratigraphic significance (Sweet, 2009) because they do not occur below the Basal Erosion surface (BES). Thus, the abrupt downward range truncation of the dinoflagellate *Chatangiella* sp. cf. *C. spectabilis* is useful to identify the position of the BES marker in those outcrop locales where no obvious lithologic evidence is present. For example, at sections ASR9A and ASR14C (Figure 2.7) in the central and eastern Smoky River regions, the position of the BES surface was identified at the abrupt cessation downwards of the taxa *Chatangiella* sp. cf. *C. spectabilis*, even though no obvious lag deposits mark the BES, as such exist in many other Smoky River sections. At section ASR3, in the western Smoky River (Figure 2.7), there is abrupt cessation downwards of the taxa *Chatangiella* sp. cf. *C. spectabilis* between samples 6ROSP75 and 6ROSP76 (Figure 2.12); this abrupt change in dinoflagellate taxa coincides with a thin conglomerate unit marking the BES surface.

Similarly, in the drill hole DDH0203 core from the Clear Hills region, the BES can be identified by an abrupt absence of *Chatangiella* sp. cf. *C. spectabilis* from sample C0203P07 to C0203P008 (Figure 2.12). There is a sampling gap of about 5 m between these two samples, which makes exact placement of the postulated BES surface uncertain; however, in drill hole DDH0203 (Figure 2.8), the postulated BES surface has been placed at a very thin concretionary layer.

The succession from the Bad Heart Formation across the ES2 erosional surface into the overlying Puskwaskau Formation appears to have occurred without any identifiable dinoflagellate range truncation (Sweet, 2009). This indicates there may not have been any significant time gap from the deposition of the Bad Heart Formation to that of the Puskwaskau Formation.

Finally, the palynology samples collected during this study, and analyzed by Boyce and Sweet (2007), from the shales stratigraphically above and below the oolitic ironstone horizon in the Botha River area north of Clear Hills, clearly show that both the underlying and overlying shales at the Botha River oolitic ironstone succession are older than Bad Heart age.

## PETROGRAPHY

The petrographic work done during the current study indicates there are four distinct sediment types within the Bad Heart Formation:

- (1) thin conglomerates (facies A), which are locally present immediately above the BES, ES1 and ES2 erosional surfaces;
- (2) dark grey to grey shale (facies B) in the lower part, but above the BES;
- (3) siltstone-sandstone to fine- to medium-grained sandstone (facies C and F) above the lower shale, and also above both the ES1 and ES2 surfaces, and finally,
- (4) oolitic sandstone to oolitic ironstone (facies D, E and G, which typically are above the non-oolitic sandstone between the BES and ES1 surfaces, and also above the ES2 surface in some sections.

In general, the two lithologies that uniquely characterize the Bad Heart Formation are sandstone, which in places is oolitic, and weakly to locally intensely oolitic ironstone.

The primary clastic grains in the Bad Heart Formation are quartz, feldspar, rock fragments, with less common mica and glauconite, and, of course, in facies D, E and G, iron ooids and locally pisoids. Quartz comprises a maximum of about 43% of the Bad Heart sedimentary clasts, and typically occurs as angular to subangular grains. In facies D and E, most of the quartz grains are scattered throughout the matrix between the ooids, although some also form the nucleus of the ooids. Feldspar is up to 9% of the sedimentary clasts and is most common within facies C, bioturbated sandstone, in the central Smoky River. Feldspar exists mostly as sub-angular to sub-rounded grains, and, as well, rare feldspar grains occur in the core of some ooids. The percentage of rock fragments varies from 0.5% to 6.5% in the Bad Heart Formation in the Smoky River region, and they comprise mostly siltstone and shale fragments. Mica fragments are a minor component, typically comprising up to a maximum of about 0.8% of the sedimentary clasts. Glauconite exists in all facies of the Bad Heart Formation, but, in

general, is less than 1% of the sedimentary grains and commonly exists only in trace amounts. Finally, iron ooids occur dominantly in facies D, E and G; the percentage of ooids varies from 1 volume % to <10% in facies D (oolitic sandstone), to >10% and locally over 90% ooids in facies E (WOIS to IOIS), or locally in facies G. Overall, the Bad Heart Formation sediments are mainly poorly sorted sandstones, thus indicating textural immaturity and minimal reworking prior to deposition (Tucker, 1981). The exception, however, is facies E oolitic ironstone, which is very well sorted; this indicates repeated reworking and is a characteristic of many oolitic ironstones (Young, 1989). Alternatively, perhaps, the oolitic-forming shoals were clastic-starved during the oolitic ironstone depositional periods.

### ***Description of ooids***

The ooids show variability in morphology, composition and texture. The ooids are light brown under the petrographic microscope in transmitted plane polarized light. The ooids are generally ellipsoidal in shape, but they vary from spheroidal to perfectly rounded, and some ooids have irregular forms. Many ooids, mostly from facies G in the Smoky River region, have been deformed so that they no longer are spherical, and can be considered as spastoliths (Young, 1989). In the spastoliths, the thickness of the concentric lamina varies and the overall ooid shape has been changed by post-depositional deformation.

The Bad Heart Formation ooids diameters range from 0.2 to 0.8 mm along the major axis. In general, the Bad Heart ooids are smaller in size than carbonate ooids; this size difference is attributed to density, in that iron ooids are heavier, hence the formation of large iron ooids would require more intense marine energy. In places, larger ooids or pisoids are present; for example, pisoids occur at the Worsley pit section in the southern Clear Hills and in the Rambling Creek sections where the pisoids are composed of a large clastic nucleus and a disproportionately small outer cortex (Figure 2.13). The ooids generally have smooth walls and show a concentric growth of a laminated cortex (sheath)

around the nucleus (core) (Figure 2.14). Internally, ooids are made up of alternate light and dark, thin, nearly continuous concentric laminae of goethite and nontronite. The number of laminae varies from less than ten up to several tens in a single ooid.

The nucleus ranges in size from 20 to 80% of the ooids diameter. The ooids nuclei consist of various materials, including quartz, ooid fragments and rare feldspar. Quartz accounts for about 30 to 40% of the total nuclei, and a rare <5% of ooids have a feldspar grain as their nucleus.

The concentric laminae are generally continuous, and the thickness varies within and among ooids. The colour of the cortex lamina, as seen under the microscope, in plane polarized light, varies from light- to pale-yellow to medium yellow-brown to dark brown. The nucleus of ooids, typically have no consistent shape and can vary from rounded to subangular. The contact between the nucleus and the cortex, and the cortex and the surrounding matrix between ooids, ranges from sharp to gradational, although sharp tends to be more common. Some ooids have cracks radiating from the nucleus.

Phanerozoic ooids are reported to have length to width ratios generally between 5:1 to 10:1 (Siddaiah, 2008), whereas in contrast, the ellipsoidal ooids from the Bad Heart Formation typically have a lower long to short axis ratio ranging from 1.2 to 1.9. The thickness of individual concentric cortex lamina varies from 2 to 15 µm. In general, the thickness of the ooid's cortex decreases towards the top of the ironstone bed; this may indicate either (1) decreasing wave agitation energy, hence decreasing the time the ooid would be suspended in the water column before its increasing density caused it to fall to the sea floor, or (2) decreasing iron activity in the sea water over time, or both.

Rohrlich (1974) showed that the ooid lamina is made of flakes, platelets and subspherical nanograins. The SEM work on the Bad Heart Formation ooids from this study shows each individual cortex lamina is composed of randomly to tangentially oriented flakes, platelets and tiny grains (Figure 2.15). The flakes are tangentially oriented to the ooids external surface and can be observed on the outer rims of the lamina (Figures 2.15B ,

2.15C). In the cortex of some ooids, the flakes and grains are coalesced (Figure 2.15D) and thus mask the initial morphology of the particles. According to Bhattacharyya and Kakimoto (1982), the tangential fabric of ferruginous ooids originated by mechanical accretion of suspended particulate matter (hydrated iron oxides and detrital clay minerals, especially kaolinite) around a nucleus in water of sufficient agitation to keep the forming-ooid above the sea floor, but not so overly strong that the agitation prevents accretion of the micro-grain to the ooid. Chamosite subsequently formed from kaolinite during early stage diagenesis in an iron-rich environment.

The broken cortex of some ooids may indicate ooid reworking before final ooid deposition. The quartz content is variable, but it is present both in the nucleus and matrix, and the quartz generally is poorly sorted, and angular to subangular. The ooids are either freely suspended within the matrix (e.g., in WOIS) or very closely packed (e.g., in IOIS). Despite the ooids common close contact or packing, little fracturing of ooids occurs, even at the point of contact of two ooids. That is, they do not show any indentation, which may indicate either the ooids are deposited in a sufficiently indurated form or the matrix is soft and acts as a cushion until the ooids are sufficiently indurated. In places, a few ooids have radial cracks from the centre, but no obvious refilling and healing are visible in the cracks, thus indicating the cracking may be post depositional (Figure 2.16).

Two distinct types of ooids were identified during the petrographic and SEM study of the Bad Heart Formation. Type 1 ooids have a thick, well developed, laminated cortex with a very small or not clearly defined nucleus (Figure 2.17). Some of these ooids show a cross-cutting texture in the cortex, indicating a period of erosion of the ooids cortex prior to the resumption of the deposition of concentric lamina and further growth of the ooids cortex (Figure 2.17D). Type 2 ooids are characterised by a large nucleus with a relatively thin, concentric laminated cortex (Figure 2.18). The nucleus in Type 2 ooids typically is quartz or an iron oxide clast and, rarely, a phosphate clast. Some Type 2 ooids with a quartz grain nucleus are cross-cut by iron oxide veins (Figure 2.18D).

## DISCUSSION

The Bad Heart Formation is distinctively anomalous in the Smoky Group because it consists of a relatively shallow marine, coarser clastic unit (mainly siltstone, sandstone, oolitic sandstone, oolitic ironstone, and local pebble conglomerate) that lies in the middle of a much deeper water, fine, clastic dominated Late Cretaceous sequence (i.e., the underlying Muskiki and Kaskapau Formation shale and the overlying Puskwaskau Formation shale). However, the extensive oolitic ironstone deposition indicates there was, at times, limited clastic supply during the Bad Heart Formation depositional period and, presumably, concomitantly the iron activity in the sea water was sufficiently elevated to cause precipitation of selected stable iron-bearing minerals. The two upward coarsening facies successions (i.e., facies succession 1 and facies succession 2) of the Bad Heart Formation also suggest deposition during two distinct stages of progradation separated by transgressive events. In this scenario, the erosional surfaces BES, ES1 and ES2 may be interpreted as transgressive wave-ravinement surfaces. Above the ES2 surface, the upward fining from ironstone-sandstone to siltstone then to Puskwaskau Formation shale indicates a regional return to deeper water conditions that are starved of coarse clastics.

The log signatures in oil-gas well sections A-A' and B-B' (Figs. 10, 11), and the geology mapped in the outcrops and the drill hole in the Rambling Creek area (Figure 2.8) in the Clear Hills region, indicate the Bad Heart Formation sandstone-ironstone total thickness ranges from 10 to 12 m. In contrast, Chen and Olson (2007), based on a regional well-log interpretation for the Upper Cretaceous in the Clear Hills region, suggested the Bad Heart Formation thickness is markedly thicker and changes drastically from up to 60 m in the west to 20 m in the eastern and northern Clear Hills. The reason for this disparity is uncertain, but might be due to the difficulty in identifying the base of the Bad Heart Formation in the sparse Clear Hills well log data set. The data in the present study, however, perhaps especially from core DDH0203, clearly show the total thickness of the

Bad Heart Formation sandstone-ironstone is about 12 m in the eastern Clear Hills region. This maximum thickness is similar to the Bad Heart sandstone-ironstone thickness measured in the outcrop at the central Smoky River (Figure 2.7) and at the Rambling Creek (Figure 2.8). In short, this study contends that, on average, the Bad Heart Formation *sensu stricto* in both the Smoky River and Clear Hills regions is a relatively thin, coarser clastic unit that typically is less than about 12 m thick (although locally up to about 18 m at ASR3 at the western Smoky River), and frequently to ubiquitously contains oolitic ironstone layers that are, in places, from 2 m to 10 m thick (e.g., section ARR3 at Rambling Creek).

The textural features described in this study for the Bad Heart oolitic ironstone strongly indicate ooid formation was authigenic; that is, the ooids formed essentially in place in relatively shallow, agitated water, and neither were transported in from elsewhere nor formed during diagenesis. For example, the petrographic features of the Bad Heart ooids, including their symmetrical shape, high sorting, rare presence of broken ooids (except in the nucleus) and delicate textural lamina of the ooid cortex, rule out their origin by transportation from a more distant source area. The local coexistence of older ironstone fragments side by side with new ooids and the occurrence of clasts with angular edges and irregular shapes indicate little transport. Instead, the ironstone clasts, which are locally present, result from *in situ* reworking of oolitic material at or above the agitated wave base. In short, the growth of the ooids, based on the petrographic data in this study, indicates the ooids formed in the water column at or near where they now occur by a process involving multi-stage, repetitive deposition of lamina to form the ooid cortex, and the ooids fell to the sea floor when their weight or mass exceeded the turbulent energy of the shallow sea waters. Once on the sea bottom, there was perhaps in places local reworking of the ooids that resulted in either continued enlargement of the cortex such that some ooids reached pisoid size or, in some cases, were fragmented and formed partial ooid clasts. The formation of ooids was a repetitive process caused by agitated sea water current or other turbulent activity resulting in ooids generation, deposition, and,

in some cases, fragmentation. Some broken clasts, being smaller, elevated into the water column, and thus acting as a nucleus or core for the formation of new ooids, with the process repeating itself. The larger size of the ooids (average 250 µm) in the Clear Hills region, in comparison to the ooids (average 35 µm) in the Smoky River Region, suggests more reworking due to shallow sea water, which led to higher turbulence and agitation in the water column, hence longer retention in the water column and also greater reworking on the sea floor, resulting in larger and a greater number of ooids and, especially, pisoids in the Clear Hills region.

Lenz's (1956) microfossil work on the Bad Heart Formation in the Clear Hills region indicated the shale directly below the sandy Bad Heart contains the microfaunal assemblage *Gaudryina irenensis* of the Upper Cenomanian Lower Kaskapau Formation. As a result, Donaldson et al. (1999) suggested that a major erosion surface (BES) at the base of Bad Heart Formation sandstone-ironstone removed about 150 m of the Muskiki and upper Kaskapau formations between the Smoky River section and the Clear Hills section. The palynology samples from this study for the Clear Hills region support this conclusion, but show a somewhat different result; that is, the range base of the biostratigraphic significant dinoflagellate *Chatangiella* sp. cf. *C. spectabilis* (Sweet, 2009) is not immediately below the clearly Bad Heart Formation sandstone in the Clear Hills, but instead, in the core from drill hole DDH0203, occurs about 4 m below the sandstone within the shale (Figure 2.8). This result from the Rambling Creek area drill core is similar to that from section ASR3 along the western Smoky River (Figure 2.7) where the abrupt truncation of the palynomorph *Chatangiella* sp. cf. *C. spectabilis* occurs in shale some 13 m below the conglomerate and sandstone immediately overlying the ES1 erosion surface.

There is debate (Donaldson et al., 1999; Collom, 2001) about both the lower pick (BES) for the basal Bad Heart Formation and, as well, but perhaps less so, for the upper pick that marks the top of the formation. This discussion involves (1) the identified erosional surfaces BES, ES1 and ES2, which are well defined in the central Smoky River sections

(Figure 2.7); (2) the palynomorph and macrofossil variations that occur across the unit and its overlying and underlying formations; and (3) the lithostratigraphic composition of the unit (i.e., the predominantly sandstone-siltstone with local thin conglomeratic layers, and especially the oolitic ironstones and sandstones therein).

Plint et al. (1990), Donaldson (1997), and Donaldson et al. (1999) showed that the lower boundary of the Bad Heart Formation is an erosion surface (BES) that occurs at the base of the facies A chert pebble conglomerate that lies about 13 m below the base of the sandy portion of the Bad Heart Formation at the original type locality near the confluence of the Smoky and Bad Heart rivers (section ASR3 in the present study) (Figure 2.19).

Further, the upper boundary is the ES2 surface at the top of Donaldson's (1997) allomember 2. Therefore, the Bad Heart Formation as defined by Donaldson et al. (1999) consists of both the Bad Heart facies succession 1 (i.e., allomember 1 from BES to ES1) and the Bad Heart facies succession 2(i.e., allomember 2 from ES1 to ES2), but it does not include the sandy and oolitic ironstone facies G that occurs above the ES2 surface. In contrast, Collom (2001) argued from his macro-paleontology data and McLearn's (1919) historic definition of the unit, that the lower Bad Heart Formation boundary should be placed at the bottom of the sandy Bad Heart interval at the original type section, or ,essentially, at Donaldson's (1997) ES1 erosion surface (Figure 2.19). Collom (2001) further suggested all the shale below this boundary corresponds to the middle Coniacian Muskiki Formation, which occurs throughout the Western Canada Sedimentary Basin. Hence, in this case, the Bad Heart Formation would be represented only by the upper sandy interval between the ES1 and ES2 erosional surfaces at section ASR3, plus facies G, which exists above the ES2 surface (Figure 2.19). In this case, the succession of sandstone and oolitic ironstones lying between the BES and ES1 surfaces at central Smoky River would not be part of the Bad Heart Formation according to Collom (2001).

In the present study, the palynology samples indicate a definite time gap across the BES surface at the ASR3 section (Sweet, 2009), as originally proposed by Plint et al. (1990)

and supported by Donaldson et al. (1999). The pick of the top of the Bad Heart Formation could be made at the upper erosion ES2, but it would mean sandstone and oolitic ironstone of facies G above this surface, as well as the MOIS to IOIS above the inferred ES2 surface at the Spirit River and Blueberry Mountain sections, would be assigned to and part of the Puskwaskau Formation, and thus would not be part of the Bad Heart Formation. However, the palynomorphs data from this study indicate no significant time gap between the Bad Heart Formation and the overlying Puskwaskau Formation. As a result, the present study suggests the Bad Heart Formation should be defined as that interval from the lower BES to the uppermost sandstone or sandstone-siltstone unit above ES2, but immediately beneath the recognizable Puskwaskau Formation shale (Figure 2.19).

Figure 2.20 provides a suggested correlation of the Bad Heart Formation between the Smoky River and Clear Hills regions. In essence, it is suggested here that (1) the base of Bad Heart Formation is marked by both a regional erosional surface and an abrupt appearance upward of the dinoflagellate *Chatangiella* sp. cf. *C. spectabilis*, whereas (2) at the top of the Bad Heart Formation, sandstone and locally thick oolitic ironstones clearly exist above the ES2 surface (e.g., at the BBM and SPRV sections, and in places at Smoky River, as shown in Figure 2.7); hence, the top of the formation should or easily could be picked at the uppermost oolitic ironstone or sandstone unit abruptly overlain by black shale of the Puskwaskau Formation. This interpretation suggests that three, rather than only two, facies successions comprise the Bad Heart Formation: (1) a lower facies succession 1 (between BES and ES1) that is upwards coarsening, (2) a middle (formerly upper, re Donaldson, 1997) facies succession 2 (between ES1 and ES2) that also is upwards coarsening, and (3) an uppermost facies succession 3 (above the ES2 surface) that is upwards fining (i.e. the ironstone, sandstone and siltstone above the ES2 erosion surface that gradationally and in places abruptly transitions to the thick black shale of the overlying Puskwaskau Formation).

This study also has shown that the Bad Heart Formation oolitic sandstone-oolitic ironstone thickness is about 5.0 m at the Worsley Pit and its thickness increases towards the northeast to 10 m near Rambling Creek (Figure 2.8). Furthermore, towards the western part of the Clear Hills, the available trenched exposures and oil/gas well logs indicate the Bad Heart Formation grades to sandstone-siltstones, and there appears to be minimal or perhaps no oolitic ironstones present. In the Naylor Hills north of the Clear Hills, a few oolitic ironstone exposures are present at the Botha River area, which previously were considered to be Bad Heart Formation (e.g., Green and Mellon, 1962; Hamilton et al, 1999). However the palynology results from this study show the Botha River oolitic ironstones are older than those of the Bad Heart Formation. Thus, the Botha River ironstone unit is within the lower Kaskapau Formation and is probably correlative with the thin oolitic ironstones that exist at the Dunvegan Crossing section (Varban and Plint, 2005). As a result, this study now suggests the northernmost extent of the Bad Heart Formation is restricted to just north of the Rambling Creek Bad Heart Formation exposures and does not extend into the northern Clear Hills region, as previously suggested by Green and Mellon (1962).

## CONCLUSIONS

The Late Cretaceous Bad Heart Formation consists of at least two, or three as suggested herein, sandstone, siltstone and oolitic ironstone successions in the Smoky River region, whereas only two successions appear to be present in the Clear Hills, except possibly at the Worsley Pit section.

At Smoky River, the two lowermost successions (i.e., succession 1 from BES to ES1 and succession 2 from ES1 to ES2) are upward coarsening facies successions, which predominantly comprise siltstone, sandstone and oolitic ironstone with minor amounts of pebble conglomerate at the base of each succession. In contrast, the uppermost succession 3, which is above the ES2 erosion surface, is upward fining and grades or abruptly transitions into Puskwaskau Formation shale. Oolitic ironstone is more prevalent

at the top of the lower succession 1, although to the west at the SPRV and BBM sections, and possibly to the north at the Worsley Pit section, at least 1 m to 2 m of oolitic ironstone may occur above the ES2 erosional surface. The thick oolitic ironstone present only in the lowermost succession along the central Smoky River indicates this area was uplifted by syn-depositional tectonic activity along two inferred faults, F2 and F3, which formed shallow shoals above the wave base where the oolitic ironstone deposits could form. In the Clear Hills region, the thickest oolitic ironstone beds are at and just westerly of the Rambling Creek exposures; thus, this area was likely formerly a shallow water shoal. The oolitic ironstone-sandstone sequence at the Botha River in the northern Naylor Hills, which formerly was believed to be of Bad Heart Formation age, is now known to be clearly older and of the Lower Kaskapau Formation age, hence probably correlative with the thin oolitic ironstone-sandstone sequence in the Lower Kaskapau Formation at Dunvegan Crossing along the Peace River. As a result, the Bad Heart Formation in the Clear Hills region is much more areally restricted and, in fact, the northern limit of the Formation may be only just to the north of the Rambling Creek locale.

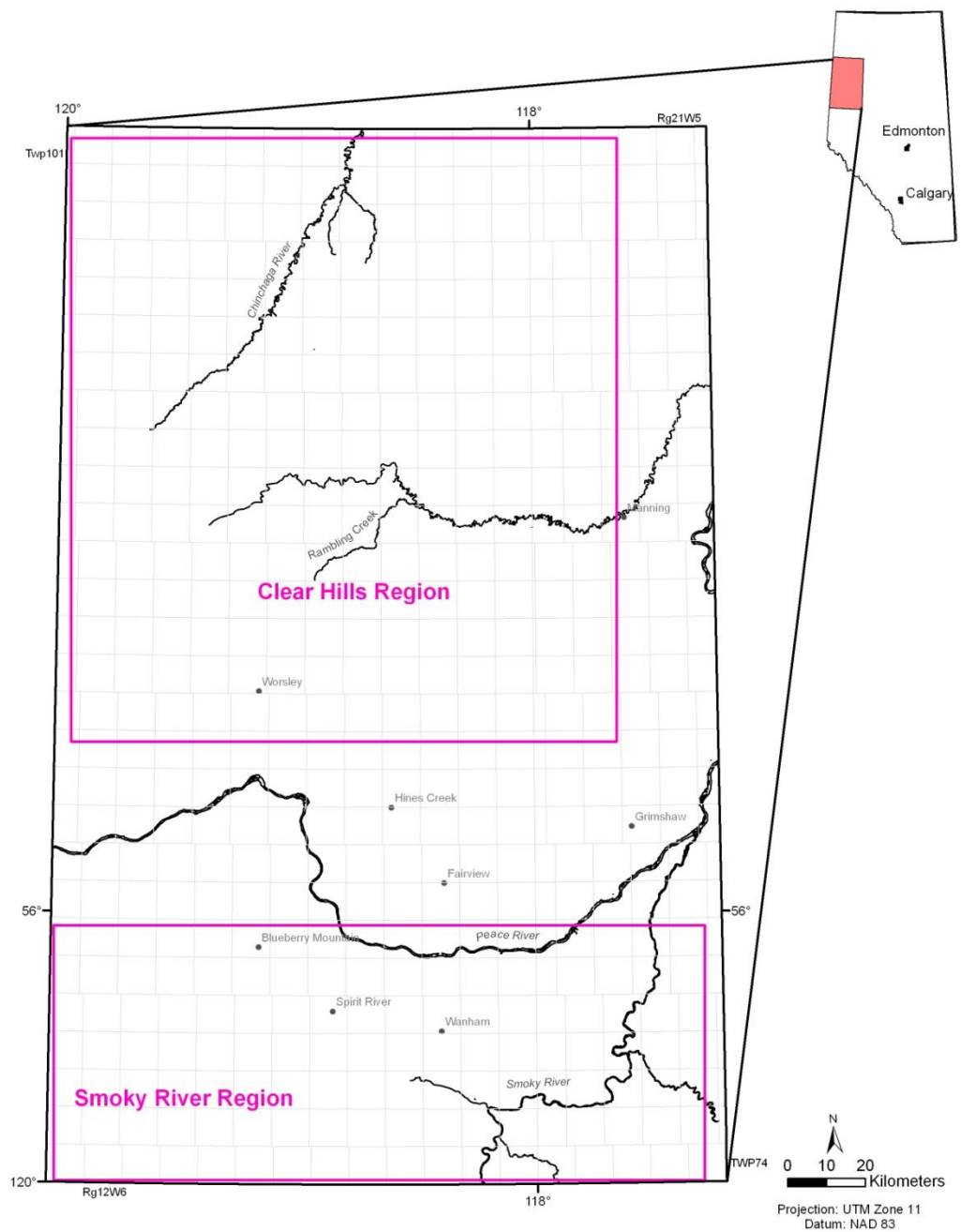
Finally, the Bad Heart Formation ironstones contain two distinct types of ooids: (1) one has a thick laminated concentric cortex, and (2) the other has a large nucleus and thin cortex. These two types of ooids likely formed in the same wave agitated environment, with deposition of the ooids occurring when their weight could not be supported in the water column by wave agitation. Thus, it is probable both ooid types have the approximate same average weight, but in the second type, the larger nucleus meant only a thinner cortex could be deposited before the ooid weight became such that it resulted in deposition on the seafloor.

Table 2.1: Summary of different facies observed within the Bad Heart Formation

Facies	Lithology , texture	Sedimentary Structure	Abundance of ooids	Depositional Environment
Facies A	Pebble conglomerate	---	Rare to Absent	Lag deposit
Facies B	Laminated Mudstone	Lenses of fine sandstone in the lower part	Absent	Quiet water below fair weather wave base with episodic storm activity
Facies C	Bioturbated sandstone	Intense bioturbation mask sedimentary structure	Rare	Quiet shelf environment below fair weather wave base
Facies D	Green oolitic sandstone with extensive Thalassinoides burrows	---	Abundant	Shallow marine oxygenated environment
Facies F	Locally stratified Skolithos Sandstone	Locally horizontally laminated and cross bedded with abundant mud filled Skolithos burrows	Rare	Shallower lower shoreface environment
Facies G	Interbedded oolitic and non-oolitic muddy sandstone; Lower muddy sandstone with calcareous cortex ooids grades to ferruginous oolitic sandstone and/or oolitic ironstone	Two generation of burrows	Abundant	Shallow marine environment

Table 2.2: Summary of formation picks criteria in selected oil and gas wells in the Clear Hills region

<b>Formation Pick</b>	<b>Criteria for Pick</b>
Bad Heart top	Picked at a medium to high gamma ray and low resistivity
Kaskapau top and/or Bad Heart bottom	Picked at a small peak in both medium gamma ray and medium resistivity. The Kaskapau top or Bad Heart bottom is difficult to pick
Dunvegan top or Kaskapau base	Picked at a abrupt drop from higher erratic to medium constant gamma ray drop and similar abrupt drop from medium to lower resistivity
Shaftesbury top or Dunvegan base	Picked at abrupt change from constant lower to higher erratic gamma ray and change from medium to higher more erratic resistivity. Note that the well log data indicate the unit becomes increasingly 'sandier' upwards
Base of Fish Scale( BFSC)	The BFSC marker is picked at markedly anomalous drop in gamma ray



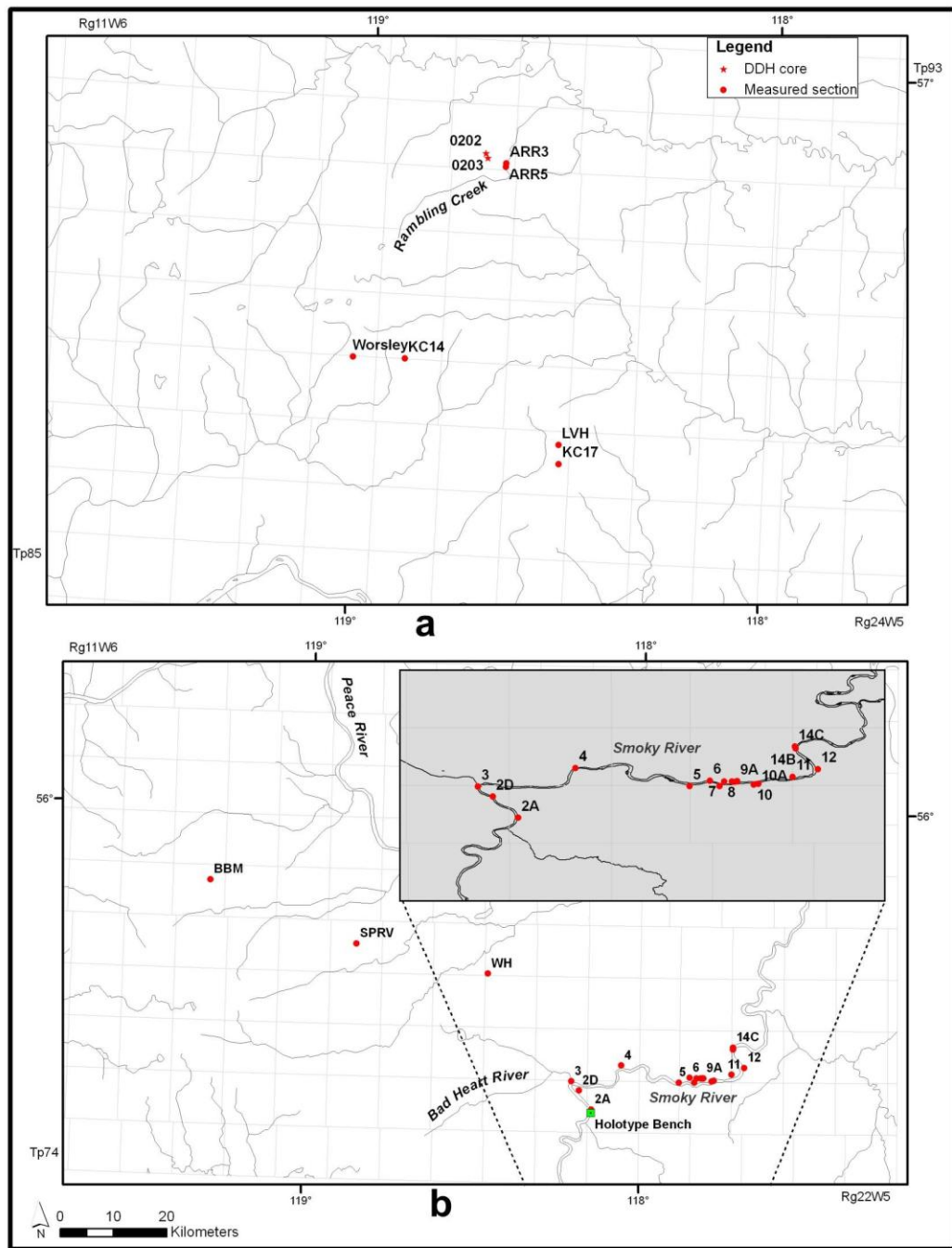


Figure 2.2 Location of mapped outcrops, diamond drill hole core and excavated trench sections; (a) Clear Hills region (b) Smoky River region

Period	Epoch	Stage	Age (Ma)	Groups and Formations		
				Northwest Plains		
Cretaceous	Late	Campanian	71.3	Wapiti		
				Puskwaskau		
		Santonian	83.5			
		Coniacian	85.8	Smoky Group	Badheart	
		Turonian	89.0		Muskihi	
					Cardium	
		Cenomanian	93.06	Kaskapau	Pouce Coupe	
					Doe Creek	
				Dunvegan		
				Shaftesbury		

Figure 2.3 Simplified stratigraphy of Late Cretaceous formations in the northwest Alberta Plains (modified from Alberta Energy and Utilities Board, 2002)

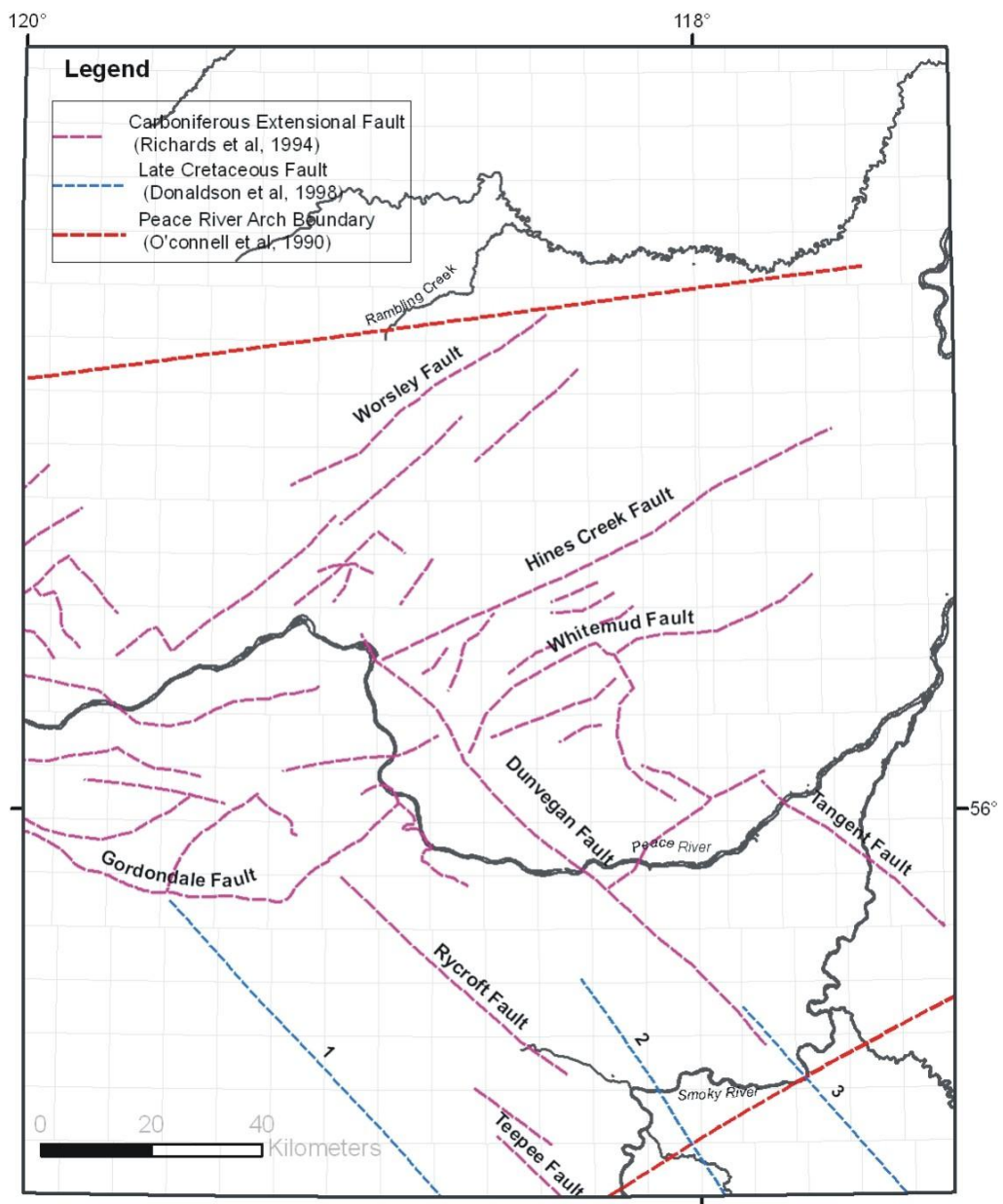


Figure 2.4 Major structural features in the Clear Hills to Smoky River region; these are derived from various sources

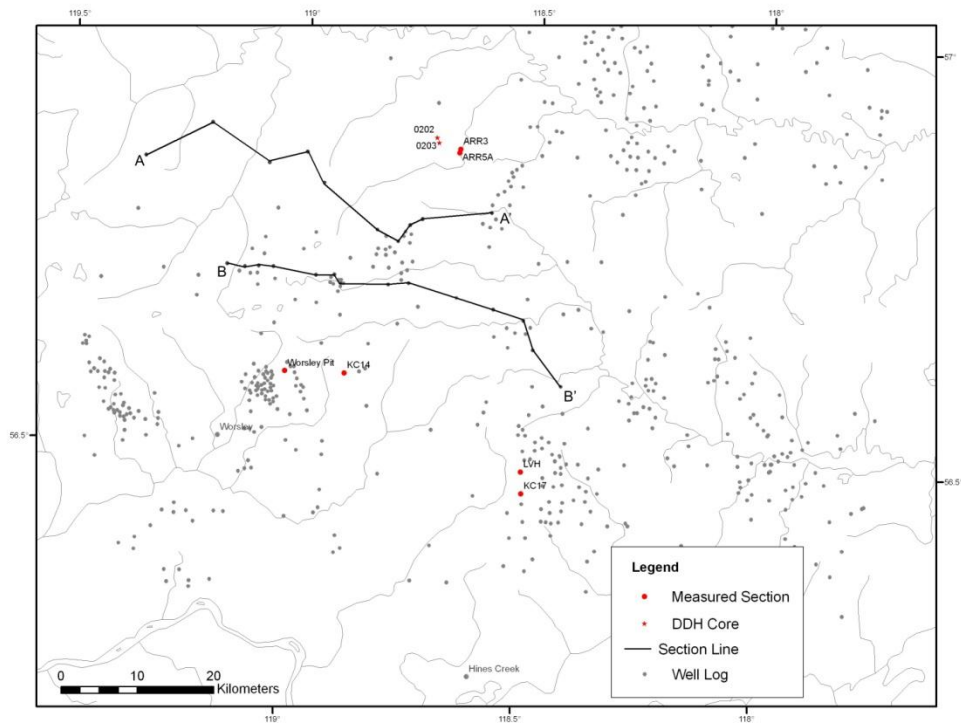


Figure 2.5 Available well logs in the Clear Hills region and the two cross sections (A-A' & B-B') that were constructed from 23 wells

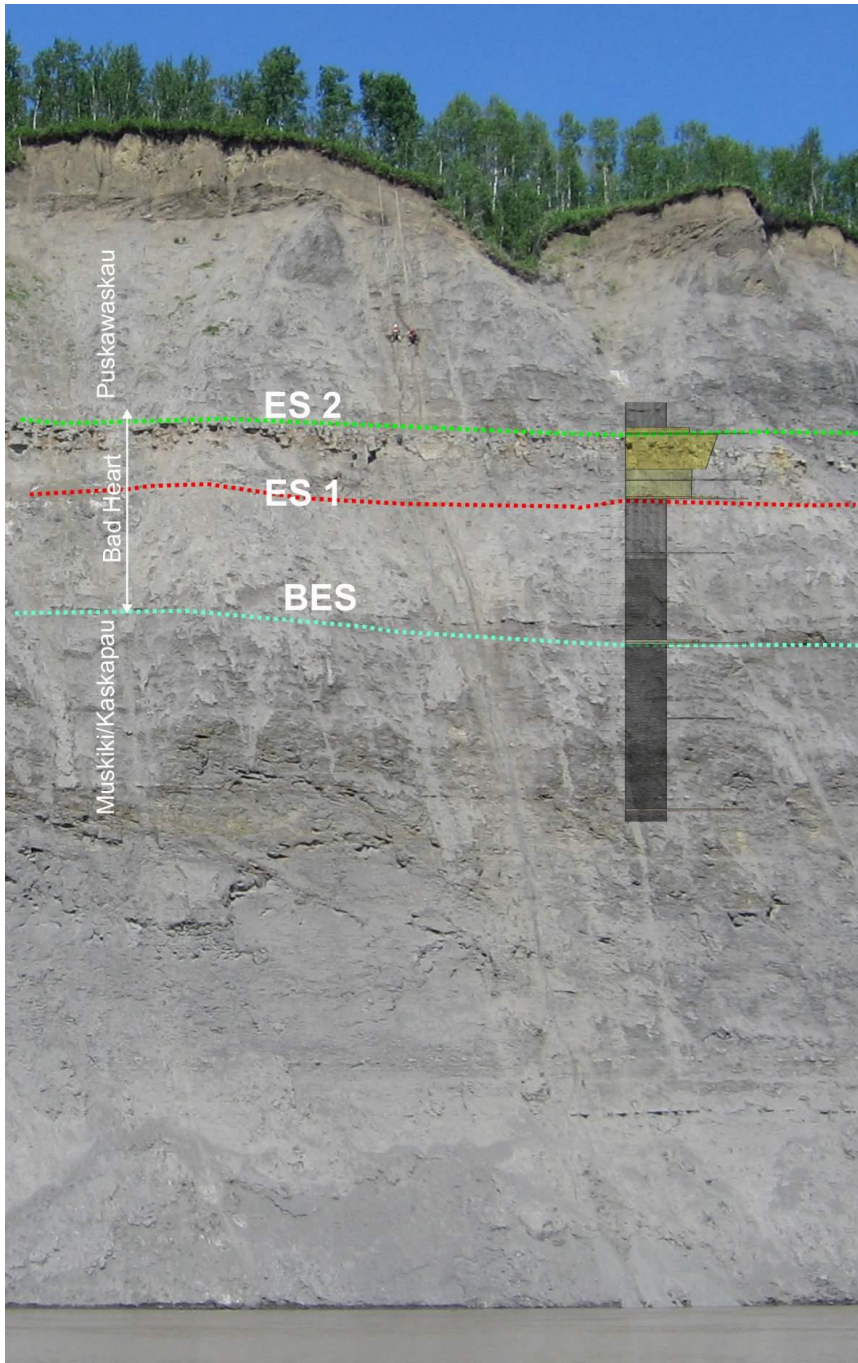


Figure 2.6 Complete Bad Heart Formation sequence near the original type section of McLearn (1919) along the Smoky River just south of the intersection with the Bad Heart River. The Basal Erosion surface (BES), Erosion Surface1 (ES1) and Erosion surface2 (ES2) originally suggested by Donaldson (1997) are shown. Also shown is a mapped section from this study

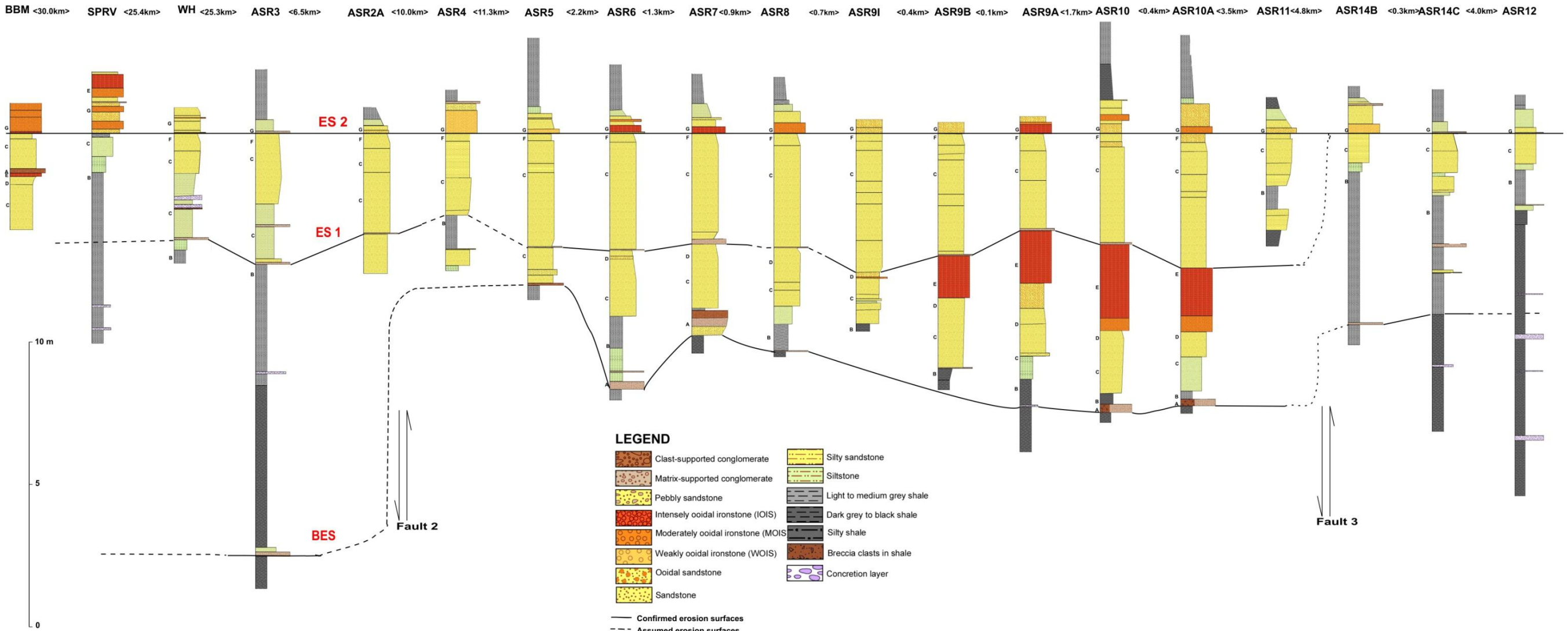


Figure 2.7 Northwest to southeast cross section of measured sections in the Smoky River region. The position of faults 2 and 3 is inferred from Donaldson et al (1998). Datum for the cross section is Erosion Surface 2 (ES2)

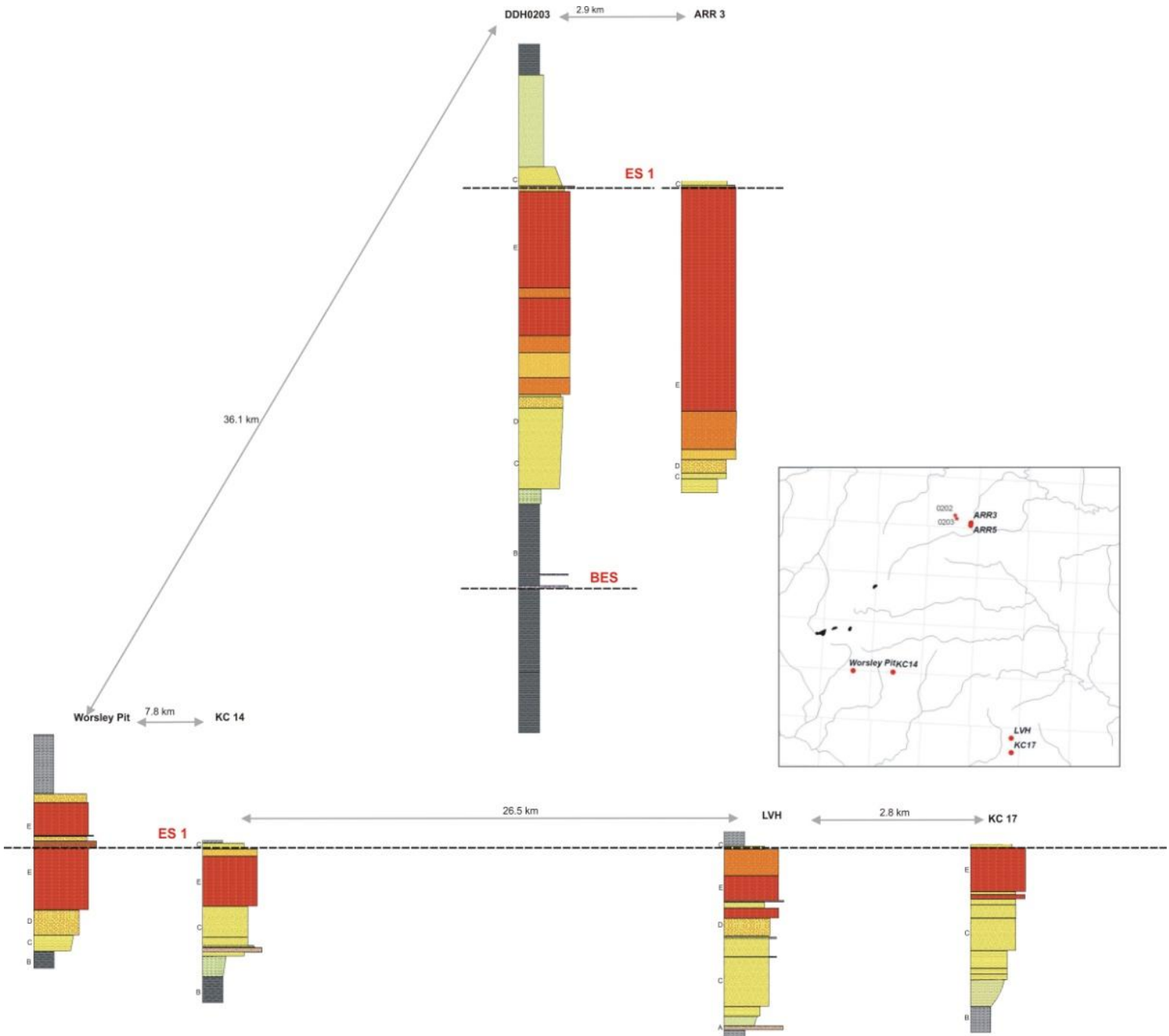


Figure 2.8 Two east-west Bad Heart Formation cross sections in the Clear Hills Rambling Creek area showing only the lower Bad Heart facies succession, with the upper Bad Heart facies succession removed by subsequent erosion. The frontal cross section is from Southern Clear Hills and the two sections in the back are from near the Rambling Creek



Figure 2.9 Bad Heart Formation Erosional surfaces ES2 and ES1 seen at section ASR9A in the cliff along central Smoky River

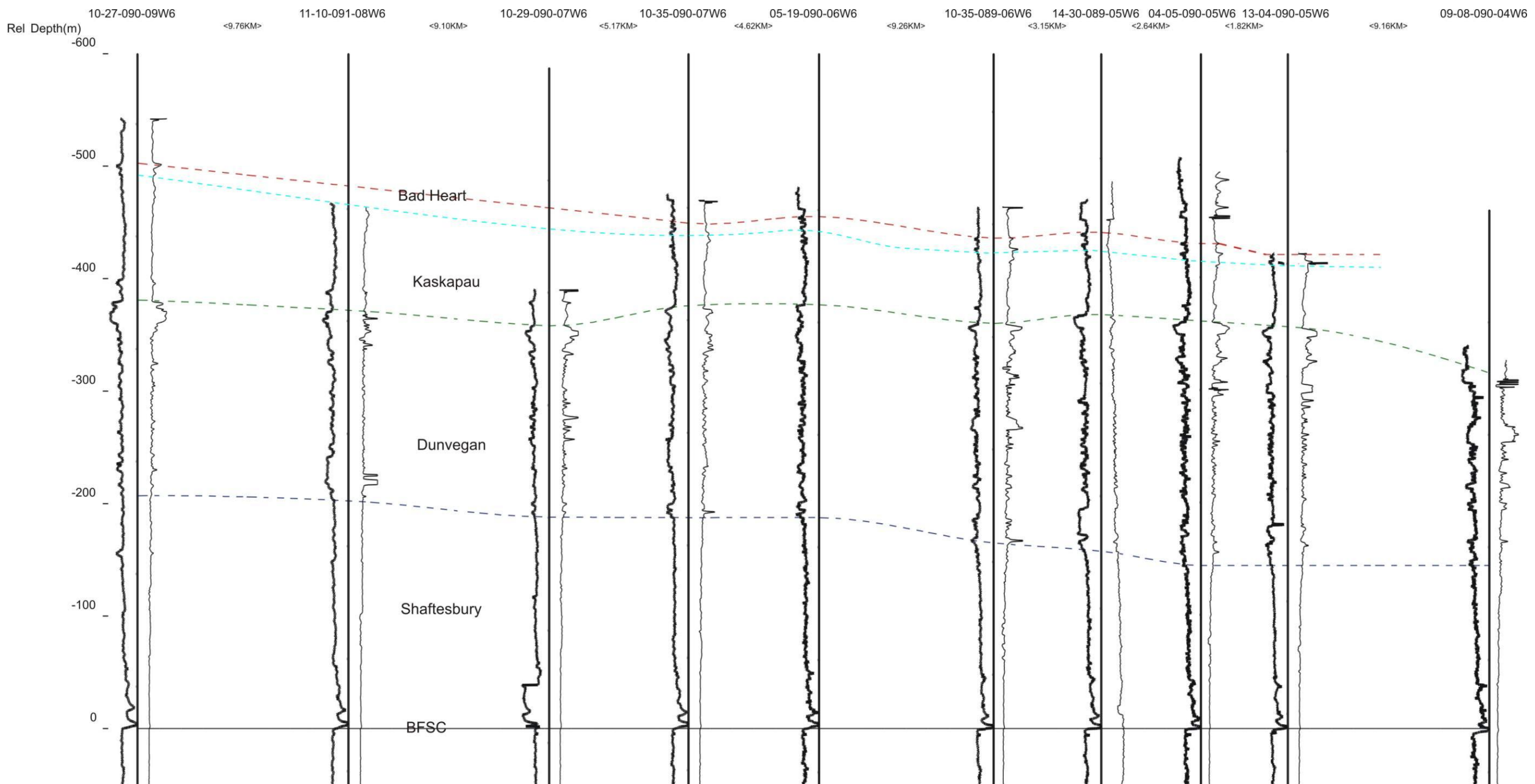


Figure 2.10 Well-log cross-section along line A-A' in the Clear Hills Region. The Base of Fish Scales (BFSC) marker is used as a datum. For each well, the log to the left is gamma and to the right is resistivity. Both logs are not always available for every well

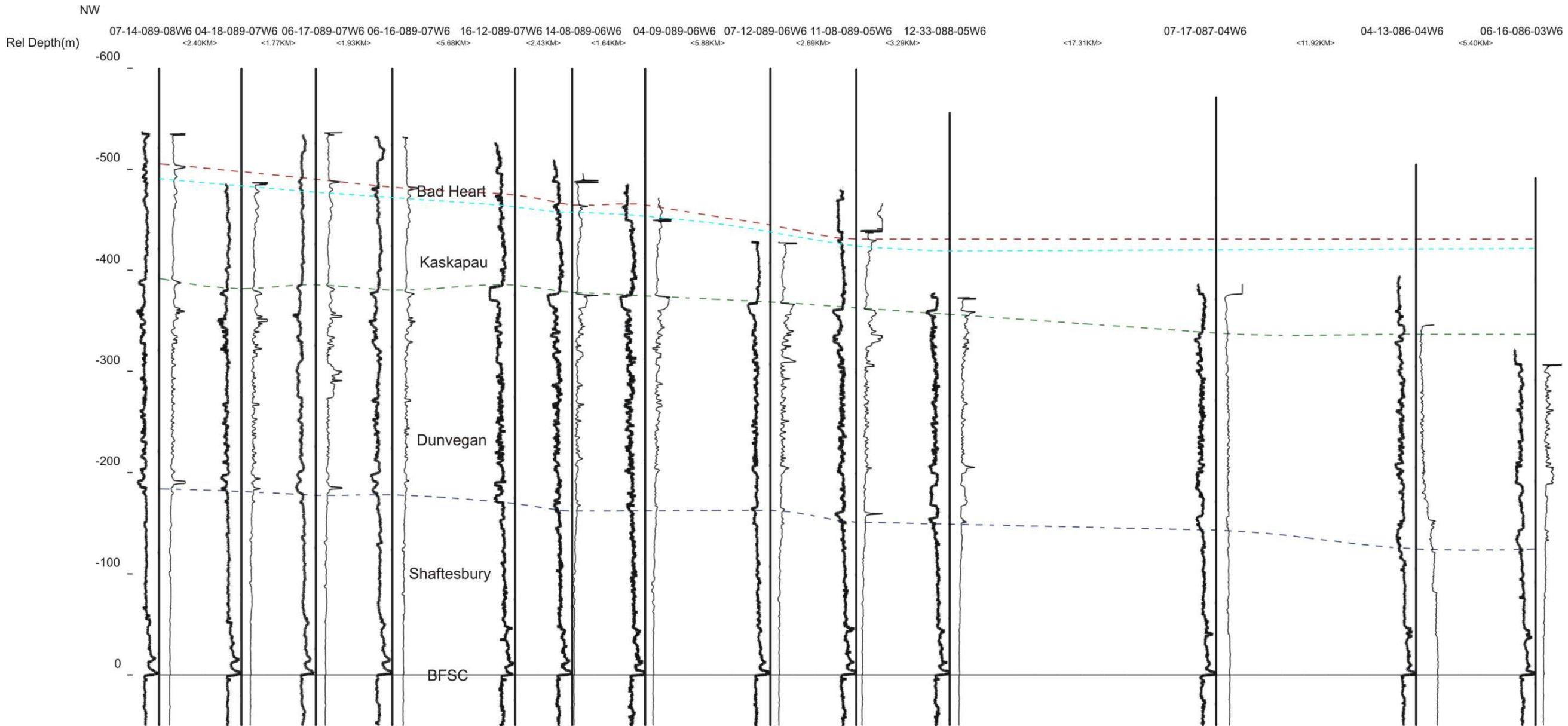


Figure 2.11 Well-log cross-section along line B-B'. The Base of Fish Scales (BFSC) is used as datum. The log to the left is gamma and to the right is resistivity. Both logs are not always available for every well

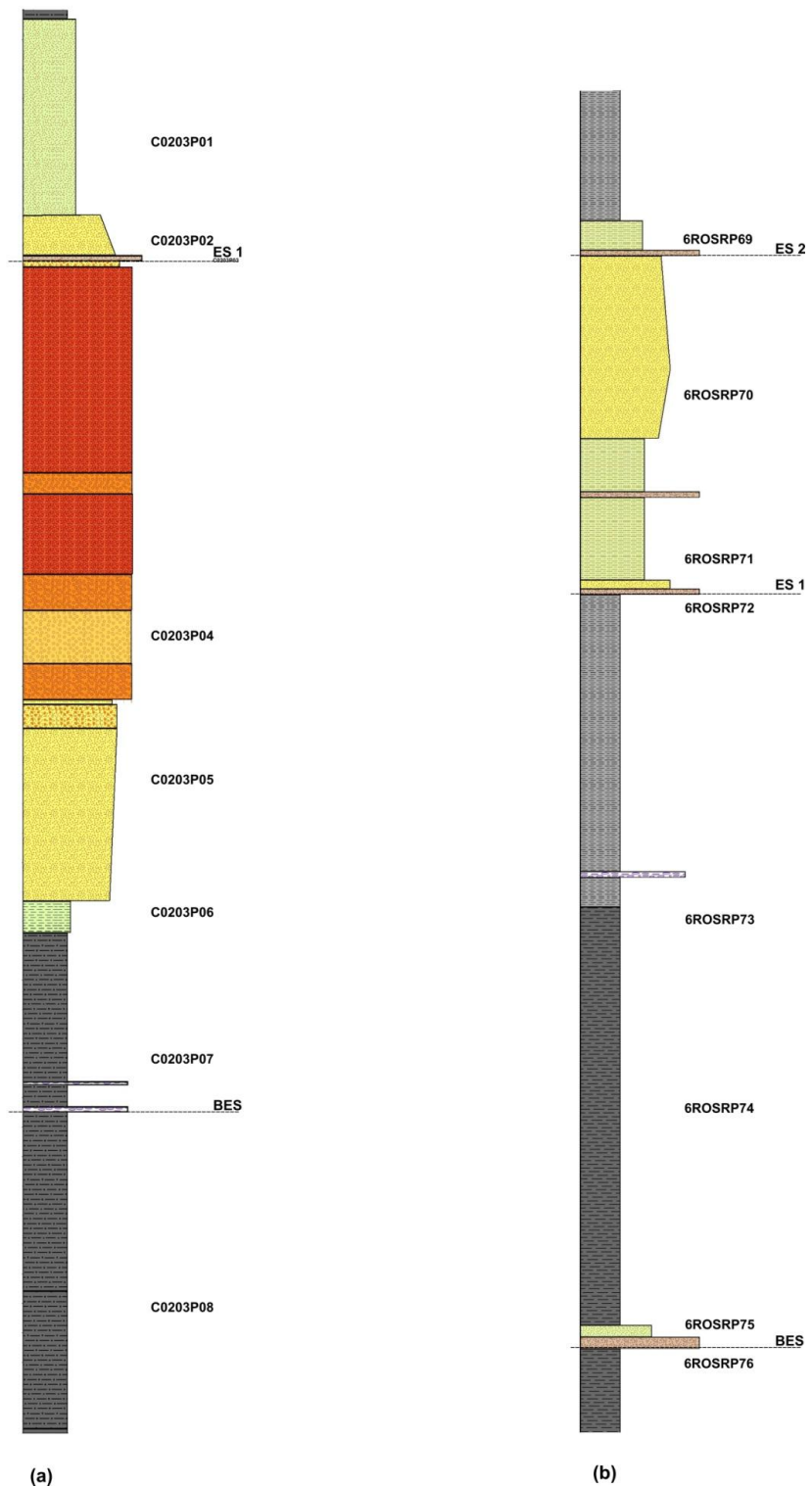


Figure 2.12 Measured stratigraphic section with selected palynology samples at (a) diamond drill core DDH0203, and (b) section ASR3

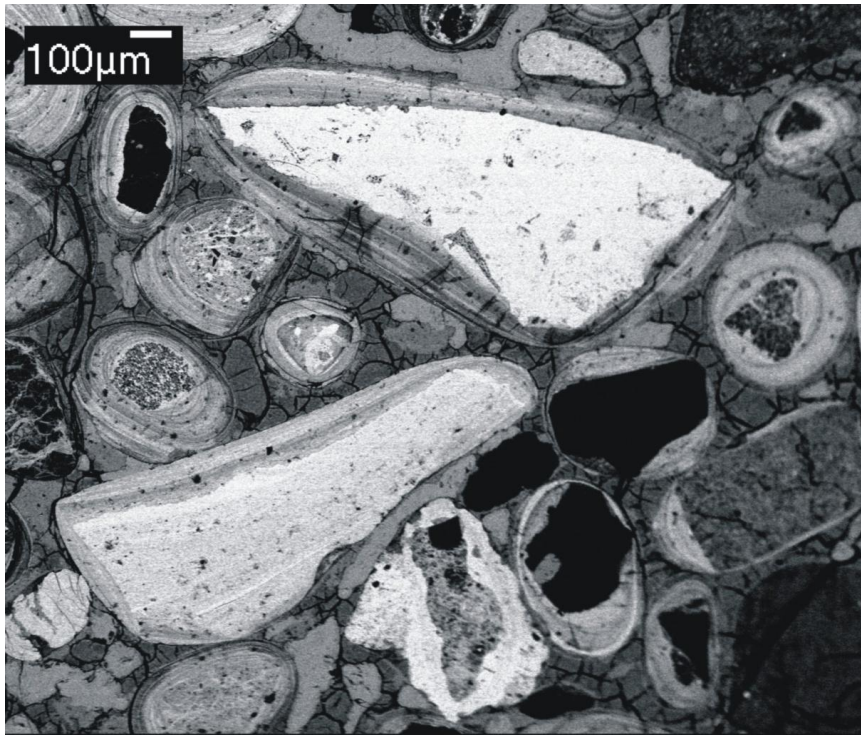


Figure 2.13 Pisoids from Bad Heart Formation at section ASR3 along Rambling Creek

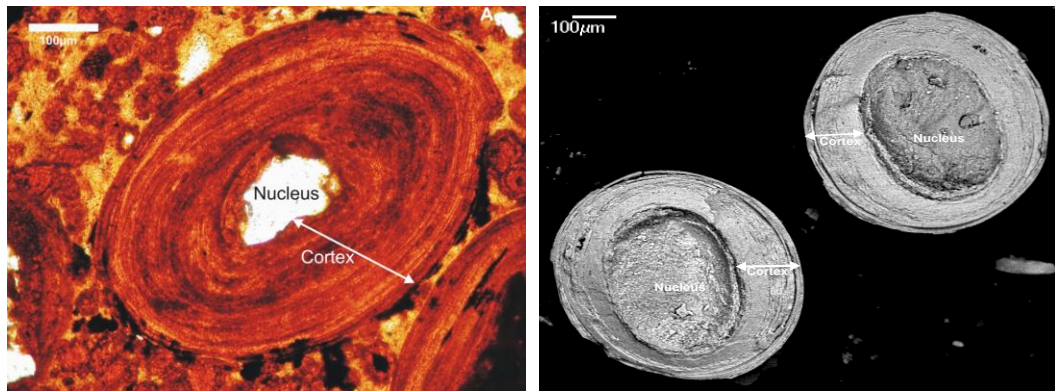


Figure 2.14 (A) Thin section view of ooids in plane polarized light; (B) SEM view of Iron ooids broken into two halves, both with a nucleus and cortex. The cortex is formed by stacking of many individual lamina

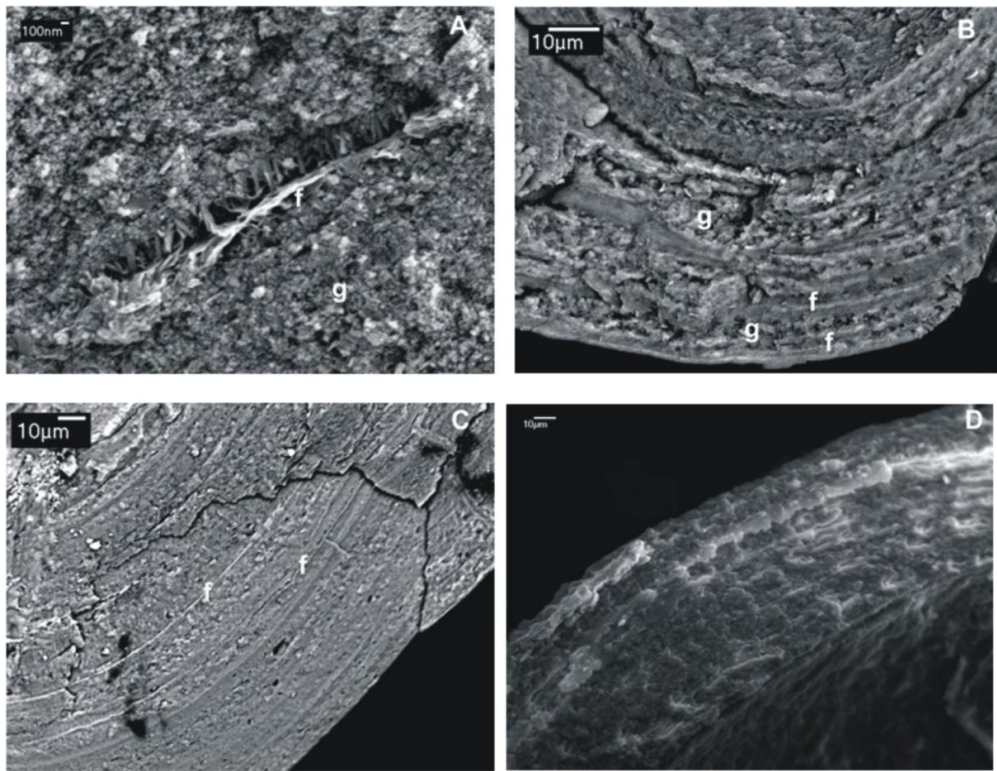


Figure 2.15 Internal morphology of ooids under SEM: (A) Detail nanostructure of lamina within an iron ooid cortex. The laminae are mainly composed of nanograins (g); (B) & (C) The flakes (f) are only observed on the outer rim of each lamina; (D) Backscattered image of ooid cortex with stacked lamina with coalesced flakes, platelets and nanograins

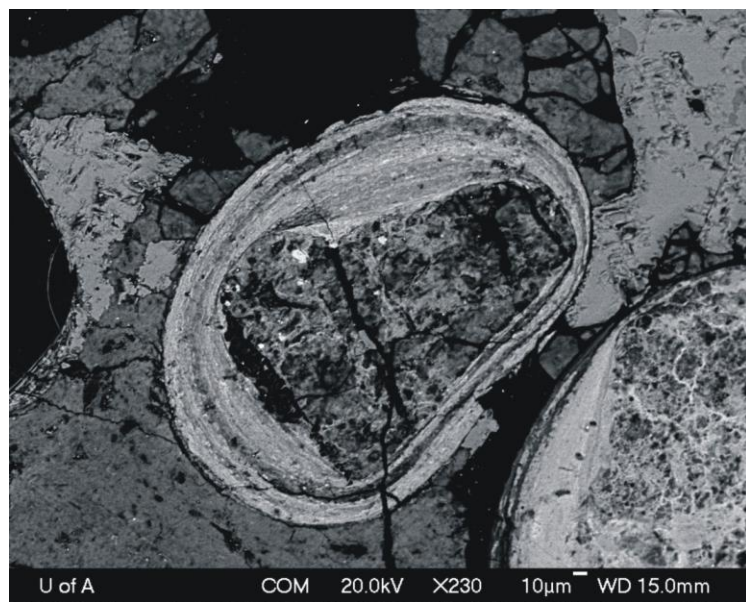


Figure 2.16 Postdepositional cracks in the ooids (Under SEM)

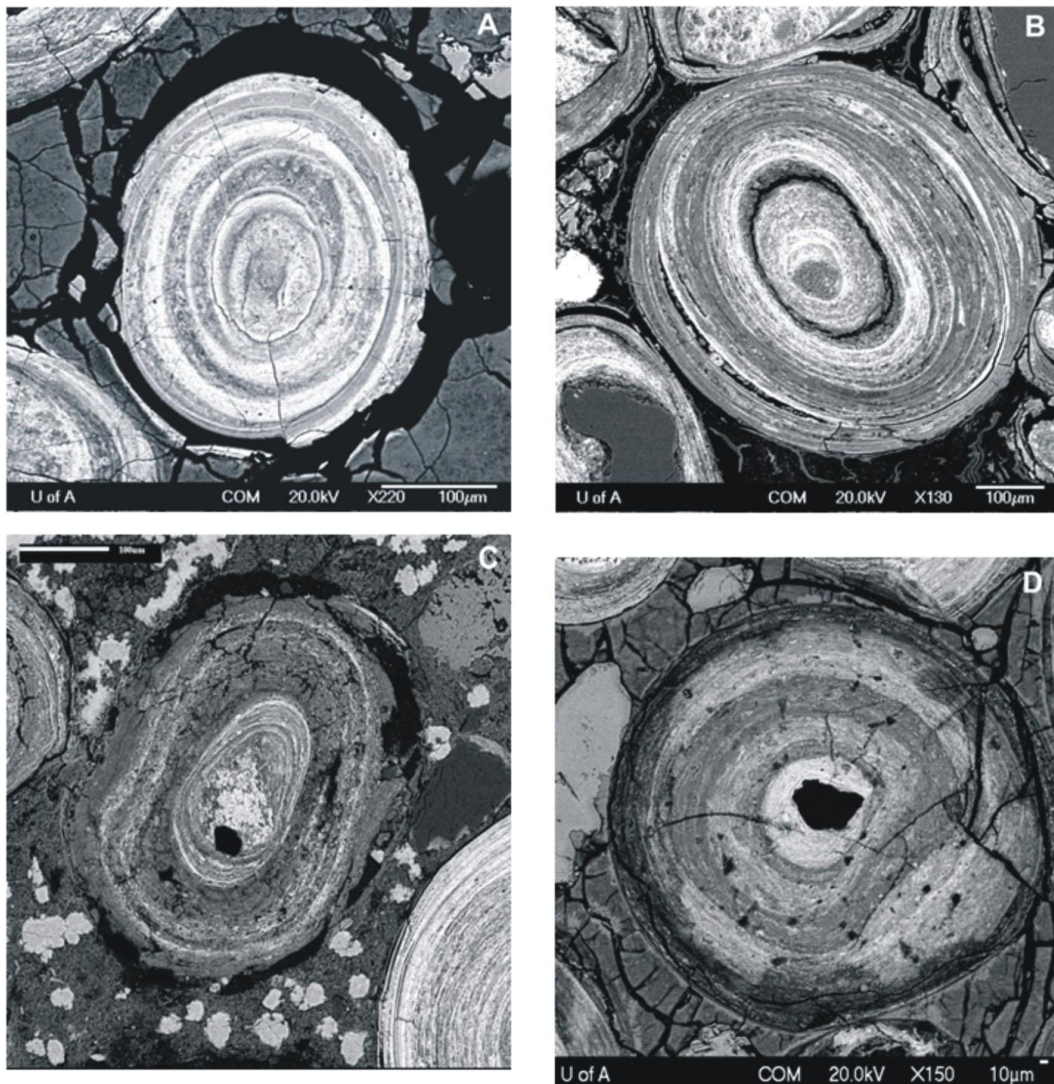


Figure 2.17 SEM of Bad Heart Type 1 iron ooids. (A) & (B) Typical Type 1 ooids from the Clear Hills region with well developed concentric laminations and a very small or not well defined nucleus. (C) Characteristics Type 1 ooid from the Smoky River region. (D) The cross cutting texture in this Type 1 ooid indicates a period of erosion before resumption of further growth (i.e., deposition of further concentric lamina) of the ooids cortex

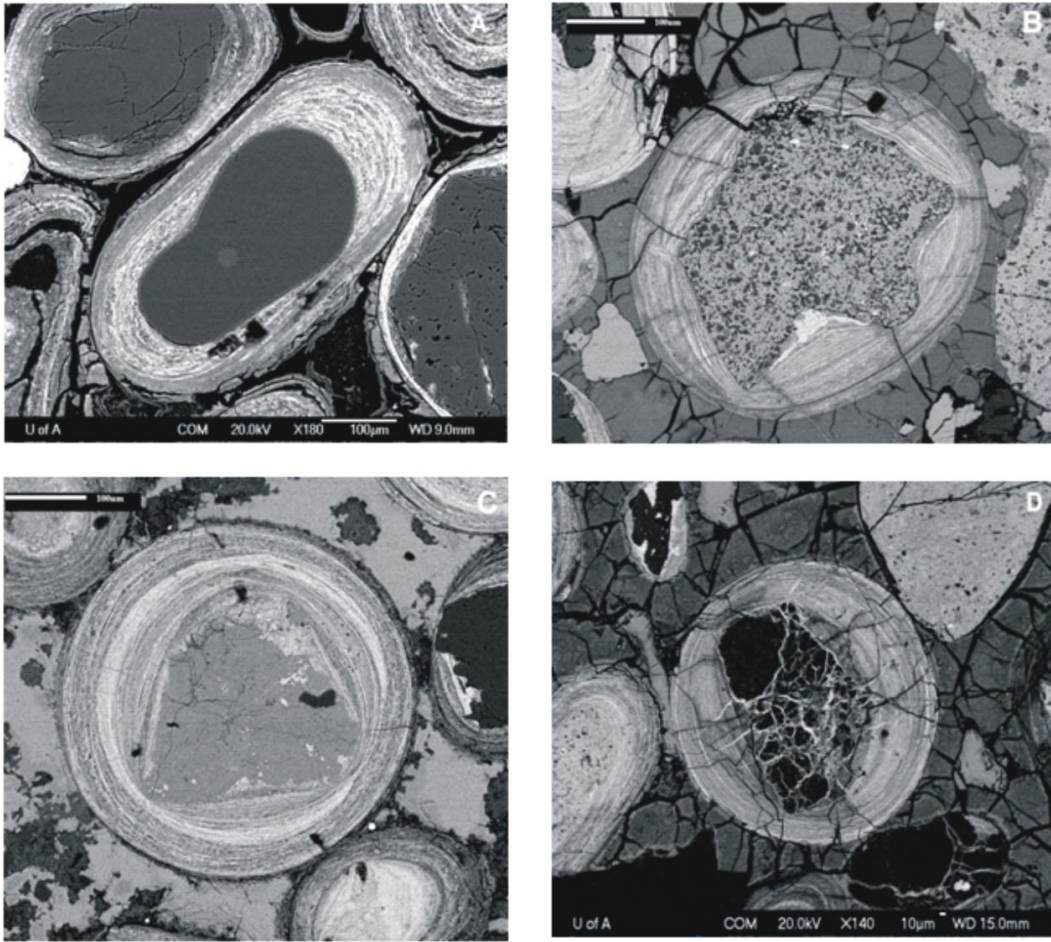


Figure 2.18 SEM Photographs of Type 2 ooids. (A) & (B) Typical Type 2 ooids from the Clear Hills region with a large nucleus and very thin concentric laminations comprising the cortex. (C) Characteristic Type 2 ooid from the Smoky River region. (D) Type 2 ooid with a quartz grain nucleus and with pervasive iron oxide veins

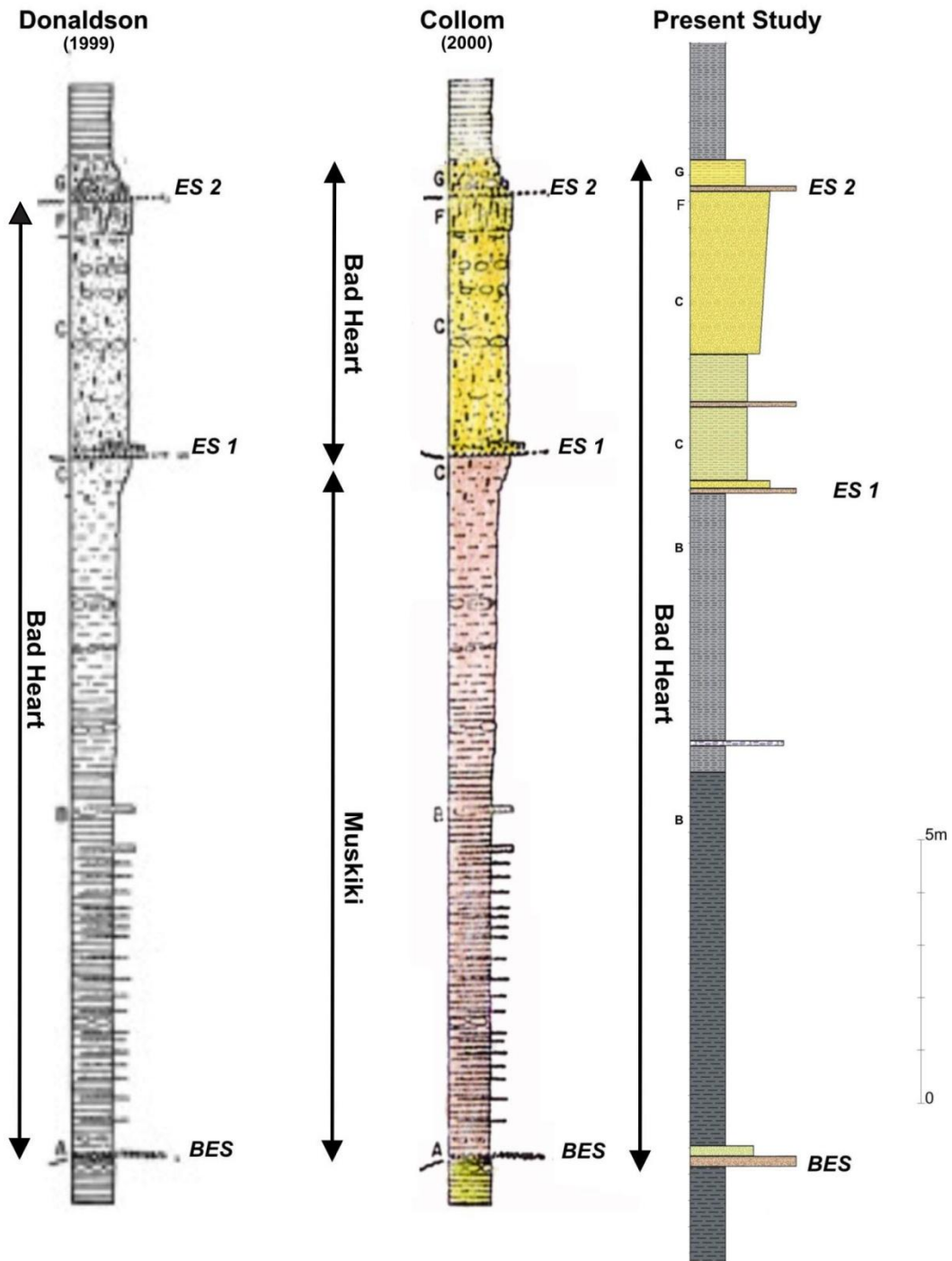


Figure 2.19 The extent of Bad Heart Formation defined from different studies

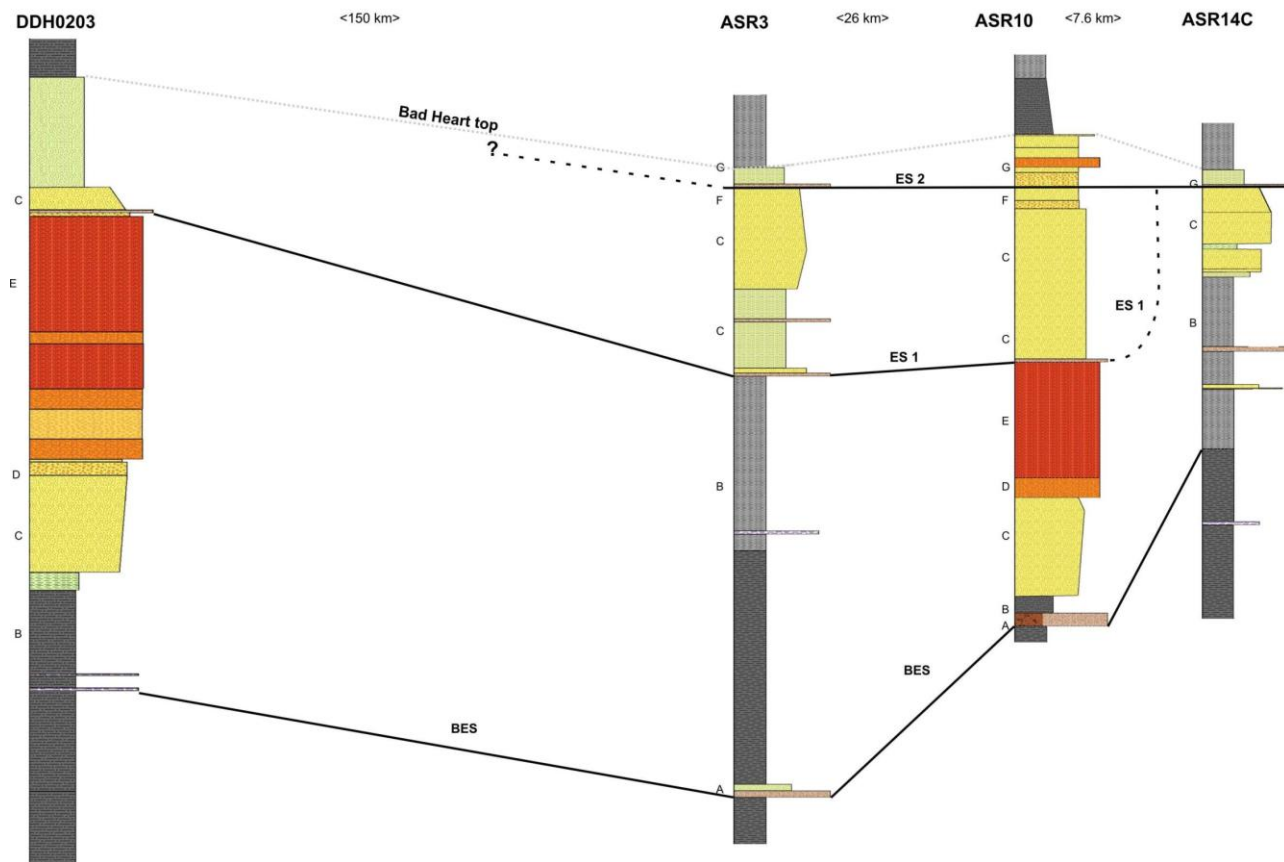


Figure 2.20 Schematic correlation diagram of Bad Heart Formation between the sections from the Smoky River and Clear Hills regions

## REFERENCES

Alberta Energy and Utilities Board. 2002. Table of Formations. Alberta Energy Resources Conservation Board, Calgary.

Bhattacharyya, D. P. and P. K. Kakimoto, 1982, Origin of ferriferous ooids; an SEM study of ironstone ooids and bauxite pisoids, *Journal of Sedimentary Petrology*, vol. 52, no. 3, p. 849-857.

Bhattacharyya, D. P. 1989. Concentrated and lean oolites: examples from the Nubia Formation at Aswan, Egypt, and significance of the oolite types in ironstone genesis. In: Phanerozoic ironstones. T.P. Young and W.E.G. Taylor(eds.). Geological Society, London, Special Publications. v. 46, p. 93-103.

Bhattacharya, J. and Walker, R. G. 1991. Allostratigraphic subdivision of the Upper Cretaceous Dunvegan, Shaftesbury, and Kaskapau formations in the northwestern Alberta subsurface. *Bulletin of Canadian Petroleum Geology*, v. 39 , p. 145-164.

Boyce, K. and Sweet, A. R. 2006. Applied Research Report on 40 Samples From the Smoky River and Clear Hills Area, West-Central Alberta (NTS 83M/09, 13, 15; 83N/12; 84D/07; 84E/09). Geological Survey of Canada, Report KJB-2006-01; ARS-2006-08, 15 p.

Boyce, K. and Sweet, A. R. 2007. Applied Research Report on 5 Core Samples From the Marum Drill Hole 9MMU006, North End of the Clear Hills, West-Central Alberta (NTS 84E/9; 57°39'16.00"N, 118°21'41.76"W). Geological Survey of Canada, Report KJB-2006-01 , 15 p.

Burkhalter, R. M. 1995. Oolitic ironstones and ferruginous microbialites: origin and relation to sequence stratigraphy (Aalenian and Bajocian, Swiss Jura Mountains). *Sedimentology*, v. 42, p. 57-74.

Chen, D. and Olson, R. A. 2007. Regional cross-sections and correlation of subsurface formations in the Clear Hills-Smoky River Region, northwestern Alberta. Alberta Geological Survey, Earth Science Reports 2007-07, 69 p.

Cobban, W. A. 1993. Diversity and distribution of Late Cretaceous ammonites, Western Interior, United States. In: Evolution of the Western Interior Basin. W.G.E. Caldwell and E.G. Kauffman (eds.). Geological Association of Canada, Special Paper , v. 39, p. 435-451.

Collom, C. J. 2001. Systematic paleontology, biostratigraphy, and paleoenvironmental analysis of the Wapiabi Formation and equivalents (upper cretaceous), Alberta and British Columbia, Western Canada .Unpublished Ph.D. thesis ,University of Calgary, Calgary, 817p.

Donaldson, W. S. 1997. The sedimentology, stratigraphy and diagenesis of the Upper Cretaceous Bad Heart Formation, NW Alberta. Ph.D. thesis, University of Western Ontario, London, Canada, 492p.

Donaldson, W. S., Plint, A. G. and Longstaffe, F. J. 1998. Basement tectonic control on distribution of the shallow marine Bad Heart Formation: Peace River Arch area, Northwest Alberta. *Bulletin of Canadian Petroleum Geology*, v. 46, p. 576-598.

Donaldson, W. S., Plint, A. G. and Longstaffe, F. J. 1999. Tectonic and eustatic control on deposition and preservation of Upper Cretaceous oolitic ironstone and associated facies: Peace River Arch area, NW Alberta, Canada. *Sedimentology*, v. 46, p. 1159-1182.

Gleddie, J. 1949. Upper Cretaceous in western Peace River Plains, Alberta. American Association of Petroleum Geologist Bulletin, v. 33, p. 511-532.

Green, R. and Mellon, G. B. 1962. Geology of the Chinchaga River and Clear Hills (north half) map-areas, Alberta. Alberta Research Council, Earth Science Reports 1962-08, 18p.

Hamilton, W. N. 1980. Clear Hills iron deposit geology, mineralogy and ore reserves. Alberta Research Council, Open File Report 1982-13, 43 p.

Hamilton,W.N., Price, M. C. and Langenberg, C. W. 1999. Geological map of Alberta. Alberta Geological Survey and Alberta Energy and Utilities Board.

Kimberley, M. M. 1979. Origin of oolitic iron formations. Journal of Sedimentary Petrology, v. 49, p. 111-131.

Leckie, D. A. and Singh, C. 1991. Estuarine deposits of the Albian Paddy Member (Peace River Formation) and lowermost Shaftesbury Formation, Alberta, Canada. Journal of Sedimentary Research, v. 61, p. 825-849.

Lenz, A. C., 1956, Oolitic iron ore, Clear Hills, Alberta. University of Alberta, Term Paper, 37p.

Macquaker, J. H. S., Taylor, K. G. Young, T. P. and Curtis, C. D. 1996. Sedimentological and geochemical controls on oolitic ironstone and "bone-bed" formation and some comments on their sequence-stratigraphical significance. In: Sequence stratigraphy in British geology. S.P. Hesselbo and D.N. Parkinson (eds.). Geological Society, London, Special Publications, v. 103, p. 97-107.

McLearn, F. H. 1919. Cretaceous, lower Smoky River, Alberta. Geological Survey of Canada, Summary Report, p. 1-7.

McLearn, F. H. 1926. New species from the Coloradoan of lower Smoky and lower Peace rivers, Alberta. Geological Survey of Canada, Bulletin v. 42, p. 117.

McLearn, F. H. and J. F. Henderson, 1944, Geology and oil prospects of Lone Mountain area, British Columbia, Geological Survey of Canada, Paper,44-2.

Mellon, G. B. 1962. Petrology of Upper Cretaceous oolitic iron-rich rocks from northern Alberta, Economic Geology and the Bulletin of the Society of Economic Geologists, v. 57, p. 921-940.

O'Connell, S. C., Dix, G. R. and Barclay, J. E. 1990. The origin, history, and regional structural development of the Peace River Arch, Western Canada. In: Geology of the Peace River Arch. S.C. O'Connell and J.S. Bell (eds.). Bulletin of Canadian Petroleum Geology, v. 38A, p. 4-24.

Olson, R. A., Weiss, J. A. and Alesi, E. J. 2006. Digital compilation of oolitic ironstone and coal data, Clear Hills - Smoky River region, northwestern Alberta]. Alberta Energy and Utilities Board, Alberta Geological Survey,Geo-Note 2005-05, 2 CD-ROM.

Plint, A. G., Norris, B. and Donaldson, W. S. 1990. Revised definitions for the Upper Cretaceous Bad Heart Formation and associated units in the foothills and plains of Alberta and British Columbia. Bulletin of Canadian Petroleum Geology, v. 38, p. 78-88.

Rohrlich, V., 1974, Microstructure and microchemistry of iron ooliths, Mineralium Deposita, vol. 9, no. 2, p. 133-142.

Siddaiah,N.S., 2008, Berthierine-rich oolitic ironstone from the Late Paleocene\_middle Eocene Subathu Formation, Dogadda area, NW Himalaya and its stratigraphic significance, Current Science, vol. 94, p. 123-127.

Stott, D. F. 1967. The Cretaceous Smoky Group, Rocky Mountain foothills, Alberta and British Columbia. Geological Survey of Canada, Bulletin,v.132. 133 p.

Sturesson, U., Heikoop, J. M. and Risk, M. J. 2000. Modern and Palaeozoic iron ooids; a similar volcanic origin. *Sedimentary Geology*, v. 136, p. 137-146.

Sweet, A.R., 2009. Applied research report summarizing the palynofacies for 47 core and outcrop samples from the southern Clear Hills, Rambling River area (NTS84D/15) and along the Smoky River (NTS83M/09 and 83N/12). Geological Survey of Canada, Paleontological Report ARS-2009-12, 15 p.

Taylor, K. G. and Curtis, C. D. 1995. Stability and facies association of early diagenetic mineral assemblages; an example from a Jurassic ironstone-mudstone succession, U.K. *Journal of Sedimentary Research, Section A: Sedimentary Petrology and Processes*, v. 65, p. 358-368.

Taylor, K. G., Simo, J. A., Yocom, D. and Leckie, D. A. 2002. Stratigraphic significance of oolitic ironstones from the Cretaceous Western Interior Seaway: the Peace River Formation, Alberta, Canada, and the Castlegate Sandstone, Utah, U.S.A. *Journal of Sedimentary Research*, v. 72, p. 316-327.

Tucker,M.E.,1981, *Sedimentary petrology: an introduction*,John Wiley & Sons, 252p.

Varban, B.L. and Plint, A. G. 2005. Allostratigraphy of the Kaskapau Formation (Cenomanian-Turonian) in the subsurface and outcrop, NE British Columbia and NW Alberta, Western Canada Foreland Basin; *Bulletin of Canadian Petroleum Geology*, vol. 53, no. 4, p. 357-389.

Wallace-Dudley, K. and D. Leckie, 1993, The lower Kaskapau Formation (Cenomanian); a multiple-frequency, retrogradational shelf system, Alberta, Canada, AAPG Bulletin, vol. 77, no. 3, p. 414-435.

Young, T. P. 1989. Phanerozoic ironstones :an introduction and review. In: Phanerozoic Ironstones . T.P. Young and W.E.G. Taylor(eds.). Geological Society, London, Special Publications, v. 46, p ix- xxv.

## **CHAPTER 3: GEOCHEMISTRY OF OOLITIC IRONSTONE, BAD HEART FORMATION, NORTHWESTERN ALBERTA**

### **INTRODUCTION**

Oolitic ironstones are sedimentary rocks with greater than 15% iron (equivalent to >21.4 wt% Fe<sub>2</sub>O<sub>3</sub>) and with >5 vol% ooids (Young, 1989; Petranek and Van Houten, 1997).

Oolitic ironstones exist worldwide and are found throughout much of the Earth's stratigraphic record, from the Precambrian to the present (Pedro et al., 1978; Kimberley, 1979; Heikoop et al., 1996; Petranek and Van Houten, 1997); however, they formed most commonly during the Phanerozoic (Petranek and Van Houten, 1997). In North America, for example, there are some 55 reported oolitic ironstone deposits in Phanerozoic strata (Van Houten, 1990). They have distinct mineral compositions, typically being composed of one or more of berthierine (Fe-rich serpentine), nontronite (Fe-rich montmorillonite clay), chamosite (Fe-rich chlorite), siderite, goethite, and hematite. Globally, Proterozoic oolitic ironstones typically have hematite as the dominant iron oxide, whereas Mesozoic and Paleozoic oolitic ironstones have goethite as the principal iron oxide (Kimberley, 1989).

The geology and genesis of oolitic ironstones have been the subject of research by both sedimentologists and economic geologists for the last two centuries. Numerous studies have been carried out on selected Phanerozoic oolitic ironstone deposits from different parts of the world, and this work has generated various interpretations as to their genesis; these include forming solely by sedimentary (Taylor and Curtis, 1995), volcanic-hydrothermal (Kimberly, 1989), or biogenic (Dahanayake and Krumbein, 1986) processes. Controversy continues regarding how the ooids were formed and especially the source of iron. This lack of agreement may be at least partly due to the wide range of depositional environments in which iron ooids are thought to be formed; these include, for example, (1) shallow marine (Maynard, 1986; Taylor et al., 2002; Macquaker et al., 1996; Sturesson et al., 2000; Donaldson et al., 1999); (2) calm, but occasionally agitated offshore transition marine (Gygi, 1981; Burkhalter, 1995); (3) restricted lagoonal marine

(Bayer, 1989); (4) coastal and deltaic settings (James and Van Houten, 1979); and even (5) continental non-marine (Siehl and Thein, 1989). Modern iron ooids have also been reported to be forming in a shallow marine environment offshore of an active volcanic island in Indonesia (Heikoop et al., 1996; Sturesson et al., 2000).

As a result of these different interpretations of genesis, three questions need to be assessed when considering the genesis of oolitic ironstones: (1) why are these rocks iron-rich? (2) why do they typically have specific silicate mineralogies? and (3) what environment(s) facilitate the development of the oolitic texture ?(Young, 1989).There are two major hypotheses regarding the source for the iron in oolitic ironstones: one hypothesis suggests the iron-enrichment can occur from normal sedimentary processes, such as weathering (Van Houten and Arthur, 1989; Young, 1989; Burkhalter, 1995; Macquaker et al., 1996); whereas the other proposal is that iron-enriched sea water results from hydrothermal and/or volcanic activity (Kimberley, 1979; Sturesson et al., 2000).

Oolitic ironstone is rare but not uncommon within the Western Canada Sedimentary Basin (WCSB; Leckie et al., 1991; Taylor et al., 2002). Nonetheless, the Late Cretaceous (Coniacian) Bad Heart Formation is a rather unique unit due to the areally extensive (~150 km), up to about 10 m thick, and potential economically important oolitic ironstones within it. Although the Bad Heart Formation is a relatively thin unit, generally being less than about 15 m thick, it is estimated to contain about 1.1 billion tonnes of oolitic ironstone in the Clear Hills region with an average grade of 34 wt% iron (Hamilton, 1980). The Bad Heart Formation crops out in northwestern Alberta in the southern and southeastern parts of the Clear Hills, to the south along Smoky River, and in the Spirit River to Birch Hills areas Figure (3.1).

## **DATABASE**

Between 2004 and 2007, the Bad Heart Formation was examined at 39 natural outcrops and 7 shallow trenches, which were either mechanically or hand excavated, in the Clear Hills and Smoky River regions (Kafle, 2009). At each locale, the stratigraphy was geologically mapped in detail, and 325 samples were collected (including duplicates) for geochemical analysis. The majority of the samples were rock chips collected systematically across the oolitic ironstones and immediately adjacent horizons; typically, the sampled interval was 0.5 m where possible, or a little smaller or larger as changes in lithology thickness varied. Out of this total, the analytical results from 215 samples from selected locations, where a complete or near complete Bad Heart section exists, are tabulated in Appendix II; this appendix provides specific sample locations, and the laboratory measured elemental and oxide concentrations in each sample. The complete set of analytical data for all the samples collected during this study has been published by the Alberta Geological Survey (Kafle, 2009).

## **PREVIOUS WORK**

Colborne (1958) was the first to undertake a detailed mineralogical and petrographic study of the Bad Heart Formation ironstone; he also compared the mineralogy of the Clear Hills ironstones to that of similar sedimentary iron deposits in Europe and the United States of America. Subsequently, Green and Mellon (1962) geologically mapped the Chinchaga and Clear Hills region at 1:250,000 scale, and Mellon (1962) did detailed petrographic and X-ray diffraction studies of oolitic ironstone from the Rambling Creek locale. The geochemistry and petrography of the Bad Heart Formation was then further studied and described in detail by Petruk (1977) and Petruk et al. (1977a, b); however, these studies were limited to the samples collected at a test pit excavated along the west side of Rambling Creek near the best exposed natural outcrop (Hamilton, 1980).

Donaldson (1997) studied the stable isotope and mineral chemistry of early diagenetic

cements to evaluate the effects of relative sea level fall, exposure, and consequent meteoric influx during the deposition of the Bad Heart Formation. Olson et al. (1999), in cooperation with the Alberta Geological Survey, conducted a preliminary study of the potential co-product trace elements within the oolitic ironstone of the Bad Heart Formation from a small set of samples from the Clear Hills region, mainly from archived samples from the Rambling Creek pit, the Worsley pit area, and a few samples from the Smoky River

## **GEOLOGICAL SETTING**

The Late Cretaceous (late Coniacian) Bad Heart Formation is a thin (generally a maximum of 10 to 15 m thick) coarser clastic unit between the shale of the underlying Kaskapau-Muskiki and overlying Puskwaskau formations. The Bad Heart Formation is a shallow water marine sequence of fine- to medium-grained siltstone and sandstone, with common oolitic ironstone interbeds and local conglomerate interlayers deposited below the wave base in a deeper water marine environment.

Donaldson (1997) suggested that the Bad Heart Formation consists of two upward coarsening sequences (allomembers) of sandstone, siltstone and, locally, mudstone , bounded by three regionally mappable erosional surfaces: (1) a Basal Erosion Surface (BES), which marks the base of the Bad Heart Formation and is a regional unconformity surface; (2) Erosion Surface 1 (ES1), which is at the top of the lower Bad Heart sequence, and (3) Erosion Surface 2 (ES2), which lies at the top of the upper Bad Heart sequence Donaldson et al. (1999) subdivided the Bad Heart Formation into seven facies that, from top to base, comprise

Facies G: Interbedded oolitic and non-oolitic muddy sandstone;

Facies F: Locally stratified sandstone with Skolithos ichnofossils;

Facies E: Oolitic Ironstone;

Facies D: Green oolitic sandstone with Thalassinoides ichnofossils;

Facies C: Bioturbated sandstone;

Facies B: Laminated Mudstone; and

Facies A: Pebble Conglomerate.

The current study, in general, confirmed that the above lithological facies are common within the Bad Heart Formation in both the Smoky River and Clear Hills regions.

## METHODOLOGY

The Lithogeochemical sampling for this study involved: (1) cleaning the surface debris (from the downslope crept material) at each Bad Heart Formation section; (2) geological mapping of the exposed section, typically at 1:50 scale; and finally (3) collecting a systematic series of rock chip samples across the sampled interval. In general, a specific chip sample comprised a constant volume or, where feasible, a constant weight of chipped sub-samples at systematic intervals (normally a maximum of about 5 to 10 cm) across a total sample width of about 0.5 m for lithologically similar material.

The geochemical whole rock analysis of the 325 predominantly rock chip samples collected during this study, with more than 50% of these samples being oolitic ironstone and the rest being from other rock types from within or immediately adjacent to the Bad Heart Formation, was done at Acme Analytical Laboratory, Vancouver. The analytical method was inductively coupled plasma mass spectrometry (ICP-MS) multi-element analysis. Standards were inserted into the sample set by AGS before shipping, and lab standards also were inserted by Acme into the analytical stream. Duplicate analyses were performed on 21 sample splits to evaluate the precision of the measurements. Appendix III includes the comparative results from the 21 duplicate sample pairs and average relative percent difference (RPD) values, which is a measure for analytical

precision (Ziegler and Combs, 1997) for each element and oxide. A lower RPD value indicates a higher level of precision. Appendix IV presents the comparative results from the standard samples inserted in the analytical stream. The Acme results were fairly accurate based on their analysis of the standards.

## RESULTS

### ***Oolitic Ironstone Mineralogy***

Petrographic observations (chapter 2) on samples of the Bad Heart oolitic ironstones indicate that they are texturally similar to other Minette-type ironstone deposits such as the Ordovician Bell Island oolitic iron ores in Newfoundland (Gross, 1996), the Silurian Clinton oolitic iron ores near Birmingham, Alabama (Simpson and Gray; 1968), the Jurassic Alsace-Lorraine oolitic iron ores in France (Bubenicek, 1968; Teyssen, 1989), and some other oolitic ironstones found elsewhere in the world (e.g., see Young and Taylor, 1989).

In the present study, oolitic ironstones are grouped into three subtypes based on the visually estimated percentage content of ooids: (1) intensely oolitic ironstone (IOIS) in which iron ooids are >70 volume per cent (vol.%), (2) moderately oolitic ironstone (MOIS) in which the ooid content ranges from <70 to  $\geq$ 30 vol.%, and (3) weakly oolitic ironstone (WOIS) in which the ooid content is from <30 to  $\geq$ 10 vol.%. Finally, in addition to these ironstone subtypes, Bad Heart Formation clastic rocks with <10 to  $\geq$ 1 vol.% ooids are defined as oolitic sandstone (OS). This visually estimated classification was established for detailed geological mapping of stratigraphic sections in the field, and also helped in examining the geochemical relationships between the various litho-units and individual samples from the Smoky River and Clear Hills regions.

The mineral composition of unweathered Bad Heart Formation ooids is typically nontronite, chamosite, siderite, quartz, and amorphous phosphate, whereas the matrix is mostly chamositic clay, ferruginous opal, or other detrital grains. However, where the Bad

Heart Formation is weathered, which it is at most of the sections mapped and sampled during this study, the iron-bearing silicate minerals have commonly been altered to goethite or limonite. Ferruginous opal is the main constituent of the matrix in the ooids from the Clear Hills Region. In thin section, the opal is pale yellow and isotropic; it absorbs water in water-saturated or humid conditions, but expels the absorbed water while drying, causing shrinkage cracks (Petruck, 1977).

According to Petruck (1977), nearly all the iron in nontronite in the unweathered or fresh lower part of the thick oolitic ironstone at Rambling Creek is ferrous ( $\text{Fe}^{2+}$ ), but on atmospheric exposure, it is progressively oxidized to the ferric ( $\text{Fe}^{3+}$ ) state. Goethite-rich ooids are dominant in the upper part of the Rambling Creek section whereas nontronite-rich ooids are dominant in the lower part. This change in iron-bearing minerals down-section is also evident from the change in colour in the outcrop at section ARR3 along Rambling Creek where the goethite-dominated ooids in the upper part are weathered to a deep orange-brown colour, whereas in the bottom part the nontronite-rich ooids are weathered to rusty greenish grey to black. The difference between the oxidized (orange-brown) goethite ooids at the top of the ARR3 section and the more reduced (rusty greenish-grey) nontronite-rich ooids in the lower part of this section, indicates either that the upper part of the section is more oxidized simply due to Recent surfacial weathering conditions that may have reached a depth of only a few meters below the top of the section, or a different depositional environment for the lower versus upper ooids at the Rambling Creek location.

Pyrite is rare to very rare in the Bad Heart Formation oolitic ironstone, and this indicates that sulfate reduction to sulfide was negligible during ironstone formation. The reported presence of pyrite by Collom (2001) in-place in the uppermost Bad Heart Formation at the 'Holotype Bench' section about 2.0 km north of the confluence of the Smoky River and Puskawaskau River is incorrect; that is, the pyrite at this location essentially exists as loose fragments sitting on the uppermost Bad Heart Formation cliff-forming sandstone exposed in the bed of the Smoky River, and thus the pyrite is placer material derived

from the overlying formations, probably the immediately overlying Puskawaskau Formation.

### ***Geochemistry***

The geochemical data for each element analyzed in this study were initially evaluated in the following ways: first, a histogram was constructed for each element to assess the underlying fundamental geochemical distribution, and then the Arithmetic Average and Median were calculated for IOIS, MOIS, and WOIS for selected sections in order to compare and contrast them. A summary of the analyses of the major, trace, and rare earth elements of the Bad Heart ooids from selected sections from the Clear Hills and Smoky River regions is presented in Tables 3.1A to 3.1D for each of the IOIS, MOIS, WOIS, and all oolitic ironstone litho-units respectively. Table 3.2 provides a summary of the underlying geochemical distribution pattern for selected elements.

Prior geochemical work by Olson et al. (1999) on selected samples from the Bad Heart Formation indicated that oolitic ironstone contains an elevated concentration (compared with Clarke's value) of some elements, such as antimony (<8 to 75 ppm), vanadium (<800 to 1,633 ppm), arsenic (<150 to 1,000 ppm), zinc (<300 to 808 ppm), and manganese (<500 to 1,661 ppm), whereas some other elements, such as aluminum and potassium, have lower concentrations.

The geochemical results from this study (Table 3.1 and Figure 3.2) show that Bad Heart Formation oolitic ironstone has very high to elevated concentrations (relative to other rocks in Bad Heart Formation) of some major oxides and also several trace elements (Table 3.3). Figures 3.2 and 3.3 show the concentration of oxides and some trace elements along a typical Bad Heart outcrop at section ASR9A in the Smoky River region, and at section ARR3 in the Clear Hills region. These figures, plus the data in Table 3.3,

show a clear correlation between the abundance of ooids and the concentration or depletion of certain major oxides and minor elements; for example, the oolitic ironstones clearly have elevated  $\text{Fe}_2\text{O}_3$ ,  $\text{CaO}$ ,  $\text{Mn}$ , and  $\text{V}$ , but lesser  $\text{SiO}_2$ , and possibly also lower amounts of  $\text{Al}_2\text{O}_3$  and  $\text{TiO}_2$ . In general, these elemental concentration trends are similar to those of the Late Cretaceous oolitic ironstones in other parts of the world (e.g., Aswan, Egypt, as reported in Bhattacharyya, 1981).

The variation in the concentration of various oxides in oolitic ironstone from the upper part of the Bad Heart Formation ooids to the lower part, just below the ES1 erosional surface, is similar in both the Clear Hills and Smoky River regions; that is, the oolitic ironstone shows an increase in the amount of  $\text{Fe}_2\text{O}_3$  and  $\text{P}_2\text{O}_5$ , and a decrease in  $\text{SiO}_2$ ,  $\text{Al}_2\text{O}_3$ ,  $\text{MgO}$ , and  $\text{TiO}_2$  from the lower to the upper part in the thick oolitic ironstone sequence below the ES1 surface.

These stratigraphic-related trends in selected elements are further supported by simple X-Y plots (Figure 3.4), which demonstrate that oolitic ironstone from the Bad Heart Formation shows a positive correlation between  $\text{SiO}_2$  and  $\text{Al}_2\text{O}_3$  (Figure 3.4a) and  $\text{Fe}_2\text{O}_3$  and  $\text{P}_2\text{O}_5$  (Figure 3.4b), and a negative correlation between  $\text{SiO}_2$  and  $\text{Fe}_2\text{O}_3$  (Figure 3.4c) and  $\text{Al}_2\text{O}_3$  and  $\text{Fe}_2\text{O}_3$  (Figure 3.4d). The negative correlation of  $\text{Fe}_2\text{O}_3$  with both  $\text{SiO}_2$  and  $\text{Al}_2\text{O}_3$  reflects the decreased deposition of both detrital quartz grains and colloidal silica in the matrix, and fine-grained detrital clay minerals, which is similar to the situation in the Sardinia oolitic ironstones reported by Franceschelli et al. (2000). Furthermore, because  $\text{TiO}_2$ ,  $\text{MgO}$ ,  $\text{Zr}$ , and  $\text{Th}$  all show strong positive correlations with  $\text{Al}_2\text{O}_3$ , this indicates that these components are primarily derived from fine-grained detrital minerals.

With respect to the trace elements present within Bad Heart oolitic ironstone, there are anomalously high concentration of manganese, vanadium, and zinc relative to other rock types from the Bad Heart Formation, in that order of abundance (Table 3.3). The average Mn concentration in the oolitic ironstone in the Clear Hills and Smoky River regions is about 1,073 ppm (median is 1,022 ppm) and locally reaches up to 2,684 ppm, whereas the non-oolitic parts of the Bad Heart Formation typically contain only about 621 ppm Mn

(median 471 ppm). The average V concentration in oolitic ironstone is 1,266 ppm (median is 1,279 ppm) and locally reaches up to 2,476 ppm, versus about 508 ppm in the non-oolitic parts of the Bad Heart Formation. In comparison, the average V concentration in the Middle to Late Cretaceous shales in northern Alberta is reported to be 118 ppm (Dufresne et al., 2001), and the Clarke values for crustal shale and sandstone are 130 and 20 ppm V, respectively (Turekian and Wedepohl, 1961). The average Zn concentration in the oolitic ironstone in the Clear Hills and Smoky River regions is about 581 ppm and locally reaches up to 1,040 ppm, whereas the non-oolitic parts of the Bad Heart Formation contain about 255 ppm. The average Zn content for Late Cretaceous shale in northern Alberta is 102 ppm (Dufresne et al., 2001), and the Clarke value for Zn in crustal shale is about 95 ppm and for sandstone is about 16 ppm (Turekian and Wedepohl, 1961). Although the barium content in the Bad Heart Formation is also elevated (compared with Clarke's value), Figure 3.3 shows that barium is typically no more elevated in oolitic ironstone than in the adjacent other parts of the Bad Heart Formation. Finally, anomalously elevated gold contents have been reported in the Bad Heart Formation (Boulay, 1995), but the gold results from this study were all low, with the highest result being 2.4 ppb Au.

### ***Rare Earth Elements***

McLennan (1989) suggested that the patterns exhibited by the rare earth elements (REE) in siliciclastic sedimentary rocks can be used to identify their source rocks because REE are transferred largely in detrital grains during the erosion and deposition of the ensuing sediments. The fraction of REE carried in solution during this erosion-sediment deposition process is very small, and is considered not to complicate the provenance/sediment REE relationship. As a result, the shale-normalized REE contents of sediments or sedimentary minerals can indicate whether or not the sedimentary deposit has typical sedimentary REE contents, and also identify subtle enrichment or deficiencies of single or a group of REE (Fleet, 1984).

Figures 3.5 to 3.7 show a comparison between the REE in the Bad Heart Formation ooids and oolitic ironstones from around the world, using either the chondrite normalized (Haskin et al., 1966) or North American Shale Composite (NASC; Gromet et al., 1984) REE patterns. In Figure 3.5, the chondrite normalized REE pattern in most Bad Heart oolitic ironstone samples is consistent with oolitic ironstones from Egypt, as reported by Bhattacharyya (1981) and Italy , being characterized by relative enrichment in the LREE (i.e., La, Ce, Pr & Nd), a negative Eu anomaly . In Figure 3.6, using the NASC normalized REE pattern, the Bad Heart ooids in comparison to the world oolitic ironstone (using data from Bhattacharyya, 1981; Sturesson, 1995; Sturesson et al., 2000; and Franceschelli et al., 2000) are characterized by a weakly upward convex shape with depleted LREE (La to Nd), a slightly depleted HREE (Ho to Lu), but a clear enrichment in intermediate REE from Sm to Tb with peak values at Gd and Tb. The data from this study show that samples with the highest phosphate contents contain the highest chondrite normalized REE, but also the most negative Eu anomaly.

The Bad Heart ooids show a somewhat higher total REE content than the sandstone and shale within the Bad Heart Formation (Table 3.4). Specifically, Facies G and Facies E (which are mainly IOIS, MOIS and WOIS) have a higher REE content compared to Facies C, D and F, which are dominantly sandstone, siltstone and, to a lesser extent, weakly oolitic sandstone (OS).

In general, most of the other sedimentary units of the Cretaceous age in Northern Alberta (Dufresne et al., 2001) yield a very similar REE enrichment pattern relative to chondritic values as follows: moderate enrichment of the LREE ( $\text{La/Sm} = 3.55$ ), moderately depleted Eu ( $\text{Eu/Eu}^* = 0.84$ ), and a relatively flat HREE profile ( $\text{Tb/Yb} = 1.62$ ). In contrast, the Bad Heart Formation oolitic ironstones exhibit only a slight enrichment in LREE ( $\text{La/Sm}=1.48$ ), a moderate negative Eu anomaly ( $\text{Eu/Eu}^*=0.72$ ) and an enhanced HREE profile ( $\text{Tb/Yb} = 2.55$ ). Further, the Cretaceous bentonites from northern Alberta (Eccles et al., 2008) (Figure 3.7) show a different REE pattern from that

exhibited by the Bad Heart Formation oolitic ironstone. Finally, the Bad Heart oolitic ironstone geochemical data from this study show the LREE (La to Sm) have a strong positive correlation between  $\text{Al}_2\text{O}_3$  and  $\text{TiO}_2$ , whereas the HREE (Eu to Lu) show a positive correlation with  $\text{P}_2\text{O}_5$ .

In summary, the Cretaceous sedimentary rocks in general in northern Alberta show enriched LREE patterns relative to HREE on chondrite-normalized diagrams, and a clear negative Eu anomaly, whereas the Bad Heart ooids show a clear negative EU anomaly, a slight enrichment in LREE, and an enriched HREE profile.

## DISCUSSION

Whether the Bad Heart Formation oolitic ironstones were primarily deposited in an oxidizing versus a reducing environment has been a subject of debate. For example, Eccles et al. (2000) argued that the presence of goethite, a negative Ce anomaly, and strong fractionation between Fe and Mn are indicative of deposition in an oxidizing environment. However, the goethite now found in ooids may reflect the fact that most samples which have historically been collected are from surface outcrops that are oxidized in the recent surfacial environment, whereas the oolitic ironstone found at depth (~70 m) in drill hole DDH0203 is dark green to black, indicating that most of the iron in the fresh, unweathered oolitic ironstones is in the reduced ferrous ( $\text{Fe}^{2+}$ ) state. Of course it also is possible that the ooids might have been deposited under oxidizing conditions and then reduced during subsequent diagenesis.

However, the environmental interpretation from the palynology samples collected during this study (Sweet, 2009) and the presence of molluscs locally within the oolitic ironstones both clearly indicate the ooids must have been formed in a well oxygenated environment. Lastly, the very minimal to generally complete lack of iron sulphide (pyrite) within the oolitic ironstone of the Bad Heart Formation suggests they were deposited in an oxidizing

environment. In short, the bulk of the above evidence indicates that the shallow sea conditions during the Bad Heart Formation time (Coniacian) were probably oxidizing, but the fact that the fresh, unweathered oolitic ironstones in hole DDH0203, as well as the lower part of the section exposed in the large pit excavated by Hamilton (1980) at Rambling Creek, have iron in the ferrous state is contradicting evidence.

The textural features of the ooids observed in this study (chapter 2) for the Bad Heart oolitic ironstone strongly indicate the ooids formation was authigenic; that is, they formed essentially in place in relatively shallow, agitated water and were neither transported in from elsewhere nor formed during diagenesis.

Perhaps the key question with respect to the Bad Heart oolitic ironstones is, what is the source of the iron that formed the over one billion tonnes of resources with an average grade of about 34% iron. In general, the consensus is that the Bad Heart oolitic ironstone was deposited in a wave-agitated shallow marine environment, but the exact origin of the high concentrations of iron and silica that presumably existed in the late Coniacian sea water is less certain (Olson et al., 1999). In general, the literature indicates at least two end-members with respect to the provenance or source of iron: (1) the iron is derived from continental sources and is transported into sea water by relatively normal continental processes (e.g., Young, 1989) or (2) the iron is of meteoric hydrothermal exhalative (fumaroles or sub-sea springs) and/or of volcanic hydrothermal origin (e.g., Kimberly, 1989).

The geochemistry of the major, trace and rare earth element contents of the oolitic ironstone can be used to try to assess the source of the iron and other elements in the Bad Heart Formation oolitic ironstone. However, the use of geochemistry to identify the source is complicated by various factors including (1) the bulk composition of the source area; (2) whether chemical weathering of the source area rocks is occurring, and the specific type of weathering (e.g., under wet tropical conditions or in dry arid to semi-arid conditions); (3) the method of transport of the element from the source area, that is, by

adsorption onto other mineral grains or completely in solution; (4) what happens geochemically during the deposition of the elements of interest at the depositional site; and lastly (5) what occurs during diagenesis to again affect the geochemistry of the element(s) in question (Fernandez and Moro, 1998).

The Bad Heart Formation ooids have lower  $\text{TiO}_2$  and higher  $\text{SiO}_2$  content in comparison with those of the Ordovician ooids from Baltoscandia (Sturesson, 1995). As well, the Recent ooids from Indonesia have very low contents of  $\text{MgO}$ ,  $\text{K}_2\text{O}$ , and  $\text{TiO}_2$  in comparison to the Bad Heart ooids. These differences in ooid composition may reflect fundamental differences in the concentration of these elements in the mineralizing waters present during deposition of the Baltoscandia and Indonesian ooids in comparison to those present during deposition of the Bad Heart oolitic ironstones. The relatively high content of  $\text{P}_2\text{O}_5$  in the samples analyzed from the Bad Heart oolitic ironstone (locally up to 3.31% and averaging about 1.56%  $\text{P}_2\text{O}_5$ ) may indicate a continental source for both phosphorous and the iron, given that phosphorous generally is believed to be leached from a continental source and then migrates to the sedimentary basin of deposition (Price, 1976). That is, phosphorous commonly is bonded to ferric iron and is believed to be transported to the sedimentary basin in the form of a ferric oxide-phosphate-clay assemblage (Manning and Gracey, 1991).

The positive correlation between elements commonly associated with a detrital source, such as Zr and  $\text{Al}_2\text{O}_3$  (0.78 correlation) and  $\text{TiO}_2$  and  $\text{Al}_2\text{O}_3$  (0.92 correlation) in the oolitic ironstone, suggests a detrital component in the oolitic ironstone. As well, the LREE (light REE) enrichment and negative Eu anomaly observed in the Bad Heart ooids are typical of material from sedimentary origin (Taylor and McClenan, 1985).

Similarly, the ratio of  $\text{TiO}_2/\text{Al}_2\text{O}_3$ , according to the criteria of (Schmidt, 1963) suggests that the Bad Heart ooids falls under 'normal' sedimentary rocks (Figure 3.8) indicating that they are from a sedimentary origin, whereas the samples from other chamosite and limonitic ooids from different parts of world falls under 'abnormal' sedimentary rocks

which are suggested to be of hydrothermal or volcanic origin; e.g., the Estonia and Russia ooids (Sturesson et al., 2000). The higher content of Zn in the Bad Heart ooids also may indicate the source of iron is from continental weathered rocks (Skocek et al., 1971). It has been postulated that zinc is transported to the depositional site by adsorption on clay minerals, iron hydroxides and organic substances given that the concentration of Zn in the surface water is very low (Guerrak, 1988).

On the other hand, the Bad Heart Formation ooids are enriched in some elements that are typically associated with hydrothermal processes; e.g., Fe, Mn, As, Ba, and Pb. As well, the Bad Heart ooids have a low concentration of  $\text{TiO}_2$ , which is not characteristic for iron ooids from a sedimentary origin (Landergren, 1948). Hegemen and Albrecht (1954), according to (Skocek et al., 1971), reported low  $\text{TiO}_2$  content in volcanic exhalative iron ores of the Lahn-dill type, which are similar to the oolitic ironstone from the Bad Heart Formation. Interestingly, Collom et al. (2001) reported the presence of volcanic glass locally within the Bad Heart oolitic ironstone, but such was not observed during the present study. Volcanic particles typically are present in some other oolitic ironstone of volcanic origin (Sturesson, 1995); hence, the absence of any volcanic particles in the detrital portion of the Bad Heart Formation oolitic ironstone, as observed in this study, indicates a volcanic-related origin of iron is unlikely for the Bad Heart Formation oolitic ironstones. As well, the REE pattern of the Bad Heart Formation ooids does not match with any Cretaceous bentonites from northern Alberta, whereas, in contrast, Sturesson (2003) found that the REE pattern of the ooids from Baltoscandia was similar to that of the stratigraphically related bentonite. Lastly, the quartz grains from within the oolitic ironstone bed are both monocrystalline and polycrystalline, but the absence of any fluid-filled vacuoles suggests that the quartz grains may be not from a hydrothermal origin (Tucker, 1981).

Hence, the high contents of  $\text{P}_2\text{O}_5$ , Zn and  $\text{TiO}_2/\text{Al}_2\text{O}_3$  ratio in the Bad Heart Formation ooids and the negative Eu anomaly suggest that the iron in ooids may be derived from

the weathering of continental rock. However, the REE pattern of the Bad Heart ooids is not similar to the general sedimentary REE pattern with enriched LREE and a flat HREE. In contrast, the absence of any volcanic particles in the detrital portion of the Bad Heart Formation oolitic ironstone, as compared to those found in some other oolitic ironstone from volcanic origin (Sturesson, 1995), and also the fact that the REE pattern of the Bad Heart ooids does not match with that of any bentonite from northern Alberta, indicate the source of the iron in the Bad Heart Formation ooids is continental sedimentary.

Lastly, the REE data from the Bad Heart Formation indicates the source must be different than that for the majority of the other Cretaceous clastic sedimentary rocks in northern Alberta (Dufresne et al., 2001). The specific source area for the Bad Heart Formation sandy units is uncertain, but may lie somewhere to the northwest, because Donaldson (1997) stated that at the Smoky River, the shallow water Bad Heart Formation was separated from a shoreline to the west by the laterally equivalent deeper water fine clastic Marshybank Formation. Similarly, deeper water fine clastic sediments also occur to the east at the Smoky River. Thus, assuming the Bad Heart Formation units at the Smoky River and the Clear Hills once formed a laterally continuous unit, although now eroded across the Peace River valley, the source of the coarser sandy clastic sediments in the Bad Heart Formation must be to the northwest, possibly from somewhere in northeastern British Columbia.

On the other hand, Olson et al. (1994) speculated, based on the large amounts of both iron and silica in the Clear Hills oolitic ironstone deposits, that "the genesis of the Clear Hills oolitic iron deposits was in some way related to either igneous fumarolic activity or to fumarolic deep-circulating hydrothermal basin fluids". In support of this alternative genesis for the source of the iron, the current study found that the Bad Heart Formation ooids are enriched in several elements (e.g., Ag, As, Ba, Cr, Fe, Mg, Mn, V and Zn,, Tables 3.1A to 3.1D) which are or may be associated with sub-sea hydrothermal or meteoric vent processes analogous to those that presently are forming the modern oxide iron deposits at the 'Paint Pots' in the Cordillera inside Kootenay National Park, about 28

km south west of Lake Louise, Alberta (Van Everdingen, 1970). As well, similar modern iron-bearing springs also exist at the Golden Deposit about 54 km northeast of Fort Norman, NWT, and in a tributary to Engineer Creek near kilometer 181 on the Dempster Highway, Yukon (Van Everdingen et al., 1985). Van Everdingen (1970) and Van Everdingen et al. (1985) concluded that the source of the iron in the Paint Pots, Golden and Engineer Creek waters was the result of oxidization of sulphides, especially pyrite, in the underlying bedrock. They also concluded that, based on oxygen- and sulphur-isotope geochemistry, the source rock was not likely to be evaporites.

In short, the ferruginous meteoric springs at the Paint Pots may be modern analogues for sub-sea springs or seeps originating from deep circulating meteoric solutions that vented onto the sea floor and were active in the Smoky River to Clear Hills region during the Coniacian time. In this event, it is likely that (1) meteoric groundwater originated in hydrographically high recharge areas in the then rising highlands of the proto Rocky Mountains to the west; (2) flowed easterly in coarser clastic units like the underlying Viking or Cardium formations; (3) leached pyrite from Colorado Group units, either the coarse clastics or the encompassing largely black shales; (4) exited to the surface along one or more northwesterly trending faults that existed in the Smoky River to Clear Hills region; and finally (5) debouched onto the sea floor during the Bad Heart Formation time as venting seeps or higher flow springs. There would have been no shortage of sulphide in the underlying Kaskapau and older formations to leach because Leckie et al. (1994, their figure 20.28) show that the upper Colorado Group typically contains about 2 to 4 per cent pyrite.

If such iron-debouching meteoric vents were present during the Bad Heart Formation time, then it is likely, or at least possible, that the waters were acidic and iron-bearing and hence were similar to the modern Paint Pots spring water and further that the water exit path(s) to the sea floor occurred along one or more of the faults that reportedly were active (Donaldson, 1997) during the deposition of the Bad Heart Formation.

## CONCLUSIONS

The bulk of the evidence indicates the depositional environment during the Coniacian Bad Heart Formation deposition was oxidizing. This is provided by the geochemical data, lack of sulphide, and common macro- and ichno-fossil assemblages. However, if this assertion is correct then because the fresh, unweathered Bad Heart Formation in drill hole DDH0203, and found locally in some outcrop exposures, is ferrous ( $\text{Fe}^{2+}$ ), the initially oxidized minerals in the ooids must have been converted during burial diagenesis to the ferrous state. The textural features of the Bad Heart Formation ooids suggest the ooids formed in place, at or near to where they now exist, by a repetitive process of growth in the water column and possible reworking on the sea floor once their weight became sufficiently large to cause them to deposit on the sea floor.

The provenance of the large amount of iron in the Bad Heart Formation oolitic ironstones remains unresolved. However, a continental sedimentary source is indicated by (1) the high concentration of  $\text{P}_2\text{O}_5$  and perhaps Zn, (2) the relatively low  $\text{TiO}_2/\text{Al}_2\text{O}_3$  ratio, and (3) a negative Eu anomaly. Further, the absence of volcanic material in the samples from this study also suggests a non-volcanic origin for the ooids. Finally, the different REE patterns of the Cretaceous northern Alberta bentonites and the Bad Heart Formation ooids are not characteristic of volcanic hydrothermal oolitic ironstone from other parts of the world. In all likelihood, the source provenance of much or all of the quartz sand in the Bad Heart Formation likely was to the northwest in northeastern B.C.

Based on the evidence from this study, it seems unlikely that, igneous or volcanic activity were important during the Bad Heart Formation time. Nevertheless, the Bad Heart ooids are enriched in some elements which are or may be associated with sub-sea hydrothermal or meteoric vent processes analogous to those presently forming the modern oxide iron deposits at the Paint Pots, Kootenay National Park. Although a continental source for the iron in the Bad Heart Formation oolitic ironstones is perhaps

marginally more likely, nonetheless the data from this study are still permissive with respect to the source of the iron being from deep circulating meteoric or possibly other, but non-igneous hydrothermal solutions that vented onto the sea floor during Bad Heart Formation time.

Table 3.1A: Concentrations of major, trace and rare earth elements and oxides in intensely oolitic ironstones (IOIS) from selected sections within the Bad Heart Formation

Section No. of samples	Clear Hills Region												Smoky River Region												
	ARR3 n=11		ARR5 n=8		KC14 n=4		KC17 n=5		LVH n=3		Worsley n=4		ASR10 n=8		ASR10A n=4		ASR9A n=7		ASR9B n=3		BBM n=1		SPRV n=2		
	Mean	Median	Mean	Median	Mean	Median	Mean	Median	Mean	Median	Mean	Median	Mean	Median	Mean	Median	Mean	Median	Mean	Median	Mean	Median	Mean	Median	
<b>Major Oxides &amp; Elements (Weight %)</b>																									
SiO <sub>2</sub>	25.02	24.52	23.92	23.93	21.64	20.10	29.28	27.12	32.11	29.88	20.79	22.73	20.00	18.80	25.18	25.13	18.69	15.74	17.23	13.87	31.67	31.67	24.77	24.77	
Al <sub>2</sub> O <sub>3</sub>	5.36	5.22	5.24	5.14	5.77	5.65	7.59	7.03	6.09	5.92	6.83	6.74	6.20	6.19	7.45	7.42	5.90	5.66	6.00	5.62	3.46	3.46	9.34	9.34	
Fe <sub>2</sub> O <sub>3</sub>	47.05	47.89	46.83	47.46	46.31	48.16	41.95	44.84	37.57	41.22	48.47	46.32	48.51	49.36	41.76	41.62	52.11	56.04	50.40	53.62	43.91	43.91	42.74	42.74	
CaO	2.04	1.94	2.08	1.94	5.33	5.39	1.45	1.44	4.37	3.84	2.69	2.41	2.52	2.54	2.88	2.79	2.23	2.11	4.29	4.56	1.71	1.71	2.37	2.37	
MgO	0.94	0.77	1.11	0.99	1.14	1.15	0.93	0.86	0.95	0.93	1.23	1.32	1.65	1.60	1.91	1.81	1.29	1.14	1.64	1.25	1.34	1.34	1.89	1.89	
Na <sub>2</sub> O	0.07	0.06	0.08	0.09	0.14	0.13	0.09	0.07	0.10	0.10	0.09	0.09	0.09	0.09	0.19	0.19	0.19	0.19	0.20	0.15	0.11	0.11	0.10	0.10	
K <sub>2</sub> O	0.52	0.47	0.46	0.44	0.62	0.62	0.80	0.75	0.80	0.80	0.72	0.71	0.56	0.57	0.81	0.82	0.46	0.37	0.49	0.36	0.55	0.55	1.14	1.14	
TiO <sub>2</sub>	0.18	0.17	0.15	0.15	0.18	0.18	0.24	0.22	0.20	0.21	0.22	0.23	0.20	0.21	0.27	0.27	0.17	0.14	0.19	0.15	0.19	0.19	0.34	0.34	
P <sub>2</sub> O <sub>5</sub>	1.60	1.62	1.60	1.60	1.69	1.64	1.39	1.49	1.61	1.75	1.63	1.70	1.64	1.62	1.56	1.43	1.65	1.84	1.97	2.07	0.66	0.66	1.03	1.03	
S	0.04	0.01	0.04	0.03	0.06	0.05	0.03	0.03	0.02	0.02	0.01	0.01	0.02	0.01	0.35	0.32	0.16	0.16	0.22	0.15	0.15	0.08	0.08	0.08	
LOI	16.84	16.80	18.09	17.90	16.80	16.95	15.84	16.10	15.87	16.30	16.80	16.85	18.29	18.10	17.55	17.55	16.86	16.70	17.23	17.50	15.90	15.90	15.85	15.85	
Total	99.65	99.46	99.59	99.64	99.65	100.00	99.59	99.95	99.70	100.97	99.47	99.08	99.67	99.06	99.90	99.33	99.71	100.09	99.85	99.37	99.65	99.65	99.63	99.63	
<b>Minor and Trace Elements (ppm except where indicated)</b>																									
Ag (ppb)	57.36	54.00	48.38	46.50	71.00	71.50	70.20	68.00	75.00	65.00	59.50	59.50	43.25	44.00	62.75	63.00	50.14	42.00	46.33	39.00	69.00	69.00	62.50	62.50	
As	249.90	255.50	339.40	369.05	171.33	172.50	142.46	155.70	162.77	166.40	218.35	218.35	254.50	264.90	188.00	200.55	188.43	200.50	161.03	174.50	74.00	74.00	208.00	208.00	
Au (ppb)	1.80	1.90	0.67	0.60	0.96	1.00	0.10	0.10	0.74	0.85	1.48	1.50	0.33	0.30	0.50	0.30	0.30	0.30	0.30	0.30	0.30	0.30	0.75	0.75	
B	28.82	30.00	54.50	52.00	41.25	41.50	25.60	30.00	26.67	28.00	42.50	42.50	58.75	59.50	54.50	56.50	65.00	66.00	59.67	61.00	19.00	19.00	33.50	33.50	
Ba	821.77	752.50	487.24	499.15	576.45	552.40	605.54	614.40	637.80	646.70	601.28	572.25	412.73	422.05	768.83	799.30	461.16	427.90	559.20	447.50	446.40	446.40	919.90	919.90	
Be	4.50	4.50	4.25	4.00	4.25	4.50	5.20	5.00	4.00	5.00	5.00	4.88	5.50	5.00	5.00	5.29	5.00	5.33	5.00	3.00	3.00	4.50	4.50		
Bi	0.68	0.69	0.76	0.76	1.02	1.01	1.20	1.12	1.05	1.07	0.92	0.96	0.96	1.01	1.01	1.09	1.08	0.97	1.03	0.26	0.26	1.56	1.56		
Cd	0.05	0.03	0.04	0.04	0.73	0.76	0.64	0.10	0.13	0.17	0.05	0.06	0.41	0.37	0.18	0.10	0.08	0.04	0.09	0.09	0.08	0.08	0.08		
Co	34.49	27.10	53.41	54.45	46.65	45.40	57.82	54.80	49.73	50.70	58.40	54.65	56.84	56.40	90.63	84.65	66.97	70.30	61.90	66.00	15.80	15.80	57.80	57.80	
Cr	124.57	123.80	118.55	118.30	141.63	141.70	148.06	150.10	131.73	137.70	160.20	160.20	151.18	151.40	123.25	123.30	167.50	167.90	155.27	167.00	34.70	34.70	151.75	151.75	
Cs	1.90	1.90	1.54	1.50	1.63	1.65	2.28	1.80	2.00	2.10	2.45	2.65	1.90	1.85	2.80	2.80	1.66	1.40	1.93	1.40	1.50	1.50	3.40	3.40	
Cu	10.15	9.90	9.54	8.60	9.88	9.80	14.62	13.30	11.47	11.80	10.23	10.45	8.83	8.85	11.13	10.80	9.09	8.00	8.57	7.50	6.50	6.50	13.60	13.60	
Ga	8.26	8.30	8.54																						

Table 3.1B: Concentrations of major, trace and rare earth elements and oxides in moderately oolitic ironstones (MOIS) from selected sections within the Bad Heart Formation

Section No. of samples	Clear Hills Region										Smoky River Region																											
	ARR3 n=3			ARR5 n=1			LVH n=2		ASR10 n=2			ASR10A n=2			ASR4 n=2			ASR6 n=2			ASR8 n=1			ASR9A n=2			ASR9B n=2			ASR9I n=1			BBM n=3			SPRV n=3		
	Mean	Median	Mean	Mean	Median	Mean	Mean	Median	Mean	Mean	Median	Mean	Mean	Median	Mean	Mean	Median	Mean	Mean	Median	Mean	Mean	Median	Mean	Mean	Median	Mean	Mean	Median	Mean	Median	Mean						
<b>Major Oxides &amp; Elements (Weight %)</b>																																						
SiO <sub>2</sub>	33.47	34.04	25.45	25.45	27.15	27.15	29.64	29.64	34.93	34.93	19.71	19.71	25.90	25.90	34.57	34.57	39.21	39.21	32.89	32.89	36.63	36.63	47.22	48.58	24.65	20.57												
Al <sub>2</sub> O <sub>3</sub>	6.45	6.91	6.48	6.48	8.65	8.65	7.19	7.19	7.46	5.03	5.03	7.67	7.67	8.99	8.99	7.20	7.20	4.87	4.87	7.72	7.72	5.00	4.94	5.94	6.18													
Fe <sub>2</sub> O <sub>3</sub>	35.08	35.07	43.16	43.16	36.23	36.23	35.84	35.84	32.50	32.50	34.73	34.73	33.96	33.96	30.21	30.21	30.62	30.62	38.02	38.02	33.20	33.20	30.81	30.86	42.16	42.14												
CaO	3.10	3.20	3.43	3.43	4.98	4.98	4.47	4.47	3.15	3.15	11.87	11.87	5.97	5.97	3.20	3.20	3.27	3.27	5.00	5.00	3.04	3.04	1.02	0.98	6.08	5.64												
MgO	1.77	1.74	1.24	1.24	1.42	1.42	2.36	2.36	1.95	1.95	2.88	2.88	2.90	2.90	1.46	1.46	1.90	1.90	1.48	1.48	2.03	2.03	0.93	0.92	1.74	1.23												
Na <sub>2</sub> O	0.10	0.10	0.12	0.12	0.14	0.14	0.21	0.21	0.18	0.18	0.19	0.19	0.29	0.29	0.14	0.14	0.23	0.23	0.20	0.20	0.24	0.24	0.07	0.06	0.10	0.11												
K <sub>2</sub> O	0.87	0.88	0.70	0.70	1.25	1.25	0.76	0.76	0.90	0.90	0.62	0.62	0.93	0.93	1.06	1.06	0.86	0.86	0.48	0.48	0.99	0.99	0.61	0.62	0.51	0.51												
TiO <sub>2</sub>	0.25	0.24	0.20	0.20	0.35	0.35	0.27	0.27	0.28	0.18	0.18	0.29	0.29	0.33	0.33	0.28	0.28	0.17	0.17	0.30	0.30	0.19	0.19	0.17	0.17													
P <sub>2</sub> O <sub>5</sub>	1.29	1.43	2.03	2.03	2.11	2.11	1.43	1.43	1.19	1.19	1.54	1.54	1.42	1.42	2.02	2.02	1.16	1.16	1.28	1.28	1.24	1.24	1.02	1.08	1.91	1.73												
S	0.37	0.18	0.03	0.03	0.05	0.05	0.20	0.20	0.48	0.48	0.53	0.53	0.46	0.46	0.66	0.66	0.54	0.54	0.34	0.34	0.21	0.21	0.05	0.05	0.05	0.05												
LOI	17.27	17.50	16.50	16.50	17.30	17.30	17.65	17.65	17.10	17.10	22.85	22.85	20.30	20.30	17.50	17.50	14.80	14.80	15.25	15.25	14.20	14.20	12.77	12.77	12.70	16.37	15.70											
Total	100.04	101.29	99.34	99.34	99.62	99.62	99.99	99.99	100.09	100.09	100.12	100.12	100.08	100.08	100.14	100.14	100.03	100.03	99.96	99.96	99.80	99.80	99.70	99.70	100.99	99.69	94.03											
<b>Minor and Trace Elements (ppm except where indicated)</b>																																						
Ag (ppb)	75.33	78.00	64.00	64.00	66.50	66.50	56.00	56.00	102.50	102.50	52.50	52.50	52.50	52.50	85.00	85.00	74.00	74.00	57.00	57.00	80.00	80.00	69.67	66.00	68.67	70.00												
As	118.33	119.40	199.60	199.60	60.70	60.70	80.95	80.95	126.95	126.95	86.85	86.85	26.20	26.20	24.00	24.00	24.00	24.00	83.05	83.05	282.30	282.30	28.70	28.70	95.17	105.20	161.37	196.00										
Au (ppb)	0.70	0.50	0.67	0.67	0.50	0.50	0.25	0.25	0.50	0.50	0.35	0.35	1.30	1.30	0.35	0.35	0.50	0.50	1.40	1.40	0.45	0.45	1.03	0.90														
B	26.67	25.00	37.00	37.00	24.00	24.00	43.50	43.50	47.00	47.00	31.50	31.50	42.50	42.50	39.00	39.00	68.00	68.00	41.00	41.00	41.00	41.00	16.00	16.00	35.67	36.00												
Ba	845.70	889.50	862.60	862.60	823.15	823.15	545.30	545.30	688.80	688.80	785.50	785.50	754.85	754.85	834.80	834.80	649.85	649.85	480.60	480.60	673.80	673.80	632.73	613.30	659.17	656.50												
Be	3.67	4.00	4.00	4.00	4.00	4.00	3.50	3.50	4.00	4.00	3.00	3.00	3.50	3.50	6.00	6.00	4.00	4.00	5.50	5.50	3.00	3.00	3.33	3.00	5.00	5.00												
Bi	0.57	0.63	0.91	0.91	0.96	0.96	0.85	0.85	1.08	1.08	0.77	0.77	0.88	0.88	1.06	1.06																						

Table 3.1C: Concentrations of major, trace and rare earth elements and oxides in weakly oolitic ironstones (WOIS) from selected sections within the Bad Heart Formation

	Clear Hills Region		Smoky River Region	
Section No. of samples	ARR3 n=1	KC14 n=1	ASR5 n=1	ASR8 n=1
<b>Major Oxides &amp; Elements (Weight %)</b>				
SiO <sub>2</sub>	38.49	22.09	27.71	32.69
Al <sub>2</sub> O <sub>3</sub>	8.34	7.3	9.24	8.97
Fe <sub>2</sub> O <sub>3</sub>	30.32	37.97	29.75	32.8
CaO	1.93	9.23	7.36	2.91
MgO	1.84	1.09	2.8	1.38
Na <sub>2</sub> O	0.09	0.16	0.25	0.13
K <sub>2</sub> O	1.11	0.88	1.09	0.97
TiO <sub>2</sub>	0.31	0.26	0.34	0.3
P <sub>2</sub> O <sub>5</sub>	0.82	3.93	2.64	1.38
S	0.17	0.03	0.34	0.98
LOI	16.3	16.6	18.4	17.9
Total	99.72	99.54	99.92	100.41
<b>Minor and Trace Elements (ppm except where indicated)</b>				
Ag (ppb)	101	74	71	63
As	125.1	165.9	17.2	30
Au (ppb)			1.8	0.2
B	31	28	41	29
Ba	1101.4	816.2	788.7	775.3
Be	4	3	5	5
Bi	0.75	1.13	1.54	0.8
Cd	0.12	0.25	0.04	0.75
Co	56.7	53	94.3	101.8
Cr	120.1	132.2	190.8	116.5
Cs	3.6	2.7	3.1	3.3
Cu	16.7	12.8	15	19.5
Ga	12.4	11.8	12.8	11.1
Hf	2.6	2.5	3.4	2.8
Hg (ppb)	34	37	47	40
Li	37.1	56.5	60.8	147.5
Mn	700	1076	480	1389
Mo	11.1	0.8	1.8	3.9
Nb	8.9	7.6	12.3	9.1
Ni	129	117	138	180
Pb	43.4	60	103.9	55.4
Rb	56.6	39.5	47.7	52.3
Sb	5.4	7	7	4.1
Sc	13	16	21	14
Se	0.7	1.5	1.5	1.1
Sn	1.3	1	2.2	1.3
Sr	181.6	418.5	326.3	151.4
Ta	0.5	0.4	0.5	0.4
Te	0.69	0.97	1.53	0.89
Th	11.5	16.9	24	12.6
Tl	0.12	0.09	0.1	0.06
U	5.6	28.6	9.9	4.4
V	1101	1468	1987	1112
W	1.5	0.8	2.3	1.7
Y	54.3	113.4	127.2	82.7
Zn	509	609	796	779
Zr	107.1	105.1	156.2	114.1
<b>Rare Earth Elements (ppm)</b>				
La	32.5	37.6	66.8	33.8
Ce	67.6	73.6	150.6	84.7
Pr	9.74	12.19	22.04	12.66
Nd	43.4	55.6	101.8	62.2
Sm	10.7	15	26.92	18.9
Eu	2.56	3.82	6.49	4.5
Gd	11.64	18.46	29.42	19.8
Tb	2.07	3.5	5.37	3.14
Dy	10.04	17.75	23.33	16.87
Ho	1.76	3.21	3.93	2.88
Er	4.35	8.14	9.95	7.28
Tm	0.63	1.03	1.31	1.03
Yb	3.79	6.58	7.9	6.14
Lu	0.52	0.92	1.07	0.81

Table 3.1D: Summary results of major, trace and rare earth elements and oxides in oolitic ironstones (including all three types) from selected sections within the Bad Heart Formation

Section No. of samples	Clear Hills Region															Smoky River Region																		
	ARR3 n=15		ARR5 n=9		KC14 n=5		KC17 n=5		LVH n=5		WORSLEY n=4		ASR10 n=10		ASR10A n=6		ASR9A n=9		ASR9B n=5		ASR4 n=2		ASR5 n=1		ASR6 n=2		ASR8 n=1		ASR9I n=1		BBM n=4		SPRV n=5	
	Mean	Median	Mean	Median	Mean	Median	Mean	Median	Mean	Median	Mean	Median	Mean	Median	Mean	Median	Mean	Median	Mean	Median	Mean	Median	Mean	Median	Mean	Median	Mean	Median	Mean	Median	Mean	Median		
<b>Major Oxides &amp; Elements (Weight %)</b>																																		
SiO <sub>2</sub>	27.61	26.21	24.09	24.26	21.73	20.66	29.28	27.12	30.13	27.12	20.79	22.73	21.93	20.76	28.43	27.02	23.25	17.55	23.49	13.87	19.71	19.71	27.71	27.71	25.90	25.90	33.63	33.63	36.63	36.63	43.34	46.48	24.70	20.57
Al <sub>2</sub> O <sub>3</sub>	5.78	5.44	5.37	5.15	6.07	5.71	7.59	7.03	7.12	7.01	6.83	6.74	6.40	6.36	7.45	7.42	6.19	5.75	5.55	5.42	5.03	5.03	9.24	9.24	7.67	8.98	8.98	7.72	7.72	4.62	4.84	7.30	6.59	
Fe <sub>2</sub> O <sub>3</sub>	43.54	45.76	46.42	47.16	44.64	47.85	41.95	44.84	37.04	44.84	48.47	46.32	45.97	47.30	38.67	38.54	47.33	51.66	45.45	52.21	34.73	34.73	29.75	29.75	33.96	33.96	31.51	31.51	33.20	33.20	34.09	31.74	42.39	42.14
CaO	2.24	1.97	2.23	1.95	6.11	5.40	1.45	1.44	1.50	2.69	2.41	2.91	2.67	2.97	3.08	2.46	2.37	4.57	4.56	11.87	11.87	7.36	7.36	5.97	5.97	3.06	3.04	1.20	1.07	4.60	2.58			
MgO	1.17	0.80	1.12	0.99	1.13	1.11	0.93	0.86	1.14	0.86	1.23	1.32	1.79	1.80	1.92	1.81	1.43	1.22	1.57	1.43	2.88	2.88	2.80	2.80	2.90	2.90	1.42	1.42	2.03	2.03	1.04	0.96	1.80	1.61
Na <sub>2</sub> O	0.08	0.07	0.08	0.09	0.14	0.13	0.09	0.07	0.11	0.07	0.09	0.09	0.12	0.10	0.19	0.19	0.20	0.19	0.19	0.20	0.15	0.19	0.25	0.25	0.29	0.29	0.14	0.14	0.24	0.24	0.08	0.08	0.10	0.11
K <sub>2</sub> O	0.63	0.56	0.49	0.46	0.67	0.65	0.80	0.75	0.98	0.57	0.72	0.71	0.60	0.58	0.84	0.83	0.55	0.45	0.48	0.36	0.62	1.09	1.09	0.93	0.93	1.02	1.02	0.99	0.99	0.60	0.59	0.76	0.59	
TiO <sub>2</sub>	0.20	0.19	0.16	0.15	0.20	0.19	0.24	0.22	0.26	0.18	0.22	0.23	0.21	0.21	0.27	0.19	0.18	0.15	0.18	0.18	0.34	0.34	0.29	0.29	0.32	0.32	0.30	0.30	0.19	0.19	0.24	0.18		
P <sub>2</sub> O <sub>5</sub>	1.49	1.57	1.65	1.65	2.13	1.75	1.39	1.49	1.81	1.50	1.63	1.70	1.60	1.59	1.43	1.40	1.54	1.78	1.69	1.70	1.54	1.54	2.64	2.64	1.42	1.42	1.70	1.70	1.24	1.24	0.93	0.99	1.56	1.45
S	0.11	0.01	0.04	0.03	0.05	0.05	0.03	0.03	0.03	0.04	0.01	0.01	0.05	0.01	0.39	0.38	0.25	0.16	0.22	0.53	0.34	0.34	0.46	0.46	0.82	0.82	0.21	0.21	0.08	0.08	0.06	0.06	0.08	0.08
LOI	16.89	16.80	17.91	17.90	16.76	16.90	15.84	16.10	16.44	15.90	16.80	16.85	18.16	18.10	17.40	17.55	16.40	16.70	16.44	17.50	22.85	22.85	18.40	18.40	20.30	20.30	17.70	17.70	14.20	14.20	13.55	13.55	16.16	15.70
Total	99.74	99.38	99.57	99.79	99.63	100.40	99.59	99.95	99.66	99.59	99.47	99.08	99.73	99.45	99.96	98.47	99.78	98.01	99.89	97.57	100.12	99.92	99.92	100.08	100.08	100.28	100.28	99.80	99.80	99.69	99.69	100.33	99.67	91.60
<b>Minor and Trace Elements (ppm except where indicated)</b>																																		
Ag (ppb)	63.87	61.00	50.11	47.00	71.60	74.00	70.20	68.00	71.60	68.00	59.50	59.50	45.80	46.00	76.00	64.50	55.44	46.00	50.60	39.00	52.50	52.50	71.00	71.00	52.50	52.50	74.00	74.00	80.00	80.00	69.50	67.50	66.20	70.00
As	215.27	253.00	323.87	367.80	170.24	171.90	142.46	155.70	121.94	155.70	218.35	218.35	219.79	246.40	167.65	166.35	165.01	169.70	209.54	174.50	86.85	86.85	17.20	17.20	26.20	26.20	27.00	27.00	28.70	28.70	89.88	89.60	180.02	196.00
Au (ppb)	1.57	1.80	0.67	0.60	0.96	1.00	0.50	0.90	0.10	0.10	0.64	0.60	1.15	1.25	0.33	0.30	0.50	0.30	1.80	1.80	0.35	0.35	0.75	0.75	1.40	1.40	0.40	0.40	0.92	0.92	0.90	0.90		
B	28.53	30.00	52.56	51.00	38.60	41.00	25.60	30.00	25.60	30.00	42.50	42.50	55.70	53.00	54.50	65.67	66.00	52.20	56.00	31.50	31.50	41.00	41.00	42.50	42.50	34.00	34.00	41.00	41.00	16.75	16.50	34.80	36.00	
Ba	845.2																																	

Table 3.2: Summary of elements and their geochemical distribution in Bad Heart Formation ironstones

<b>Major &amp; Minor Element</b>	<b>Description of Geochemical Distribution</b>	<b>Comments about the Distribution</b>
Ag	Unimodal, symmetric	Average may be best estimator for the distribution
Al	Unimodal, positively skewed, not lognormal	Median may be best estimator for the distribution
As	Bimodal	
B	Unimodal, positively skewed	Median may be best estimator for the distribution
Ba	Unimodal, positively skewed	Median may be best estimator for the distribution
Ca	Bimodal	
Co	Unimodal, positively skewed	Median may be best estimator for the distribution
Cr	Bimodal	
Cu	Bimodal	
Fe	Bimodal	
Hg	Bimodal	
K	Bimodal	
Li	Bimodal	
Mg	Bimodal	
Mn	Unimodal, positively skewed, log normal	Median may be best estimator for the distribution
Mo	Unimodal symmetric	Average may be best estimator for the distribution
Na	Unimodal, positively skewed, lognormal	Median may be best estimator for the distribution
Ni	Unimodal, positively skewed, not lognormal	Median may be best estimator for the distribution
P	Unimodal, positively skewed, not lognormal	Median may be best estimator for the distribution
Pb	Unimodal, positively skewed, lognormal	Median may be best estimator for the distribution
Rb	Unimodal, positively skewed, lognormal	Median may be best estimator for the distribution
S	Unimodal, positively skewed, lognormal	Median may be best estimator for the distribution
Sr	Unimodal, positively skewed, not lognormal	Median may be best estimator for the distribution
Ti	Unimodal, positively skewed, lognormal	Median may be best estimator for the distribution
U	Unimodal, positively skewed	Median may be best estimator for the distribution
V	Unimodal symmetric	Average may be best estimator for the distribution
Y	Bimodal	
Zn	Unimodal symmetric	Average may be best estimator for the distribution
Zr	Bimodal	

Table 3.3: Summary of major oxides and trace element averages and maximum contents in the Bad Heart Formation ironstones

Oxide or Element	Clarke value <sup>1</sup>	Other Bad Heart Litho-units		Average Content in Ooidal Ironstone				Maximum Content in OIS
		Sandstone, Siltstone & shale	OS	WOIS	MOIS	IOIS	Overall OIS	
<b>Major Oxides &amp; Elements (Weight %)</b>								
SiO <sub>2</sub>		56.5(60.9)	39.8(37.9)	30.2(30.2)	32.0(31.1)	23.4(23.4)	26.2(24.9)	52.2
Al <sub>2</sub> O <sub>3</sub>		8.9(7.8)	6.1(6.6)	8.5(8.7)	6.6(6.5)	6.1(5.9)	6.4(6)	11.9
Fe <sub>2</sub> O <sub>3</sub>		15.3(13.1)	29.3(27.5)	32.7(31.6)	35.2(34.9)	46.6(47.2)	42.7(43.8)	62
CaO		3.0(1.1)	4.3(3.7)	5.4(5.1)	4.5(3.3)	2.6(2.3)	3.3(2.6)	12.7
MgO		1.4(1.3)	1.8(1.9)	1.8(1.6)	1.8(1.6)	1.3(1.2)	1.5(1.3)	3.1
TiO <sub>2</sub>		0.4(0.4)	0.3(0.3)	0.3(0.3)	0.2(0.2)	0.2(0.2)	0.2(0.2)	0.4
P <sub>2</sub> O <sub>5</sub>		0.6(0.2)	1.1(1)	2.2(2)	1.5(1.4)	1.6(1.6)	1.6(1.6)	3.9
S		0.5(0.4)	0.3(0.2)	0.4(0.3)	0.3(0.2)	0.1(0.1)	0.2(0.1)	1
LOI		11.6(10)	15.9(15.8)	17.3(17.3)	16.8(16.8)	17.1(17.1)	17(17)	23.9
Total		98.2(95.2)	98.9(94.9)	98.8(97.1)	98.9(96.0)	99.0(99.0)	99.1(97.5)	
<b>Minor and Trace Elements (ppm except where indicated)</b>								
Ag (ppb)	0.07(ppm)	83.8(81.5)	73.0(71)	77.3(72.5)	68.9(65.5)	56.5(54)	61.1(61.5)	115
As	13	64.8(41.2)	87.5(71)	84.6(77.6)	110.4(85.6)	221.8(216.4)	182.7(182.2)	498.8
B	100	22(20)	35.8(37)	32.3(30)	36.4(35.5)	45.2(44.5)	42.0(39.5)	101
Ba	580	790.4(741.2)	868.7(714)	870.4(802.5)	701.5(686.8)	602.6(550.9)	643.1(614.6)	1605.2
Co	19	26.8(20.6)	51.8(50.2)	76.5(75.5)	57.6(52.1)	54.5(54.7)	56.3(54.4)	133.1
Cr	90	45.4(34.8)	72.0(56.8)	139.9(126.2)	118.1(115.2)	138.3(137.5)	132.4(128.2)	204.8
Hg (ppb)	0.4(ppm)	48.0(35.5)	26.5(25)	39.5(38.5)	46.3(33.5)	22.1(16)	30.2(25)	221
Li	66	60.3(55.1)	53.1(35.7)	75.5(58.7)	44.4(33.2)	23.5(20.2)	31.8(25.3)	150.6
Mn	850	515.8(280.5)	1091.1(993)	873.3(823)	1119.5(1056)	1066.2(1029.5)	1073(1022.5)	2684
Ni	68	51(45)	88.6(78)	141.0(133.5)	97.7(84.5)	93.0(89.5)	96.5(90)	225
Pb	20	28.1(22.4)	39.6(36.1)	65.7(57.7)	54.9(52.2)	51.1(48.1)	52.9(49.1)	122
Rb	140	75.3(60.7)	41.2(40.3)	49(50)	36.3(36.2)	29.3(26.4)	32.2(29.2)	75.1
Sr	300	173.9(143.2)	208.3(158.5)	269.5(254)	194.7(185.4)	162.2(158.8)	176.3(164.8)	418.5
V	130	451.3(356)	764.4(591)	1417(1290)	1165.2(1040)	1299.9(1290.5)	1266.2(1279.5)	2476
Y	26	36.9(30.6)	58.3(56.1)	94.4(98.1)	70.6(65.1)	72.4(68.9)	72.9(68.4)	135.5
Zn	95	223.4(164)	395.8(378)	673.3(694)	519.3(500.5)	602.2(587.5)	581.4(582)	1040
Zr	160	154(155.5)	111.1(107.8)	120.6(110.6)	110.1(104.9)	98.1(93.1)	102.6(96.6)	175.5

<sup>1</sup>Clarke values are from Turekian and Wedepohl (1961)

The values in parentheses are median values

Table 3.4: Summary of average and maximum rare earth element contents in Bad Heart Formation ironstones

REE	Clarke value <sup>1</sup>	Other Bad Heart Litho-units		Average Content in Ooidal Ironstone				Maximum Content in OIS
		Sandstone, Siltstone & shale	OS	WOIS	MOIS	IOIS	Overall OIS	
La	92	29.7(30.3)	28(28.2)	42.7(35.7)	32.2(30.3)	33.2(32.6)	33.3(32.5)	66.8
Ce	59	60.3(61.3)	61.5(58.1)	94.1(79.2)	69.5(64.8)	66.1(63.0)	68.3(63.9)	150.6
Pr	5.6	7.8(8.0)	9(8.2)	14.2(12.4)	10.6(10.1)	10.4(10.2)	10.6(10.2)	22
Nd	24	32(31.1)	41.3(37.3)	65.8(58.9)	48.5(45.9)	48.1(46.8)	49.0(46.7)	101.8
Sm	6.4	7.3(6.5)	11.0(10.0)	17.9(17.0)	13.2(11.9)	13.3(13.2)	13.5(13.1)	29.7
Eu	1	1.7(1.4)	2.7(2.5)	4.3(4.2)	3.3(3.0)	3.3(3.3)	3.4(3.2)	7.4
Gd	6.4	7.2(5.6)	12.5(11.7)	19.8(19.1)	15(13.6)	15.1(14.3)	15.3(14.3)	33.5
Tb	1	1.2(0.9)	2.2(1.9)	3.5(3.3)	2.7(2.5)	2.7(2.6)	2.7(2.6)	5.4
Dy	4.6	6.5(5.2)	10.9(10.7)	17(17.3)	13.5(13.4)	13.8(13.3)	13.9(13.4)	28.6
Ho	1.2	1.2(1.0)	1.9(1.9)	2.9(3.0)	2.3(2.1)	2.3(2.2)	2.4(2.2)	4.9
Er	2.5	3.2(2.9)	4.9(4.8)	7.4(7.7)	6.0(5.8)	6.1(5.9)	6.2(5.9)	12.5
Tm	0.2	0.5(0.5)	0.7(0.7)	1.0(1.0)	0.8(0.8)	0.8(0.8)	0.8(0.8)	1.6
Yb	2.6	2.9(2.9)	3.9(4.0)	6.1(6.4)	4.9(4.6)	5.0(4.8)	5.0(4.8)	9.7
Lu	0.7	0.4(0.4)	0.5(0.5)	0.8(0.9)	0.7(0.6)	0.7(0.6)	0.7(0.6)	1.2
TREE		161.9(157.7)	191.1(180.5)	297.6(266.1)	223.3(209.4)	220.9(213.6)	225(214.1)	456.93

<sup>1</sup>Clarke values are from Turekian and Wedepohl (1961)

The values in parentheses are median values

TREE: Total Rare earth elements

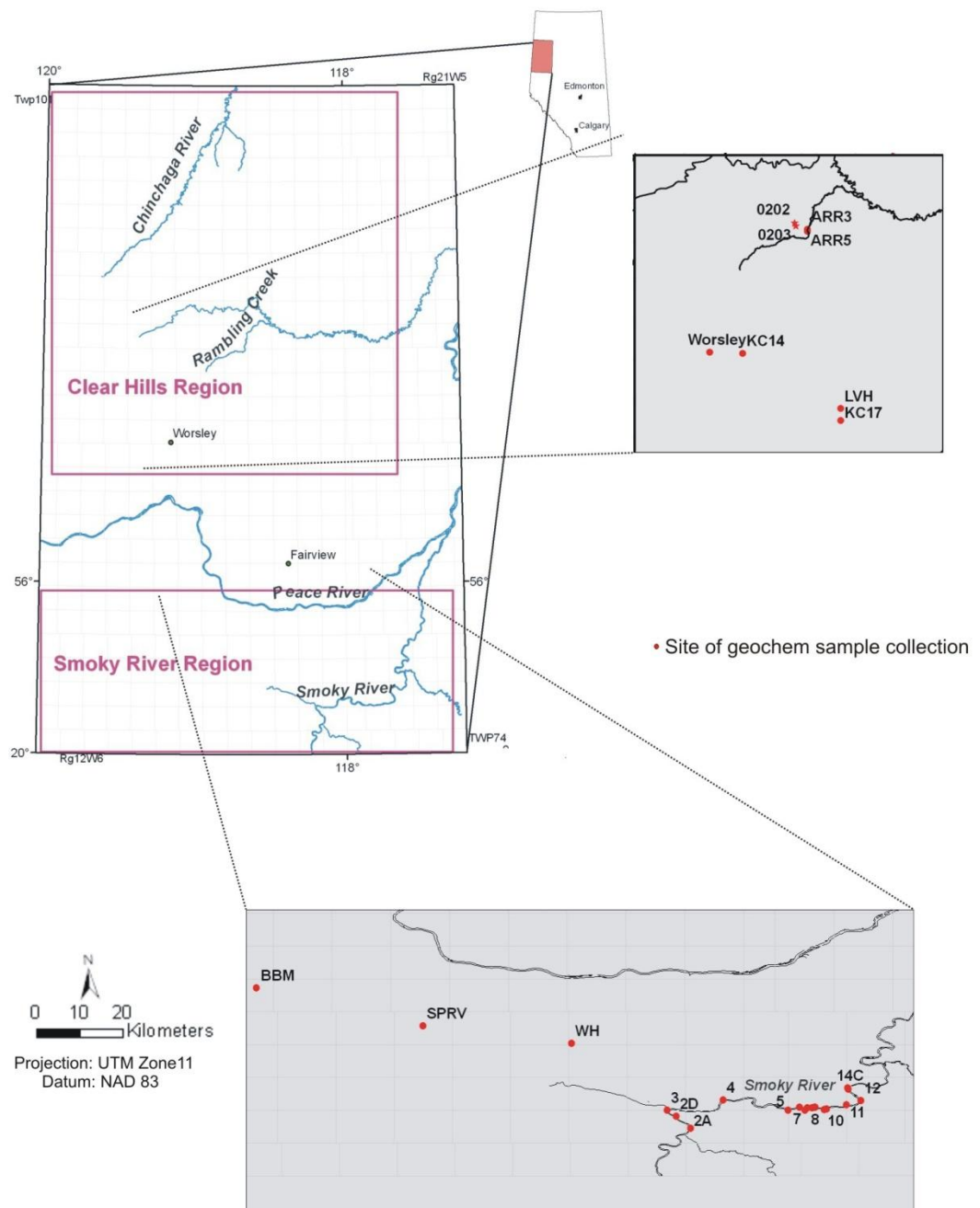


Figure 3.1 Location map of the study area

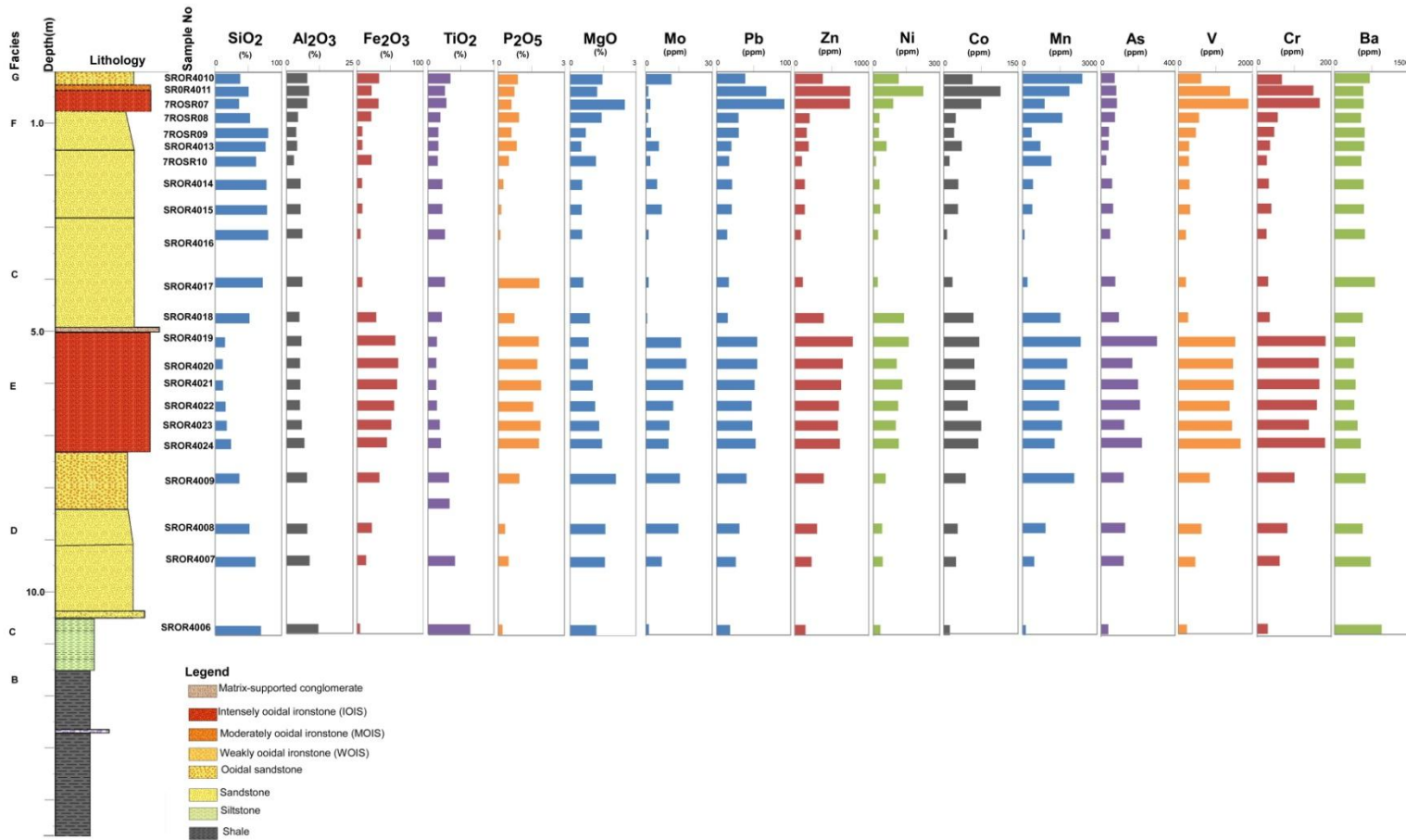


Figure 3.2 Variation in oxides and selected trace elements along Bad Heart Formation section ASR9A in the Smoky River region

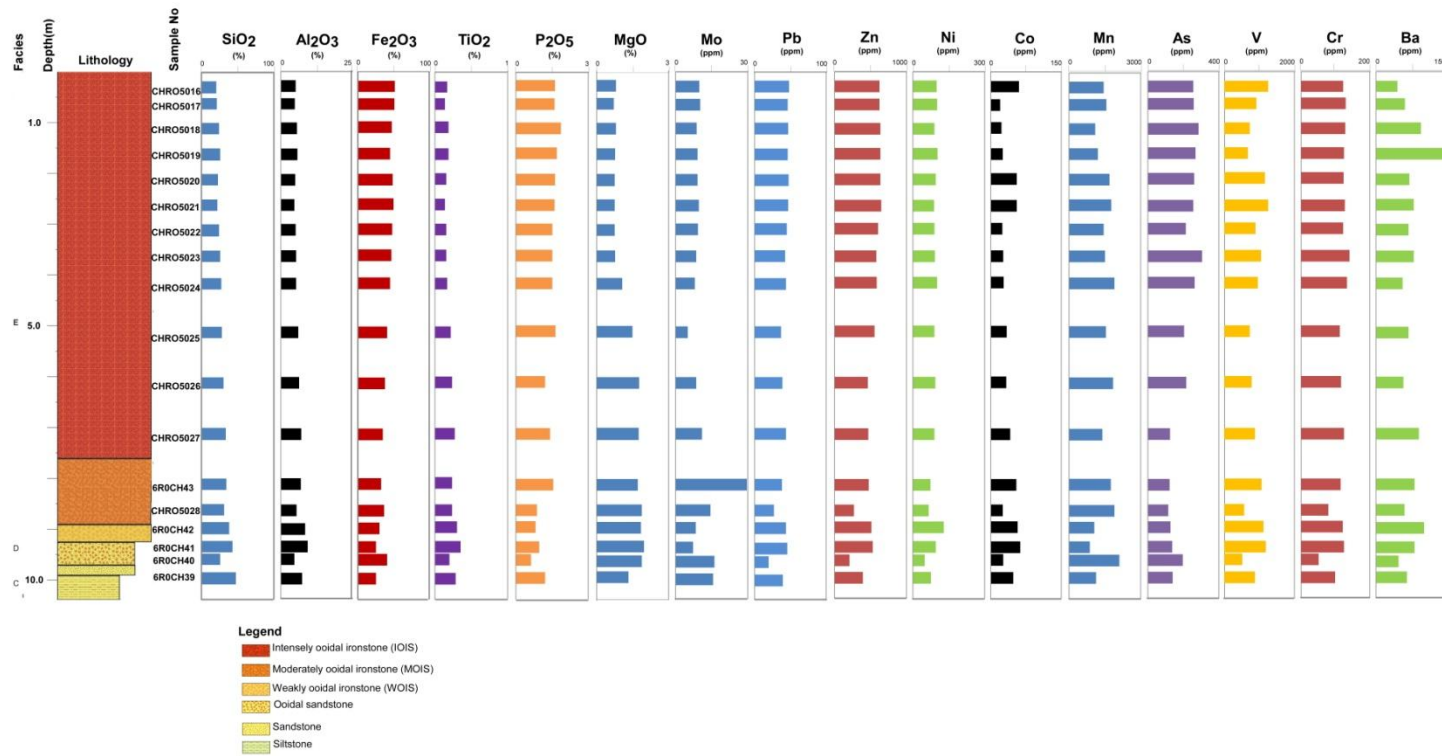
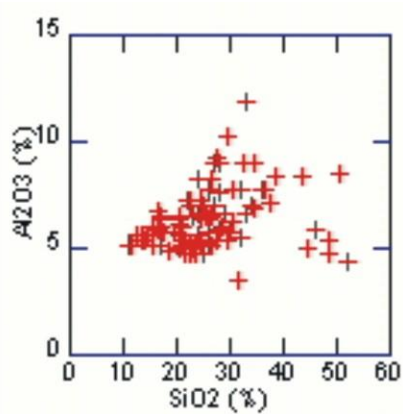
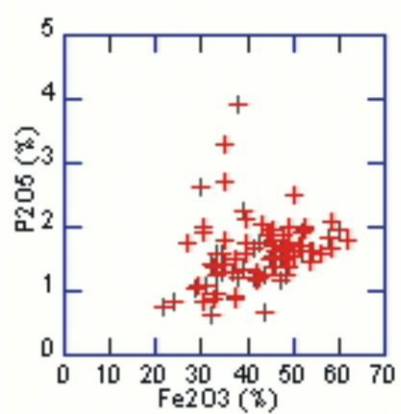


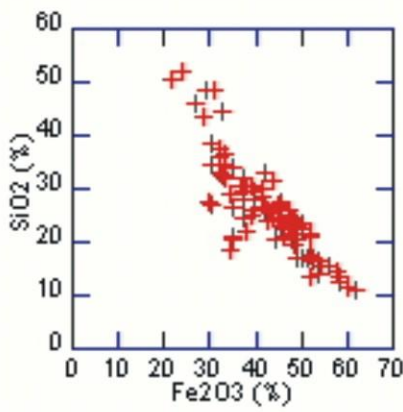
Figure 3.3 Variation in oxides and selected trace elements along the Bad Heart Formation section ARR3 near Rambling Creek in the Clear Hills region



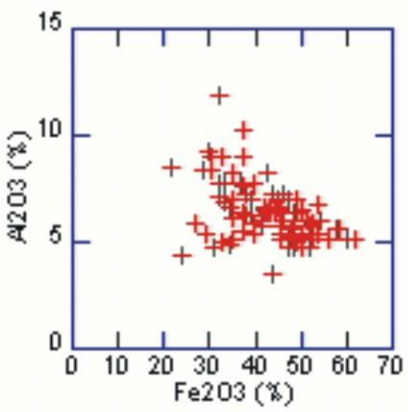
a



b



c



d

Figure 3.4 Correlation diagrams of various oxides from Bad Heart Formation oolitic ironstone

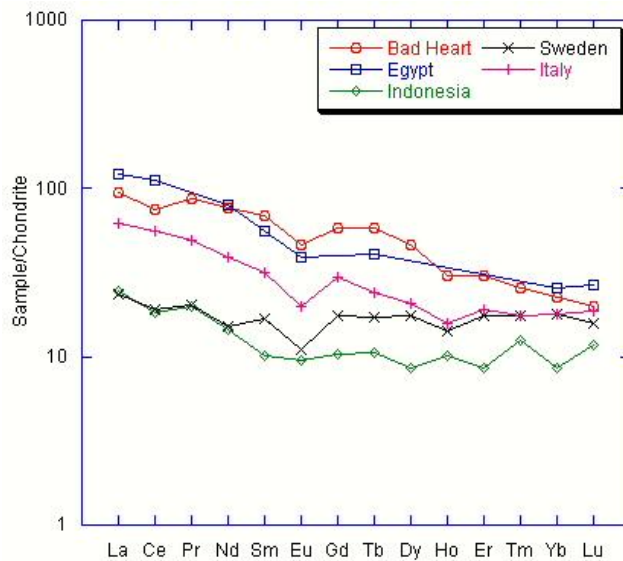


Figure 3.5 Comparison of chondrite normalized patterns of REE for Bad Heart Formation ooids with other oolitic ironstones from around the world, including Egypt (Bhattacharyya, 1981); Indonesia (Sturesson et al., 2000); Sweden (Sturesson, 1995); and Italy (Franceschelli et al., 2000)

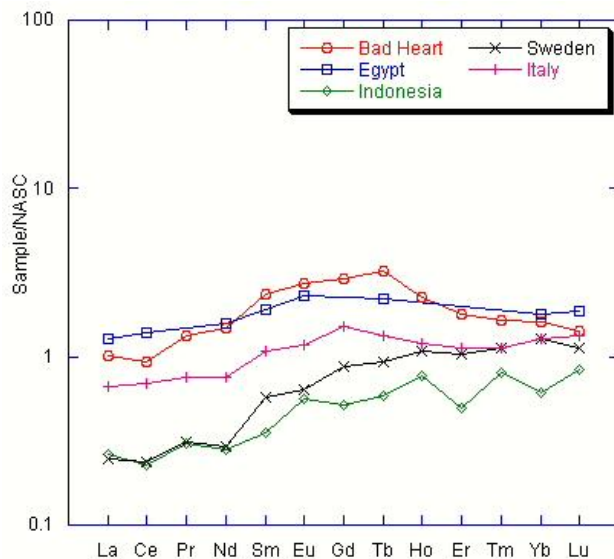


Figure 3.6 Comparison of NASC normalized patterns of REE for Bad Heart Formation ooids with other oolitic ironstones from around the world, including Egypt (Bhattacharyya, 1981); Indonesia (Sturesson et al., 2000); Sweden (Sturesson, 1995); and Italy (Franceschelli et al., 2000)

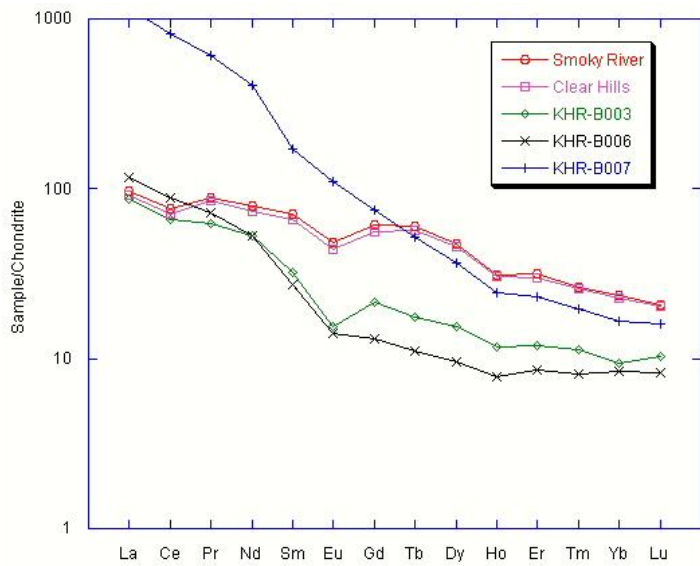


Figure 3.7 Comparison of chondrite normalized REE patterns for the Bad Heart

Formation ooids with Cretaceous bentonite (KHR-B003 & KHR-B006), kimberlite-sourced bentonite (KHR-B007) from northern Alberta. The bentonite data are from Eccles et al. (2008)

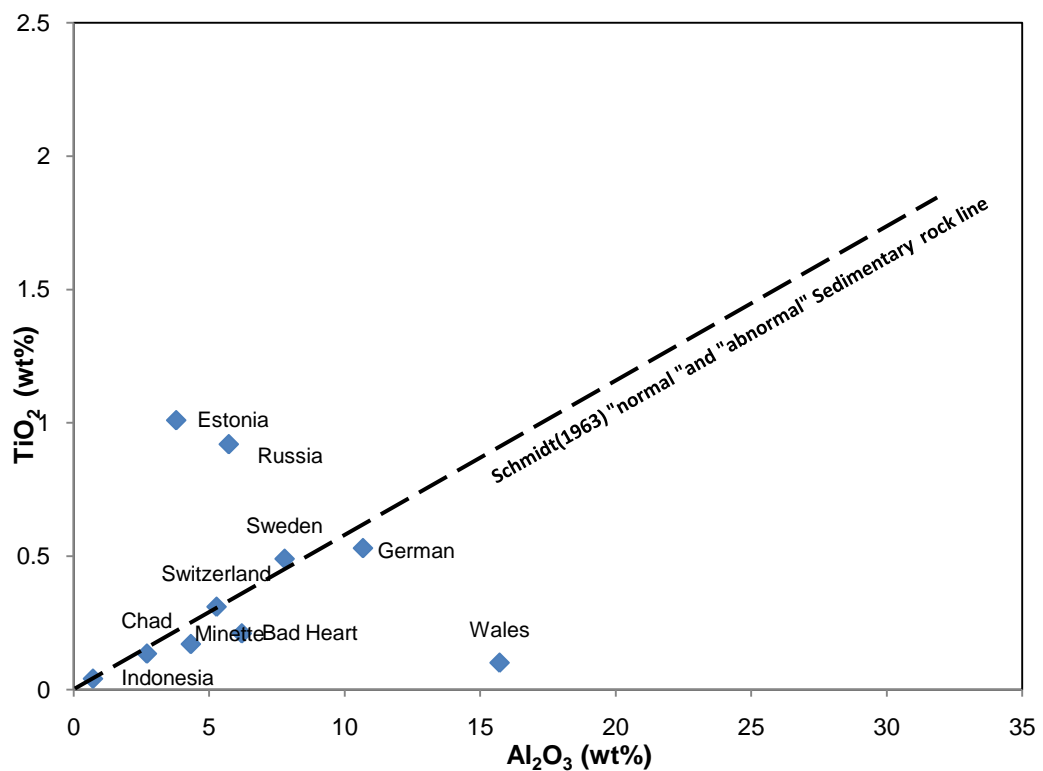


Figure 3.8 Ratio of  $\text{TiO}_2$  and  $\text{Al}_2\text{O}_3$  for iron ooids from different parts of the world. The dotted line in the middle approximates the limit of  $\text{TiO}_2/\text{Al}_2\text{O}_3$  ratios between “Normal” sedimentary rocks (below the line) and “Abnormal” sedimentary rocks (above the line) (Schmidt, 1963)

## REFERENCES

- Bayer, U., 1989, Stratigraphic and environmental patterns of ironstone deposits; Phanerozoic ironstones, Geological Society Special Publications, vol. 46, p. 105-117.
- Bhattacharyya, D., 1981, Sedimentology of the Late Cretaceous Nubia Formation at Aswan, southeast Egypt, and origin of the associated ironstones, Unpublished Ph.D. thesis, Princeton University, Princeton, USA, 229 p.
- Boulay,R.A., 1995, Report on Ironcap gold property, Peace River Area , Alberta, Unpublished Mineral assessment Report Prepared By Marum Resources, Inc., 26 p.
- Bubenicek, L., 1968, Geologie des minerais de fer oolithiques. Geology of oolitic iron ores, Mineralium Deposita, vol. 3, no. 2, p. 89-108.
- Burkhalter, R. M., 1995, Oolitic ironstones and ferruginous microbialites; origin and relation to sequence stratigraphy (Aalenian and Bajocian, Swiss Jura Mountains), Sedimentology, vol. 42, no. 1, p. 57-74.
- Colborne, G. L., 1958, Sedimentary iron in the Cretaceous of the Clear Hills area, Alberta, Master's thesis, University of Alberta, Edmonton, Canada ,102 p.
- Collom, C. J. 2001. Systematic paleontology, biostratigraphy, and paleoenvironmental analysis of the Wapiabi Formation and equivalents (Upper Cretaceous), Alberta and British Columbia, Western Canada .Unpublished Ph.D. thesis, University of Calgary, Calgary, 817 p..
- Collom, C. J., P. A. Johnston, and Anonymous, 2001, Oolitic ironstones; products of exhalative paleoenvironments in shallow epeiric seas; Earth system processes; programmes with abstracts, Geological Society of America and Geological Society of London.

Dahanayake, K. and W. E. Krumbein, 1986, Microbial structures in oolitic iron formations, Mineralium Deposita, vol. 21, no. 2, p. 85-94.

Donaldson, W. S., 1997, The sedimentology, stratigraphy and diagenesis of the Upper Cretaceous Bad Heart Formation, NW Alberta, Unpublished Ph.D. thesis, University of Western Ontario, London, Canada ,490 p.

Donaldson, W. S., A. G. Plint, and F. J. Longstaffe, 1999, Tectonic and eustatic control on deposition and preservation of Upper Cretaceous oolitic ironstone and associated facies; Peace River Arch area, NW Alberta, Canada, Sedimentology, vol. 46, no. 6, p. 1159-1182.

Dufresne, M. B., D. R. Eccles, and D. A. Leckie, 2001, The geological and geochemical setting of the Mid-Cretaceous Shaftesbury Formation and other Colorado Group sedimentary units in northern Alberta, EUB/AGS, Special report 09,55 p.

Eccles, D. R., R. A. Olson, C. J. Collom, and J. M. Peter, 2000, Trace element geochemical study of the Clear Hills iron deposits; genetic origin and potential co-products; GeoCanada 2000; the millennium geoscience summit, Abstract Volume (Geological Association of Canada), vol. 25.

Eccles, D. R., L. M. Heaman, and A. R. Sweet, 2008, Kimberlite-sourced bentonite, its paleoenvironment and implication for the Late Cretaceous K14 kimberlite cluster, northern Alberta, Canadian Journal of Earth Sciences, vol. 45, no. 5, p. 531-547.

Fernandez, A. and M. C. Moro, 1998, Origin and depositional environment of Ordovician stratiform iron mineralization from Zamora (NW Iberian Peninsula), Mineralium Deposita, vol. 33, no. 6, p. 606-619.

Fleet, A. J., 1984, Aqueous and sedimentary geochemistry of the rare earth elements, *in* Henderson, P., ed., Rare earth element geochemistry, Netherlands, Elsevier Sci. Publ. Co., Amsterdam, Netherlands , vol. 2.

Franceschelli, M., M. Puxeddu, and M. Carta, 2000, Mineralogy and geochemistry of Late Ordovician phosphate-bearing oolitic ironstones from SE Sardinia, Italy, *Mineralogy and Petrology*, vol. 69, no. 3-4, p. 267-293.

Green, R. and Mellon, G. B. 1962. Geology of the Chinchaga River and Clear Hills (north half) map-areas, Alberta. Alberta Research Council, Earth Science Reports 1962-08, 18 p.

Gross,G.A. 1996. Ironstone; in *Geology of Canada, Mineral Deposit Types*, ed. O.R. Eckstrand, W.D. Sinclair, and R.I. Thorpe, Geological Survey of Canada, *Geology of Canada*, no.8, p. 73-80

Gromet, L. P., R. F. Dymek, L. A. Haskin, and R. L. Korotev, 1984, The "North American shale composite"; its compilation, major and trace element characteristics, *Geochimica et Cosmochimica Acta*, vol. 48, no. 12, p. 2469-2482.

Guerrak, S., 1988, Ordovician ironstone sedimentation in Ougarta Ranges; north western Sahara (Algeria), *Journal of African Earth Sciences* (1983), vol. 7, no. 4, p. 657-678.

Gygi, R. A., 1981, Oolitic iron formations; marine or not marine? *Eclogae Geologicae Helvetiae*, vol. 74, no. 1, p. 233-254.

Hamilton, W. N., 1980, Clear Hills iron deposit geology, mineralogy and ore reserves; Alberta Research Council, EUB/AGS Open File Report 1982-13.\_43 p..

Haskin, L. A., T. R. Wildeman, F. A. Frey, K. A. Collins, C. R. Keedy, and M. A. Haskin, 1966, Rare earths in sediments, *Journal of Geophysical Research*, vol. 71, no. 24, p. 6091-6105.

Heikoop, J. M., C. J. Tsujita, M. J. Risk, T. Tomascik, and A. J. Mah, 1996, Modern iron ooids from a shallow-marine volcanic setting; Mahengetang, Indonesia, *Geology (Boulder)*, vol. 24, no. 8, p. 759-762.

James, H. E., Jr and F. B. van Houten, 1979, Miocene goethic and chamositic oolites, northeastern Colombia, *Sedimentology*, vol. 26, no. 1, p. 125-133.

Kafle, B. (2009): Geochemistry and preliminary stratigraphy of oolitic ironstone of the Bad Heart Formation, Clear Hills and Smoky River regions, northwestern Alberta; Energy Resources Conservation Board, ERCB/AGS Open File Report 2009-01, 97 p.

Kimberley, M. M., 1979, Origin of oolitic iron formations, *Journal of Sedimentary Petrology*, vol. 49, no. 1, p. 111-131.

Kimberley, M. M., 1989, Exhalative origins of iron formations, *Ore Geology Reviews*, vol. 5, no. 1-2, p. 13-145.

Landergren, S., 1948, On the geochemistry of Swedish iron ores and associated rocks; a study on iron-ore formation, *Sveriges Geologiska Undersökning, Serie C, Avhandlingar och Uppsatser*, vol. 5, no. 496, p. 182.

Leckie, D. A., C. Singh, M. J. Farabee, and L. N. Ford Jr., 1991, A shallow condensed section in the Cretaceous Shaftesbury Formation of northern Alberta; an integrated study; American Association of Stratigraphic Palynologists, 23<sup>rd</sup> annual meeting, *Palynology*, vol. 15, p. 246.

Leckie, D.A., J.P. Bhattacharya, J. Bloch, C.F. Gilboy and B. Norris, 1994, Cretaceous Colorado/Alberta Group of the Western Canada Sedimentary Basin, in G. Mossop & I. Shetsen (Eds.) *Atlas of the Western Canada Sedimentary Basin*, chapter 20, p. 335-352.

Macquaker, J. H. S., K. G. Taylor, T. P. Young, and C. D. Curtis, 1996, Sedimentological and geochemical controls on oolitic ironstone and "bone-bed" formation and some comments on their sequence-stratigraphical significance; *Sequence stratigraphy in British geology*, Geological Society Special Publications, vol. 103, p. 97-107.

Manning, P. G. and K. J. Gracey, 1991, Form and availability of inorganic phosphorus in suspended particulates of the Trent-Severn Waterway, Ontario, *The Canadian Mineralogist*, vol. 29, p. 575-585.

Maynard, J. B., 1986, Geochemistry of oolitic iron ores, an electron microprobe study, *Economic Geology and the Bulletin of the Society of Economic Geologists*, vol. 81, no. 6, p. 1473-1483.

McLennan, S. M., 1989, Rare earth elements in sedimentary rocks; influence of provenance and sedimentary processes; *Geochemistry and mineralogy of rare earth elements*, *Reviews in Mineralogy*, vol. 21, p. 169-200.

Mellon, G. B., 1962, Petrology of Upper Cretaceous oolitic iron-rich rocks from northern Alberta, *Economic Geology and the Bulletin of the Society of Economic Geologists*, vol. 57, no. 6, p. 921-940.

Olson, R.A., M.B. Dufresne, M.E. Freeman, R.J.H. Richardson, and D.R. Eccles, 1994, Regional Metallogenic Evaluation of Alberta. Alberta Energy and Utilities Board/Alberta Geological Survey, Open File Report 1994-08, 158 p.

Olson, R.A., D.R. Eccles, and C.J. Collom, 1999, A Study of Potential Co-Product Trace Elements Within the Clear Hills Iron Deposits, Northwestern Alberta; Alberta Energy and Utilities Board/Alberta Geological Survey Special Report 08, 87 p.

Pedro, G., J. P. Carmouze, and B. Velde, 1978, Peloidal nontronite formation in Recent sediments of Lake Chad, *Chemical Geology*, vol. 23, no. 2, p. 139-149.

Petranek, J. and F. B. Van Houten, 1997, Phanerozoic oolitic ironstones, Czech Geological Survey Special Papers, vol. 7, p. 71.

Petrak, W., 1977, Mineralogical characteristics of an oolitic iron deposit in the Peace River District, Alberta, *The Canadian Mineralogist*, vol. 15, p. 3-13.

- Petruk, W., D. M. Farrell, E. E. Laufer, R. J. Tremblay, and P. G. Manning, 1977a, Nontronite and ferruginous opal from the Peace River iron deposit in Alberta, Canada, The Canadian Mineralogist, vol. 15, p. 14-21.
- Petruk, W., I. B. Klymowsky, and G. O. Hayslip, 1977b, Mineralogical characteristics and beneficiation of an oolitic iron ore from the Peace River District, Alberta, CIM Bulletin, vol. 70, no. 786, p. 122-131.
- Price, N. B., 1976, Chemical diagenesis in sediments, *in* Riley, J. P. and R. Chester, eds., Chemical oceanography; Volume 6, United States (USA), Acad. Press, Inc.
- Schmidt, R. G., 1963, Geology and ore deposits of the Cuyuna North range, Minnesota, U.S. Geological Survey Professional Paper, vol. P0407, p. 96.
- Siehl, A. and J. Thein, 1989, Minette-type ironstones; Phanerozoic ironstones, Geological Society Special Publications, vol. 46, p. 175-193.
- Simpson, T.A. and Gray, T. R., 1968, The Birmingham Red-Ore District, Alabama; *in* Ridge, J.D. (Ed.) Ore Deposits of the United States, 1933-1967, the Graton-Sales Volume, p. 187-206.
- Skocek, V., N. Al-Qaraghuli, and A. A. Saadallah, 1971, Composition and Sedimentary Structures of Iron Ores from the Wadi Husainiya Area, Iraq, Economic Geology and the Bulletin of the Society of Economic Geologists, vol. 66, no. 7, p. 995-1004.
- Sturesson, U., 1995, Llanvirnian (Ord.) iron ooids in Baltoscandia; element mobility, REE distribution patterns, and origin of the REE, Chemical Geology, vol. 125, no. 1-2, p. 45-60.
- Sturesson, U., 2003, Lower Palaeozoic iron oolites and volcanism from a Baltoscandian perspective, Sedimentary Geology, vol. 159, no. 3-4, p. 241-256.

Sturesson, U., J. M. Heikoop, and M. J. Risk, 2000, Modern and Palaeozoic iron ooids; a similar volcanic origin, *Sedimentary Geology*, vol. 136, no. 1-2, p. 137-146.

Sweet, A.R., 2009. Applied research report summarizing the palynofacies for 47 core and outcrop samples from the southern Clear Hills, Rambling River area (NTS84D/15) and along the Smoky River (NTS83M/09 and 83N/12). Geological Survey of Canada, Paleontological Report ARS-2009-12, 15 p.

Taylor, S. R. and S. M. McClenan, 1985, The continental crust; its composition and evolution; an examination of the geochemical record preserved in sedimentary rocks, United Kingdom , Blackwell Sci. Publ., Oxford.

Taylor, K. G. and C. D. Curtis, 1995, Stability and facies association of early diagenetic mineral assemblages; an example from a Jurassic ironstone-mudstone succession, U.K, *Journal of Sedimentary Research, Section A: Sedimentary Petrology and Processes*, vol. 65, no. 2, p. 358-368.

Taylor, K. G., J. A. Simo, D. Yocum, and D. A. Leckie, 2002, Stratigraphic significance of oolitic ironstones from the Cretaceous Western Interior Seaway; the Peace River Formation, Alberta, Canada, and the Castlegate Sandstone, Utah, U.S.A, *Journal of Sedimentary Research*, vol. 72, no. 2, p. 316-327.

Teyssen, T., 1989, A depositional model for the Liassic Minette ironstones (Luxembourg and France), in comparison with other Phanerozoic oolitic ironstones; in Young, T.P. and Taylor, W.E.G. (Eds.), *Phanerozoic Ironstones*; published by The Geological Society of London as Special Publication No. 46, p. 79-92.

Tucker, M. E., 1981, *Sedimentary petrology : an introduction*, Toronto, John Wiley & Sons, 252 p.

Turekian, K. K. and K. H. Wedepohl, 1961, Distribution of the elements in some major units of the earth's crust, Geological Society of America Bulletin, vol. 72, no. 2, p. 175-191.

Van Everdingen, R.O., 1970, The Paint Pots, Kootenay National Park, British Columbia - acid spring water with extreme heavy-metal content, Canadian Journal of Earth Sciences, vol. 7, p. 831-852.

Van Everdingen, R.O., M.A. Shakur, and F.A. Michel, 1985, Oxygen- and sulfur-isotope geochemistry of acidic groundwater discharge in British Columbia, Yukon and District of Mackenzie, Canada, Canadian Journal of Earth Science, vol. 22, p. 1689-1695.

Van Houten, F. B., 1990, Palaeozoic oolitic ironstones on the North American Craton, Palaeogeography, Palaeoclimatology, Palaeoecology, vol. 80, no. 3-4, p. 245-254.

Van Houten, F. B. and M. A. Arthur, 1989, Temporal patterns among Phanerozoic oolitic ironstones and oceanic anoxia; Phanerozoic ironstones, Geological Society Special Publications, vol. 46, p. 33-49.

Young, T. P., 1989, Phanerozoic ironstones:an introduction and review; in Young, T.P. and Taylor, W.E.G. (Eds.), Phanerozoic Ironstones; published by The Geological Society of London as Special Publication No. 46, p. iv-xxv.

Young, T.P. and Taylor, W.E.G. (Eds.), Phanerozoic Ironstones, 1989; published by The Geological Society of London as Special Publication No. 46, 251 p.

Ziegler, A.C. and Combs, L.J., 1997,, Baseline data-collection and quality-control protocols and procedures for the Equus beds ground-water recharge demonstration project near Wichita, Kansas, 1995-06; U.S. Geological Survey, Open-File Report 97-235, 23 p.

## CHAPTER 4: CONCLUSIONS

This thesis presents new stratigraphy and geochemistry data from the Bad Heart Formation. It is proposed herein that the late Coniacian Bad Heart Formation consists of three sandstone, siltstone and oolitic ironstones successions in the Smoky River region, whereas only two successions are present in the Clear Hills region. The new palynology data collected during this study show that downward range truncation of the dinoflagellate *Chatangiella sp. cf. C. spectabilis* is at the lower boundary of the Bad Heart Formation.

At the Smoky River, the two lowermost Bad Heart Formation successions both comprise upward coarsening facies, which predominantly comprise siltstone, sandstone and oolitic ironstone with minor amounts of pebble conglomerate at the base of each succession. These lower successions are bound by three erosion surfaces: (1) a basal erosion surface (BES) and (2) erosion surfaces at the top of each succession (named ES1 and ES2, respectively). In contrast, the third or uppermost Bad Heart Formation succession occurs above the ES2 erosion surface, is upward fining, and grades into the Puskwaskau Formation shale. Oolitic ironstone is more prevalent at the top of succession 1 along the central parts of Smoky River, although at the Spirit River (SPRV) and Blueberry Mountain (BBM) sections, which are northwest of the Smoky River, and at the Worsley Pit section in the Clear Hills region, a 1 m to 2 m thick oolitic ironstone is present above the ES2 erosional surface. The thick oolitic ironstone present only in the lowermost succession along the central Smoky River, plus the associated ichno-fossils, shows that the ooids formed in a shallow marine, wave-agitated environment, and thus indicate this area was uplifted by syn-depositional tectonic activity along two inferred faults, F2 and F3, which resulted in shallow shoals above the wave base where the oolitic ironstone deposits could form. In the Clear Hills region, the thickest oolitic ironstone beds are at and just westerly of the Rambling Creek exposures, which indicates this area was also a wave-

agitated shallow shoal during the deposition of the thick ironstone which occurs in this region.

The oolitic ironstone-sandstone sequence at the Botha River in the northern Naylor Hills, which formerly was believed to be Bad Heart Formation, now is known, based on the palynology data from this study, to be clearly older and of Lower Kaskapau Formation age and hence is probably correlative with the thin oolitic ironstone-sandstone sequence in the Lower Kaskapau Formation, which is observed at Dunvegan Crossing along the Peace River. As a result, the Bad Heart Formation in the Clear Hills region is much more areally restricted, and thus the northern limit of the Bad Heart Formation may be only just to the north of the Rambling Creek locale.

The textural features of the Bad Heart Formation ooids suggest the ooids formed in place, at or near to where they now exist, in a wave-agitated environment by a repetitive process of concentric growth of the ooids in the water column; once their weight became sufficiently heavy, and/or the wave energy decreased, the ooids deposited on the sea floor, in places, some further reworking possibly resulted, in increased ooid enlargement to form pisoids. Further, the larger size of the ooids in the Clear Hills region suggests either higher wave energy or more reworking on the sea floor, or both, in comparison to the smaller ooids at the Smoky River region. There are two distinct types of ooids: (1) one has a thick laminated concentric cortex, and (2) the other has a large nucleus and thin cortex. In general, their average size (diameter) is about the same, which indicates their weight or mass is equivalent; hence, the ooids with a larger nucleus could not be supported long enough in the water column to form a thick laminated cortex.

The bulk of the evidence indicates the depositional environment during the Coniacian Bad Heart Formation deposition was oxidizing. This conclusion is supported by the geochemical data, lack of sulphide, and common macro- and ichno-fossil assemblages. However, the unweathered oolitic ironstone in the core from drill hole DDH0203, which is west of the Rambling Creek oolitic ironstone outcrops in the eastern Clear Hills, is dark green in colour, indicating the iron now is in the ferrous ( $\text{Fe}^{2+}$ ) state. Thus, this suggests

that the initially oxidized ferric ( $\text{Fe}^{3+}$ ) minerals in the ooids were converted to the ferrous state during burial diagenesis.

The exact provenance of the large amount of iron in the Bad Heart Formation oolitic ironstones is still not resolved. However, some geochemical data from this present study, such as high  $\text{P}_2\text{O}_5$  and Zn, low  $\text{TiO}_2/\text{Al}_2\text{O}_3$  and negative Eu anomaly, indicate a continental sedimentary source for the iron. As well, the absence of volcanic material in the samples from this study and the different REE pattern of Cretaceous northern Alberta bentonites and Bad Heart Formation ooids are not characteristic of the volcanic hydrothermal oolitic ironstone from other parts of the world. Based on the evidence from this study, igneous or volcanic activity was unlikely to have been important during the Bad Heart Formation time. Having said this, the Bad Heart ooids are enriched in some elements associated with sub-sea hydrothermal or meteoric vent processes analogous to those presently forming the modern oxide iron deposits at the Paint Pots in Kootenay National Park, British Columbia. The data from this study indicate a continental source of iron for Bad Heart Formation may be more likely, but at the same time the data are still permissive and thus the source of iron could be from deep circulating meteoric or possibly other hydrothermal solutions that vented onto the sea floor during the Bad Heart Formation time. However, it is considered highly unlikely that the source of the iron was from volcanic or other igneous sources.

Some suggestions for future work include:

1. More closely spaced shallow well-log data (which are now starting to become available after the ERCB directive in late 2006 that in the future, all oil and gas drilling must collect well-log data from the ground surface) could be used to construct a more detailed subsurface stratigraphy of the Bad Heart Formation, especially in the Clear Hills region, which has very few natural outcrops, drill cores or oil/gas geophysical well-log data.

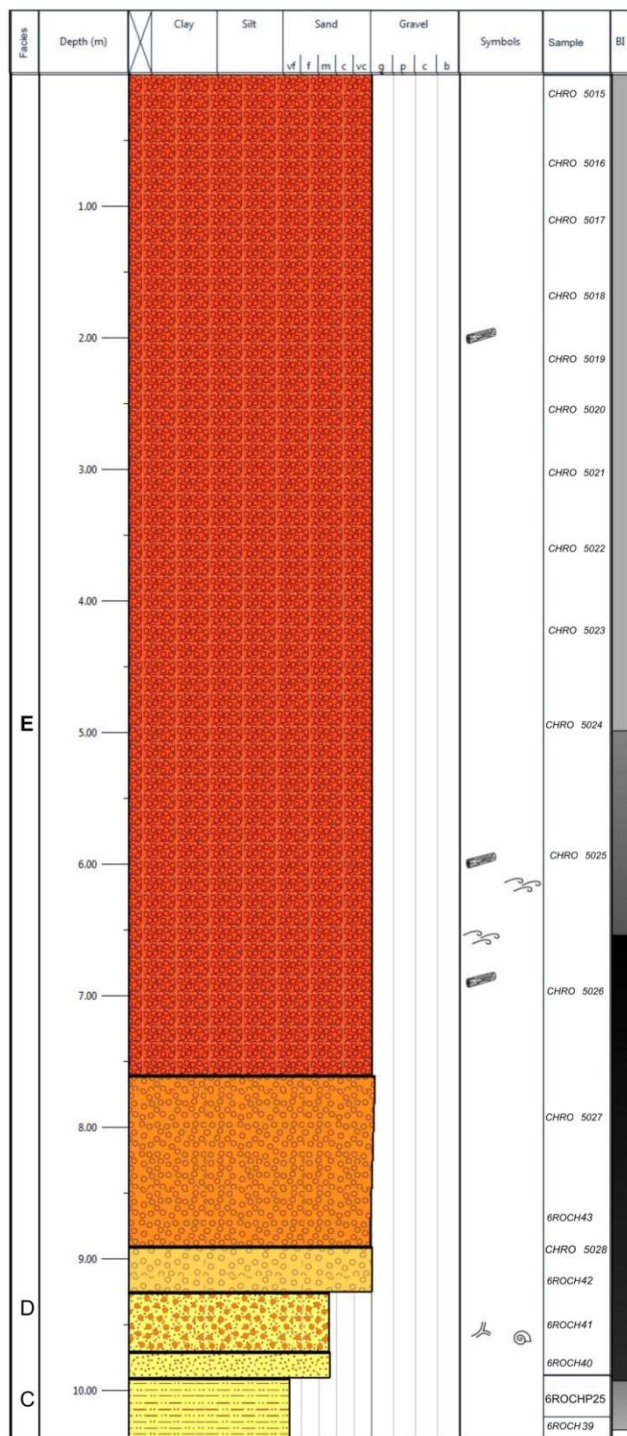
2. Various isotopic studies could be used to evaluate the provenance of the detrital, oolitic and matrix components of the Bad Heart Formation. For example, a study of the oxygen isotope composition of the detrital quartz grains could assist in determining the provenance of the coarser clastic content of the Bad Heart Formation sediments.

## APPENDIX I: STRATIGRAPHIC SECTIONS

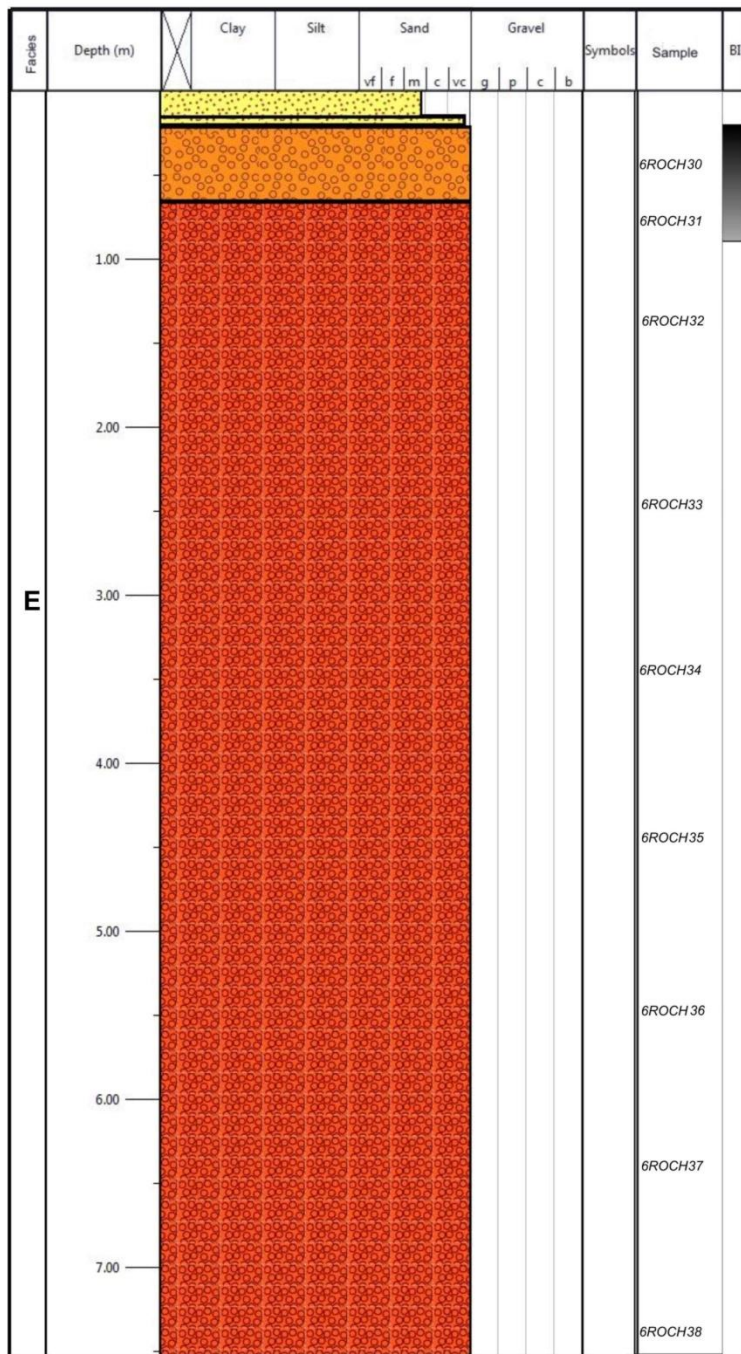
### LEGEND

Lithology	Symbols
Till	
Clast-supported conglomerate	
Matrix-supported conglomerate	
Pebbly sandstone	
Intensely ooidal ironstone (IOIS) (>70% ooids)	
Moderately ooidal ironstone (MOIS) (30-70% ooids)	
Weakly ooidal ironstone (WOIS) (10-30% ooids)	
Ooidal sandstone (<10% ooids)	
Sandstone	
Silty sandstone	
Siltstone	
Light to medium grey shale	
Dark grey to black shale	
Silty shale	
Breccia clasts in shale	
Concretion layer	

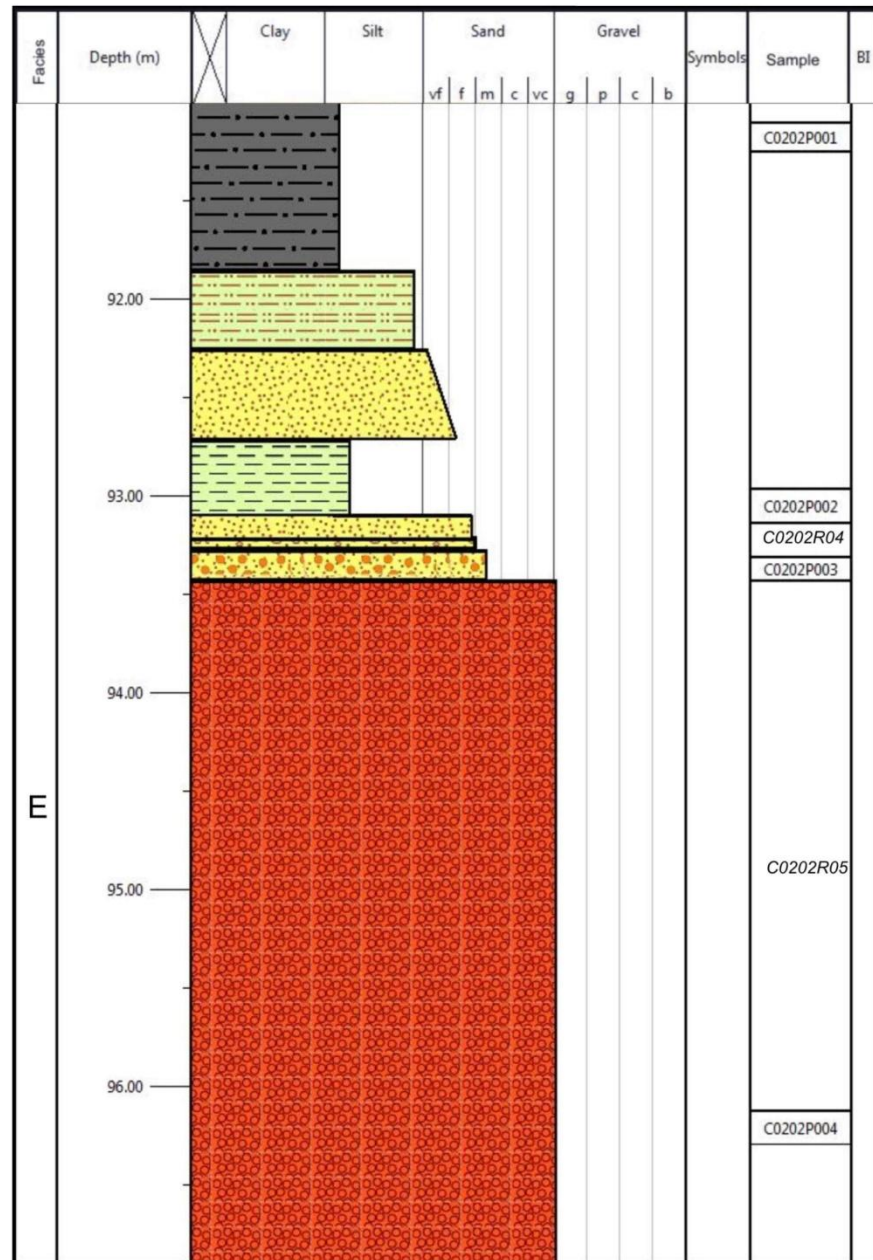
### Section ARR3

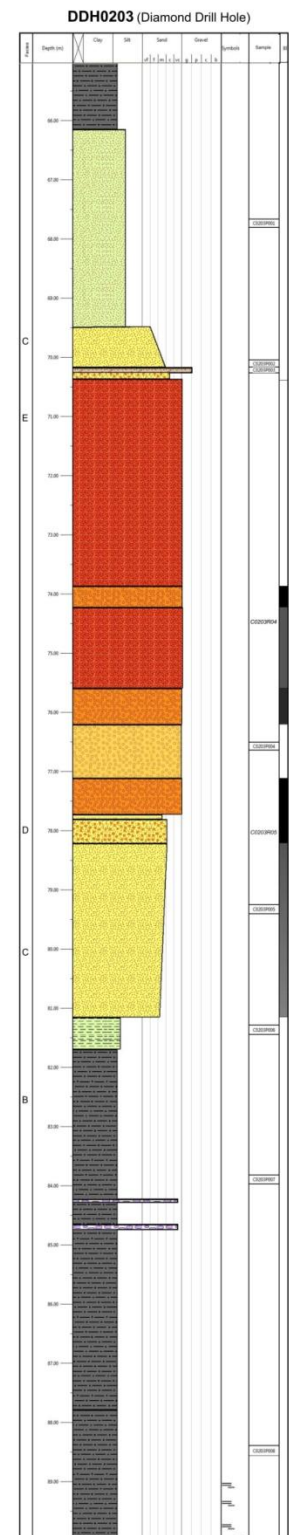


### Section ARR5

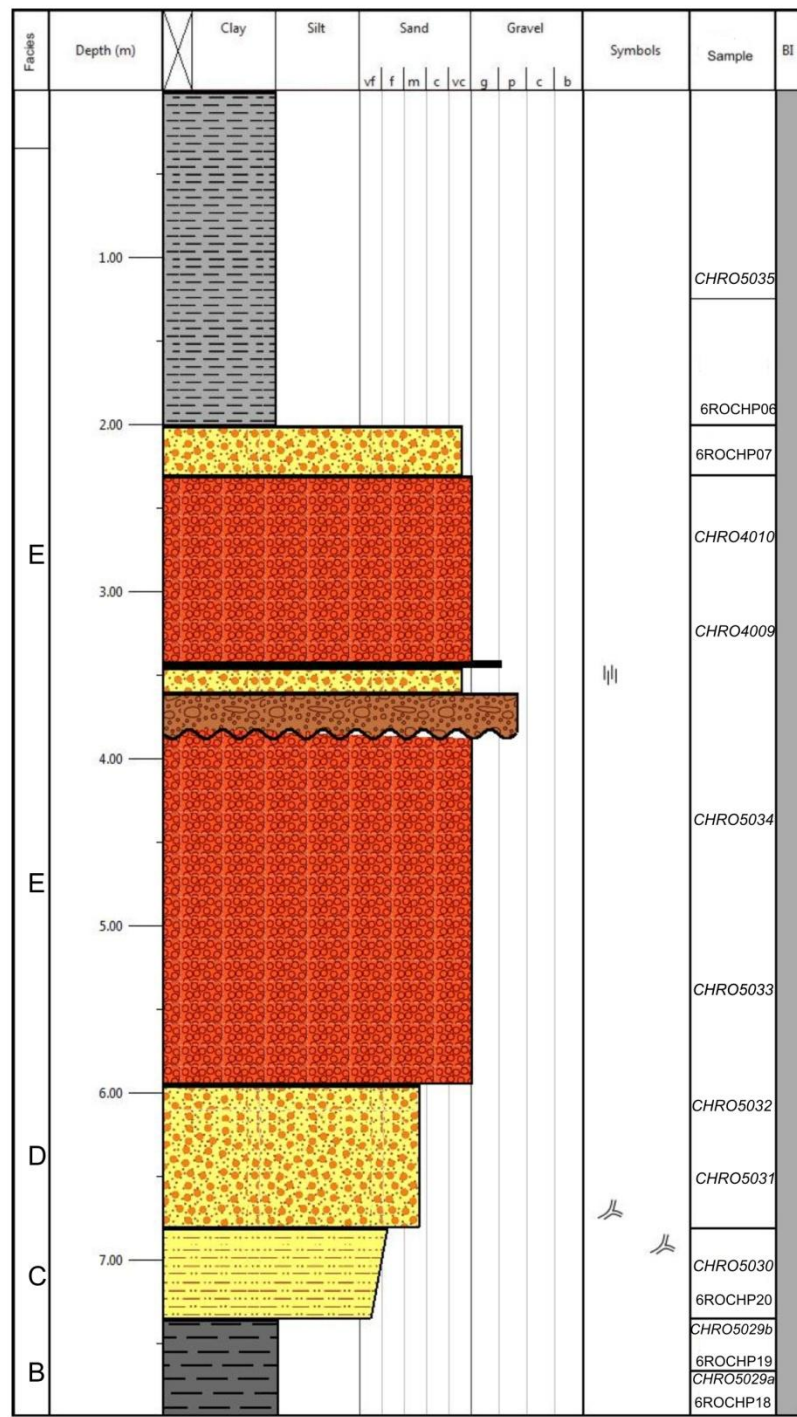


## DDH0202(Diamond Drill Hole)

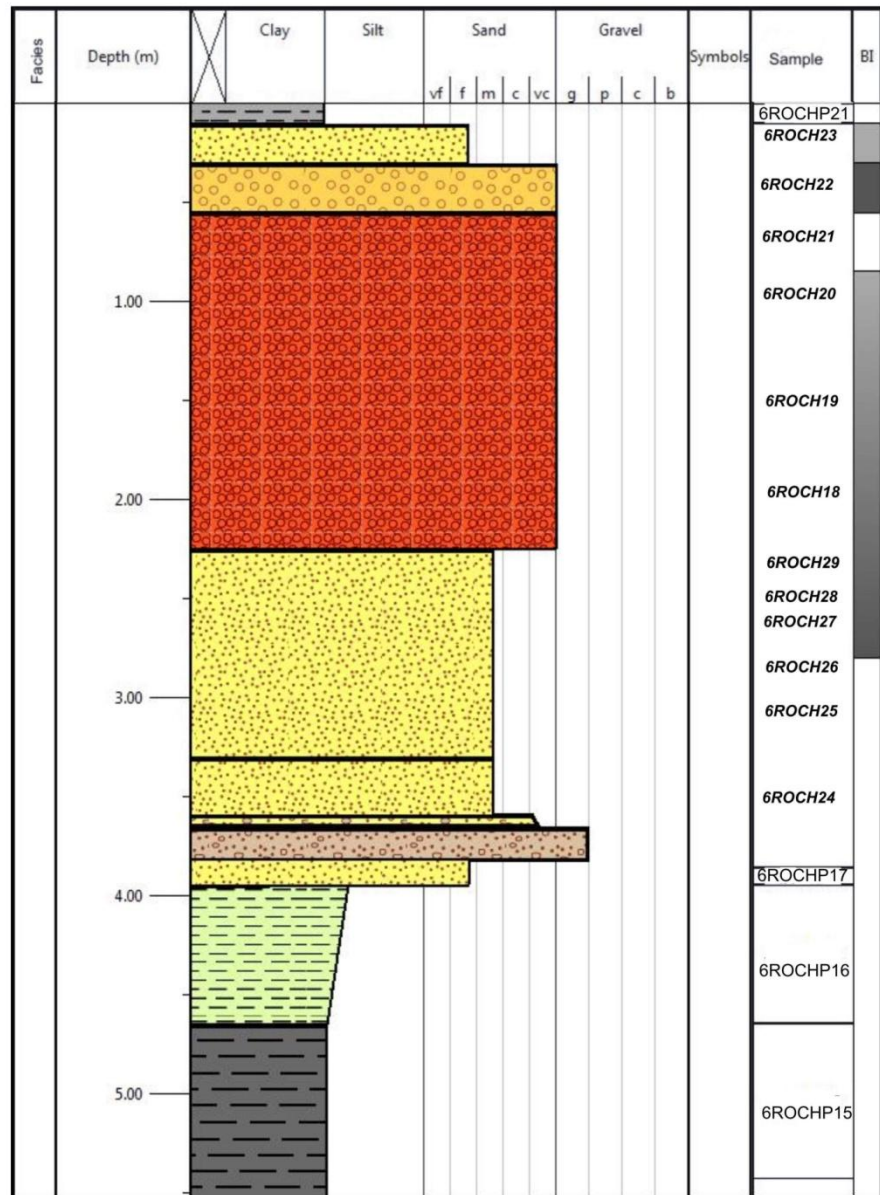




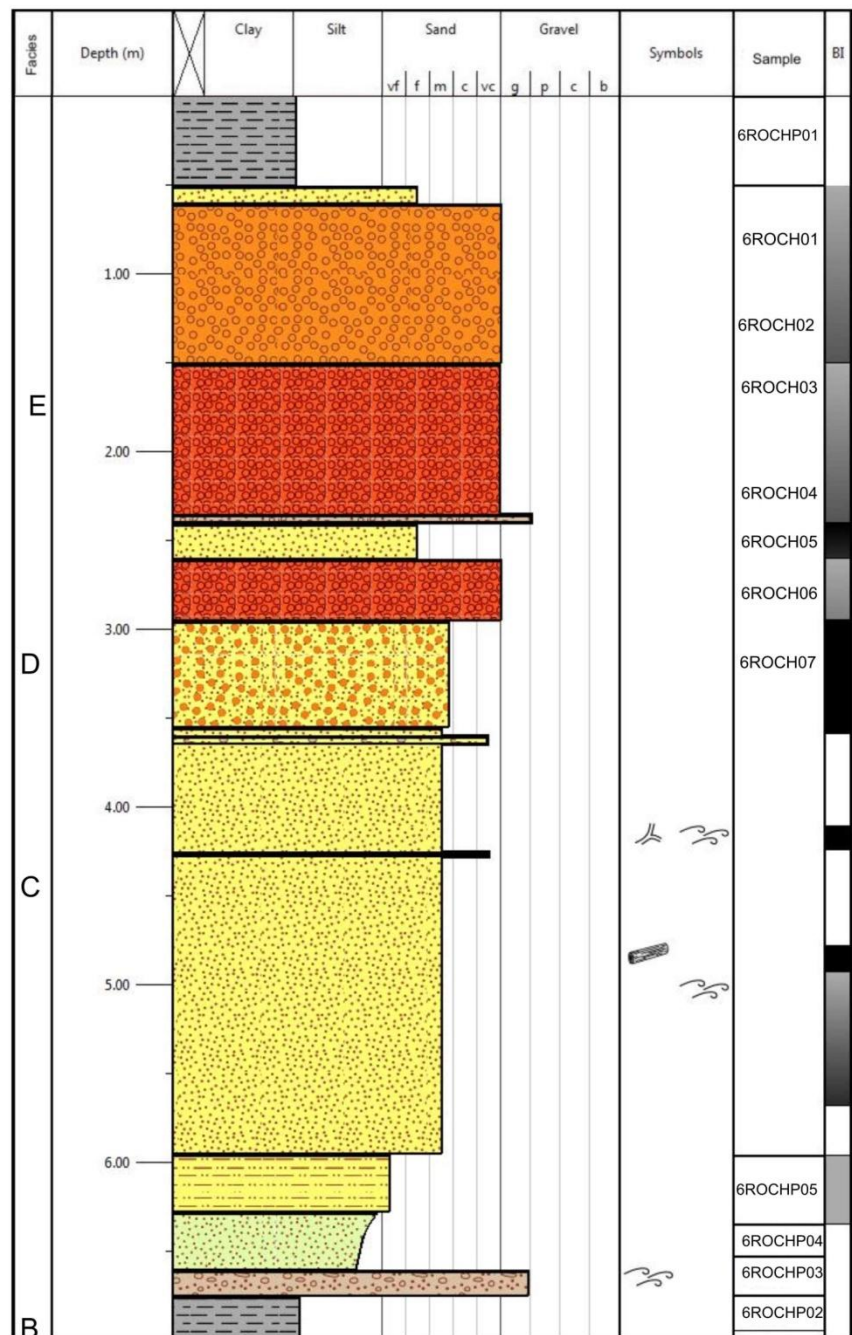
## Section Worsley



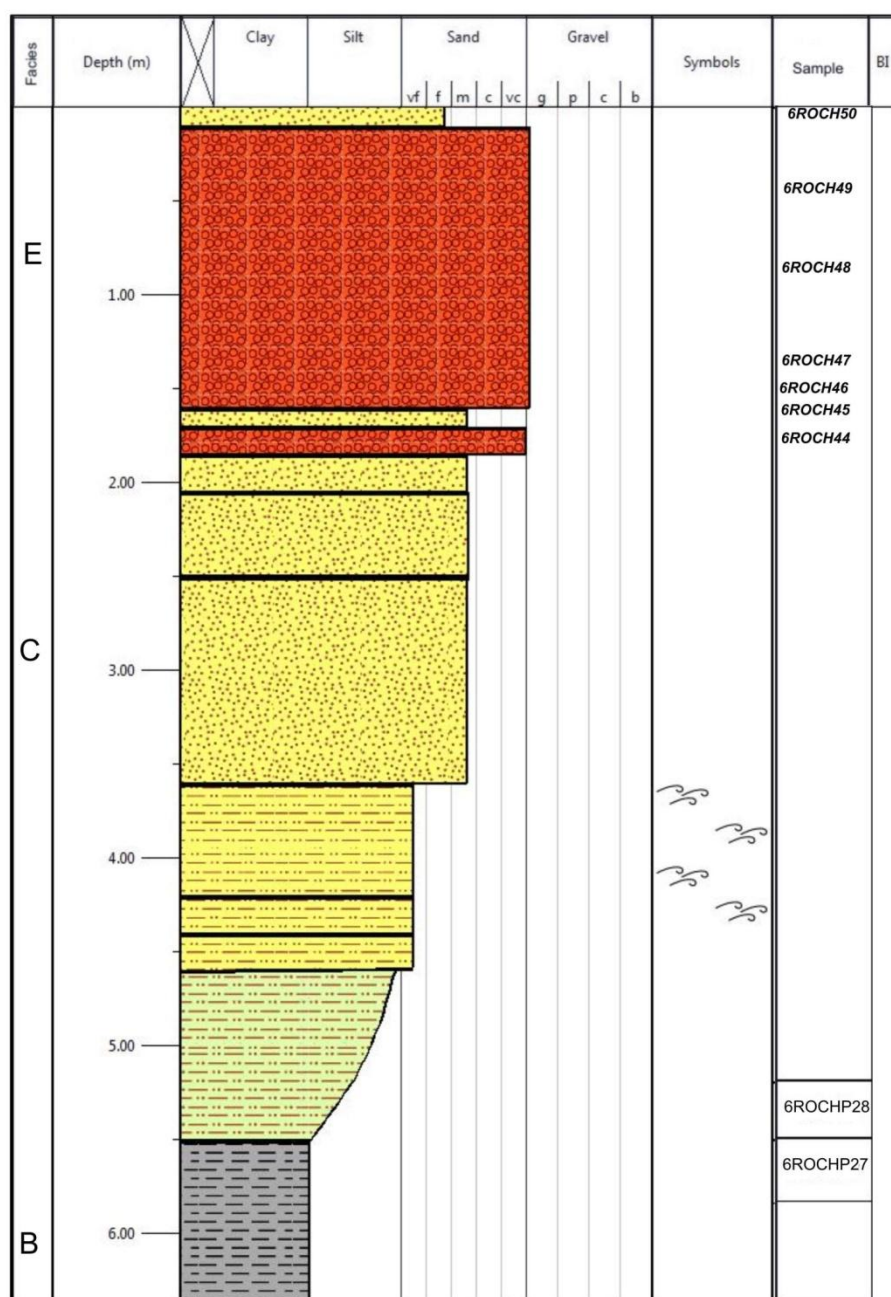
Section KC14



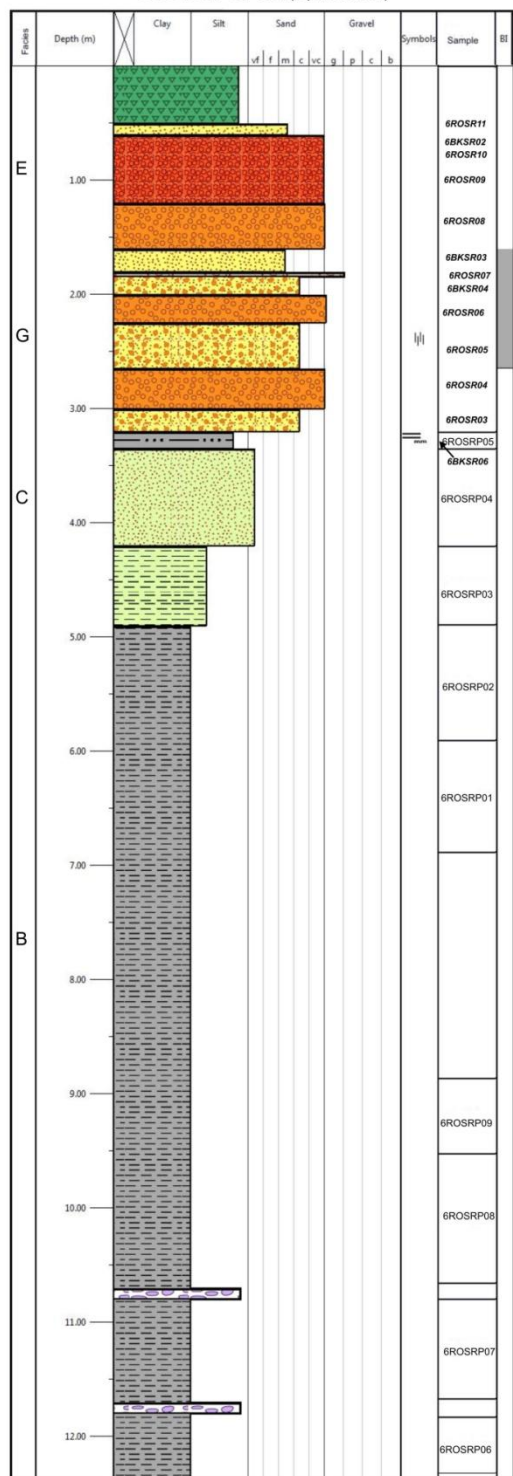
## Section LVH



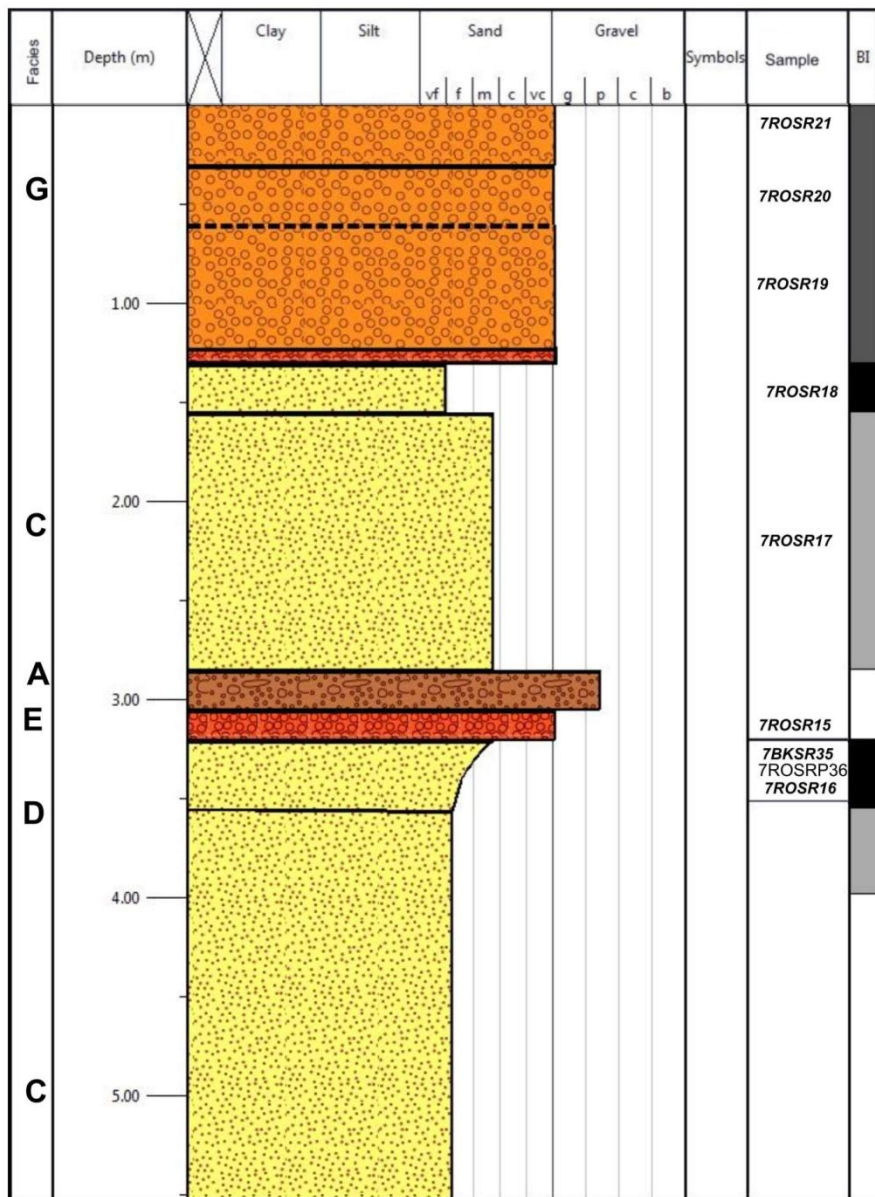
Section KC17



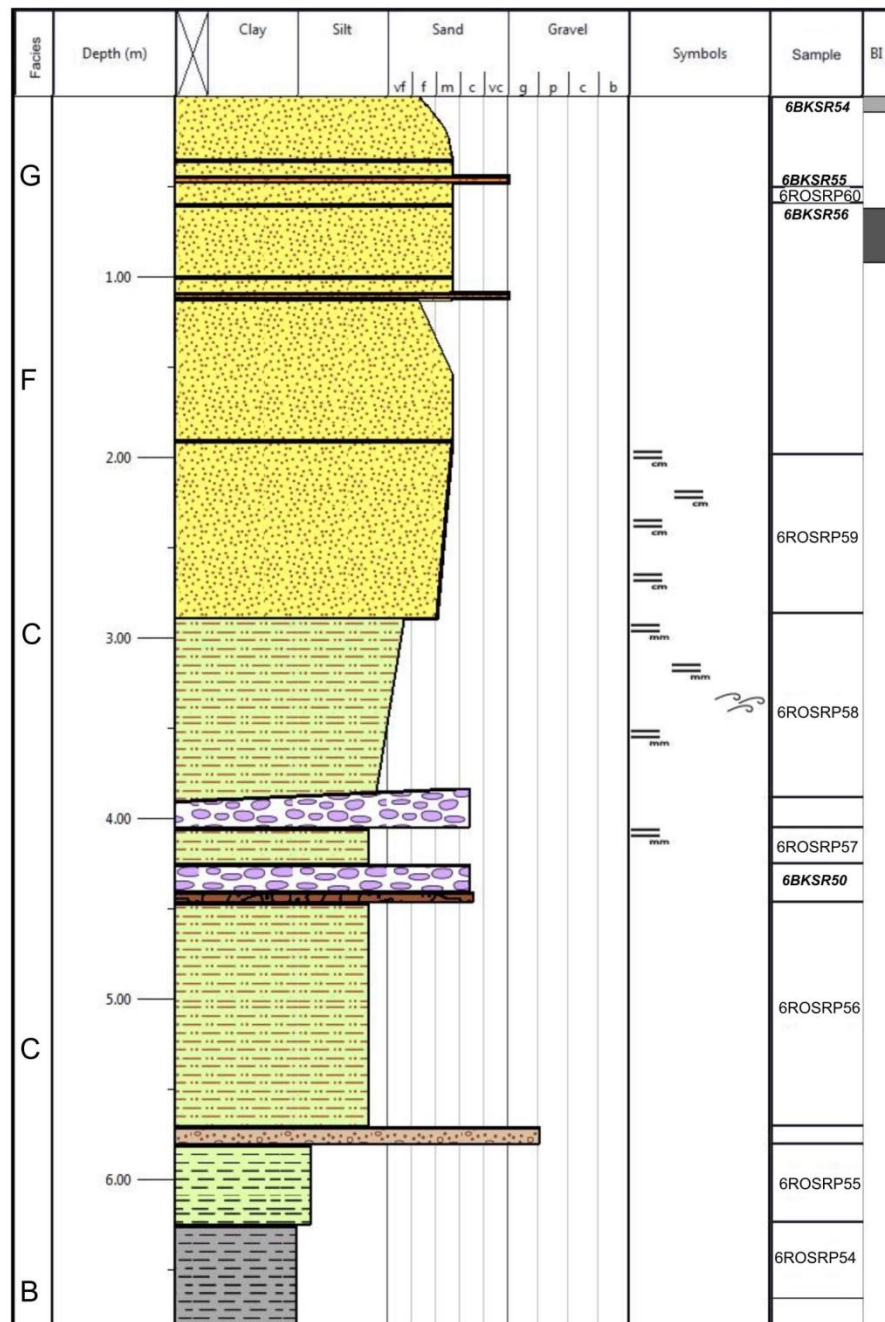
**Section SPRV(Spirit River)**

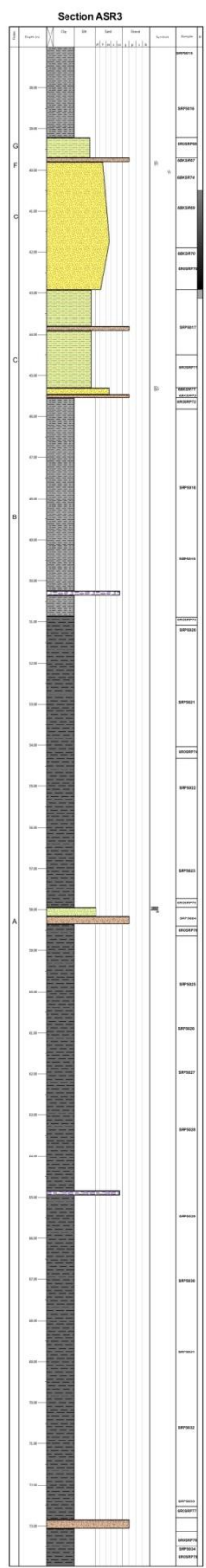


## Section BBM(Blueberry Mountain)

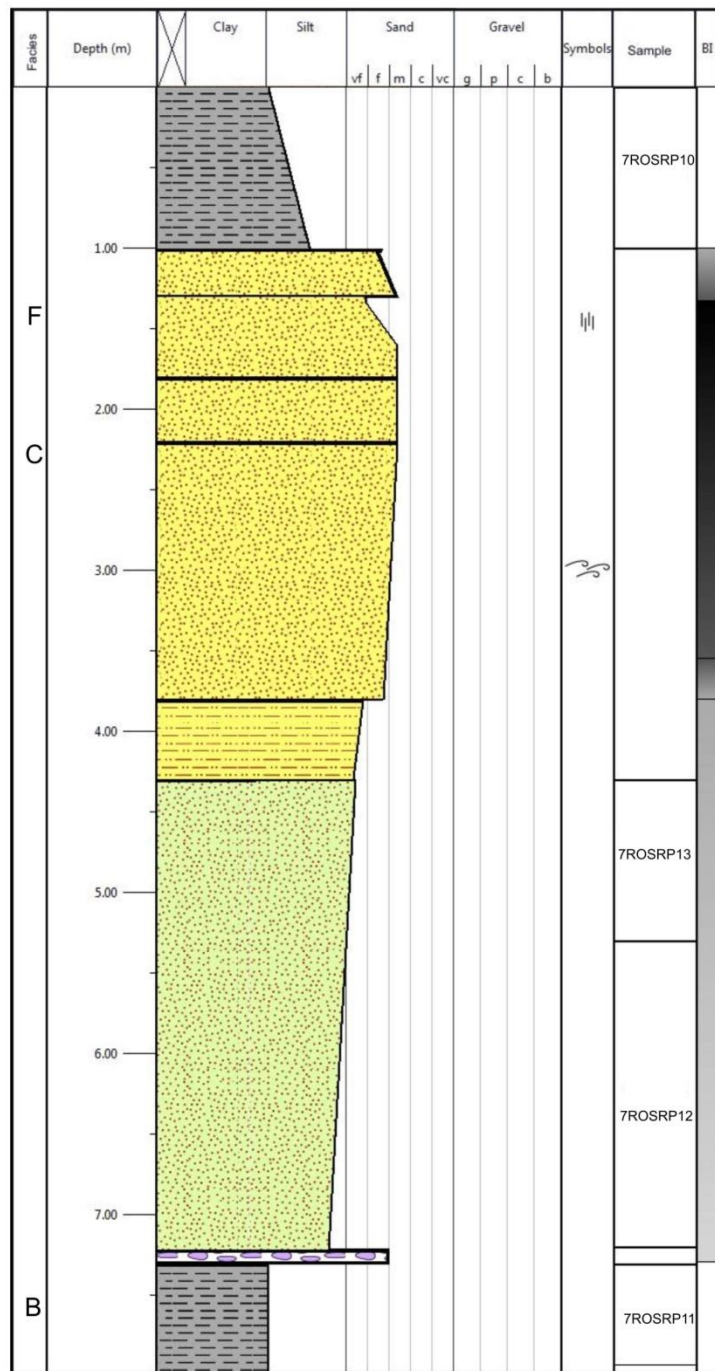


## **Section WH(Wanham)**

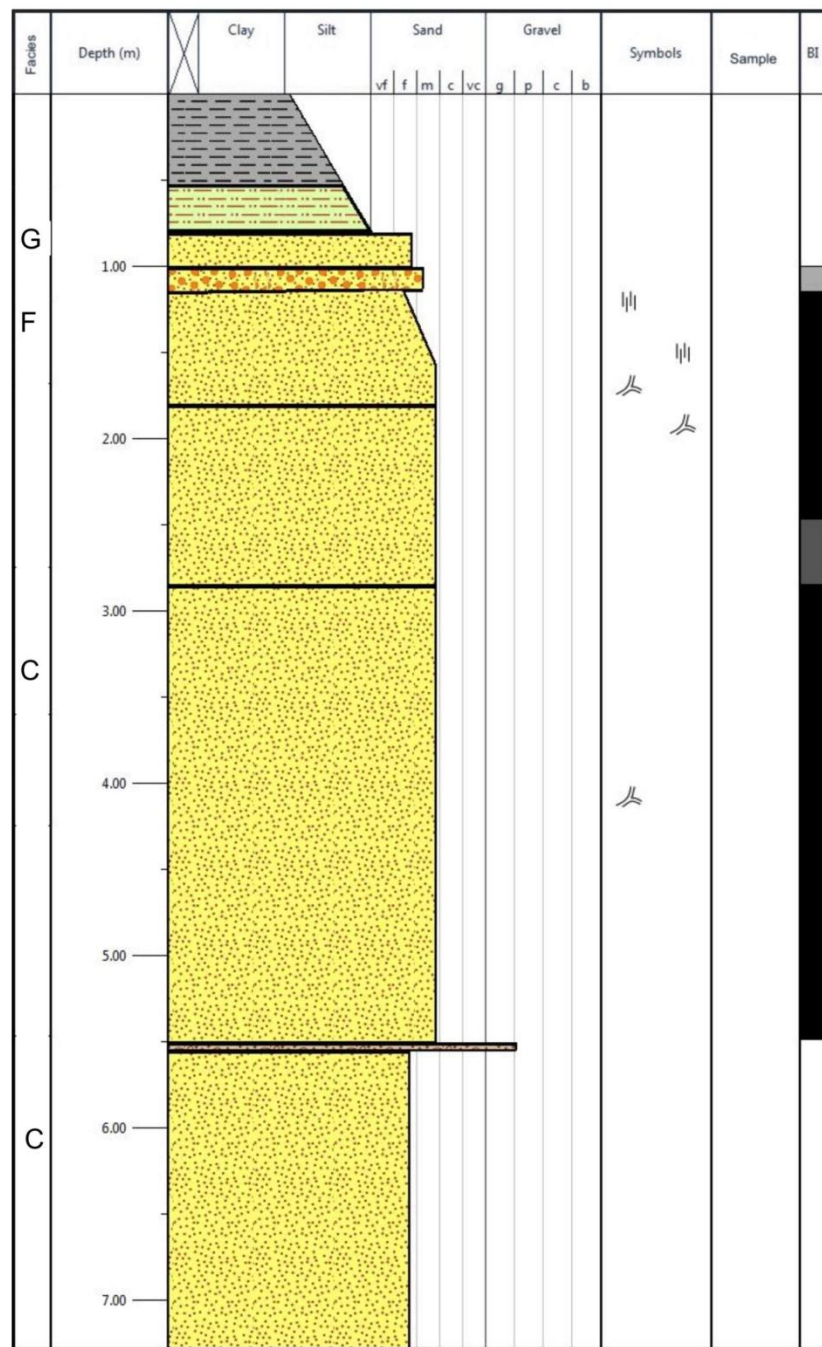




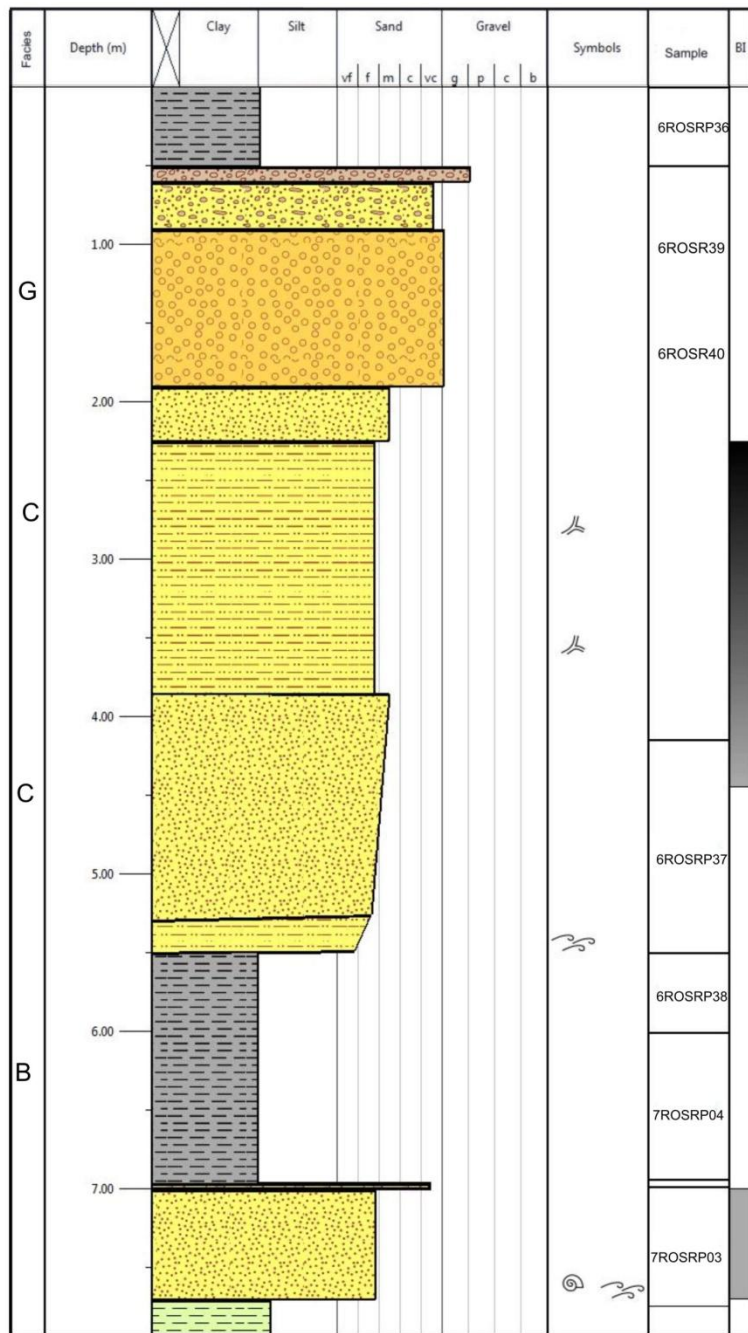
### Section ASR2D



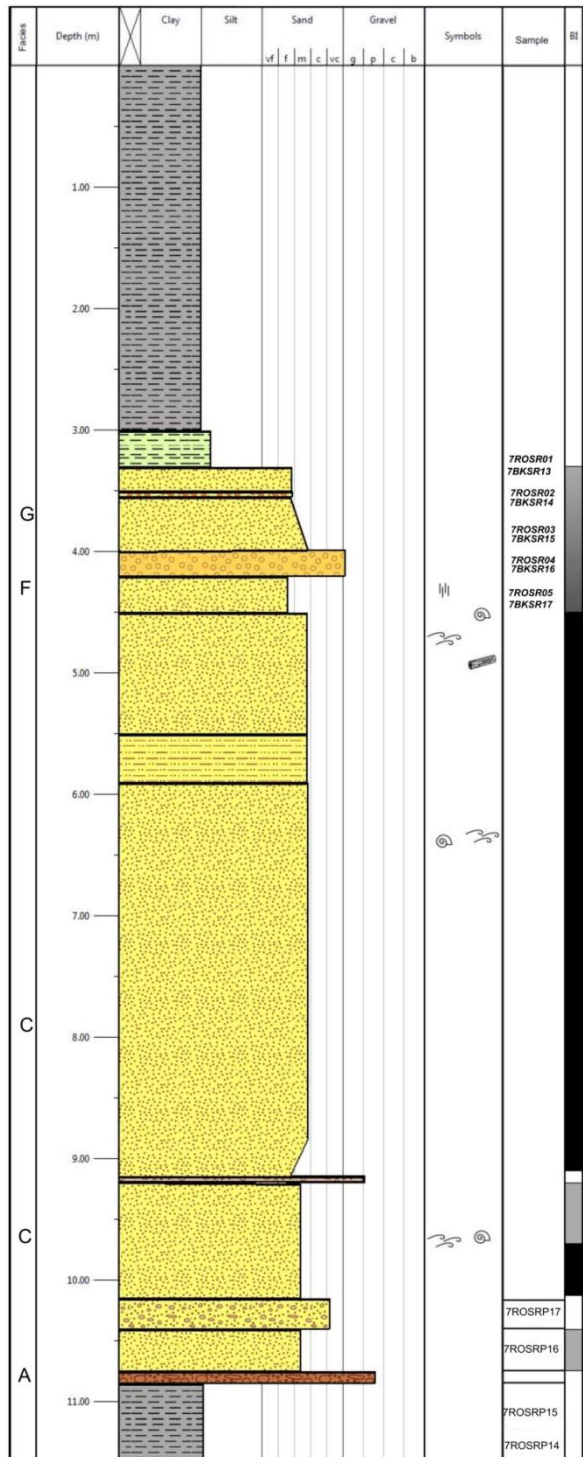
### Section ASR2A



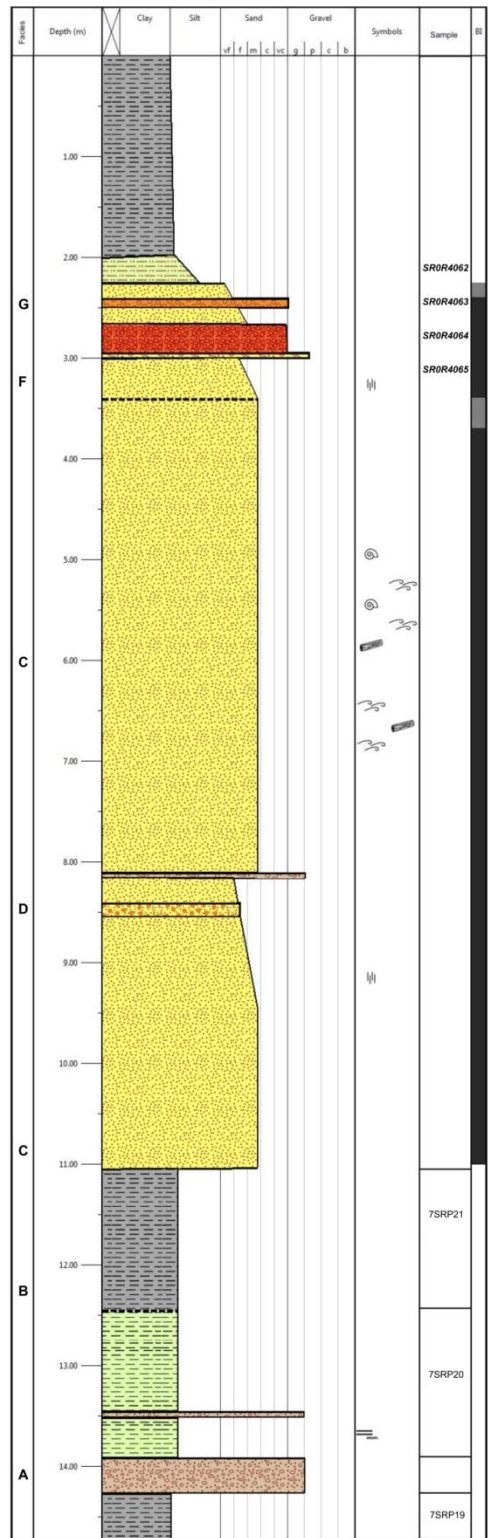
### Section ASR4



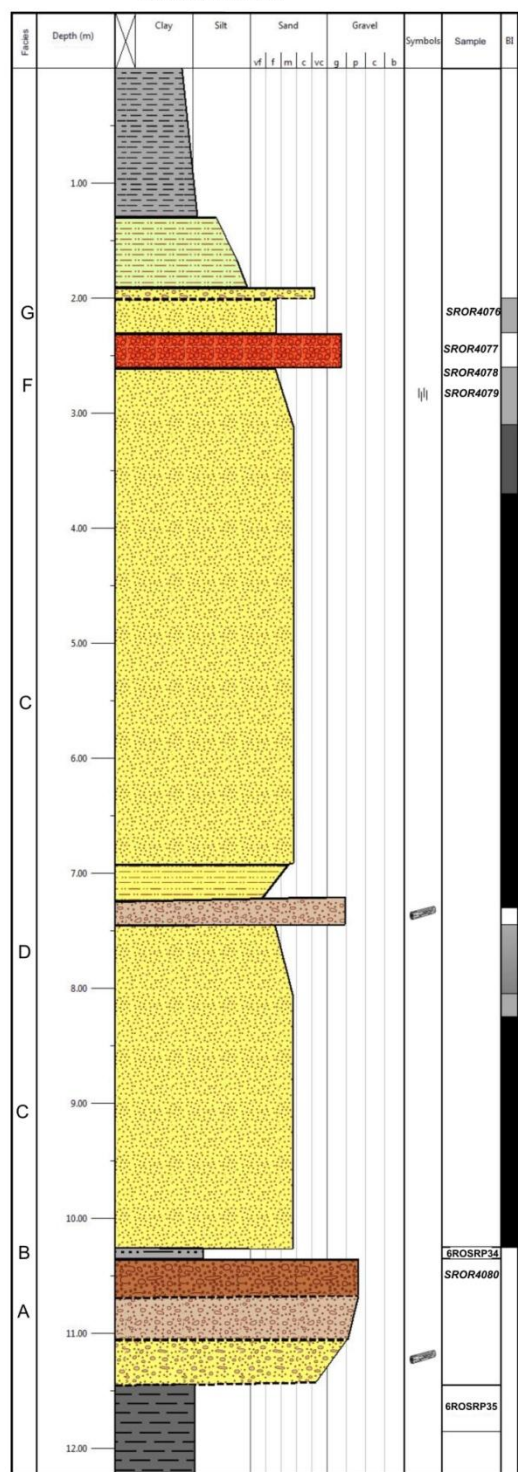
### Section ASR5



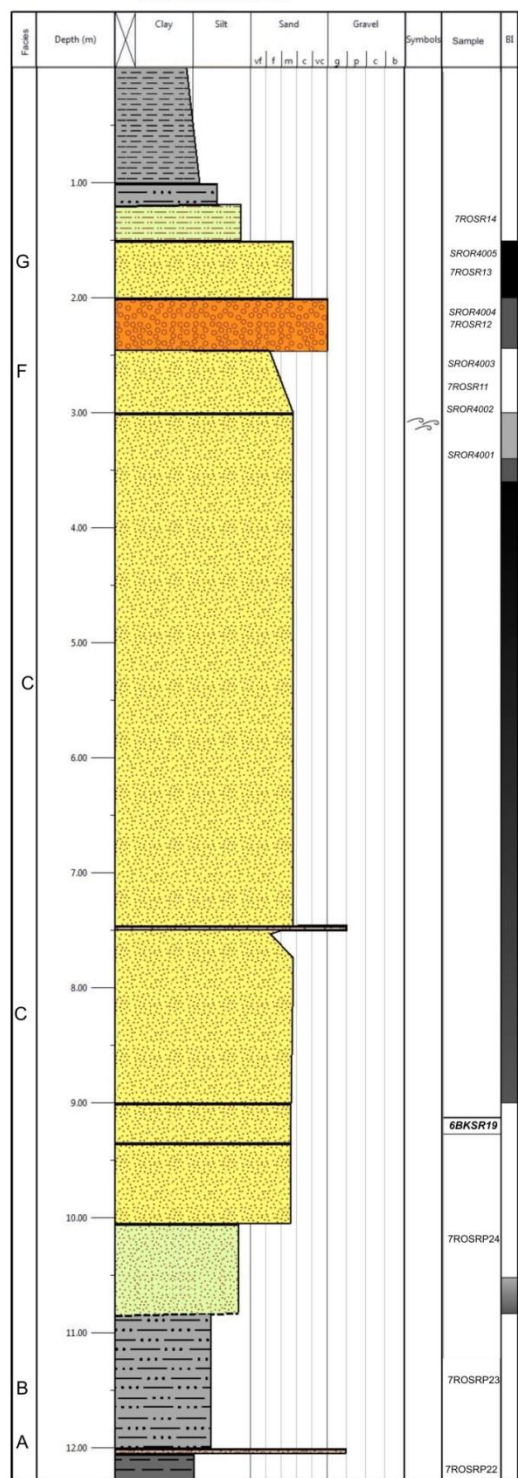
**Section ASR6**



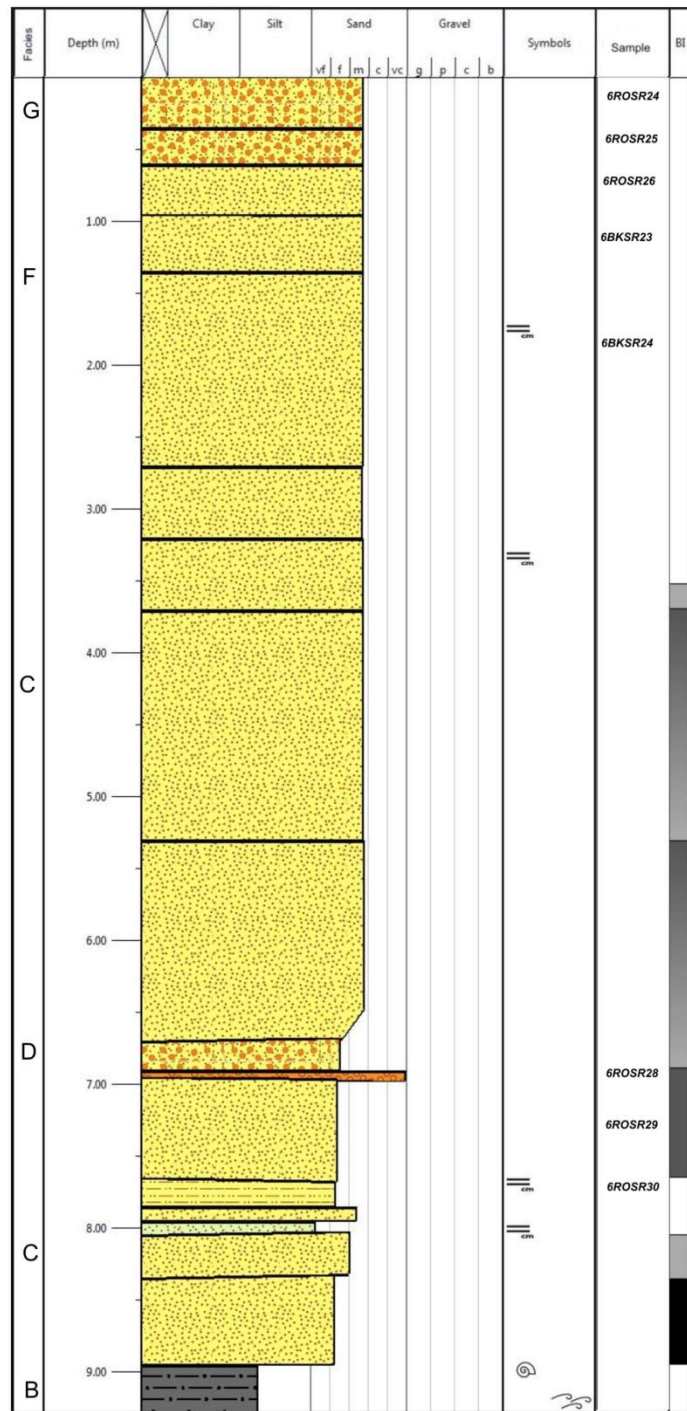
**Section ASR7**



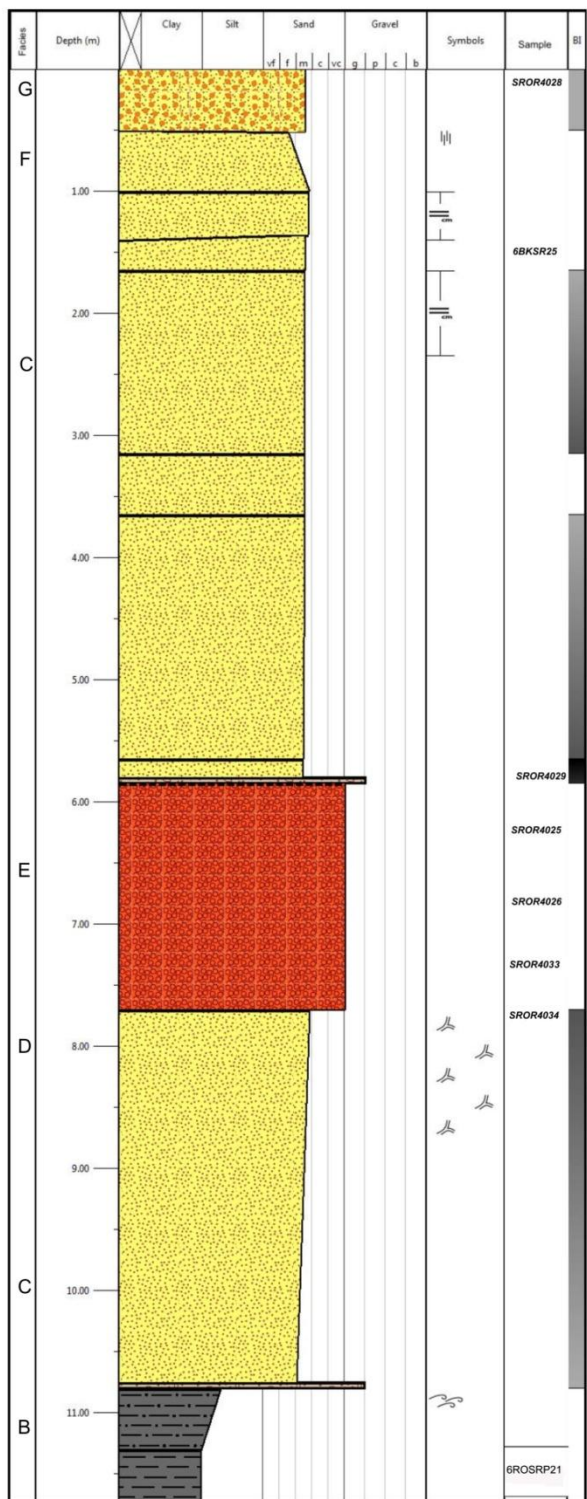
### Section ASR8



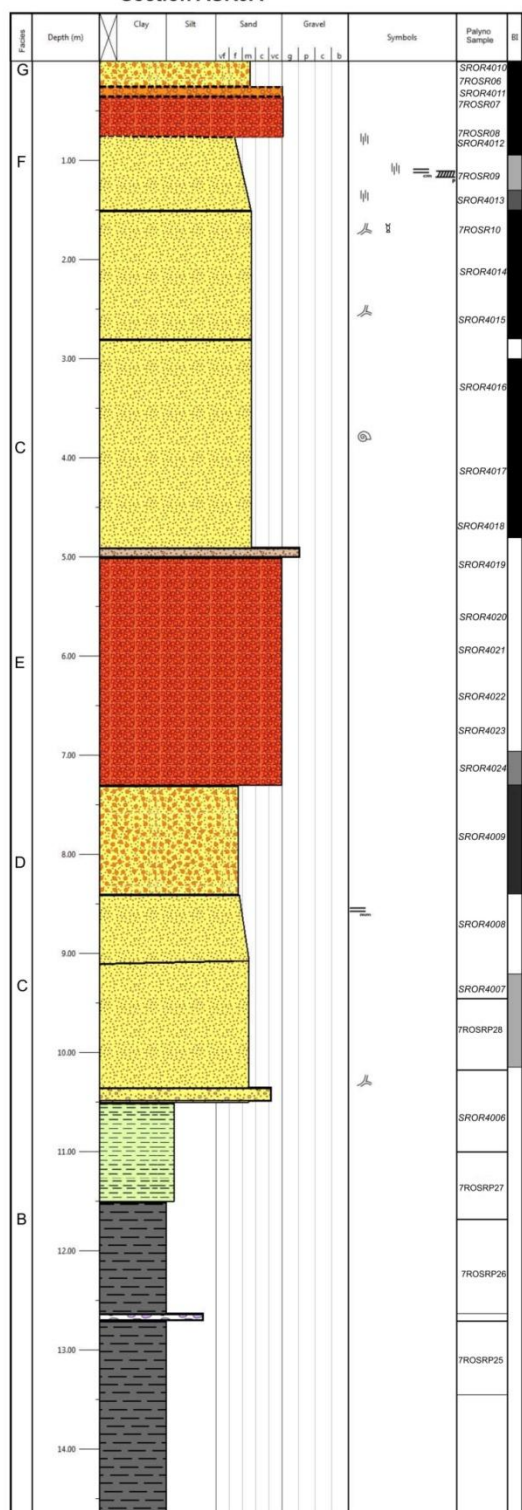
### Section ASR91



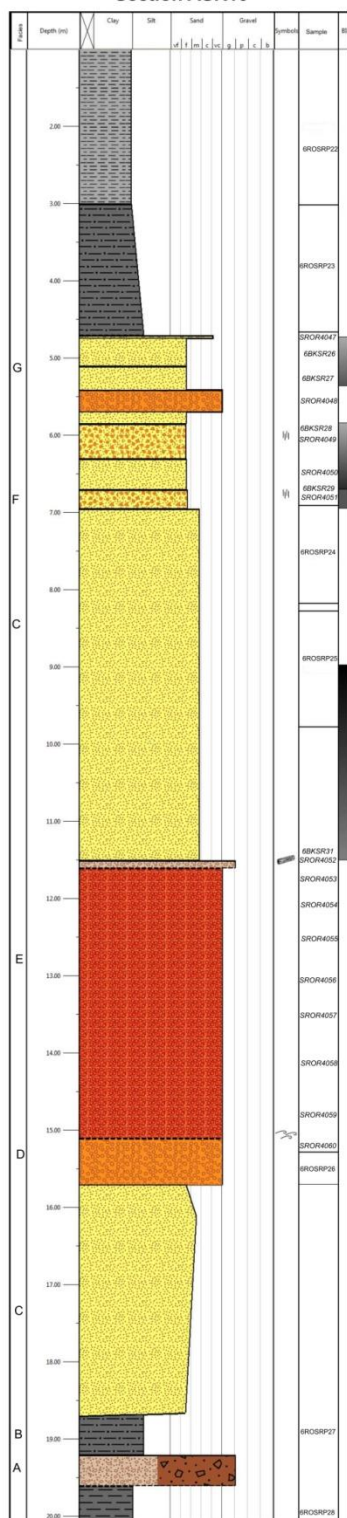
### Section ASR9B



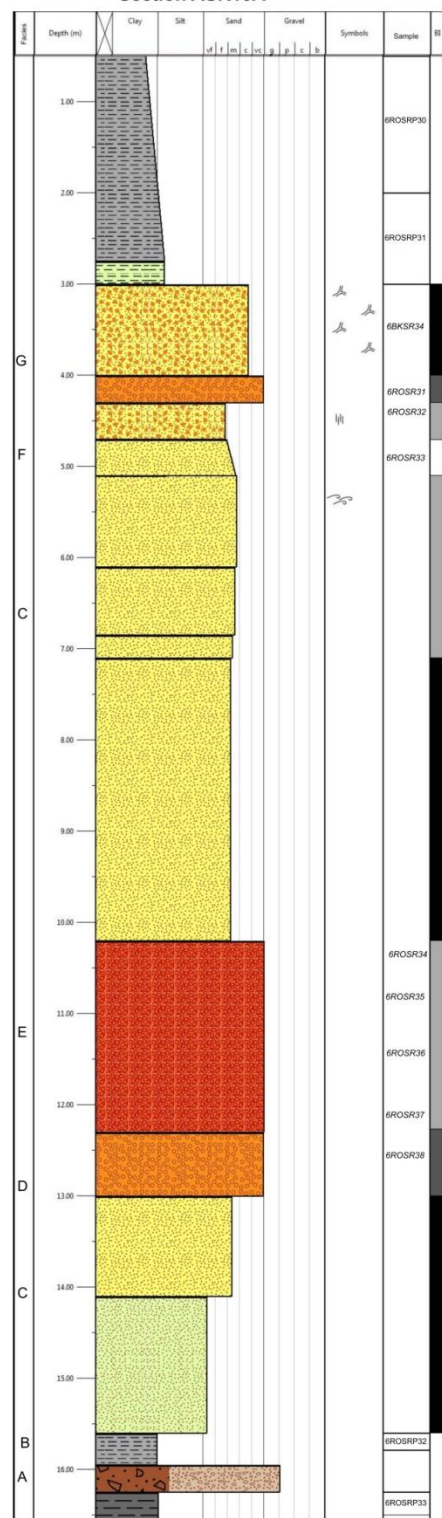
**Section ASR9A**



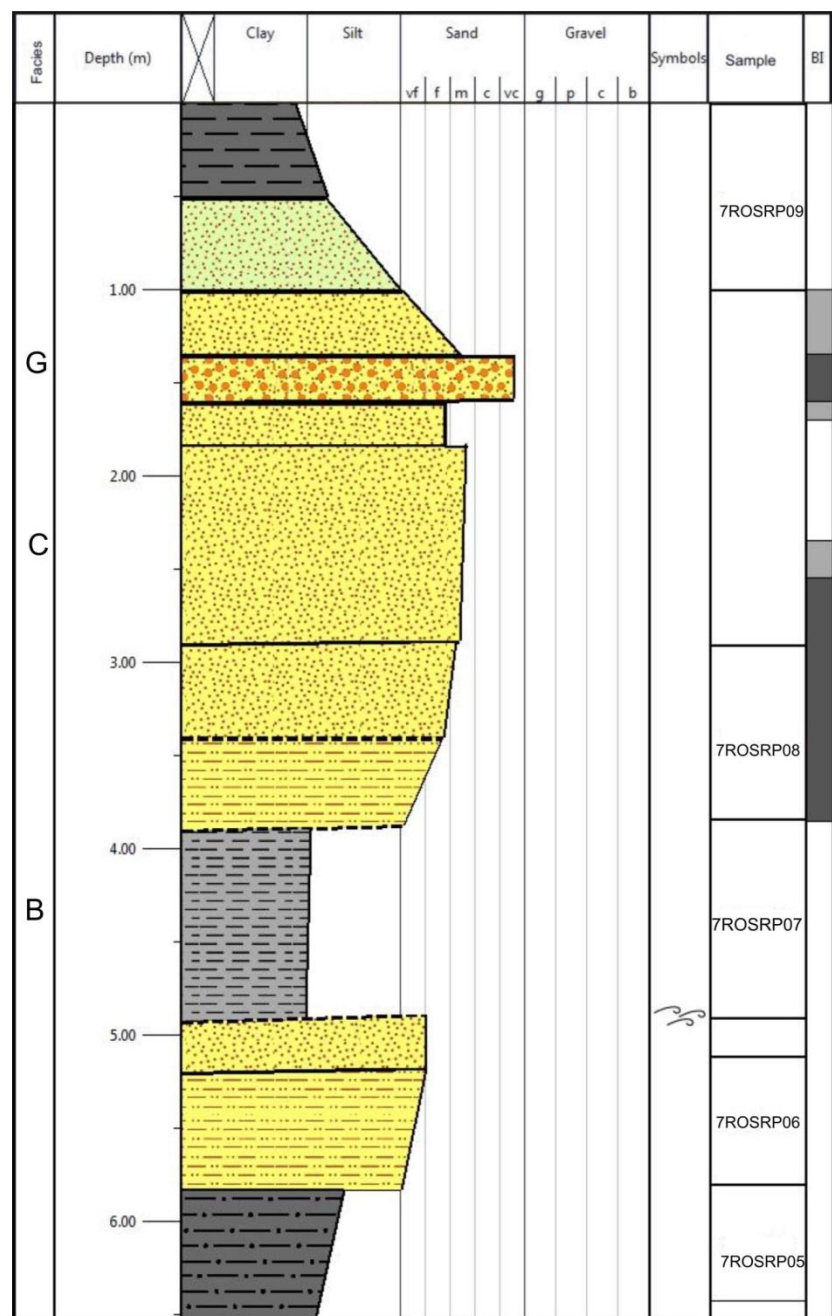
### Section ASR10



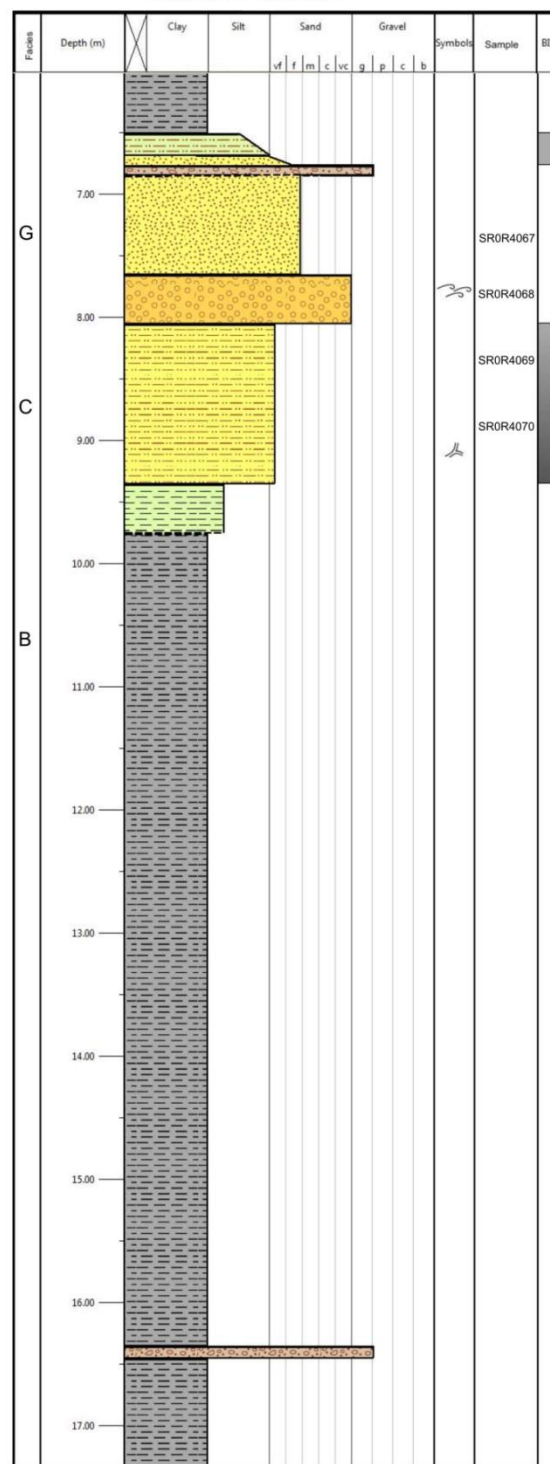
**Section ASR10A**



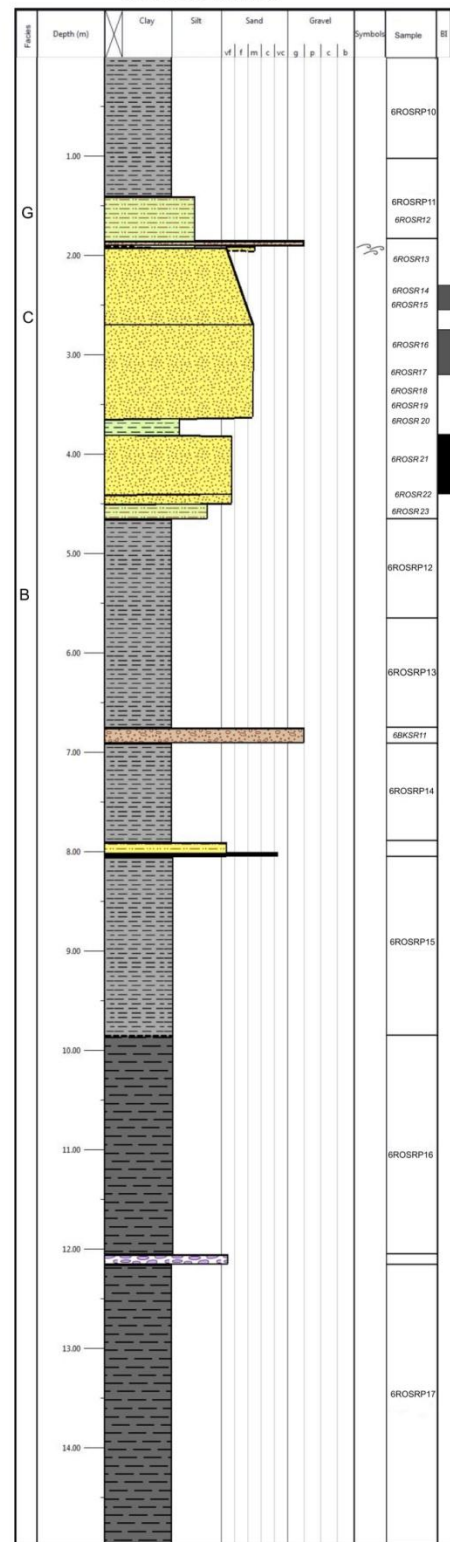
## Section ASR11



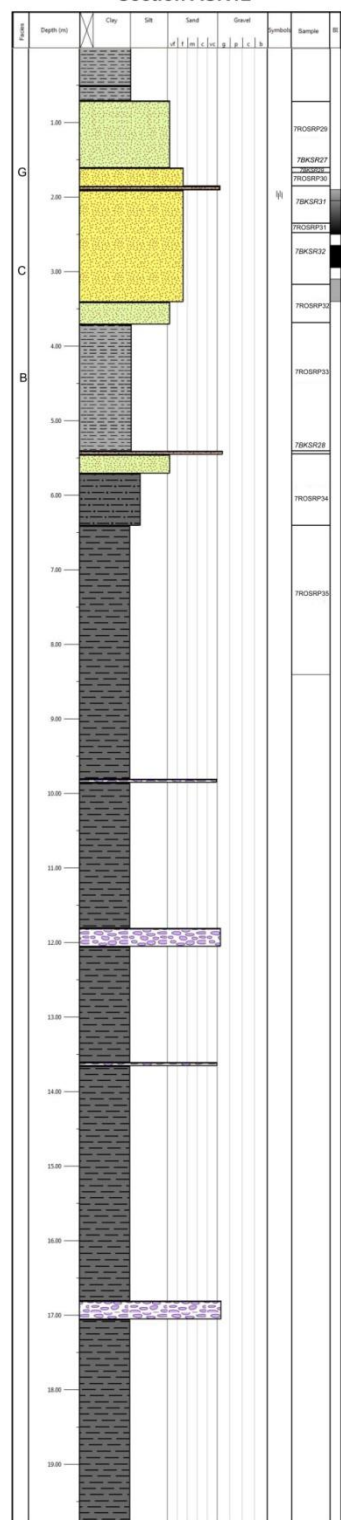
### Section ASR14B



**Section ASR14C**



**Section ASR12**



APPENDIX II :ANALYTICAL RESULTS FOR 215 SELECTED ROCK SAMPLES FROM BAD HEART FORMATION IN THE CLEAR HILLS AND SMOKY RIVER REGIONS

Section	Sample	Lithology	Facies	Mo (ppm)	Cu (ppm)	Pb (ppm)	Zn (ppm)	Ag (ppb)	Ni (ppm)	Co (ppm)	Mn (ppm)	Fe (%)	As (ppm)	U (ppm)	Au (ppb)	Th (ppm)	Sr (ppm)	Cd (ppm)	Sb (ppm)	Bi (ppm)	V (ppm)	La (ppm)	Cr (ppm)	Ba (ppm)	W (ppm)	Zr (ppm)
ARR3	CHRO5016	IOIS	E	13.3	9.7	47.9	622	52	99	59.3	962	39.15	253	5.7	1.9	10.4	115.5	0.03	11.2	0.68	1233	37.6	121.5	493.6	5.7	78.2
ARR3	CHRO5017	IOIS	E	13.7	8.4	46.2	623	50	100	19.7	1034	39.51	255.5	6.6	2	10.7	121.6	0.02	10.8	0.71	901	38	129	666.6	4.5	84.8
ARR3	CHRO5018	IOIS	E	11.6	9.9	46.5	633	61	90	22	735	35.14	281.3	6.1	1.7	10.5	148.8	0.13	9.6	0.69	714	37.3	127.3	1035	4.2	78.8
ARR3	CHRO5019	IOIS	E	12.1	10.7	45.9	636	54	103	25.6	806	36.74	265.5	6.3	2	10.6	165.2	0.08	9.6	0.71	664	36.5	123.8	1605	3.6	78.3
ARR3	CHRO5020	IOIS	E	12.1	9.6	47.4	633	53	94	54.6	1124	37.86	257.8	7.1	1.7	10.5	142.1	0.04	9.4	0.68	1142	32.6	122.1	767.1	4.7	71.9
ARR3	CHRO5021	IOIS	E	13.05	9.2	46.7	647.5	54	86.5	54.95	1174	37.34	253.4	6.45	1.95	10.3	154.8	0.03	10.4	0.695	1238	34.35	126.3	865.6	4.8	74.1
ARR3	CHRO5022	IOIS	E	12.5	10.3	44.5	603	48	89	24.1	968	36.73	210	7.1	1.8	9.7	155.7	0.03	9.4	0.65	882	37.4	121.3	746.4	4	87.7
ARR3	CHRO5023	IOIS	E	11.5	9.3	42.4	580	57	92	25.9	1000	35.7	300	6.7	1.8	11.2	162.7	0.03	9	0.75	1038	35.7	139.7	867	4	82.2
ARR3	CHRO5024	IOIS	E	10.7	10.6	43.5	588	65	100	27.1	1267	34.3	259.3	6.2	1.9	10.7	151.9	0.05	8.8	0.72	945	35.9	132.6	644.7	3.6	77.6
ARR3	CHRO5025	IOIS	E	6.8	11.7	36.7	556	67	90	33.7	1025	30.85	200.1	5.7	2.1	9.3	176.7	0.08	7.1	0.59	713	34.2	111.1	752.5	3.6	76.2
ARR3	CHRO5026	IOIS	E	11.4	12.2	38.6	462	70	93	32.4	1220	29.32	213	4.8	1	9.3	162.3	0.02	7.6	0.58	770	32.1	115.6	625.8	3.2	88
ARR3	CHRO5027	MOIS	E	14.7	14.5	43.7	468	86	90	40.6	928	26.98	123.4	5.6	0.5	10.2	201.4	0.05	7.1	0.63	867	35.7	123.2	990.5	2	87.5
ARR3	6ROCH43	MOIS	E	39.8	16.3	37.8	473	78	72	54.4	1164	23.95	119.4	6.7	0.5	10.5	209.9	0.09	8.2	0.7	1044	29.8	113.7	889.5	2	89
ARR3	CHRO5028	MOIS	E	19.5	11	26.6	273	62	66	25.6	1260	28.21	112.2	3.5	1.1	6.6	136.1	0.02	4.9	0.39	556	23.6	78.9	657.1	1.1	65.5
ARR3	6ROCH42	WOIS	E	11.1	16.7	43.4	509	101	129	56.7	700	22.81	125.1	5.6	BDL	11.5	181.6	0.12	5.4	0.75	1101	32.5	120.1	1101	1.5	107.1
ARR3	6ROCH41	OS	D	9.7	25.4	45.3	532	106	95	61.9	578	19.44	136.4	6	0.7	11.7	179.5	0.1	5.8	0.75	1172	35.2	123.3	882.5	1.6	113.4
ARR3	6ROCH40	Sandstone	C	21.6	10.1	19.3	210	40	48	26	1395	30.72	192.8	2.6	BDL	4.4	104.8	0.05	6.6	0.3	504	16.4	50.6	521.2	1	56.6
ARR3	6ROCH39	Sandstone	C	20.9	12.6	39.1	395	73	75	47.2	754	19.16	136.6	4.9	0.4	9.2	184.1	0.09	6.9	0.58	868	30.8	97.9	711.4	1.1	97.1
ARR5	6ROCH30	MOIS	E	14.1	13.4	52.7	623	64	91	51.1	2684	33	199.6	11.4	BDL	13.8	177.2	0.67	8.7	0.91	1344	35.8	137.9	862.6	4.3	97.4
ARR5	6ROCH31	IOIS	E	10.1	8.2	36.8	574	45	70	46.3	1328	37.15	266.6	6.8	BDL	12.1	168	0.02	8.3	0.79	1164	31.7	117.1	583.4	5	86.1
ARR5	6ROCH32	IOIS	E	11.6	7.8	42.9	561	43	78	57.9	982	35.18	367.8	6.6	1.1	10.5	131.8	0.05	9.6	0.75	1351	29.7	122.9	505.1	4.8	78.7
ARR5	6ROCH33	IOIS	E	11.7	7.9	44.1	548	43	54	59	914	34.97	386.3	6.7	0.9	10	164.6	0.02	10.4	0.73	1305	30.7	118.6	493.2	4.3	67.5
ARR5	6ROCH34	IOIS	E	13.3	11.6	43.5	567	47	80	56	892	35.36	370.3	6.9	0.5	9.9	158.7	0.03	10.8	0.74	1334	32.2	113.7	507.1	4.3	90.8
ARR5	6ROCH35	IOIS	E	13.1	8.5	45.1	593	46	69	49.8	901	35.7	381.8	6.8	0.5	10.2	186	0.03	10.6	0.76	1259	30.7	118	424.9	4.1	77
ARR5	6ROCH36	IOIS	E	12.2	8.7	42.3	563	52	66	54.7	960	34.06	372.3	6.4	0.6	10.8	159.9	0.04	9.8	0.79	1311	32.5	120	540.8	4	72.2
ARR5	6ROCH37	IOIS	E	10.1	11.4	44	550	57	61	54.2	1276	32.99	318.6	5.9	0.7	10.7	158.6	0.07	8.5	0.8	1208	27.1	123	399.9	4	88.9
ARR5	6ROCH38	IOIS	E	7.1	12.2	39.9	524	54	61	49.4	1825	32.04	251.5	5.2	0.4	9.9	159.6	0.09	7.1	0.73	1128	27.6	115.1	443.5	4.4	76.9
KC14	6ROCH23	Sandstone		1	10.3	41.4	370	68	57	38.3	1716	37.09	52.2	5.9	0.5	10.6	163.1	0.2	4	0.63	852	28.5	61.2	860.2	0.8	82.5
KC14	6ROCH22	WOIS	E	0.8	12.8	60	609	74	117	53	946	27.41	165.9	28.6	BDL	16.9	418.5	0.25	7	1.13	1468	37.6	132.2	816.2	0.8	105.1
KC14	6ROCH21	IOIS	E	5.9	11.9	54.7	1040	74	95	46.6	1076	35.93	190.5	8.1	BDL	16.3	261	2.4	12.9	1.15	1405	30	151.5	698.9	4.8	98.9
KC14	6ROCH20	IOIS	E	6.3	10.2	34.4	573	69	78	41.1	927	32.86	149.8	6.1	BDL	12.8	189.8	0.48	5.9	0.92	1119	27.3	131.6	531.5	5.7	102.7
KC14	6ROCH19	IOIS	E	7.6	8	39.6	542	53	75	44.2	910	34.91	171.9	4.8	BDL	13.1	165.7	0.02	7.4	0.92	1207	24.6	138.4	502.1	7.2	105.2
KC14	6ROCH18	IOIS	E	6.1	9.4	44.4	595	88	102	54.7	850	30.99	173.1	5.3	BDL	15.5	332.2	0.03	7.5	1.09	1281	29.9	145	573.3	6.5	87.5
KC14	6ROCH29	Sandstone	C	18	5.2	24.1	203	83	57	29.2	645	17.21	32.1	3.4	BDL	6.8	408.2	0.1	3	0.35	531	16.1	46.2	537.8	0.7	101.8
KC14	6ROCH28	Sandstone	C	14.1	9.5	23.7	146	100	33	16.4	40	5.61	.84	1.9	BDL	6.7	103.1	0.02	2.7	0.26	397	17.7	37.7	601.9	0.8	174.3
KC14	6ROCH27	Sandstone	C	8.8	6.5	17.4	143	68	26	25.2	423	12.09	57.2	2.2	BDL	4.1	993.5	0.07	1.7	0.2	360	13.2	27.3	452.8	0.5	62.6
KC14	6ROCH26	OS	C	5.6	8.4	61.6	545	64	78	57.2	501	19.38	45.4	4.3	BDL	15.2	896.6	0.1	6.4	1.07	1433	28.4	131.3	546	0.9	89.7
KC14	6ROCH25	Sandstone	C	7.8	7.4	22.8	211	45	37	31.7	1059	19.13	69.9	4.2	0.6	6	915	0.07	2.5	0.33	476	17.6	45.1	455.6	0.6	72.7
KC14	6ROCH24	Sandstone	C	2.6	12.6	38.6	276	70	46	33.3	281	13.09	256	10.7	0.3	9.6	717.3	0.05	4	0.56	707	24.8	76.5	626.9	0.9	162.8
KC17	6ROCH50	Sandstone		1.6	34.1	74.5	274	29	30	14.8	118	16.21	90.9	7.2	1.2	15	123.9	0.44	4.8	0.92	1424	36.8	111.5	735.7	1.4	141.9
KC17	6ROCH49	IOIS	E	3.7	17.2	66.9	587	64	91	54.8	1100	27.52	92.2	6.1	1	14	129.6	1.52	5.5	1	1554	38.6	110.2	725.5	2.2	130.7
KC17	6ROCH48	IOIS	E	6.9	13.3	56.3	637	69	67	48.2	781	35	182.9	6.8	1.2	14.6	101.9	0.31	7.9	1.12	1571	30.1	150.1	515.8	8.2	110.8
KC17	6ROCH47	IOIS	E	6.1	12.2	46.7	563	68	54	37.7	1379	36.54	155.7	5.9	1	10.9	102.3	0.83	6.3	0.87	1286	25.6	114.6	557.2	6.4	86.1
KC17	6ROCH46	IOIS	E	7.5	11.8	58.4	687	60	91	59	839	35.49	178	5.3	0.9	15.5	98.8	0.48	9	1.31	1832	32.1	160.6	614.4	8.2	95.2
KC17	6ROCH45	Sandstone		3	17.1	35.8	494	108	111	58.3	159.4	29.17	85.9	7	0.6	8.3	185.6	1.43	4.3	0.57	758	37.1	72.6	650.9	2.2	88.1
KC17	6ROCH44	IOIS	E	5.6	18.6	78.5	872	90	139	89.4	469	21.82	103.5	6.8	0.7	21	133.6	0.64	9.9	1.69	2476	36.4	204.8			

Section	Sample	Lithology	Facies	Ce (ppm)	Sn (ppm)	Y (ppm)	Nb (ppm)	Ta (ppm)	Be (ppm)	Sc (ppm)	Li (ppm)	S (%)	Rb (ppm)	Hf (ppm)	B (ppm)	Tl (ppm)	Hg (ppb)	Se (ppm)	Te (ppm)	Ga (ppm)	Cs (ppm)	SiO2 (%)	Al2O3 (%)	Fe2O3 (%)	MgO (%)
ARR3	CHRO5016	IOIS	E	66.8	1.2	64.3	6.3	0.3	4	14	14.5	0.005	21.4	1.5	27	0.02	2.5	0.05	0.35	8.8	1.6	20.91	5.14	52.07	0.8
ARR3	CHRO5017	IOIS	E	70.7	1.1	71.6	5.1	0.1	5	12	12.3	0.005	20.2	1.6	30	0.02	7	0.05	0.43	6.6	1.4	21.34	4.79	51.84	0.71
ARR3	CHRO5018	IOIS	E	69.7	1.2	66	5.1	0.3	4	12	19.8	0.005	29	1.9	28	0.03	6	0.05	0.51	8.6	2.1	24.19	5.63	47.89	0.79
ARR3	CHRO5019	IOIS	E	68.5	1.2	66	4.8	0.3	4	12	19.2	0.01	28.2	1.7	25	0.03	5	0.05	0.5	7.8	2.2	25.94	5.71	45.76	0.77
ARR3	CHRO5020	IOIS	E	61	1.2	60.3	5.9	0.3	5	13	15.4	0.005	20.9	2	31	0.02	2.5	0.05	0.48	8.5	1.5	23.22	4.97	49.26	0.74
ARR3	CHRO5021	IOIS	E	64.9	1.15	65.6	5.7	0.3	4.5	13	12.35	0.005	18.2	1.55	30	0.02	5	0.05	0.395	8.7	1.3	22.58	4.755	50.3	0.75
ARR3	CHRO5022	IOIS	E	70.4	1	70.8	5.1	0.3	5	12	15.5	0.005	23.8	2.1	24	0.03	2.5	0.05	0.38	7.7	1.6	24.52	5.16	48.57	0.75
ARR3	CHRO5023	IOIS	E	68.8	1.2	66	5.2	0.3	5	12	18.2	0.005	24.7	1.7	33	0.04	5	0.1	0.71	8.3	1.9	26.21	5.22	47.1	0.76
ARR3	CHRO5024	IOIS	E	68.3	1.2	64.5	5.1	0.2	5	11	15.8	0.005	26.5	1.8	34	0.03	14	0.2	0.67	8.3	2	27.41	5.32	45.48	1.06
ARR3	CHRO5025	IOIS	E	66.8	1.1	57.1	5.3	0.3	4	11	22.4	0.1	36.1	1.9	30	0.05	18	0.3	0.62	9.3	2.6	28.43	6	41.29	1.49
ARR3	CHRO5026	IOIS	E	61.7	1.1	54.9	6	0.4	4	13	28.4	0.26	39.3	1.8	25	0.11	21	0.4	0.6	8.3	2.7	30.51	6.31	38	1.77
ARR3	CHRO5027	MOIS	E	69	1.4	59	7.4	0.4	4	14	35.7	0.18	47.2	2	25	0.1	26	0.6	0.57	10.3	3.4	34.04	7.01	35.07	1.74
ARR3	6ROCH43	MOIS	E	64.8	1.1	50.4	7.2	0.4	4	12	28.8	0.18	44.1	2.5	35	0.11	28	0.6	0.64	10.3	2.9	34.41	6.91	33.01	1.71
ARR3	CHRO5028	MOIS	E	45.3	1	36.5	5.9	0.3	3	11	32.2	0.76	36.8	1.4	20	0.07	18	0.5	0.35	7.8	2.5	31.95	5.44	37.17	1.87
ARR3	6ROCH42	WOIS	E	67.6	1.3	54.3	8.9	0.5	4	13	37.1	0.17	56.6	2.6	31	0.12	34	0.7	0.69	12.4	3.6	38.49	8.34	30.32	1.84
ARR3	6ROCH41	OS	D	76.7	1.7	57.6	10.4	0.5	3	14	45.8	0.17	65.5	3.1	29	0.12	38	1	0.75	13.9	4.4	43.25	9.31	25.79	1.96
ARR3	6ROCH40	Sandstone	C	33.2	0.8	23.3	5.4	0.3	5	7	25.6	1.47	33.8	1.4	25	0.1	22	0.7	0.29	6.7	2.2	26.48	4.69	41.13	1.88
ARR3	6ROCH39	Sandstone	C	67.9	1.1	50.8	7.9	0.4	3	12	37.9	0.52	52.3	2.7	27	0.09	28	1	0.55	10.5	3.3	48.42	7.31	25.29	1.32
ARR5	6ROCH30	MOIS	E	68	1.2	81.3	7.5	0.4	4	15	34.1	0.03	28.8	2.2	37	0.15	32	1.6	0.84	11.4	1.8	25.45	6.48	43.16	1.24
ARR5	6ROCH31	IOIS	E	59.8	0.9	69.3	6	0.2	4	12	14.2	0.02	23.2	2	49	0.03	14	0.9	0.76	8.9	1.5	17.16	5.08	52.4	1.3
ARR5	6ROCH32	IOIS	E	58.3	1.1	59.3	6.3	0.3	4	13	11.2	0.03	21.5	1.8	53	0.04	7	0.3	0.67	8.8	1.5	21.49	5.37	48.62	0.96
ARR5	6ROCH33	IOIS	E	60.2	1.1	62.3	5.7	0.2	4	11	10	0.03	19.2	1.8	62	0.03	BDL	0.2	0.68	7.9	1.5	22.52	5.15	47.75	0.99
ARR5	6ROCH34	IOIS	E	62.8	1.1	67.7	6	0.3	5	12	10.8	0.04	20.5	2.1	59	0.03	9	0.2	0.72	8.9	1.4	24.26	5.42	45.69	0.98
ARR5	6ROCH35	IOIS	E	62.7	1.1	70.9	5.9	0.3	4	12	10.7	0.08	19.7	1.7	70	0.02	7	0.3	0.75	8.2	1.3	23.59	4.75	48.35	0.96
ARR5	6ROCH36	IOIS	E	62.9	1.2	62.1	5.8	0.3	4	11	11.4	0.03	20.6	1.6	51	0.03	12	0.2	0.67	8.1	1.5	25.21	4.8	47.16	0.82
ARR5	6ROCH37	IOIS	E	55.6	1.2	55.6	6.4	0.3	5	11	15.1	0.03	23.8	2	47	0.04	6	0.4	0.79	8.5	1.7	26.45	5.12	45.32	1.11
ARR5	6ROCH38	IOIS	E	56.1	1	54.2	6.5	0.3	4	11	16.2	0.06	29.3	2	45	0.05	25	0.6	0.73	9	1.9	30.7	6.2	39.33	1.76
KC14	6ROCH23	Sandstone		57.7	0.9	64.2	6.9	0.3	4	16	35.5	0.02	41.9	2.2	22	0.09	33	1.3	0.48	8.9	2.8	22.95	6.62	47.47	0.83
KC14	6ROCH22	WOIS	E	73.6	1	113.4	7.6	0.4	3	16	56.5	0.03	39.5	2.5	28	0.09	37	1.5	0.97	11.8	2.7	22.09	7.3	37.97	1.09
KC14	6ROCH21	IOIS	E	60.8	1.3	70.5	8.7	0.3	4	14	32.8	0.05	29.3	2.4	38	0.11	72	1	1.11	10.3	1.9	17.07	6.36	49.19	1.04
KC14	6ROCH20	IOIS	E	53	1.1	63.1	6.5	0.3	5	13	20.8	0.05	29	2.3	42	0.06	17	0.9	0.88	8.8	1.8	19.54	5.71	48.46	1.11
KC14	6ROCH19	IOIS	E	47.2	1.1	60.7	6.2	0.3	5	13	16.3	0.05	23.4	2.3	44	0.04	13	0.9	1.06	9	1.5	20.66	5.58	47.85	1.22
KC14	6ROCH18	IOIS	E	63.9	1.2	66.6	6.4	0.3	3	14	20.7	0.07	22.7	1.8	41	0.07	14	0.9	1.31	8.2	1.3	29.27	5.41	39.74	1.19
KC14	6ROCH29	Sandstone	C	35.2	0.5	21.4	4	0.2	1	6	13.9	0.01	23.1	2.6	16	0.06	5	0.7	0.41	4.6	1.1	48.78	3.32	23.06	1.1
KC14	6ROCH28	Sandstone	C	38.4	0.8	15	6.3	0.4	1	5	32.4	0.02	40.5	4.6	11	0.14	9	0.3	0.17	8	2.3	77.1	5.06	8.02	0.77
KC14	6ROCH27	Sandstone	C	28.7	0.4	16.5	4	0.2	1	5	17.2	0.02	32.4	1.6	12	0.08	9	0.6	0.23	5.3	1.7	45.01	3.58	16.5	0.99
KC14	6ROCH26	OS	C	59	1.1	62.1	7.7	0.4	3	13	40	0.04	32.9	2.3	25	0.07	13	0.7	1.07	9.8	1.8	27.05	6.27	25.8	1.77
KC14	6ROCH25	Sandstone	C	35.9	0.8	27.6	5.2	0.3	2	8	23.8	0.04	37.2	1.8	20	0.1	11	0.5	0.34	6.8	2.3	31	4.82	24.69	1.33
KC14	6ROCH24	Sandstone	C	49.3	1.2	40.9	8.5	0.5	3	11	47.1	0.16	57.3	4.6	21	0.14	19	0.4	0.56	10.3	3.6	46.52	7.78	18.31	1.24
KC17	6ROCH50	Sandstone		97.4	1.8	66.3	13.5	0.8	3	21	79.8	0.18	87.3	4.5	14	0.14	51	1.3	0.57	16.2	6.4	45.65	13.09	21.51	1.09
KC17	6ROCH49	IOIS	E	95.1	1.4	79	11.1	0.6	4	17	57.2	0.03	63.2	3.4	20	0.12	35	0.8	0.76	12.4	4.1	29.59	10.2	37.36	1.1
KC17	6ROCH48	IOIS	E	69.8	1.6	74.7	8.6	0.4	7	16	33.3	0.02	40	2.7	31	0.07	23	0.5	0.96	11.4	2.5	22.73	7.03	48.92	0.81
KC17	6ROCH47	IOIS	E	54.9	1.1	68.5	6	0.3	5	12	20.8	0.04	28.1	2	30	0.06	12	0.4	0.8	8.2	1.7	23.55	5.29	50.22	0.73
KC17	6ROCH46	IOIS	E	68.7	1.2	84.9	7.1	0.3	6	16	22.4	0.03	23.9	2.1	31	0.05	10	0.6	1.24	9.8	1.3	27.12	7.01	44.84	0.86
KC17	6ROCH45	Sandstone		80.9	1	107.4	5.9	0.3	5	10	33.2	0.05	38.2	2.4	23	0.11	18	0.6	0.55	7.5	2.2	32.4	6.1	39.33	0.75
KC17	6ROCH44	IOIS	E	84.4	1.8	101.8	10.6	0.5	4	19	52.8	0.04	34.5	3.5	16	0.07	18	0.8	1.72	13.4	1.8	43.39	8.43	28.4	1.16
LVH	6ROCH01	MOIS	E	69.5	1.2	76.2	9.1	0.5	3	17	62.2	0.07	54.8	2.6	27	0.12	32	2.3	0.58	11.7	3.7	26.3	8.31	35.22	1.37
LVH	6ROCH02	MOIS	E	63.8	1.7	52.3	10.5	0.5	5	16	58.4	0.02	55.1	3.4	21	0.09	39	1.5	0.82	12.3	3.7	28	8.99	37.24	1.47
LVH	6ROCH03	IOIS	E	61.6	1.4	71.6	8.1	0.4	4	15	32.6	0.02	34.5	2.3	32	0.05	17	1.3	1.07	11.3	2.3	20.37	6.55	44.45	1.02
LVH	6ROCH04	IOIS	E	54.9	1.3	60.9	7.1	0.3	5	14	23.4	0.02	24.9	2.2	28	0.04									

Section	Sample	Lithology	Facies	CaO (%)	Na2O (%)	K2O (%)	TiO2 (%)	P2O5 (%)	LOI (%)	Pr (ppm)	Nd (ppm)	Sm (ppm)	Eu (ppm)	Gd (ppm)	Tb (ppm)	Dy (ppm)	Ho (ppm)	Er (ppm)	Tm (ppm)	Yb (ppm)	Lu (ppm)
ARR3	CHRO5016	IOIS	E	1.93	0.08	0.45	0.17	1.63	16.4	10.6	48.4	13.7	3.38	14.15	2.53	13.04	2.22	5.73	0.73	4.6	0.59
ARR3	CHRO5017	IOIS	E	1.79	0.06	0.4	0.14	1.62	17	11.17	51.5	14.6	3.48	14.53	2.62	13.83	2.42	6.17	0.81	4.63	0.65
ARR3	CHRO5018	IOIS	E	2.16	0.07	0.56	0.19	1.89	16.3	10.66	49.1	13.1	3.27	13.5	2.44	12.93	2.26	5.46	0.75	4.62	0.6
ARR3	CHRO5019	IOIS	E	2.09	0.07	0.56	0.19	1.72	16.8	10.64	46.9	13.2	3.22	13.47	2.51	12.91	2.17	5.71	0.79	4.53	0.59
ARR3	CHRO5020	IOIS	E	1.97	0.06	0.44	0.16	1.63	17.1	9.43	42.7	12.8	2.99	12.77	2.09	12.06	1.99	5.01	0.75	4.27	0.54
ARR3	CHRO5021	IOIS	E	1.935	0.055	0.38	0.14	1.615	17	10.2	45.95	13.3	3.095	13.98	2.505	13.1	2.21	5.62	0.805	4.365	0.585
ARR3	CHRO5022	IOIS	E	1.66	0.06	0.46	0.16	1.53	16.7	10.87	50.1	13.9	3.43	14.91	2.57	13.56	2.32	6.14	0.78	4.78	0.63
ARR3	CHRO5023	IOIS	E	1.76	0.06	0.47	0.16	1.53	16.4	10.65	47.9	14.2	3.31	14.31	2.38	12.87	2.2	5.95	0.8	4.38	0.56
ARR3	CHRO5024	IOIS	E	1.92	0.06	0.51	0.17	1.53	16.2	10.58	46.3	13.4	3.32	13.93	2.43	13.61	2.15	5.7	0.82	4.04	0.59
ARR3	CHRO5025	IOIS	E	2.65	0.08	0.68	0.22	1.66	17.2	9.79	42.5	12	3.12	12.4	2.2	11.84	2.06	4.97	0.74	3.91	0.58
ARR3	CHRO5026	IOIS	E	2.55	0.09	0.79	0.24	1.22	18.1	9.5	41	11.2	2.9	12.7	1.92	10.3	1.78	4.71	0.71	3.96	0.5
ARR3	CHRO5027	MOIS	E	2.83	0.09	0.92	0.28	1.43	16.3	10.24	45.3	11.8	3.04	13.27	2.08	10.98	2	5.18	0.71	4.23	0.57
ARR3	6ROCH43	MOIS	E	3.2	0.1	0.88	0.24	1.57	17.5	9.15	40.2	10.3	2.52	11.18	1.98	9.41	1.58	4.1	0.6	3.44	0.48
ARR3	CHRO5028	MOIS	E	3.28	0.1	0.82	0.24	0.88	18	6.6	28.1	7.5	1.93	8.15	1.28	6.82	1.17	3.16	0.45	2.64	0.39
ARR3	6ROCH42	WOIS	E	1.93	0.09	1.11	0.31	0.82	16.3	9.74	43.4	10.7	2.56	11.64	2.07	10.04	1.76	4.35	0.63	3.79	0.52
ARR3	6ROCH41	OS	D	2.03	0.11	1.31	0.36	0.97	14.5	10.98	46.5	11.5	2.84	12.55	2.26	11	1.88	4.82	0.68	4.03	0.57
ARR3	6ROCH40	Sandstone	C	2.52	0.09	0.7	0.2	0.63	21.3	4.68	19.2	4.7	1.13	4.88	0.91	4.45	0.76	2.06	0.29	1.72	0.25
ARR3	6ROCH39	Sandstone	C	2.4	0.18	1.11	0.29	1.22	12.2	9.65	41.6	10.3	2.49	11.08	2	9.19	1.62	4.32	0.6	3.55	0.48
ARR5	6ROCH30	MOIS	E	3.43	0.12	0.7	0.2	2.03	16.5	12.02	54.7	13.7	3.42	15.57	2.85	14.21	2.45	6.12	0.76	4.83	0.71
ARR5	6ROCH31	IOIS	E	3.01	0.09	0.51	0.15	1.96	17.9	10.53	46.7	12.3	3.05	13.84	2.51	12.47	2.05	5.22	0.66	4.21	0.58
ARR5	6ROCH32	IOIS	E	1.95	0.09	0.49	0.15	1.55	18.9	9.46	42	11.6	2.79	12.86	2.38	11.18	1.9	5.04	0.72	4.05	0.54
ARR5	6ROCH33	IOIS	E	1.92	0.08	0.41	0.14	1.65	19	9.8	43.5	11.7	2.89	13.25	2.49	11.76	1.99	5.15	0.7	4.05	0.56
ARR5	6ROCH34	IOIS	E	2	0.08	0.42	0.14	1.78	18.8	10.23	46.9	12.6	3.13	14.3	2.62	12.42	2.11	5.25	0.75	4.28	0.59
ARR5	6ROCH35	IOIS	E	1.8	0.09	0.36	0.14	1.66	17.9	10.34	47.7	13	3.19	14.98	2.7	13.19	2.2	5.42	0.76	4.47	0.6
ARR5	6ROCH36	IOIS	E	1.64	0.05	0.39	0.14	1.49	17.8	9.84	42.9	11.9	3.03	13.37	2.55	11.59	2.01	5.05	0.73	3.98	0.56
ARR5	6ROCH37	IOIS	E	1.86	0.06	0.46	0.17	1.38	17.6	8.94	40.2	10.1	2.64	12.02	2.19	10.75	1.84	4.75	0.62	3.79	0.53
ARR5	6ROCH38	IOIS	E	2.42	0.1	0.64	0.19	1.35	16.8	8.57	38.5	10.2	2.49	11.42	2.14	10.31	1.75	4.64	0.65	3.79	0.52
KC14	6ROCH23	Sandstone		2.74	0.15	0.94	0.26	2.22	15.3	9.2	40.6	10.5	2.58	11.76	2.2	11.33	2	5.3	0.65	4.19	0.61
KC14	6ROCH22	WOIS	E	9.23	0.16	0.88	0.26	3.93	16.6	12.19	55.6	15	3.82	18.46	3.5	17.75	3.21	8.14	1.03	6.58	0.92
KC14	6ROCH21	IOIS	E	5.37	0.12	0.65	0.21	1.98	17.5	10.33	46.6	12.5	3.08	14.35	2.66	13.94	2.3	5.74	0.73	4.77	0.68
KC14	6ROCH20	IOIS	E	5.4	0.1	0.66	0.19	1.53	17	9.02	40.7	11.1	2.74	12.7	2.33	11.82	1.98	5.16	0.65	4.27	0.59
KC14	6ROCH19	IOIS	E	4.99	0.2	0.56	0.16	1.48	16.9	8.3	39.6	10.5	2.56	12.4	2.25	11.68	2.03	4.94	0.65	4.03	0.58
KC14	6ROCH18	IOIS	E	5.55	0.13	0.59	0.16	1.75	15.8	9.95	45.8	12.3	3.03	13.69	2.53	12.82	2.2	5.45	0.71	4.46	0.63
KC14	6ROCH29	Sandstone	C	8.49	0.07	0.62	0.14	0.33	13.9	4.51	17.8	4.8	1.04	4.55	0.86	4.24	0.73	1.89	0.22	1.57	0.23
KC14	6ROCH28	Sandstone	C	1.78	0.1	1	0.24	0.17	5.7	5.01	19.8	4.1	0.91	3.47	0.61	2.97	0.5	1.27	0.17	1.22	0.19
KC14	6ROCH27	Sandstone	C	14.91	0.08	0.71	0.16	0.28	17.6	3.87	16.2	3.6	0.83	3.52	0.63	3.21	0.53	1.35	0.17	1.29	0.18
KC14	6ROCH26	OS	C	14.74	0.12	0.79	0.21	1.45	21.5	9.53	43	11.3	2.74	12.74	2.44	11.73	2.08	5.32	0.67	4.32	0.6
KC14	6ROCH25	Sandstone	C	15.35	0.15	0.84	0.21	0.52	20.7	5.24	21.7	5.2	1.18	5.42	0.98	4.88	0.86	2.21	0.28	1.97	0.28
KC14	6ROCH24	Sandstone	C	7.61	0.24	1.33	0.35	0.52	15.9	7.11	30.6	7	1.66	7.5	1.35	6.86	1.26	3.32	0.41	2.85	0.43
KC17	6ROCH50	Sandstone		1.11	0.23	1.8	0.52	1.19	13.5	13.1	55.2	13	3.06	13.12	2.47	12.13	2.16	5.71	0.85	5.23	0.74
KC17	6ROCH49	IOIS	E	1.44	0.13	1.34	0.39	1.49	16.5	13.07	56.9	14.4	3.67	16.21	3.11	15.01	2.61	6.88	0.97	5.63	0.79
KC17	6ROCH48	IOIS	E	1.24	0.07	0.75	0.26	1.36	16.4	10.64	48.1	12.8	3.26	15.21	2.88	14.12	2.45	6.23	0.93	5.21	0.72
KC17	6ROCH47	IOIS	E	1.5	0.07	0.56	0.18	1.56	15.9	9.47	43	11.6	2.97	13.63	2.64	12.45	2.17	5.79	0.78	4.55	0.64
KC17	6ROCH46	IOIS	E	1.3	0.07	0.57	0.17	1.5	16.1	11.74	52.3	14.9	3.74	17.16	3.3	15.65	2.71	7	0.93	5.68	0.77
KC17	6ROCH45	Sandstone		3	0.09	0.78	0.22	2.47	14.5	14.26	68.9	17.4	4.36	20.5	3.66	17.32	3.09	8.16	1.11	6.24	0.93
KC17	6ROCH44	IOIS	E	1.77	0.1	0.76	0.22	1.04	14.3	14.65	67.1	18.6	4.65	21.59	4.02	19.01	3.3	8.48	1.17	6.99	0.94
LVH	6ROCH01	MOIS	E	6.59	0.19	1.21	0.34	3.31	16.7	10.46	46.5	11.7	2.84	13.53	2.5	13.47	2.46	6.27	0.83	5.09	0.75
LVH	6ROCH02	MOIS	E	3.37	0.09	1.29	0.35	0.9	17.9	10.05	44	11.3	2.73	11.83	2.23	11.79	2	4.92	0.65	4.29	0.63
LVH	6ROCH03	IOIS	E	5.91	0.12	0.8	0.22	1.89	18.3	10.27	46.5	12.6	3.24	14.54	2.79	13.75	2.46	6.07	0.79	4.96	0.72
LVH	6ROCH04	IOIS	E	3.36	0.07	0.7	0.17	1.2	16.3	8.99	41	11.2	2.95	13.21	2.49	12.83	2.19	5.44	0.68	4.5	0.62
LVH	6ROCH05	Sandstone	D	5.24	0.08	0.78	0.19	1.62	15.2	6.67	29.9	7.6	1.9	8.45	1.57	7.92	1.4	3.53	0.46	2.94	0.42
LVH	6ROCH06	IOIS	E	3.84	0.1	0.9	0.21	1.75	13	10.02	45.9	12.5	3.16	14.43	2.77	14.39	2.38	6.03	0.78	4.88	0.72
LVH	6ROCH07	OS	D	3.09	0.09	0.87	0.19	0.59	9.9	5.44	23.3	5.8	1.35	5.91	1.09	5.4	0.92	2.48	0.29	1.97	0.28
Worsley	CHRO5035	Shale	Puskawakau	0.4	0.45	2.56	0.72	0.14	8	8.37	31.2	5.85	1.07	3.94	0.69	3.94	0.81	2.32	0.43	2.57	0.37
Worsley	CHRO4010	IOIS	E	2.68	0.08	0.74	0.24	1.16	16.3	9.02	42.8	12.1	3.21	14.42	2.37	12.61	2.22	5.73	0.87	4.95	0.69
Worsley	CHRO4009	IOIS	E	4.61	0.1</																

Section	Sample	Lithology	Facies	Mo (ppm)	Cu (ppm)	Pb (ppm)	Zn (ppm)	Ag (ppb)	Ni (ppm)	Co (ppm)	Mn (ppm)	Fe (%)	As (ppm)	U (ppm)	Au (ppb)	Th (ppm)	Sr (ppm)	Cd (ppm)	Sb (ppm)	Bi (ppm)	V (ppm)	La (ppm)	Cr (ppm)	Ba (ppm)	W (ppm)	Zr (ppm)
Worsley	CHRO5033	IOIS	E	6.1	12.1	52.7	544	NA	68	63.8	903	34.93	NA	7.3	NA	NA	143.1	NA	10.7	NA	1283	33.6	NA	716	2.9	123.9
Worsley	CHRO5032	OS	D	17.2	10.4	36.1	353	NA	58	44.6	956	31.21	NA	4.5	NA	NA	226.6	NA	5.3	NA	973	28	NA	631.9	0.8	100.8
Worsley	CHRO5031	OS	D	7.1	11.8	68.8	630	NA	57	50.7	640	25.65	NA	5.5	NA	NA	191.1	NA	7.5	NA	1459	30.8	NA	785.2	0.9	120.1
Worsley	CHRO5030	Silty Sandstone	C	7.9	13.7	34.4	342	NA	45	43.9	1715	16.85	NA	4.9	NA	NA	164	NA	6	NA	637	25.6	NA	635.4	1.1	119.5
Worsley	CHRO5029b	Shale	B	4.4	7.7	32.5	89	NA	16	7.2	41	9.44	NA	1.8	NA	NA	197	NA	3	NA	451	23.1	NA	832.9	1.3	209.6
Worsley	CHRO5029a	Shale	B	3.9	10	22.6	35	NA	5	5.1	26	2.51	NA	3.1	NA	NA	207.9	NA	2.5	NA	377	31.5	NA	1041	1.2	217.1
ASR10	SROR4047	Sandstone	G	0.7	18.1	29	380	59	137	59.5	653	13.13	64.4	7.4	0.1	7.1	180.1	0.42	1.8	0.35	393	37.2	54.8	793.7	1.2	164.7
ASR10	SROR4048	MOIS	G	1.3	13.7	59.4	585	53	131	77.8	1139	26	87	4.9	0.3	14.4	178.9	0.2	4.5	0.92	1163	36.7	139.8	655.1	1.4	117.8
ASR10	SROR4049	OS	F	0.5	8.4	23.9	291	88	89	46.3	1234	17.34	70	2.6	0.1	7.3	169.5	0.13	1.8	0.34	448	23.1	52.8	572.9	0.6	122.5
ASR10	SROR4050	Sandstone	F	1.6	12.2	23.7	231	109	80	51.8	228	7.5	104.8	2.5	0.4	6.6	95.4	0.09	1.9	0.3	352	18.8	44.9	551	0.7	105.8
ASR10	SROR4051	Sandstone	F	1	7.2	25.7	241	85	46	32.5	867	13.06	61.4	4.5	0.2	7.9	183.8	0.11	1.8	0.36	452	23.8	53.7	586.2	0.7	112
ASR10	SROR4052	Sandstone	C	0.5	7.3	23.7	464	103	201	105.6	953	16.97	200.6	2.8	1.4	6.7	160.5	0.21	2.1	0.32	474	30.2	59.9	595.6	0.5	92
ASR10	SROR4053	IOIS	E	8.8	8.2	56.4	551	31	78	51.1	374.1	36.79	286	4.8	1.1	12.8	164.9	0.02	7.1	0.93	1448	34.5	150.1	390.4	8.9	97.9
ASR10	SROR4054	IOIS	E	10.4	8.1	53.5	579	38	79	54.4	1137	38.65	278.2	5.2	0.1	14.6	132.3	0.02	7.9	1.02	1433	32.4	157.5	334.2	9.3	95
ASR10	SROR4055	IOIS	E	9.5	9.3	50.7	552	45	93	60.7	1084	36.8	313.8	5.9	1.2	14	201.6	0.08	7.8	1	1310	33.4	152.1	424.9	7.2	92.9
ASR10	SROR4056	IOIS	E	9.1	7.8	52.9	576	38	81	55.8	1212	38.04	254.5	5.7	0.5	13.8	161.7	0.04	8.3	0.98	1335	33.1	150.7	371.1	7.3	86
ASR10	SROR4057	IOIS	E	7.7	9.3	49.6	526	43	89	58.7	1063	35.08	275.3	4.8	0.7	13.9	139.5	0.08	7	0.96	1225	29.4	152.3	424.6	6.7	88.1
ASR10	SROR4058	IOIS	E	6	8.4	48.6	489	47	82	63.2	1245	33.57	238.3	4.6	0.2	13.3	150.7	0.06	6.8	0.91	1145	28.7	141.1	419.5	6.5	84.5
ASR10	SROR4059	IOIS	E	4.8	9.9	46.6	507	50	86	53.8	990	30.74	183.9	4	1.1	13.2	141.7	0.06	6.5	0.92	1251	27.6	149.8	445.7	5.1	101.7
ASR10	SROR4083	IOIS	E	5	9.6	50	540	54	80	57	1039	32.17	206	4.3	1	14.3	152.9	0.07	6.9	0.95	1342	29.1	155.8	491.4	5	98.1
ASR10	SROR4060	MOIS	D	3.7	9.8	40.3	442	59	76	47.5	814	25.16	74.9	6.3	0.2	10.9	184.8	0.07	4.8	0.77	965	26.6	116.2	435.5	0.9	95.7
ASR10A	6ROSR31	MOIS	G	2.5	10.9	76.5	732	90	182	102.4	1005	23.6	151.3	5.2	0.8	16.7	245.6	0.25	5.3	1.19	1562	42	142.1	708	4.5	122
ASR10A	6ROSR32	OS	F	0.8	5.8	22.8	192	96	50	28.5	807	13.97	63.1	2.5	0.2	5.5	116	0.15	1.5	0.25	341	17.5	33.6	576.2	0.7	107.8
ASR10A	6ROSR33	Sandstone	F	0.9	9.1	33.3	289	122	66	49.1	375	7.97	102	2.4	0.2	7.9	123	0.18	2.1	0.41	482	21.4	48.3	545.2	0.9	109.1
ASR10A	6ROSR34	IOIS	E	5.7	12.4	62.3	771	60	135	133.1	1602	31.23	219.7	10.8	1.1	13.2	195.6	0.29	5.6	1.04	1295	48.8	125.9	944.8	9	133.2
ASR10A	6ROSR35	IOIS	E	6.9	10.7	55.2	677	64	197	92.7	1669	33.31	239.4	5.9	1.6	13.2	158.5	0.29	6.7	1.01	1169	39.6	120.5	858.5	11.1	126.7
ASR10A	6ROSR36	IOIS	E	5.3	10.5	58.1	720	62	174	76.6	1114	31.39	181.4	4.8	1.8	13	144.5	0.61	6.9	0.97	1150	36.9	123.1	740.1	7.9	110.8
ASR10A	6ROSR37	IOIS	E	3	10.9	57.7	614	65	96	60.1	959	28.35	111.5	5.2	1.4	13	168	0.44	5.2	1	1186	37.6	123.5	531.9	4	124.2
ASR10A	6ROSR38	MOIS	D	4.7	13.3	53.9	529	115	115	53.6	116.6	24.23	102.6	4	0.2	12.8	170.4	0.48	4.8	0.96	1032	30.3	109.3	669.6	1.4	127
ASR4	6ROSR39	MOIS	G	3.2	8	37.8	383	49	52	35.5	1012	25.03	99.4	4.5	BDL	10.4	258.7	0.06	5	0.7	1008	29.5	95.6	809.5	2.2	82.5
ASR4	6ROSR40	MOIS	G	1.7	8.7	44.9	420	56	68	39.8	1092	25.44	74.3	8.8	BDL	11.4	261.6	0.07	5.1	0.84	1036	25	94.2	761.5	1.4	88.8
ASR5	7ROSR01	Sandstone	G	5.9	6.5	20.2	156	38	41	19.7	1373	32.09	16.5	2.6	0.6	3.6	175.3	0.06	2.1	0.2	391	18.1	22.2	621.4	1.1	89.3
ASR5	7ROSR02	OS	G	1.6	14.4	90.9	476	77	68	50.2	993	23.14	15.6	7.7	0.6	17.9	333.7	0.08	4.9	1.06	1285	53.1	121.3	862.9	1.8	156.7
ASR5	7ROSR03	Sandstone	G	2.2	10.1	52.7	356	53	51	42.2	1184	25.8	10.8	6.8	1.6	10.7	309	0.11	3.9	0.68	987	35	82.2	744.4	1.3	101.5
ASR5	7ROSR04	WOIS	G	1.8	15	103.9	796	71	138	94.3	480	23.49	17.2	9.9	1.8	24	326.3	0.04	7	1.54	1987	66.8	190.8	788.7	2.3	156.2
ASR5	7ROSR05	OS	F	1.1	6	24.8	166	70	25	19.6	921	22.38	34.4	2.2	BDL	6.5	162.6	0.06	2	0.3	529	16.2	40.6	551.2	0.7	123.3
ASR6	SROR62	Siltstone	G	0.8	9	22.5	195	52	53	32.7	1123	25.59	38.2	2.9	0.7	5.7	173.6	0.11	1.5	0.28	380	26.7	39.6	741.1	1.4	112.4
ASR6	SROR63	MOIS	G	6.1	9.6	37.3	302	42	103	42.8	1331	27.01	32.4	3.8	0.2	8.9	186	0.21	3.2	0.51	835	30.7	71.9	725	1.1	88.4
ASR6	SROR64	MOIS	G	3.8	12.1	74.4	694	63	130	80.9	714	22.16	20	6.8	0.5	18.4	281.9	0.1	5.9	1.24	1795	47.5	179.3	784.7	1.7	155.4
ASR6	SROR65	Sandstone	F	2.2	4.9	15.8	125	65	26	19.4	873	16.83	32.4	1.9	0.5	4.7	128.7	0.1	1.2	0.17	327	17.2	28.4	513	0.7	94.1
ASR7	SROR4076	Siltstone	G	2.05	23.05	47.05	314.5	67	56	33.7	189	60.05	40.45	4	0.75	10.15	81.2	0.08	2.55	0.545	692.5	33.3	69.1	798	2.15	198.9
ASR7	SROR4077	OS	G	0.5	9.6	27.6	272	39	79	38	1645	26.73	49.2	2.5	0.6	6.8	173.2	0.34	1.9	0.36	512	26.6	51.5	846.8	1.4	83.7
ASR7	SROR4078	OS	G	0.5	12.4	54.1	731	71	238	118.3	1785	18.72	104.2	6.2	0.1	13.6	219.3	0.72	3.6	0.8	1173	41.9	105.2	842.7	1.8	127.7
ASR7	SROR4079	Sandstone	F	2	5	18.7	217	64	58	33.1	1246	15.65	35.3	1.6	0.5	5.5	155.5	0.31	1	0.23	403	18.4	35.5	598.6	0.8	86.3
ASR7	SROR4080	Conglomerate	A	4.8	8.9	47.3	358	54	54	37	1027	20.6	127	7.7	0.1	8.6	363.4	0.21	3	0.46	612	37.7	72.1	656	1.1	88.3
ASR8	7ROSR14	Sandy Siltstone	G	1.5	24.6	31.5	313	49	97	39.2	196	8.02	55	3.2	0.5	8.3	77.3	0.34	2	0.44	474	26.1	50.2	809	1.9	236.1
ASR8	SROR4005	OS	G	4.8	28.1	37	567	53	157	77.2	1167	21.25	56.6	4	0.1	8.1	11									

Section	Sample	Lithology	Facies	Ce (ppm)	Sn (ppm)	Y (ppm)	Nb (ppm)	Ta (ppm)	Be (ppm)	Sc (ppm)	Li (ppm)	S (%)	Rb (ppm)	Hf (ppm)	B (ppm)	Tl (ppm)	Hg (ppb)	Se (ppm)	Te (ppm)	Ga (ppm)	Cs (ppm)	SiO2 (%)	Al2O3 (%)	Fe2O3 (%)	MgO (%)
Worsley	CHRO5033	IOIS	E	62.6	1.4	65.7	8.5	0.3	4	16	26.5	NA	49.3	3	NA	NA	NA	NA	NA	12.2	2.9	24.11	8.21	42.75	1.36
Worsley	CHRO5032	OS	D	54.1	1.2	46	7.5	0.2	4	13	26.7	NA	48.1	2.4	NA	NA	NA	NA	NA	10.6	3	21.2	6.87	40.09	1.58
Worsley	CHRO5031	OS	D	62.7	1.5	66.9	9.8	0.5	3	14	34.8	NA	47.8	3	NA	NA	NA	NA	NA	13.1	2.8	34.38	8.08	32.18	1.85
Worsley	CHRO5030	Silty Sandstone	C	52.2	1.1	45.1	7.7	0.4	3	11	40.1	NA	54.8	3.1	NA	NA	NA	NA	NA	9.2	3.2	42.7	6.68	22.4	1.09
Worsley	CHRO5029b	Shale	B	43.3	1.2	10.9	9.9	0.5	1	7	49.6	NA	76	6	NA	NA	NA	NA	NA	12.7	4.2	63.47	6.66	13.38	0.64
Worsley	CHRO5029a	Shale	B	64.3	1.4	15.1	11.6	0.7	1	9	45.4	NA	100.6	5.8	NA	NA	NA	NA	NA	14.2	6	76.31	8.79	3.56	0.69
ASR10	SROR4047	Sandstone	G	94.1	1.5	92.2	10.4	0.6	3	12	108.7	0.37	73.7	4.2	35	0.07	66	1	0.26	10.5	4.7	53.41	9.5	18.39	1.32
ASR10	SROR4048	MOIS	G	86.6	1.2	83.7	8.8	0.4	4	15	92.4	0.15	41.9	2.9	49	0.05	35	1.2	0.99	10.9	2.6	30.32	7.71	37	2.31
ASR10	SROR4049	OS	F	55.8	0.7	48	4.4	0.3	3	7	49.6	0.19	28.8	2.9	38	0.05	16	0.6	0.36	5.9	1.6	51.77	4.17	23.88	1.51
ASR10	SROR4050	Sandstone	F	44.9	1	25.1	6.1	0.4	1	7	92.6	0.57	44.7	2.9	26	0.09	24	0.6	0.22	7	2.8	71.47	5.95	10.31	0.93
ASR10	SROR4051	Sandstone	F	57.1	1	40.7	5.2	0.4	2	7	30.6	0.05	33.6	2.9	33	0.05	13	0.6	0.31	5.6	2	59.52	4.24	18.36	1.3
ASR10	SROR4052	Sandstone	C	58.1	0.7	58.9	4.9	0.3	2	7	34.2	0.26	43	2.3	40	0.04	14	0.7	0.28	6.4	2.2	48.94	4.86	23.79	1.64
ASR10	SROR4053	IOIS	E	63.1	1.2	73.2	8	0.4	6	15	17.8	0.005	25.4	2.2	69	0.03	29	0.4	0.72	9.2	1.7	17.25	6.03	51.1	1.44
ASR10	SROR4054	IOIS	E	61.1	1.4	69.3	7.6	0.3	6	15	13.7	0.005	24.2	2.2	65	0.03	17	0.2	0.6	9.5	1.6	15.39	6.02	54.28	1.42
ASR10	SROR4055	IOIS	E	61.8	1.4	70.1	8.1	0.3	6	14	18.1	0.005	29.1	2.4	64	0.03	13	0.4	0.67	9.8	1.9	16.97	6.44	50.25	1.45
ASR10	SROR4056	IOIS	E	62.9	1.2	68.3	7.4	0.3	5	14	14.6	0.005	23.2	2	68	0.03	9	0.4	0.6	8.6	1.7	16.6	5.92	52.76	1.32
ASR10	SROR4057	IOIS	E	56.7	1.2	61.7	7.7	0.3	5	14	18.5	0.005	29.5	2.2	55	0.04	14	0.6	0.76	9.4	2	20.34	6.36	48.46	1.74
ASR10	SROR4058	IOIS	E	53.7	1.3	57.2	7.1	0.3	6	13	16.9	0.005	26.3	2.1	51	0.04	24	0.6	0.85	8.1	1.8	21.17	6.03	46.14	1.85
ASR10	SROR4059	IOIS	E	53.2	1.5	57.7	7.6	0.3	3	14	19.2	0.05	31.9	2.8	49	0.05	26	0.8	0.91	9.4	2.3	25.77	6.35	42.81	1.97
ASR10	SROR4083	IOIS	E	55.1	1.5	62.6	8.7	0.4	2	14	20.5	0.06	34.6	2.4	49	0.06	29	0.8	0.84	9.3	2.2	26.5	6.45	42.25	1.99
ASR10	SROR4060	MOIS	D	50.1	1.4	50.5	7.1	0.3	3	13	25.3	0.25	33.8	2.1	38	0.07	22	0.8	0.66	9.3	2.4	28.95	6.67	34.68	2.4
ASR10A	6ROSR31	MOIS	G	99.3	1.5	101.6	9	0.4	4	17	65.8	0.43	35.5	2.8	57	0.06	44	0.9	1.24	9.6	2.3	37.7	7.16	31.92	1.52
ASR10A	6ROSR32	OS	F	35.7	0.6	21.6	4.3	0.2	2	6	24	0.12	31.7	3	36	0.07	13	0.5	0.18	4.8	1.9	61.61	3.85	19.81	1.05
ASR10A	6ROSR33	Sandstone	F	47	1	31.9	5.7	0.3	1	8	38.1	0.11	40.2	2.6	31	0.08	23	0.6	0.35	6.1	2.2	71.57	5.25	11.14	0.79
ASR10A	6ROSR34	IOIS	E	105.5	1.4	126.4	9.1	0.4	5	16	34.4	0.46	38.2	3.2	63	0.08	49	0.7	0.88	9.9	2.7	25.97	7.75	39.49	1.63
ASR10A	6ROSR35	IOIS	E	85.5	1.6	96.8	8.5	0.5	6	14	35.1	0.31	41	3.3	61	0.08	33	0.5	0.78	9.7	2.8	22.39	7.19	46.22	1.67
ASR10A	6ROSR36	IOIS	E	84.3	1.4	94	8.1	0.4	4	14	30.7	0.33	37.7	2.6	52	0.08	37	0.6	0.83	9	2.8	24.28	7.24	43.75	1.95
ASR10A	6ROSR37	IOIS	E	79.3	1.5	85.8	9	0.4	5	15	30.1	0.31	43.3	3	42	0.08	37	0.6	0.86	9.9	2.9	28.06	7.6	37.58	2.39
ASR10A	6ROSR38	MOIS	D	66.7	1.2	64.9	9.2	0.5	4	14	39.3	0.52	45.1	2.8	37	0.1	25	0.7	0.94	10.8	3.2	32.16	7.76	33.08	2.37
ASR4	6ROSR39	MOIS	G	62.9	1	50.4	6	0.3	3	12	25.8	0.64	26.4	2	33	0.1	161	0.7	0.81	7	1.5	18.49	4.88	34.25	3.12
ASR4	6ROSR40	MOIS	G	52.7	1	52.8	6.4	0.3	3	13	28.2	0.42	27	2.3	30	0.07	35	1.3	0.81	7.8	1.7	20.92	5.17	35.21	2.64
ASR5	7ROSR01	Sandstone	G	39.1	0.9	34.6	5.6	0.3	4	10	33.8	0.29	30.9	2.2	37	0.07	19	0.5	0.18	6.2	2	18.97	4.45	38.68	3.99
ASR5	7ROSR02	OS	G	131.7	1.8	98.7	11.4	0.6	5	16	67.6	0.2	57.2	4	53	0.08	23	1.6	1.02	12	3.4	36.41	8.81	27.37	2.35
ASR5	7ROSR03	Sandstone	G	79.2	1.3	66.4	7.1	0.3	4	15	40.3	0.24	35.3	2.2	41	0.13	28	1	0.57	8	2.3	19.26	5.78	31.12	2.68
ASR5	7ROSR04	WOIS	G	150.6	2.2	127.2	12.3	0.5	5	21	60.8	0.34	47.7	3.4	41	0.1	47	1.5	1.53	12.8	3.1	27.71	9.24	29.75	2.8
ASR5	7ROSR05	OS	F	36.4	0.6	28.2	4.1	0.2	4	7	21	0.25	22.9	2.7	30	0.06	14	0.6	0.29	5.4	1.2	42.45	3.23	27.64	2.39
ASR6	SROR62	Siltstone	G	58.7	0.9	46.7	7.2	0.4	2	10	48.3	0.09	49.9	3	30	0.07	24	0.8	0.25	7.7	3.1	32.41	6	31.77	3.32
ASR6	SROR63	MOIS	G	71.5	1.1	72.5	6.6	0.3	4	14	54.8	0.53	44.4	2.6	47	0.06	26	0.9	0.46	8.5	3	24.7	6.32	37.41	3.1
ASR6	SROR64	MOIS	G	97.7	1.8	90	10.3	0.4	3	19	47.5	0.39	47.9	3.6	38	0.05	38	1.2	1.25	12.5	3.2	27.1	9.02	30.51	2.69
ASR6	SROR65	Sandstone	F	34	1.9	20.7	3.7	0.2	2	7	19.8	0.13	26.3	2.6	22	0.05	20	0.4	0.18	4	1.2	46.52	3.05	22.74	2.16
ASR7	SROR4076	Siltstone	G	66.45	1.45	29.65	13.25	0.8	3	13	77.85	0.275	94.6	5.85	21	0.075	56	0.8	0.415	15.3	5.75	61.44	11.51	13.33	1.045
ASR7	SROR4077	OS	G	53.6	0.9	59.5	6	0.4	3	10	76.6	0.12	41.1	1.9	40	0.06	25	0.6	0.29	7.1	2.1	26.81	5.87	37.03	2.64
ASR7	SROR4078	OS	G	97.2	0.7	145.8	8	0.3	4	16	149.8	0.52	45.5	3.4	39	0.05	32	1	0.79	8.7	2.2	39.47	7.84	25.9	1.56
ASR7	SROR4079	Sandstone	F	40.6	0.05	40	3.3	0.2	2	6	45	0.12	26.4	2	30	0.04	6	0.3	0.2	4.2	0.7	46.14	3.27	21.54	1.8
ASR7	SROR4080	Conglomerate	A	70.1	0.2	70.4	6.4	0.4	3	13	32.5	0.34	41.1	2.3	42	0.09	39	0.7	0.41	7.5	1.9	25.42	5.45	29.27	2.38
ASR8	7ROSR14	Sandy Siltstone	G	54.3	1.9	30.7	13.5	0.8	3	11	89.6	0.36	85.9	6	22	0.11	58	1.1	0.34	13.2	5.4	63.29	11.25	11.08	1.07
ASR8	SROR4005	OS	G	69.1	1.4	74.2	9.4	0.5	6	12	134.2	0.84	64.2	3.7	33	0.09	39	1.3	0.38	10.8	3.9	40.91	9.4	27.45	1.3
ASR8	7ROSR13	OS	G	82.9	1.1	111	7.2	0.4	4	11	144.7	1.13	40.3	2.7	48	0.1	30	0.9	0.41	7.5	2.6	27.55	6.85	37.21	1.92
ASR8	SROR4004	WOIS	G	84.7	1.3	82.7	9.1	0.4	5	14	147.5	0.98	52.3	2.8	29	0.06	40	1.1	0.89	11.1	3.3	32.69	8.97	32.8	1.38
ASR8	7ROSR12	MOIS	G	110.1	1.9	120.4	10.3	0.5	6	16	118.1	0.66	49.7	3.7	39	0.08	43	1							

Section	Sample	Lithology	Facies	CaO (%)	Na2O (%)	K2O (%)	TiO2 (%)	P2O5 (%)	LOI (%)	Pr (ppm)	Nd (ppm)	Sm (ppm)	Eu (ppm)	Gd (ppm)	Tb (ppm)	Dy (ppm)	Ho (ppm)	Er (ppm)	Tm (ppm)	Yb (ppm)	Lu (ppm)
Worsley	CHRO5033	IOIS	E	2.14	0.09	1.01	0.29	1.74	17.9	10.48	46.1	13.27	2.95	13.46	2.5	13.25	2.2	5.67	0.89	4.8	0.63
Worsley	CHRO5032	OS	D	7.3	0.09	0.96	0.28	1.3	20.1	8.6	37.3	9.95	2.31	9.98	1.8	9.5	1.59	4.01	0.64	3.39	0.48
Worsley	CHRO5031	OS	D	3.2	0.14	1.02	0.28	0.92	17.7	10.23	43.3	13.51	3.07	14.27	2.66	14	2.36	5.9	0.88	4.94	0.67
Worsley	CHRO5030	Silty Sandstone	C	8.38	0.23	1.12	0.29	1.02	15.8	7.74	33.9	8.9	2	9.1	1.62	8.59	1.44	3.72	0.6	3.37	0.46
Worsley	CHRO5029b	Shale	B	0.33	0.54	1.65	0.39	0.18	12.7	5.24	19.2	2.97	0.52	1.88	0.31	1.99	0.35	0.97	0.21	1.21	0.2
Worsley	CHRO5029a	Shale	B	0.33	0.35	1.8	0.49	0.14	7.5	7.79	28.3	5.65	0.93	3.36	0.55	2.84	0.51	1.47	0.24	1.73	0.26
ASR10	SROR4047	Sandstone	G	3.05	0.32	1.55	0.48	1.71	10	13.22	61.5	17	4.23	19.22	3.1	16.4	3	7.99	0.99	5.71	0.84
ASR10	SROR4048	MOIS	G	3.14	0.13	0.82	0.29	1.28	16.9	12.27	57.5	16.9	4.11	18.5	3.03	15.66	2.83	7.46	1.02	5.71	0.84
ASR10	SROR4049	OS	F	3.41	0.09	0.63	0.18	1.31	12.8	7.27	33.8	9.1	2.28	10.29	1.62	8.72	1.54	4.32	0.55	3.03	0.49
ASR10	SROR4050	Sandstone	F	1.57	0.1	0.98	0.26	0.2	7.9	5.62	25	6.2	1.39	5.74	0.9	5.01	0.91	2.47	0.33	1.93	0.31
ASR10	SROR4051	Sandstone	F	3.62	0.1	0.73	0.19	1.45	10.2	7.22	32.4	8.4	2.02	8.67	1.41	7.42	1.32	3.6	0.47	2.7	0.42
ASR10	SROR4052	Sandstone	C	5.1	0.08	0.96	0.19	0.51	13.7	8.23	37.4	9.9	2.49	11.83	1.92	9.41	1.65	4.46	0.58	2.83	0.42
ASR10	SROR4053	IOIS	E	2.39	0.11	0.52	0.19	1.71	18.9	9.94	54.3	13.9	3.43	15.41	2.67	13.53	2.27	6.26	0.82	5.29	0.72
ASR10	SROR4054	IOIS	E	1.9	0.08	0.48	0.18	1.62	18.3	9.79	48.1	13.4	3.38	14.8	2.63	13.28	2.22	6.07	0.8	5.02	0.7
ASR10	SROR4055	IOIS	E	3.26	0.1	0.57	0.21	2.52	17.9	9.44	48.3	12.2	3.21	14.06	2.49	12.39	2.17	6.08	0.8	5.09	0.72
ASR10	SROR4056	IOIS	E	2.43	0.09	0.48	0.19	1.98	17.9	9.57	47.6	13.2	3.26	14.24	2.61	12.81	2.22	5.91	0.79	4.89	0.64
ASR10	SROR4057	IOIS	E	2.09	0.08	0.58	0.22	1.27	18.5	8.63	43.4	11.5	2.85	12.55	2.33	11.94	1.97	5.26	0.72	4.49	0.63
ASR10	SROR4058	IOIS	E	2.78	0.09	0.56	0.2	1.61	19.2	8.36	41.5	11	2.64	11.61	2.16	11.18	1.81	5.17	0.65	4.25	0.59
ASR10	SROR4059	IOIS	E	2.69	0.09	0.63	0.21	1.22	17.9	7.88	37.4	10.1	2.73	11.95	2.19	11.03	2.06	5.04	0.72	4.61	0.56
ASR10	SROR4083	IOIS	E	2.65	0.1	0.63	0.21	1.17	17.7	8.2	41	10.9	2.96	12.91	2.27	11.79	2.13	5.4	0.74	4.8	0.59
ASR10	SROR4060	MOIS	D	5.79	0.28	0.7	0.24	1.57	18.4	7.27	34.2	9.2	2.31	10.34	1.79	8.97	1.7	4.19	0.6	3.65	0.48
ASR10A	6ROSR31	MOIS	G	3.07	0.13	0.79	0.24	1.42	15.7	15.1	67.8	18.3	4.69	22.31	3.99	20.8	3.22	8.87	1.07	6.62	0.91
ASR10A	6ROSR32	OS	F	1.82	0.09	0.77	0.18	0.45	10.2	4.74	18.4	4.5	1.03	4.84	0.82	4.36	0.7	1.99	0.23	1.68	0.23
ASR10A	6ROSR33	Sandstone	F	2.34	0.12	0.96	0.23	0.18	7.3	6.29	25.3	6.4	1.47	7.04	1.28	6.7	1.05	2.78	0.34	2.28	0.31
ASR10A	6ROSR34	IOIS	E	3.51	0.21	0.87	0.26	2.13	17.6	16.04	72.3	19.2	4.92	25.2	4.64	23.42	3.78	10.21	1.26	7.52	1.08
ASR10A	6ROSR35	IOIS	E	2.44	0.14	0.76	0.27	1.37	17.1	13.22	57.6	15.7	3.92	19.76	3.64	18.9	3.07	8.41	0.97	6.1	0.85
ASR10A	6ROSR36	IOIS	E	2.49	0.17	0.73	0.27	1.25	17.5	13.51	60.3	16.2	4.07	20.13	3.69	19.21	3.02	8.25	1.03	6.19	0.88
ASR10A	6ROSR37	IOIS	E	3.08	0.23	0.88	0.28	1.48	18	13.13	58	15	3.66	17.58	3.26	16.6	2.65	7.45	0.93	5.82	0.8
ASR10A	6ROSR38	MOIS	D	3.22	0.23	1	0.31	0.95	18.5	10.63	48.9	12	2.99	13.93	2.57	13.43	2.34	5.83	0.75	4.52	0.66
ASR4	6ROSR39	MOIS	G	12.72	0.15	0.6	0.18	1.3	23.9	9.79	43.8	11.1	2.65	11.9	2.11	10.37	1.85	4.45	0.57	3.51	0.52
ASR4	6ROSR40	MOIS	G	11.02	0.23	0.63	0.18	1.78	21.8	8.07	36.5	9.5	2.5	10.94	2.15	11.06	1.93	4.86	0.63	3.93	0.57
ASR5	7ROSR01	Sandstone	G	5.81	0.21	0.72	0.24	0.68	25.9	5.18	22	5.35	1.29	6.1	1.11	5.17	0.99	2.79	0.4	2.42	0.34
ASR5	7ROSR02	OS	G	4.5	0.3	1.34	0.42	2.27	15.8	19.44	88.3	23.98	5.5	24.85	4.3	17.94	3.19	8.08	1.06	6.36	0.89
ASR5	7ROSR03	Sandstone	G	12.98	0.2	0.81	0.25	1.83	24.7	11.22	52	13.39	3.18	14.64	2.61	11.64	2.05	5.15	0.75	4.2	0.57
ASR5	7ROSR04	WOIS	G	7.36	0.25	1.09	0.34	2.64	18.4	22.04	101.8	26.92	6.49	29.42	5.37	23.33	3.93	9.95	1.31	7.9	1.07
ASR5	7ROSR05	OS	F	4.79	0.16	0.58	0.15	0.52	17.8	4.77	21.4	5.02	1.19	5.69	1.06	4.6	0.87	2.33	0.35	2.05	0.3
ASR6	SROR62	Siltstone	G	3.8	0.27	1	0.33	1.03	19.9	7.96	36.2	9.1	2.17	9.49	1.5	8.07	1.5	4.04	0.54	2.85	0.42
ASR6	SROR63	MOIS	G	3.95	0.26	0.89	0.28	0.93	21.8	9.82	48.3	13.5	3.63	15.88	2.7	13.7	2.44	5.81	0.76	5.01	0.63
ASR6	SROR64	MOIS	G	7.98	0.32	0.96	0.3	1.91	18.8	13.44	64	16.8	4.76	19.67	3.41	17.59	3.02	7.77	1.06	6.72	0.84
ASR6	SROR65	Sandstone	F	7.1	0.15	0.59	0.15	0.31	16.9	4.35	19	4	1.07	4.37	0.72	4	0.69	1.79	0.26	1.74	0.2
ASR7	SROR4076	Siltstone	G	0.31	0.32	1.77	0.57	0.215	8.95	8.495	37.25	7.25	1.655	6.39	1.065	5.64	1.07	2.95	0.46	3.29	0.405
ASR7	SROR4077	OS	G	3.79	0.16	0.8	0.26	1.21	21.1	8.19	39.4	10.3	2.77	12.63	2.15	10.97	1.9	4.89	0.64	4.08	0.55
ASR7	SROR4078	OS	G	5.72	0.13	0.88	0.25	1.66	16	15.7	81.4	23.1	6.29	29.59	5.07	25.74	4.6	11.54	1.53	9.18	1.17
ASR7	SROR4079	Sandstone	F	8.32	0.09	0.55	0.13	0.44	17.3	5.61	25.8	7	1.87	8.64	1.38	7.23	1.29	3.29	0.44	2.7	0.33
ASR7	SROR4080	Conglomerate	A	12.83	0.18	0.81	0.23	1.46	19.1	10.18	46.3	11.4	2.93	13.25	2.15	11.16	1.98	4.99	0.7	4.43	0.57
ASR8	7ROSR14	Sandy Siltstone	G	0.27	0.38	1.92	0.61	0.2	9.7	6.79	28.1	5.49	1.13	4.89	0.93	4.52	0.87	2.68	0.41	2.5	0.38
ASR8	SROR4005	OS	G	2.08	0.23	1.21	0.39	0.87	15.5	10.05	51.5	15	3.53	15.99	2.49	14.24	2.45	6.52	0.89	5.04	0.68
ASR8	7ROSR13	OS	G	3.96	0.19	0.9	0.29	1	19.6	13.23	66.8	17.74	4.42	22.3	3.9	17.05	3.1	8.15	1	5.68	0.84
ASR8	SROR4004	WOIS	G	2.91	0.13	0.97	0.3	1.38	17.9	12.66	62.2	18.9	4.5	19.8	3.14	16.87	2.88	7.28	1.03	6.14	0.81
ASR8	7ROSR12	MOIS	G	3.2	0.14	1.06	0.33	2.02	17.5	17.91	84.8	23.44	5.63	25.84	4.66	20.43	3.58	9.06	1.24	6.94	0.97
ASR8	SROR4003	Sandstone	F	4.03	0.1	0.61	0.16	0.93	17.1	9.13	47.3	13.6	3.48	15.87	2.58	13.16	2.42	6.35	0.82	4.51	0.63
ASR8	7ROSR11	Sandstone	F	11.6	0.13	0.54	0.1	0.42	16.9	4.17	19.3	4.53	1.03	4.97	0.87	3.94	0.72	1.91	0.26	1.53	0.22
ASR8	SROR4002	Sandstone	F	12.62	0.11	0.61	0.13	0.22	14.2	4.42	20.6	5.3	1.26	6	0.96	4.87	0.93	2.37	0.3	1.71	0.24
ASR8	SROR4001	Sandstone	F	1.05	0.18	0.94	0.21	0.33	4.9	4.36	18.7	5	1.07	4.49	0.75	4.12	0.71	2.01	0.28	1.62	0.25
ASR9A	SROR4010	OS	G	1.96	0.25	1.04	0.34	0.89	14.6	7.65	35.4	10	2.52	11.65	1.93	10.69	1.96	5.08	0.7	4.04	0.54
ASR9A</																					

Section	Sample	Lithology	Facies	Mo (ppm)	Cu (ppm)	Pb (ppm)	Zn (ppm)	Ag (ppb)	Ni (ppm)	Co (ppm)	Mn (ppm)	Fe (%)	As (ppm)	U (ppb)	Au	Th (ppm)	Sr (ppm)	Cd (ppm)	Sb (ppm)	Bi (ppm)	V (ppm)	La (ppm)	Cr (ppm)	Ba (ppm)	W (ppm)	Zr (ppm)
ASR9A	7ROSR07	IOIS	E	1.3	14.4	90.6	748	87	90	75.9	592	25.84	86.9	5.4	0.5	21.4	174.6	0.05	7.1	1.34	1892	35.6	169	586.9	1	162.2
ASR9A	SROR4012	OS	F	8.4	9.6	29.6	369	88.5	146.5	55.1	1284	15.65	179.7	2.4	0.2	7.55	140.7	0.72	3.8	0.375	493.5	29.55	56.8	587.4	0.7	114.1
ASR9A	7ROSR08	Sandstone	F	0.6	7.1	29	201	92	28	24.4	1070	15.88	75.9	6.4	0.2	8.5	179.4	0.1	1.9	0.43	562	21.1	55.6	535.7	0.6	140
ASR9A	7ROSR09	Sandstone	F	1.5	6.2	29.1	161	80	25	21.4	247	5.93	43.7	3.3	0.6	8	121	0.05	1.9	0.36	473	21.1	46.2	609.7	0.7	110.6
ASR9A	SROR4013	Silty Sandstone	F	3.9	6.6	19.6	187	52	60	36.9	482	5.94	41.2	2.6	0.6	5.3	146.8	0.17	1.2	0.19	289	17.5	35.3	604.8	1.2	86.5
ASR9A	7ROSR10	Sandstone	F	1.3	5.2	16.3	96	81	12	11.9	775	17.55	29.2	3.4	0.2	4.7	113	0.04	1.1	0.17	279	14.4	25.9	541.8	0.4	121.4
ASR9A	SROR4014	Silty Sandstone	C	3.4	9.2	20.5	134	47	28	29.5	280	5.88	60.9	2.1	0.1	5.4	103.1	0.1	1.6	0.19	297	16.1	31.7	592.7	0.9	125.2
ASR9A	SROR4015	Sandstone	C	4.8	9.3	19.7	138	46	31	29.2	265	6.34	64.9	1.7	0.3	5.8	80.1	0.1	1.6	0.22	313	14.6	38.6	595.7	1.4	107.7
ASR9A	SROR4016	Sandstone	C	0.8	8.4	13.6	85	41	21	7.3	56	4.19	50.4	1.9	0.9	4.4	83.1	0.04	1.1	0.13	204	17.5	25.7	617	0.6	155
ASR9A	SROR4017	Silty Sandstone	C	0.8	11.2	15.8	109	45	20	18	136	5.89	77.5	6	0.5	4.6	254.5	0.2	1.3	0.14	199	34.8	29.9	818	1.5	143.2
ASR9A	SROR4018	Sandstone	C	0.4	8.7	15.2	393	78	138	60.2	1012	21.94	97.3	4	0.3	4.9	122.9	0.84	1.4	0.17	263	30.1	34.2	570.5	0.8	142.3
ASR9A	SROR4019	IOIS	E	10.6	9.7	54.6	785	41	159	71.7	1563	44.75	302.9	4.8	0.1	15.7	145.4	0.57	8.6	1.08	1536	44.7	185.1	417.4	8.6	92.6
ASR9A	SROR4020	IOIS	E	12.2	7.1	54.8	651	35	106	62.4	1200	46.71	169.7	4.4	0.1	15.7	126.1	0.05	9.6	1.08	1477	31.4	166.8	394.9	8.1	100.4
ASR9A	SROR4021	IOIS	E	11.2	7.4	51.3	629	38	131	64	1133	45.8	200.5	5.2	0.6	14.8	158.8	0.25	8.4	1.04	1497	36.7	167.9	427.9	8.7	98
ASR9A	SROR4022	IOIS	E	8.2	7	47.5	599	42	112	48.8	981	41.4	211.6	5.4	0.5	14.5	160.6	0.21	7.3	1.03	1390	31.2	161.3	400.4	8.3	86.2
ASR9A	SROR4023	IOIS	E	7.1	8	48.3	584	46	102	75.7	1055	37.62	126.5	5.6	0.3	12.2	193.5	0.1	6.8	0.91	1453	34.3	139.5	468.6	7.8	93.2
ASR9A	SROR4024	IOIS	E	6.8	10	52.4	612	62	115	70.3	859	32.1	220.9	7.2	0.2	15.9	204.6	0.04	8.2	1.15	1673	40.3	182.9	532	4.4	135
ASR9A	SROR4009	OS	D	10.2	14.7	40.3	395	68	55	44.5	1387	25.13	122.2	3.9	0.5	9.7	152.2	0.06	4.6	0.64	840	30.3	100.3	626.4	1.1	116.3
ASR9A	SROR4008	Silty Sandstone	C	9.8	14	30.7	300	75	40	28.7	616	16.7	130.7	2.7	0.1	8.4	86.8	0.06	4.6	0.51	623	24.3	81.4	572.9	1	112.4
ASR9A	SROR4007	Silty Sandstone	C	4.8	18.2	25.8	227	87	42	25	315	10.21	122	3.2	0.7	7	116.6	0.07	2.7	0.38	454	32	61.1	733	1.6	173.1
ASR9A	SROR4006	Shale	B	0.9	22.9	18.2	143	105	32	13	91	3.57	39.5	3.8	0.1	5.2	109.2	0.08	1.4	0.25	227	34.8	28.6	953.7	1.9	216.5
ASR9B	SROR4027	IOIS	G	1.8	10.9	51.9	435	62	87	52.3	1364	27.9	78.2	6.5	1.1	12.5	348.3	0.19	4.2	0.81	1241	39.9	125.2	786.7	1.7	112.2
ASR9B	SROR4028	MOIS	F	1	7.4	29.2	264	83	47	31.1	1103	17.59	65.8	3.9	0.7	8.3	186.8	0.18	2.2	0.42	654	26.2	65.1	563.7	1.1	129.8
ASR9B	SROR4029	OS	C	0.7	8	19.7	378	72	85	77.2	679	18.33	76.2	4.3	0.1	5	143.1	0.18	1.4	0.21	320	29.8	40	543.9	0.6	134.7
ASR9B	SROR4025	IOIS	E	9.6	7.3	51.8	602	39	94	66	1261	42.84	174.5	5.6	0.1	14.5	180.3	0.04	7.5	1.03	1803	43.4	167	447.5	11.3	95.7
ASR9B	SROR4026	IOIS	E	9.4	7.5	53.7	593	38	88	67.4	778	38.8	230.4	4.6	0.3	14.6	185.3	0.005	7.9	1.07	1620	30.6	173.6	443.4	10.6	92.4
ASR9B	SROR4033	MOIS	E	8.9	6.4	54.9	617	31	110	67.1	756	37.37	498.8	4.6	0.3	15	177.4	0.01	17.9	1.1	1639	33	176.9	397.5	9.1	90.5
ASR9B	SROR4034	OS	D	6.3	12.1	42.3	453	68	78	57.4	911	27.58	335	5.1	0.6	11.3	158.5	0.12	9.1	0.8	1039	32.3	124.5	546.9	1.4	99.5
ASR9I	6ROSR24	OS	G	2.2	10.3	46.5	323	57	51	31.4	1236	27.42	71	5.6	1.2	9.8	247.6	0.16	3.7	0.64	784	23.6	72.9	838.5	1.7	104.4
ASR9I	6ROSR25	OS	G	1	11.4	61.3	548	101	91	67.3	856	17.02	109.9	6.9	1.4	16.1	374.1	0.12	4.9	0.93	1322	57.1	115.2	968.6	2.2	192.9
ASR9I	6ROSR26	Sandstone	F	0.7	7.2	46.2	320	85	48	40.2	1131	15.36	106.4	4.3	1.4	11	198.1	0.06	3.1	0.67	872	24.5	71.5	669.7	1.4	129.2
ASR9I	6ROSR28	MOIS	D	3.3	12.4	62.8	566	80	64	53	869	24.15	28.7	4.2	1.4	15.4	216.6	0.06	4.9	1.17	1250	30.3	138.6	673.8	1.7	130.2
ASR9I	6ROSR29	Sandstone	D	3.1	11.9	43.7	401	91	70	49.9	724	21.46	73.6	3.6	0.8	10	160.6	0.07	3.8	0.72	861	27.7	82.3	650.7	1.8	133.6
ASR9I	6ROSR30	Silty Sandstone	D	8.7	14.7	37.3	225	245	46	30.3	83	10.87	336.6	2.8	BDL	9.2	74.1	0.06	6.1	0.64	672	21.6	84	650.6	2.7	154.4
BBM	7ROSR21	MOIS	G	1.5	8.3	34.8	336	60	75	65.6	990	22.74	105.2	6	0.5	8.8	67.1	0.11	3.6	0.57	673	25.2	72.7	613.3	1	88.6
BBM	7ROSR20	MOIS	G	1.8	8.5	47.5	405	66	66	48.6	667	22.68	119.1	5.1	0.4	11.9	77.7	0.04	4.3	0.86	960	28.6	107.7	699.8	1.3	116.2
BBM	7ROSR19	MOIS	G	0.9	9.7	45.6	422	83	79	55.6	1668	26.82	61.2	4.8	BDL	11.6	75.4	0.08	4.3	0.86	912	23.7	100.9	585.1	0.7	118.3
BBM	7ROSR18	Sandstone	C	0.4	7.4	33.5	252	64	39	31.8	1385	23.54	32	4.5	0.2	6.8	131.7	0.04	2.6	0.43	557	35.5	50.1	521.8	0.6	132.2
BBM	7ROSR17	Sandstone	C	10.7	7.8	22.2	124	72	27	29.2	462	8.02	53.9	1.8	BDL	4.8	61.3	0.05	1.7	0.21	336	18.1	32.9	470	0.7	152.1
BBM	7ROSR15	IOIS	E	0.7	6.5	26.7	177	69	24	15.8	2485	35.13	74	2	0.3	5.4	76.2	0.09	1.4	0.26	364	18.2	34.7	446.4	0.7	112.1
BBM	7ROSR16	Sandstone	D	1.4	12.8	153.4	1354	67	137	126.2	371	23.41	632.1	5.4	BDL	30.9	221	0.1	15.2	2.46	2654	63.2	267.6	639.6	1	187
SPRV	6ROSR11	Sandstone		0.6	9.2	35	272	53	31	23.3	1284	31.92	49.8	5.7	0.5	7	211.7	0.1	2	0.52	634	22.1	50.6	851.9	1.7	88.7
SPRV	6ROSR10	IOIS	E	0.8	17.5	122	868	71	150	78.8	519	23.82	228.4	5.9	0.6	21.2	136.6	0.08	8	1.77	1768	34.1	166.2	1118	1.5	175.5
SPRV	6ROSR09	IOIS	E	7.1	9.7	75.7	600	54	102	36.8	1135	37.92	187.6	4.7	0.9	16.3	120.1	0.07	8.5	1.34	1455	28.1	137.3	721.6	6.7	93.6
SPRV	6ROSR08	MOIS	E	7.5	7.1	51.7	528	56	133	36.9	1020	35.6	196	5.7	0.9	12.9	172.9	0.03	8.2	1.01	1297	30.2	122.6	656.5	7.1	90.9
SPRV	6ROSR07	OS	G	1	6.8	32.3	295	90	58	45.7	700	20.13	52.5	3.3	BDL	6.7	122.7	0.16	3	0.48	506	16.4	53.4	4704	0.8	77.6
SPRV	6ROSR06	MOIS	G	7.1	10.5	92.																				

Section	Sample	Lithology	Facies	Ce (ppm)	Sn (ppm)	Y (ppm)	Nb (ppm)	Ta (ppm)	Be (ppm)	Sc (ppm)	Li (ppm)	S (%)	Rb (ppm)	Hf (ppm)	B (ppm)	Tl (ppm)	Hg (ppb)	Se (ppm)	Te (ppm)	Ga (ppm)	Cs (ppm)	SiO2 (%)	Al2O3 (%)	Fe2O3 (%)	MgO (%)
ASR9A	7ROSR07	IOIS	E	80.9	2	76	10.3	0.5	5	18	43.6	0.3	39.5	3.5	64	0.08	26	1.1	1.51	11.5	2.5	36.13	7.81	32.29	2.48
ASR9A	SROR4012	OS	F	60.2	0.8	79.6	5.9	0.3	2	8	61.65	0.65	38.4	3.15	40.5	0.115	27	1.25	0.42	6.8	2.35	57.14	5.26	20.54	0.99
ASR9A	7ROSR08	Sandstone	F	45.8	0.9	45.2	5.7	0.3	3	8	23.8	0.22	29.1	3.4	40	0.09	13	1	0.41	5.9	1.6	52.63	4.26	21.59	1.43
ASR9A	7ROSR09	Sandstone	F	49.2	0.9	39.4	5.2	0.4	2	6	21	0.09	27.3	2.7	24	0.05	13	0.6	0.33	4.9	1.3	79.6	3.62	8.16	0.7
ASR9A	SROR4013	Silty Sandstone	F	42.3	0.7	30.6	4.2	0.3	2	5	62.1	0.64	30.3	2.4	21	0.06	16	0.4	0.2	5.4	1.6	75.81	3.99	8.09	0.51
ASR9A	7ROSR10	Sandstone	F	31.7	0.7	19.6	4.4	0.2	2	5	15.2	0.18	23.4	2.8	33	0.07	10	0.4	0.08	4	1.2	61.72	2.73	21.98	1.17
ASR9A	SROR4014	Silty Sandstone	C	32.7	1	16.5	5.4	0.3	2	6	76.5	0.44	43.4	3.4	16	0.07	15	0.6	0.16	6.7	2.6	77.18	5.32	7.55	0.54
ASR9A	SROR4015	Sandstone	C	29.6	0.8	15.1	5.3	0.3	1	5	70.3	0.22	42	2.8	21	0.08	10	0.8	0.15	7.4	2.3	77.97	5.27	8.17	0.53
ASR9A	SROR4016	Sandstone	C	33.9	0.8	16.7	5.1	0.4	1	5	53.2	0.24	48.4	4	16	0.07	20	0.5	0.05	7.6	2.9	79.96	5.99	5.52	0.55
ASR9A	SROR4017	Silty Sandstone	C	79.2	0.9	64.4	5	0.3	2	7	51.4	0.38	49.7	3.9	24	0.09	13	0.8	0.06	7.4	2.9	71.77	5.96	7.76	0.59
ASR9A	SROR4018	Sandstone	C	64.5	0.8	75.8	5.2	0.2	3	6	42	0.24	42.3	4	44	0.1	20	1	0.09	6.2	2.6	51.64	4.87	28.73	0.89
ASR9A	SROR4019	IOIS	E	86.9	1.4	135.1	7.7	0.3	6	15	31.7	0.16	18.2	1.9	66	0.04	35	0.8	0.8	9	1.4	14.67	5.66	57.5	0.83
ASR9A	SROR4020	IOIS	E	58.9	1.2	77.1	7.5	0.3	5	15	19	0.09	16.2	2.4	72	0.02	8	0.2	0.44	9.6	1.2	11.18	5.12	62.04	0.8
ASR9A	SROR4021	IOIS	E	64.2	1.2	95.4	7.5	0.3	5	14	25.2	0.13	17.7	2.1	71	0.03	10	0.3	0.54	9	1.2	11.71	5.15	60.22	1.02
ASR9A	SROR4022	IOIS	E	59	1.1	75.5	7.8	0.3	6	13	27.3	0.19	18.8	2.2	67	0.02	15	0.4	0.64	8.9	1.4	15.74	5.1	56.04	1.14
ASR9A	SROR4023	IOIS	E	66.2	1.2	75.6	8.3	0.3	6	14	34.2	0.12	25.3	2.1	57	0.05	34	0.6	0.54	9.7	1.8	17.55	5.75	51.66	1.32
ASR9A	SROR4024	IOIS	E	75.8	1.5	91.9	9.8	0.4	4	17	43.5	0.16	30.5	3.1	58	0.16	55	1.3	1.08	10.9	2.1	23.88	6.68	45	1.45
ASR9A	SROR4009	OS	D	58.1	1.6	48.6	9.5	0.5	4	12	39	0.1	54.9	2.9	34	0.08	24	0.7	0.46	11.7	3.7	36.49	7.7	33.46	2.07
ASR9A	SROR4008	Silty Sandstone	C	45.7	1.6	31.4	8.8	0.5	2	10	42.1	0.58	53.5	3	23	0.07	24	0.7	0.38	10.4	3.8	51.57	7.83	22.13	1.59
ASR9A	SROR4007	Silty Sandstone	C	61.2	1.7	35.3	10.5	0.6	2	11	55.3	0.85	75.6	4.6	19	0.07	30	0.9	0.26	12.4	4.9	60.67	8.68	13.68	1.57
ASR9A	SROR4006	Shale	B	64.5	2	27.8	14.6	0.9	2	11	75.1	0.46	109.6	6.3	16	0.07	39	0.7	0.04	15.4	7.5	69.13	12	4.48	1.18
ASR9B	SROR4027	IOIS	G	82.5	1.3	75.2	8.1	0.3	5	15	36.9	0.33	42.2	2.6	56	0.06	16	1.4	0.85	11.3	3	25.17	7.04	39.26	2.47
ASR9B	SROR4028	MOIS	F	54.6	0.8	39.8	5.7	0.3	4	9	20.8	0.14	32.1	2.9	30	0.05	10	0.8	0.43	6.8	1.9	52.23	4.32	23.83	1.43
ASR9B	SROR4029	OS	C	59.8	0.7	40	5	0.3	2	6	24.5	0.13	37.6	3.4	37	0.08	25	1.5	0.14	6.2	2.1	51.07	4.52	24.53	1.41
ASR9B	SROR4025	IOIS	E	80.9	1.3	97.9	9.1	0.4	5	16	14.1	0.22	20.3	2.1	61	0.03	40	0.6	0.59	9.7	1.4	12.64	5.62	58.33	1.19
ASR9B	SROR4026	IOIS	E	60	1.3	78.4	8.1	0.3	6	14	12.6	0.1	18.5	1.8	62	0.03	31	0.5	0.76	9.8	1.4	13.87	5.34	53.62	1.25
ASR9B	SROR4033	MOIS	E	62.9	1.2	81.6	8.1	0.2	7	15	9.4	0.53	16.4	2	52	0.26	70	0.7	0.8	8.6	1.1	13.55	5.42	52.21	1.53
ASR9B	SROR4034	OS	D	62.3	1.4	59.6	8.8	0.5	3	13	27.8	0.69	44.6	2.4	39	0.11	53	1	0.78	10.9	3.1	27.26	7.07	37.95	2.26
ASR91	6ROSR24	OS	G	49.6	1	39	7.4	0.4	4	12	34.7	0.46	47.2	2.6	52	0.12	33	1.2	0.55	8.1	2.9	31.81	6.57	36.52	2.2
ASR91	6ROSR25	OS	G	131	1.4	105.7	8.7	0.4	2	17	35.7	0.31	40.1	4.6	50	0.1	40	0.8	0.94	9.6	2.5	48.54	6.67	22.35	1.68
ASR91	6ROSR26	Sandstone	F	58.8	0.9	45.3	6.3	0.3	2	9	22.6	0.28	32.5	3	40	0.07	19	0.6	0.7	6.2	1.8	51.97	4.8	21.23	1.4
ASR91	6ROSR28	MOIS	D	64.7	1.7	65.2	9.8	0.5	3	15	38.4	0.21	44.6	2.9	41	0.07	32	1.3	0.92	10.2	2.7	36.63	7.72	33.2	2.03
ASR91	6ROSR29	Sandstone	D	57.7	1.4	47.6	9	0.5	4	12	31.1	0.37	49.8	3.5	25	0.08	26	0.7	0.6	9.4	3.4	40.89	6.92	28.96	2.55
ASR91	6ROSR30	Silty Sandstone	D	41.3	1.5	17.3	9	0.5	2	10	39.8	2.25	60.6	3.7	16	0.23	54	0.9	0.6	10.9	4	58	7.72	15.83	1.31
BBM	7ROSR21	MOIS	G	48.6	0.9	49.3	5.8	0.3	3	9	21.9	0.06	31	2.3	17	0.11	30	0.9	0.51	7.4	1.7	48.58	4.74	30.86	0.92
BBM	7ROSR20	MOIS	G	59.2	1.3	62.9	6.8	0.3	4	11	27.7	0.04	27.7	2.5	16	0.08	68	1	0.79	8.5	1.5	48.71	5.32	28.96	0.89
BBM	7ROSR19	MOIS	G	52.2	1.2	53.9	6.5	0.3	3	10	25.4	0.06	25.5	2.7	15	0.1	46	0.6	0.7	7.7	1.6	44.38	4.94	32.62	0.99
BBM	7ROSR18	Sandstone	C	78.4	0.7	71.4	4.7	0.2	3	9	19.4	0.06	19.8	2.7	16	0.07	20	0.6	0.37	4.8	1.1	51.22	3.45	28.52	0.7
BBM	7ROSR17	Sandstone	C	37.4	0.8	17.2	6.1	0.3	1	6	35.1	0.04	34.5	3.8	11	0.08	15	0.5	0.19	6.3	2.1	75.17	4.53	11.19	0.62
BBM	7ROSR15	IOIS	E	39.2	0.7	30.6	5.3	0.3	3	7	15.8	0.15	25.3	2.9	19	0.06	16	0.5	0.15	4.9	1.5	31.67	3.46	43.91	1.34
BBM	7ROSR16	Sandstone	D	134.9	2.4	150	13.7	0.5	3	28	41	0.14	22.5	3.6	21	0.56	322	0.8	2.16	13.3	1.6	30.49	8.73	30.46	1.71
SPRV	6ROSR11	Sandstone		42	1.1	37.4	6.8	0.4	4	12	25.3	0.03	45.1	2.1	27	0.09	35	0.8	0.4	7.6	3	22.86	6.32	43.4	1.73
SPRV	6ROSR10	IOIS	E	72.2	2.4	77.6	12.1	0.7	3	22	66.6	0.08	75.1	4.1	26	0.08	123	1	1.45	16	4.7	32.96	11.89	31.92	2.16
SPRV	6ROSR09	IOIS	E	58.3	1.5	64.7	7.2	0.3	6	16	22.4	0.08	32.4	1.9	41	0.06	48	0.8	0.86	9.4	2.1	16.57	6.79	53.56	1.61
SPRV	6ROSR08	MOIS	E	60	1.3	65.4	5.8	0.3	6	13	14.1	0.02	22	2.1	36	0.04	36	0.4	0.79	8.6	1.5	20.57	5.06	49.07	1.23
SPRV	6ROSR07	OS	G	34.2	0.8	28.2	4	0.3	2	8	19.2	0.15	28.9	1.8	21	0.07	44	0.3	0.37	6	1.7	41.17	4.34	27.17	2.3
SPRV	6ROSR06	MOIS	G	66.6	1.8	73.3	9.2	0.4	5	17	25.2	0.07	22.9	3.1	40	0.12	221	0.4	1.67	9.4	1.4	32.98	6.59	42.14	1.23
SPRV	6ROSR05	OS	G	22.7	0.5	13.2	3.2	0.2	2	4	15	0.15	21.9	1.7	25	0.08	13	0.3	0.13	3.9	1.3	36.13	2.73	33.7	2.08
SPRV	6ROSR04	MOIS	G	83.2	1.5	105.3	7.5	0.4	4	19	26.3	BDL	25.7	2.2	31	0.06	37	0.6	1.66	9.7	1.5	20.41	6.18	35.27	2.76
SPRV	6ROSR03	OS	G	28	0.8	24.1	3.9	0.2	4	7	16.5	0.03	23.6	2											

Section	Sample	Lithology	Facies	CaO (%)	Na2O (%)	K2O (%)	TiO2 (%)	P2O5 (%)	LOI (%)	Pr (ppm)	Nd (ppm)	Sm (ppm)	Eu (ppm)	Gd (ppm)	Tb (ppm)	Dy (ppm)	Ho (ppm)	Er (ppm)	Tm (ppm)	Yb (ppm)	Lu (ppm)
ASR9A	7ROSR07	IOIS	E	1.78	0.33	0.85	0.28	0.61	17.1	11.69	53.6	14.38	3.39	15.85	3.04	13.64	2.45	6.36	0.85	5.07	0.76
ASR9A	SROR4012	OS	F	3.1	0.15	0.83	0.225	0.735	10.4	9.05	45.05	11.9	3.065	15.57	2.295	12.37	2.245	5.755	0.735	4.095	0.56
ASR9A	7ROSR08	Sandstone	F	5.68	0.14	0.72	0.19	0.94	12.1	6.14	27.8	6.53	1.57	7.71	1.39	6.29	1.2	3.28	0.45	2.62	0.38
ASR9A	7ROSR09	Sandstone	F	1.27	0.16	0.74	0.16	0.6	4.8	6.21	26.9	6.78	1.58	7.35	1.3	5.97	1.08	2.81	0.39	2.19	0.31
ASR9A	SROR4013	Silty Sandstone	F	2.48	0.14	0.74	0.16	0.84	6.7	5.51	26.4	7.2	1.73	7.15	1.16	6.3	1.08	2.75	2.58	0.31	
ASR9A	7ROSR10	Sandstone	F	1.8	0.1	0.62	0.15	0.49	9	3.95	16.5	3.64	0.83	3.82	0.69	3.07	0.55	1.56	0.21	1.36	0.2
ASR9A	SROR4014	Silty Sandstone	C	1.15	0.13	0.98	0.22	0.23	6.2	4.22	18.9	4.8	1.06	4.21	0.63	3.76	0.68	1.81	0.26	1.71	0.25
ASR9A	SROR4015	Sandstone	C	0.53	0.19	0.97	0.22	0.15	5.5	3.55	14.5	3.6	0.78	3.22	0.48	2.57	0.52	1.54	0.23	1.42	0.22
ASR9A	SROR4016	Sandstone	C	0.51	0.25	1.14	0.26	0.1	5.1	4.07	18.1	3.5	0.78	3.34	0.53	3.02	0.58	1.71	0.23	1.46	0.23
ASR9A	SROR4017	Silty Sandstone	C	3.15	0.24	1.1	0.26	1.87	6.8	10.95	51.2	13.7	3.17	14.29	2.1	11.53	2.05	5.23	0.67	4.27	0.55
ASR9A	SROR4018	Sandstone	C	1.38	0.17	0.86	0.21	0.73	10	9.72	47.3	11.9	3.14	14.98	2.24	12.1	2.16	5.37	0.66	3.78	0.52
ASR9A	SROR4019	IOIS	E	1.8	0.2	0.37	0.14	1.84	16.4	15.07	73.3	21.9	5.5	26.95	4.37	22.85	4.12	10.46	1.35	7.69	1.04
ASR9A	SROR4020	IOIS	E	1.54	0.19	0.31	0.13	1.78	16.4	9.74	46.5	13.8	3.47	16.16	2.64	14.62	2.57	6.66	0.93	5.35	0.68
ASR9A	SROR4021	IOIS	E	2.11	0.19	0.33	0.13	1.94	16.7	10.99	54.2	15.3	3.94	19.18	2.94	16.31	2.94	7.5	0.99	5.8	0.78
ASR9A	SROR4022	IOIS	E	2.56	0.13	0.37	0.14	1.59	16.7	9.52	44.8	13.4	3.35	15.66	2.55	14.22	2.52	6.43	0.87	5.04	0.64
ASR9A	SROR4023	IOIS	E	2.89	0.14	0.45	0.18	1.92	17.8	10.04	49.4	13.7	3.53	15.62	2.76	14.09	2.37	6.49	0.82	5.48	0.75
ASR9A	SROR4024	IOIS	E	2.93	0.15	0.57	0.2	1.86	16.9	11.8	58.2	16.2	4.04	18.86	3.35	16.98	2.78	7.73	0.98	6.66	0.9
ASR9A	SROR4009	OS	D	2.48	0.16	1.07	0.32	0.96	14.8	8.22	37.3	9.8	2.35	10.21	1.68	9.44	1.68	4.43	0.65	3.73	0.52
ASR9A	SROR4008	Silty Sandstone	C	1.06	0.2	1.11	0.33	0.32	13.4	5.93	26.2	6.5	1.48	6.5	1.09	5.95	1.07	2.91	0.4	2.74	0.36
ASR9A	SROR4007	Silty Sandstone	C	1.14	0.3	1.41	0.41	0.47	11.2	7.62	33.6	7.8	1.67	7.35	1.13	6.25	1.19	3.16	0.48	3.04	0.38
ASR9A	SROR4006	Shale	B	0.46	0.4	2.2	0.64	0.19	8.8	7.34	28.7	5.8	1.15	4.5	0.69	4.33	0.87	2.64	0.39	2.73	0.41
ASR9B	SROR4027	IOIS	G	4.56	0.29	0.77	0.27	2.23	17.5	11.16	52.6	14.6	3.53	16.43	2.81	14.39	2.39	6.45	0.81	5.66	0.74
ASR9B	SROR4028	MOIS	F	3.91	0.14	0.64	0.19	0.85	12	6.82	31.7	8.8	2.05	9.13	1.52	7.98	1.39	3.56	0.45	2.97	0.45
ASR9B	SROR4029	OS	C	3.31	0.1	0.75	0.2	0.67	13	7.23	32.4	7.6	1.81	8.8	1.36	7	1.18	3.13	0.41	2.47	0.35
ASR9B	SROR4025	IOIS	E	2.54	0.15	0.36	0.15	2.07	16.6	12.41	62.4	17.4	4.49	20.37	3.56	18.08	3.03	8.06	1.03	7.18	0.93
ASR9B	SROR4026	IOIS	E	5.77	0.15	0.33	0.14	1.62	17.6	9.48	46.4	13.5	3.5	16.11	2.79	15.1	2.43	6.47	0.88	5.75	0.74
ASR9B	SROR4033	MOIS	E	6.09	0.25	0.31	0.14	1.7	18.5	10.12	48.4	14.8	3.66	17.24	2.93	15.28	2.55	6.72	0.87	5.74	0.74
ASR9B	SROR4034	OS	D	3.38	0.26	0.8	0.27	1.18	19.2	8.84	42.2	11.5	2.7	12.38	2.08	11.06	1.9	5.07	0.66	4.62	0.64
ASR91	6ROSR24	OS	G	3.72	0.43	1.02	0.29	1.22	15.8	7.02	28.7	7.5	1.74	8.33	1.47	8.28	1.32	3.64	0.48	3.12	0.44
ASR91	6ROSR25	OS	G	4.54	0.4	0.91	0.27	2.78	11.4	19.05	84.2	22	5.63	25.17	4.6	23.07	3.52	9.52	1.16	7.41	1
ASR91	6ROSR26	Sandstone	F	6.23	0.26	0.78	0.2	0.88	12	8.12	34.8	9.4	2.31	10.65	1.98	10.14	1.56	4.37	0.55	3.36	0.47
ASR91	6ROSR28	MOIS	D	3.04	0.24	0.99	0.3	1.24	14.2	10.26	46.5	12.4	2.93	13.81	2.6	13.93	2.15	5.97	0.78	4.92	0.67
ASR91	6ROSR29	Sandstone	D	2.63	0.18	1.04	0.3	0.92	15.4	8.45	36.7	9.4	2.23	10.52	1.88	9.97	1.54	4.33	0.59	3.7	0.51
ASR91	6ROSR30	Silty Sandstone	D	0.44	0.26	1.34	0.37	0.24	14.4	5.51	21.2	4.2	0.89	3.72	0.63	3.56	0.58	1.69	0.24	1.69	0.25
BBM	7ROSR21	MOIS	G	0.98	0.06	0.66	0.19	1.08	11.6	7.18	31.5	7.78	1.85	8.86	1.66	7.49	1.35	3.53	0.47	2.83	0.4
BBM	7ROSR20	MOIS	G	1.15	0.05	0.62	0.19	1.08	12.7	9.1	40.7	11.15	2.65	12.73	2.32	10.18	1.87	4.87	0.67	3.82	0.54
BBM	7ROSR19	MOIS	G	0.94	0.09	0.56	0.18	0.89	14	7.76	35.1	9.36	2.31	10.79	2.03	9.21	1.68	4.31	0.58	3.6	0.48
BBM	7ROSR18	Sandstone	C	2.64	0.07	0.47	0.15	1.93	10.5	11.03	49	12.81	3.13	15.08	2.68	11.75	2.07	5.06	0.64	3.63	0.49
BBM	7ROSR17	Sandstone	C	0.65	0.09	0.7	0.22	0.15	6.6	4.67	19.2	4.05	0.89	3.81	0.69	3.02	0.54	1.55	0.21	1.4	0.21
BBM	7ROSR15	IOIS	E	1.71	0.11	0.55	0.19	0.66	15.9	5.35	22	5.6	1.33	6.03	1.11	5.04	0.93	2.38	0.32	1.92	0.26
BBM	7ROSR16	Sandstone	D	5.77	0.08	0.5	0.25	3.34	18.3	22.07	97.1	28.52	6.82	33	6.06	26.21	4.7	12.04	1.63	9.42	1.25
SPRV	6ROSR11	Sandstone		5.48	0.11	1	0.29	1.59	16.8	5.82	24.6	6	1.46	6.97	1.29	7.14	1.21	3.42	0.46	2.91	0.42
SPRV	6ROSR10	IOIS	E	2.16	0.11	1.6	0.44	0.61	15.7	11.48	49.9	13.8	3.34	15.46	3.12	17.04	2.76	7.91	1.05	6.9	0.98
SPRV	6ROSR09	IOIS	E	2.58	0.08	0.67	0.24	1.45	16	9.69	42.6	12.5	3.09	14.28	2.67	14.32	2.22	6.12	0.82	4.9	0.69
SPRV	6ROSR08	MOIS	E	5.64	0.11	0.43	0.16	1.73	15.7	9.92	43.1	11.9	3.03	13.73	2.55	13.44	2.1	5.86	0.75	4.68	0.66
SPRV	6ROSR07	OS	G	6.39	0.07	0.65	0.17	0.58	16.4	4.99	21.9	5.5	1.26	5.94	1.09	5.9	0.91	2.64	0.35	2.17	0.3
SPRV	6ROSR06	MOIS	G	2.28	0.07	0.51	0.18	1.31	12.3	10.85	48.1	14	3.58	16.63	3.11	16.07	2.53	6.92	0.89	5.42	0.76
SPRV	6ROSR05	OS	G	5.24	0.08	0.52	0.13	0.9	18.3	2.93	11.3	2.6	0.62	2.8	0.5	2.68	0.44	1.17	0.15	0.98	0.14
SPRV	6ROSR04	MOIS	G	10.33	0.13	0.59	0.17	2.7	21.1	13.74	62	18.1	4.55	21.28	4.1	21.65	3.46	9.4	1.17	7.4	1.01
SPRV	6ROSR03	OS	G	4.63	0.15	0.58	0.14	0.36	18.9	4.14	18.1	4.5	1.07	4.95	0.94	4.98	0.79	2.28	0.3	1.87	0.29
ASR14C	6ROSR12	Siltstone	G	0.89	0.41	2.08	0.63	0.18	9.1	9.59	41	9.1	2.18	10.23	1.78	9.65	1.53	4.53	0.55	3.55	0.57
ASR14C	6ROSR13	Sandstone	C	3.41	0.31	1.34	0.4	0.55	14.1	7.31	30.8	7.4	1.69	7.52	1.37	7.28	1.17	3.38	0.45	2.93	0.43
ASR14C	6ROSR14	Sandstone	C	0.78	0.3	1.57	0.47	0.25	9.1	8.31	35.1	8.4	1.92	8.86	1.67	9.05	1.41	4.1	0.54	3.62	0.5
ASR14C	6ROSR15	Sandstone	C	7.63	0.23	0.79	0.23	1.56	21.8	7.46	32.4	7.8	1.88	8.55	1.49	7.98	1.21	3.6	0.42	2.92	0.4
ASR14C	6ROSR16	Sandstone	C	1.65	0.27	1.46	0.44	0.85	9.3	9.48	39.6	9.3	2.18	9.82	1.75	9.04	1.44	4.09	0.53	3.29	0.48
ASR14C	6ROSR1																				

Section	Sample	Lithology	Facies	Mo (ppm)	Cu (ppm)	Pb (ppm)	Zn (ppm)	Ag (ppb)	Ni (ppm)	Co (ppm)	Mn (ppm)	Fe (%)	As (ppm)	U (ppb)	Au	Th (ppm)	Sr (ppm)	Cd (ppm)	Sb (ppm)	Bi (ppm)	V (ppm)	La (ppm)	Cr (ppm)	Ba (ppm)	W (ppm)	Zr (ppm)	
ASR14C	6ROSR19	Sandstone	C	0.8	7	22	178	49	28	20.8	1381	18.6	41.2	5.3	0.3	5.7	359.7	0.06	1.7	0.25	444	25.1	39.4	642.2	0.9	68.7	
ASR14C	6ROSR20	Siltstone	C	13.6	9.7	39.7	142	77	14	8.3	77	10.81	257.5	1.7	0.3	5.6	90	0.02	6.5	0.39	623	18.4	41.9	641.8	1.9	157.3	
ASR14C	6ROSR21	Siltstone	C	7	13.9	27.3	209	87	40	31.1	512	8.95	81.6	2.7	0.3	8	126.9	0.07	2.1	0.33	484	26.6	46.5	788.1	1.6	171.1	
ASR14C	6ROSR22	Sandstone	C	3.5	7.5	11.2	78	46	22	13.1	1479	26.3	38.2	2.3	0.3	2.9	181.4	0.06	0.8	0.12	231	22.9	18.3	567.7	0.8	78.6	
ASR14C	6ROSR23	Siltstone	C	9.2	17.6	25.5	204	91	30	23.9	155	5.01	77.4	2.9	2.9	BDL	6.9	102.8	0.06	1.8	0.28	397	25.8	41.7	832	1.6	187.7
ASR14B	SROR4066	Silty Sandstone		0.7	19.7	33.7	350	71	159	72.5	471	10.14	282.6	3.2	0.1	7.6	102.8	0.35	3.7	0.38	396	35.2	44.7	730.9	1.7	159.1	
ASR14B	SROR4067	Sandstone	G	19.1	11.8	48	288	61	78	51.8	774	15.91	57.8	6.7	0.4	9.6	188	0.07	3.7	0.51	697	30.3	68.4	717.8	1.6	109	
ASR14B	SROR4068	Sandstone	G	4.2	16.9	57.5	448	100	80	53	386	12.76	51.3	4.1	0.6	14.6	133.9	0.12	4.2	0.74	1021	35.8	109.1	730	2.1	149.8	
ASR14B	SROR4069	Silty Sst	C	6.5	9.7	33.2	259	58	43	34.6	861	16.63	38	2.5	0.6	9.1	165.7	0.06	2.7	0.42	634	24.1	64.6	589.9	1.2	95.3	
ASR14B	SROR4070	Silty Sst	C	7.9	15.4	26.5	186	75	23	24.6	581	13.11	81.9	2.4	0.8	7.6	99.4	0.08	2.2	0.3	439	24.1	45	629	1.3	145.5	
ASR3	SRP5001	Shale	Puskawakau	4.2	41.5	19.2	126	126	28	9.1	142	4.13	16.6	4	1	4.7	138	0.12	1	0.32	257	38.1	26.4	999.5	1.9	172.1	
ASR3	SRP5002	Shale	Puskawakau	7.8	41.4	22.1	132	178	33	9.3	120	4.25	19.4	4.7	1.1	5.2	155.9	0.27	0.8	0.35	248	38.3	24.9	1050	1.7	170.8	
ASR3	SRP5003	Shale	Puskawakau	3.5	36.1	20.4	135	132	38	9.3	120	4.14	15.7	4.2	0.5	5.8	149.4	0.17	0.7	0.33	244	38.5	27.9	931.4	1.9	167.9	
ASR3	SRP5004	Shale	Puskawakau	5	30.2	21.1	123	143	42	9.9	121	3.87	17.9	4.5	0.5	5.5	155.1	0.2	0.9	0.33	252	39.4	25.1	1103	1.7	181.8	
ASR3	SRP5005	Shale	Puskawakau	2	35.7	20.5	153	107	44	10.2	128	3.86	14	4.1	0.8	5.9	157.1	0.16	0.7	0.32	242	39.9	27.4	1025	2.1	171.4	
ASR3	SRP5006	Shale	Puskawakau	1.5	32.6	23.2	151	86	44	10.4	109	4.13	21.9	4.2	0.4	5.6	161.7	0.09	0.7	0.33	258	42.5	27.2	1179	2.4	168.9	
ASR3	SRP5007	Shale	Puskawakau	1.1	32.8	22.9	162	82	40	12.5	117	3.99	26.1	4.2	0.9	5.6	156.3	0.1	0.8	0.33	281	43.8	28.3	1081	2	188.6	
ASR3	SRP5008	Shale	Puskawakau	0.9	32.5	20.9	159	83	49	15.2	149	4.26	24.3	4.2	0.5	5.5	150.2	0.12	0.9	0.31	283	42.5	26	1199	2.1	189.8	
ASR3	SRP5009	Shale	Puskawakau	0.9	30.8	19.6	164	81	45	13.1	128	4.08	23.1	4.1	0.9	5.1	150.4	0.09	1	0.29	272	41.3	27.3	1057	2	196.7	
ASR3	SRP5010	Shale	Puskawakau	1.1	30.2	19.6	142	91	45	13.3	105	3.99	25.4	4.6	0.5	5.4	141.8	0.11	1	0.31	272	41.2	27.1	1019	1.7	181.9	
ASR3	SRP5011	Shale	Puskawakau	0.9	31.3	17.6	159	91	42	13	100	3.8	23.4	4.7	0.6	5.3	141.9	0.11	0.9	0.29	264	41.5	27.8	1069	1.8	200.6	
ASR3	SRP5012	Shale	Puskawakau	0.8	27.4	19.8	146	80	41	13.1	102	3.81	23	4.1	0.3	5.2	134.6	0.08	0.9	0.29	253	40.8	25.4	1011	2	196.4	
ASR3	SRP5013	Shale	Puskawakau	0.9	26	17.1	146	80	42	12.4	95	3.56	24.9	4.3	0.1	5	137.3	0.09	0.9	0.27	259	39.7	25.4	1058	2	218.1	
ASR3	SRP5014	Shale	Puskawakau	1.2	25.2	17.9	157	107	48	16.8	138	3.19	25.7	4.2	0.8	4.4	138.1	0.12	0.9	0.23	234	38.5	21.7	1450	2.1	234.9	
ASR3	SRP5015	Shale	Puskawakau	1.2	21.1	15	122	81	37	10.8	78	2.91	48.8	3.8	0.4	4.7	96.1	0.07	0.9	0.2	212	31.5	22.7	886	1.8	223.4	
ASR3	SRP5016	Silty Shale	Puskawakau	3.6	21.3	17.3	144	74	41	13.2	79	3.36	62.2	4	0.6	4.8	98.7	0.08	1.4	0.23	241	36.1	24	1001	1.7	239.7	
ASR3	SRP5017	Siltstone	C	1.3	17.2	18.3	123	103	29	13.9	61	2.83	46.9	2.8	0.3	4.7	121.3	0.06	1	0.2	203	29.3	22.4	984.7	1.4	244.2	
ASR3	SRP5018	Shale	B	2	20.7	16.3	109	138	36	9.3	77	3.02	16.7	3.2	0.3	3.9	129.9	0.05	1	0.19	190	33.5	18.2	993.3	1.6	254.8	
ASR3	SRP5019	Shale	B	1.3	23.65	15.6	142	112.5	42.5	12.9	146	3.205	14.7	3.55	0.4	4.6	122	0.1	0.95	0.205	191.5	34.1	20.1	938.8	1.85	246.4	
ASR3	SRP5020	Shale	B	1.2	23.5	17.2	144	113	42	11.9	112	2.71	12.2	3.8	0.3	4.9	121.7	0.1	0.9	0.21	195	35	19.9	917.7	1.8	259.6	
ASR3	SRP5021	Shale	B	1.2	24.9	18.7	143	108	46	11	115	2.85	12.5	3.9	0.4	4.7	124.2	0.09	0.9	0.2	195	35.9	20.7	960.2	1.7	247.7	
ASR3	SRP5022	Shale	B	1.3	25.9	18.7	147	114	49	11.3	125	2.87	15.4	3.6	0.4	4.8	131.1	0.07	0.9	0.21	201	37.1	21.4	1046	1.9	248.2	
ASR3	SRP5023	Shale	B	2.8	26.7	20.3	153	104	45	13.1	105	2.78	20.4	4	0.3	5.1	131.9	0.07	1.1	0.25	227	36.9	23.6	977.2	1.6	219.7	
ASR3	SRP5024	Conglomerate	A	1.1	9.9	30.3	193	69	9	9.7	1216	28.93	15.4	3	1	4.9	274.6	0.05	1.5	0.21	326	25.9	33	1030	0.7	70.9	
ASR3	SRP5025	Shale	Kaskapau	1.4	27.9	18.4	154	84	47	12	85	3.36	23	4	0.3	5.1	143.1	0.08	1	0.25	234	39.9	23.8	993.9	2.4	186.9	
ASR3	SRP5026	Shale	Kaskapau	1	27.9	18.4	152	86	51	13	82	3.29	22.3	4.2	0.4	5	142.2	0.09	0.9	0.25	234	39.2	24.4	986.3	1.9	206.2	
ASR3	SRP5027	Shale	Kaskapau	1.4	24.7	19	137	84	52	13.8	89	3.43	18.9	4.1	0.2	5.2	143.3	0.08	0.9	0.25	230	38.9	22.7	1008	1.9	209.2	
ASR3	SRP5028	Shale	Kaskapau	1	27.8	20.8	164	96	60	15	87	3.31	22.2	4.4	0.2	5.4	153.7	0.12	1.1	0.29	250	41	24.2	1057	1.8	191.3	
ASR3	SRP5029	Shale	Kaskapau	1.2	27.2	17.8	159	98	53	13.8	85	3.26	21.4	4.5	0.3	5.6	143.1	0.1	1	0.27	263	40.3	24.6	1034	2	209	
ASR3	SRP5030	Shale	Kaskapau	1.1	28.2	19.7	157	100	59	14.5	83	3.21	19.2	4	0.6	5.8	147	0.12	0.9	0.27	245	41	24.5	1047	1.4	205.8	
ASR3	SRP5031	Shale	Kaskapau	1	27.8	17.7	159	104	55	13.9	80	3.15	17.8	4.1	0.5	5.9	140.2	0.1	1	0.26	239	38.8	24.8	989.9	1.7	198.7	
ASR3	SRP5032	Shale	Kaskapau	0.8	26	18.2	149	99	51	14.4	78	3.16	15.8	4.5	0.7	5.9	151.7	0.1	0.9	0.28	241	42.7	24	1054	1.8	205.9	
ASR3	SRP5033	Shale	Kaskapau	1.2	26.2	24	174	105	51	14.8	77	3.32	14.8	3.9	0.7	6.3	140.3	0.11	1.1	0.26	242	39.7	27.9	969.2	1.5	207	
ASR3	SRP5034	Shale	Kaskapau	1	29.1	19.1	166	117	49	14.8	80	3.13	17	4.2	0.7	6	147.8	0.13	1.1	0.27	223	39.5	27.4	1054	1.5	201.1	

Section	Sample	Lithology	Facies	Ce (ppm)	Sn (ppm)	Y (ppm)	Nb (ppm)	Ta (ppm)	Be (ppm)	Sc (ppm)	Li (ppm)	S (%)	Rb (ppm)	Hf (ppm)	B (ppm)	Tl (ppm)	Hg (ppb)	Se (ppm)	Te (ppm)	Ga (ppm)	Cs (ppm)	SiO2 (%)	Al2O3 (%)	Fe2O3 (%)	MgO (%)
ASR14C	6ROSR19	Sandstone	C	52.9	0.7	43	4.3	0.2	3	14	22.1	0.2	30.2	1.5	28	0.08	21	0.5	0.29	4.6	2	28.52	4.12	23.86	2.22
ASR14C	6ROSR20	Siltstone	C	34.8	1.3	11.1	8.6	0.5	1	7	30.4	1.92	58.6	3.8	16	0.17	61	0.8	0.3	9.6	3.8	60.29	6.37	15.58	0.67
ASR14C	6ROSR21	Siltstone	C	56.7	1.2	29.8	9	0.5	1	10	44	0.63	64.7	4.2	20	0.1	29	0.6	0.23	9.8	4	62.79	7.79	13.29	1.33
ASR14C	6ROSR22	Sandstone	C	49.1	0.6	41.5	4.4	0.3	2	9	21.7	0.22	33.5	2	24	0.07	15	0.4	0.04	4.8	2.2	22.41	3.84	36.83	3.87
ASR14C	6ROSR23	Siltstone	C	55.2	1.4	22.9	10.4	0.7	1	9	56	0.42	78.7	5.2	15	0.1	32	1	0.21	11.3	5.2	64.23	8.38	6.2	0.93
ASR14B	SROR4066	Silty Sandstone		82.3	1.4	78.9	11	0.7	2	12	123.9	0.68	85.9	4.6	31	0.1	76	1	0.18	11.7	5.3	58.33	11.1	14.21	1.46
ASR14B	SROR4067	Sandstone	G	60.5	0.7	49.1	8.7	0.5	2	11	45.3	0.44	60.8	2.5	26	0.07	36	0.7	0.47	9.6	3.4	46.23	7.72	22.43	2.15
ASR14B	SROR4068	Sandstone	G	71.2	1.4	40.6	11.1	0.7	1	13	55.9	0.39	76.2	4.2	21	0.08	45	0.9	0.68	13	4.5	58.52	9.55	17.3	1.69
ASR14B	SROR4069	Silty Sst	C	48.3	0.9	34.3	6.6	0.4	2	11	32.3	0.38	44.3	2.3	22	0.05	31	0.7	0.42	7.4	2.4	40.32	5.79	22.83	2.32
ASR14B	SROR4070	Silty Sst	C	47.7	1.3	24.2	8.3	0.5	2	9	48	0.65	63.4	3.9	17	0.07	31	0.6	0.25	9.4	3.6	55.75	7.32	18.07	1.97
ASR3	SRP5001	Shale	Puskawakau	71.7	2.3	23.2	16	1.2	1	14	70.7	1.06	129.9	5.5	18	0.19	93	1.6	0.05	19.5	9.3	61.75	15.24	5.45	1.41
ASR3	SRP5002	Shale	Puskawakau	71.5	2.5	26.9	16.7	1.1	2	14	81.1	1.95	126.8	5.1	21	0.25	111	2.7	0.06	19.7	8.9	59.41	14.5	5.82	1.41
ASR3	SRP5003	Shale	Puskawakau	70.5	2.3	25.9	16.4	1.2	2	15	86.2	1.56	131.8	4.8	15	0.17	91	1.7	0.07	19.2	9.5	60.9	14.9	5.64	1.45
ASR3	SRP5004	Shale	Puskawakau	73.5	2.4	27.2	16.9	1.1	2	14	86.5	1.58	129.8	5.2	16	0.19	88	2.1	0.07	19.4	9.2	62.08	14.37	5.2	1.41
ASR3	SRP5005	Shale	Puskawakau	74.1	2.3	28.9	16.7	1.1	2	15	97.5	1.46	137.4	4.9	19	0.12	83	1.4	0.06	20.2	9.7	61.44	15.13	5.14	1.54
ASR3	SRP5006	Shale	Puskawakau	78.1	2.1	28.6	17.1	1.1	1	16	103.7	1.35	145.8	4.8	19	0.1	94	1.1	0.07	21.4	10.4	60.29	16.1	5.73	1.5
ASR3	SRP5007	Shale	Puskawakau	81.1	2.4	30.8	18.4	1.1	2	16	114.2	0.72	154.6	5.3	20	0.09	88	0.9	0.09	21.7	11.2	63.1	15.93	5.25	1.49
ASR3	SRP5008	Shale	Puskawakau	76.7	2.3	32.9	17.7	1.2	2	15	110.8	0.73	148.1	5.4	20	0.09	90	0.8	0.08	21.5	11.2	63.29	15.62	5.58	1.49
ASR3	SRP5009	Shale	Puskawakau	77.6	2.4	30.5	17.4	1.1	2	15	109.9	0.69	144.5	5.3	18	0.09	92	0.9	0.08	21.3	10.3	64.62	15.16	5.3	1.43
ASR3	SRP5010	Shale	Puskawakau	76.9	2.4	28.2	16.3	1.1	2	15	112	0.93	141.4	5.3	20	0.09	86	1	0.06	20.4	10.8	63.72	15.29	5.24	1.45
ASR3	SRP5011	Shale	Puskawakau	78.6	2.3	30.4	17.6	1.2	1	15	108.9	0.84	143.4	5.5	19	0.09	76	1	0.06	21.2	10.6	64.5	15.23	5	1.38
ASR3	SRP5012	Shale	Puskawakau	77.4	2.1	28.2	16.4	1.2	2	14	104.2	0.68	138.1	6.3	18	0.09	82	0.9	0.08	19.8	9.6	65.41	15.05	5	1.4
ASR3	SRP5013	Shale	Puskawakau	75.2	2.4	30.3	17.2	1.1	2	14	94.3	0.66	138.6	6	15	0.08	82	0.8	0.06	19.5	9.5	66.71	14.38	4.82	1.34
ASR3	SRP5014	Shale	Puskawakau	73	2.2	35.4	15.4	1.1	1	13	96.2	0.59	122	6.7	17	0.08	72	0.5	0.07	17.8	8.5	68.07	13.22	4.21	1.24
ASR3	SRP5015	Shale	Puskawakau	61.6	2	26.5	13.7	0.9	1	12	77.2	0.54	105.3	6.6	15	0.08	68	0.6	0.06	14.9	7.1	72.69	11.84	3.78	1.09
ASR3	SRP5016	Silty Shale	Puskawakau	68.3	2	27.9	14.7	0.9	2	13	83.8	0.55	118.4	6.6	14	0.08	63	0.9	0.05	16.8	8.1	70.13	13.05	4.29	1.25
ASR3	SRP5017	Siltstone	C	54.6	1.5	23.6	12.2	0.7	1	9	59.1	0.98	86.4	6.8	11	0.07	52	0.5	0.09	12.9	5.8	77.42	9.45	3.71	0.91
ASR3	SRP5018	Shale	B	61.4	1.8	23.2	14.3	0.9	1	10	71.7	1.19	103.6	7.7	14	0.09	87	0.7	0.05	14	7	71.49	11.15	3.95	1.01
ASR3	SRP5019	Shale	B	63.2	1.95	28.25	14.1	1.05	1	11.5	74.5	0.85	105.9	6.9	14	0.07	70.5	0.65	0.045	15	6.95	71.02	12.06	4.165	1.145
ASR3	SRP5020	Shale	B	66.4	2	29.3	14.8	1	1	11	75.6	0.36	109.8	7.5	15	0.05	51	0.7	0.05	16	7.4	72.4	12.19	3.68	1.16
ASR3	SRP5021	Shale	B	66.7	2	28.5	14.9	1	1	11	79.8	0.32	110.4	6.8	15	0.06	56	0.6	0.05	15.4	7.3	72.51	12.29	3.67	1.14
ASR3	SRP5022	Shale	B	67.8	2.3	29.2	15.3	1	1	12	81.7	0.28	112.5	6.8	14	0.05	46	0.7	0.06	15.9	7.9	71.97	12.67	3.68	1.12
ASR3	SRP5023	Shale	B	71.1	2.2	28.6	15.6	1.1	2	13	84.4	0.33	121.9	7.1	16	0.06	58	0.6	0.04	17.1	8.6	69.47	13.85	3.72	1.16
ASR3	SRP5024	Conglomerate	A	52.3	0.7	46.9	4.3	0.3	3	15	34.2	0.14	38.8	2.1	30	0.04	36	0.7	0.14	5.5	2.4	26.68	4.9	37.55	2.14
ASR3	SRP5025	Shale	Kaskapau	73	2.4	29	15.2	1	1	14	88.4	0.81	125.9	5.6	13	0.07	82	0.7	0.07	18.3	8.9	66.5	14.83	4.3	1.23
ASR3	SRP5026	Shale	Kaskapau	74.5	2.5	30	15.6	1.1	2	14	92.2	0.82	126.7	5.9	15	0.08	92	0.8	0.07	17.6	8.9	68.22	14.45	4.24	1.21
ASR3	SRP5027	Shale	Kaskapau	74.2	2.5	30.3	16.2	1.1	2	14	87.7	0.92	125.1	6.1	12	0.05	81	0.7	0.05	18.3	8.7	68.14	14.27	4.51	1.24
ASR3	SRP5028	Shale	Kaskapau	79.9	2.5	31.4	16.3	1.2	2	15	98.2	0.77	138.2	5.4	13	0.07	86	0.8	0.07	19.5	10.1	65.77	15.68	4.54	1.34
ASR3	SRP5029	Shale	Kaskapau	77.4	2.5	31.1	15.8	1	1	14	90.8	0.7	134.4	6	15	0.08	90	0.8	0.06	18.4	9.5	68.42	14.65	4.22	1.24
ASR3	SRP5030	Shale	Kaskapau	78.3	2.3	32.1	15.2	1.1	2	15	94.9	0.73	132.4	5.7	14	0.07	82	0.9	0.08	18.5	9.6	67.46	14.9	4.26	1.25
ASR3	SRP5031	Shale	Kaskapau	74.8	2.3	31.4	14.7	1.1	2	14	89.8	0.8	124.1	6	15	0.08	89	0.7	0.06	18.5	8.6	68.01	14.3	4.17	1.18
ASR3	SRP5032	Shale	Kaskapau	81.2	2.3	32.6	15.7	1.1	2	15	96.4	0.68	136.2	5.9	16	0.07	80	0.8	0.06	19.2	9.5	66.79	15	4.31	1.22
ASR3	SRP5033	Shale	Kaskapau	77.1	2.2	32.6	14.5	1	2	14	88	0.62	124.5	5.5	15	0.05	81	0.9	0.06	18.1	8.6	67.72	14.35	4.52	1.19
ASR3	SRP5034	Shale	Kaskapau	80.6	2.2	30.3	14.9	1.2	2	15	91.2	0.74	129.8	5.9	24	0.11	98	0.9	0.06	18.5	9.2	68.04	14.26	4.33	1.17

Section	Sample	Lithology	Facies	CaO (%)	Na2O (%)	K2O (%)	TiO2 (%)	P2O5 (%)	LOI (%)	Pr (ppm)	Nd (ppm)	Sm (ppm)	Eu (ppm)	Gd (ppm)	Tb (ppm)	Dy (ppm)	Ho (ppm)	Er (ppm)	Tm (ppm)	Yb (ppm)	Lu (ppm)
ASR14C	6ROSR19	Sandstone	C	15.52	0.22	0.7	0.19	2.43	21.8	7.33	30.8	7.7	1.89	8.97	1.56	8.38	1.37	3.85	0.49	3.04	0.41
ASR14C	6ROSR20	Siltstone	C	0.91	0.73	1.3	0.35	0.14	13.6	4.21	14.8	2.8	0.52	2.12	0.38	2.06	0.37	1.19	0.17	1.23	0.19
ASR14C	6ROSR21	Siltstone	C	2.26	0.26	1.41	0.39	0.44	9.9	7.45	31.4	6.6	1.47	6.63	1.14	6.51	0.96	2.81	0.35	2.43	0.34
ASR14C	6ROSR22	Sandstone	C	5.39	0.18	0.73	0.2	1.21	25.1	6.51	28.7	6.5	1.55	7.66	1.36	7.18	1.21	3.39	0.39	2.62	0.38
ASR14C	6ROSR23	Siltstone	C	0.55	0.3	1.59	0.41	0.13	17.2	7.01	26.8	5.8	1.18	5.05	0.89	4.83	0.76	2.35	0.33	2.2	0.33
ASR14B	SROR4066	Silty Sandstone		1.34	0.36	1.88	0.56	0.21	10	11.82	53.8	13.9	3.61	16.61	2.82	13.89	2.48	6.75	0.86	5.42	0.67
ASR14B	SROR4067	Sandstone	G	4.79	0.48	1.23	0.37	1.18	13	7.9	36.2	8.6	2.11	9.98	1.7	8.74	1.64	4.4	0.6	4.12	0.5
ASR14B	SROR4068	Sandstone	G	1.16	0.39	1.47	0.43	0.45	8.5	9.17	39	9	2.28	9.26	1.56	7.96	1.4	3.83	0.56	3.72	0.45
ASR14B	SROR4069	Silty Sst	C	8.83	0.25	0.91	0.26	0.44	17.7	6.37	28.7	6.9	1.75	7.57	1.24	6.75	1.12	3.03	0.45	3.03	0.38
ASR14B	SROR4070	Silty Sst	C	1.95	0.27	1.29	0.36	0.18	12.4	5.91	24.8	5.3	1.25	4.82	0.82	4.34	0.8	2.28	0.34	2.27	0.31
ASR3	SRP5001	Shale	Puskawakau	0.68	0.57	2.68	0.78	0.16	11.2	8.38	29.5	4.9	1.05	3.6	0.58	3.58	0.71	2.45	0.38	2.4	0.39
ASR3	SRP5002	Shale	Puskawakau	0.55	0.56	2.62	0.79	0.15	14.1	8.62	32.5	5.6	1.24	4.7	0.71	4.32	0.87	2.6	0.42	2.62	0.42
ASR3	SRP5003	Shale	Puskawakau	0.78	0.58	2.73	0.79	0.15	12	8.41	30.9	5.7	1.21	4.46	0.72	3.83	0.81	2.46	0.39	2.41	0.4
ASR3	SRP5004	Shale	Puskawakau	0.58	0.56	2.66	0.79	0.15	12	8.81	32	5.8	1.26	4.49	0.76	4.59	0.86	2.7	0.47	2.77	0.41
ASR3	SRP5005	Shale	Puskawakau	0.5	0.64	2.82	0.8	0.17	11.6	9.06	33.4	6.7	1.25	4.72	0.78	4.67	1.01	2.68	0.49	2.54	0.43
ASR3	SRP5006	Shale	Puskawakau	0.43	0.66	2.97	0.81	0.18	11.1	9.26	34	6.8	1.28	4.73	0.71	4.47	0.93	2.61	0.44	2.66	0.46
ASR3	SRP5007	Shale	Puskawakau	0.33	0.62	2.99	0.82	0.16	9.1	9.63	36.1	6.6	1.41	5.1	0.82	4.64	0.95	2.8	0.49	3.12	0.48
ASR3	SRP5008	Shale	Puskawakau	0.4	0.59	2.9	0.82	0.16	8.9	9.32	34.6	7.4	1.48	5.63	0.93	5.21	0.97	3.07	0.51	3.14	0.46
ASR3	SRP5009	Shale	Puskawakau	0.39	0.61	2.82	0.79	0.16	8.5	9.07	33.1	6.4	1.32	5.18	0.81	4.28	0.88	2.78	0.45	2.94	0.44
ASR3	SRP5010	Shale	Puskawakau	0.38	0.63	2.84	0.79	0.15	9.3	9.21	34.8	6.2	1.38	4.74	0.82	4.89	0.91	2.67	0.44	2.86	0.41
ASR3	SRP5011	Shale	Puskawakau	0.32	0.57	2.77	0.78	0.16	9.2	9.29	34.1	6.4	1.34	5.21	0.86	4.75	1.01	2.92	0.45	2.68	0.44
ASR3	SRP5012	Shale	Puskawakau	0.35	0.59	2.85	0.79	0.15	8.2	8.97	33	6.4	1.22	4.49	0.77	4.37	0.9	2.79	0.45	2.92	0.4
ASR3	SRP5013	Shale	Puskawakau	0.3	0.55	2.75	0.79	0.15	8	8.82	32.6	5.8	1.27	4.6	0.73	4.41	0.95	2.88	0.46	2.86	0.46
ASR3	SRP5014	Shale	Puskawakau	1.69	0.52	2.52	0.74	0.14	7.5	8.62	32.7	6.6	1.59	5.85	0.98	5.74	1.11	3.18	0.46	3.17	0.44
ASR3	SRP5015	Shale	Puskawakau	0.2	0.53	2.35	0.69	0.14	6.6	7.21	25.8	5.3	1.17	4.16	0.71	4.05	0.8	2.48	0.38	2.68	0.4
ASR3	SRP5016	Silty Shale	Puskawakau	0.21	0.52	2.51	0.76	0.15	6.9	8.34	30.5	6	1.3	4.48	0.73	4.31	0.85	2.62	0.38	3.03	0.38
ASR3	SRP5017	Siltstone	C	0.46	0.42	1.89	0.55	0.17	4.8	6.73	23.5	4.5	1.09	4.11	0.69	3.78	0.77	2.17	0.36	2.43	0.35
ASR3	SRP5018	Shale	B	0.5	0.52	2.29	0.66	0.15	8.2	7.14	24.5	4.2	0.92	3.51	0.63	3.51	0.72	2.24	0.38	2.53	0.4
ASR3	SRP5019	Shale	B	0.525	0.5	2.43	0.69	0.195	7.05	7.605	27.15	5.2	1.115	4.71	0.78	4.46	0.875	2.695	0.43	2.87	0.42
ASR3	SRP5020	Shale	B	0.46	0.51	2.48	0.71	0.19	6	8.03	28.4	5.2	1.21	4.67	0.81	4.4	0.87	2.85	0.46	2.97	0.47
ASR3	SRP5021	Shale	B	0.45	0.53	2.51	0.71	0.19	5.9	8.03	28.2	5.6	1.1	4.92	0.77	4.62	0.9	2.83	0.44	2.89	0.44
ASR3	SRP5022	Shale	B	0.43	0.56	2.53	0.73	0.18	5.9	8.14	29.2	5.8	1.24	5	0.84	4.77	0.86	2.82	0.48	2.78	0.45
ASR3	SRP5023	Shale	B	0.37	0.57	2.69	0.78	0.17	7	8.29	29	6	1.23	4.67	0.84	4.43	0.86	2.75	0.43	3.11	0.46
ASR3	SRP5024	Conglomerate	A	4.38	0.24	0.81	0.25	1.18	21.5	7.46	31.6	8.4	2.13	8.94	1.55	8.42	1.51	3.86	0.55	3.4	0.49
ASR3	SRP5025	Shale	Kaskapau	0.41	0.58	2.78	0.8	0.2	8.3	8.76	31.9	6.1	1.37	5.15	0.89	4.66	0.86	2.93	0.46	2.94	0.45
ASR3	SRP5026	Shale	Kaskapau	0.31	0.61	2.74	0.78	0.17	7.2	8.8	31.2	6.1	1.26	4.94	0.83	4.59	0.97	2.75	0.49	2.98	0.45
ASR3	SRP5027	Shale	Kaskapau	0.43	0.64	2.79	0.78	0.19	6.8	8.75	29.9	6.2	1.28	4.98	0.93	5.07	0.95	2.87	0.49	3.1	0.44
ASR3	SRP5028	Shale	Kaskapau	0.41	0.63	2.93	0.81	0.21	7.6	9.28	33.2	6.7	1.41	5.38	0.95	5.2	0.96	2.92	0.47	3.22	0.48
ASR3	SRP5029	Shale	Kaskapau	0.35	0.62	2.84	0.77	0.21	6.6	9.08	32.9	6.6	1.36	5.07	0.87	5.38	1.02	3.12	0.5	3.2	0.46
ASR3	SRP5030	Shale	Kaskapau	0.31	0.62	2.82	0.77	0.2	7.2	9.2	33.7	6.7	1.42	5.64	0.87	5.17	1.07	2.96	0.51	3	0.48
ASR3	SRP5031	Shale	Kaskapau	0.26	0.56	2.74	0.76	0.18	7.6	8.93	33.4	5.9	1.42	5.76	0.9	5.11	1.04	2.9	0.49	3.04	0.46
ASR3	SRP5032	Shale	Kaskapau	0.3	0.6	2.9	0.8	0.2	7.8	9.4	34.5	7.4	1.42	5.71	0.92	5.31	0.96	3.11	0.47	3.22	0.46
ASR3	SRP5033	Shale	Kaskapau	0.35	0.6	2.69	0.73	0.22	7.4	8.88	34.9	6.6	1.56	6.04	0.95	5.66	1.01	3.04	0.48	3.04	0.45
ASR3	SRP5034	Shale	Kaskapau	0.31	0.59	2.73	0.77	0.21	7.5	8.7	34.1	6.2	1.22	4.9	0.94	4.75	1	3.04	0.48	2.95	0.43

Note: IOIS(Intensely Ooidal ironstone,>70% ooids);MOIS(Moderately ooidal ironstone,30%-70% ooids);WOIS(Weakly ooidal ironstone,10%-30% ooids);OS(ooidal sandstone,<10% ooids) BDL: Below detection Limit, NA:Not available

APPENDIX III: COMPARATIVE RESULTS FROM DUPLICATE SAMPLE PAIRS

Unit	Mo ppm	Cu ppm	Pb ppm	Zn ppm	Ag ppm	Ni ppb	Co ppm	Mn ppm	Fe %	As ppm	U ppm	Au ppb	Th ppm	Sr ppm	Cd ppm	Sb ppm	Bi ppm	V %	Ca %	P ppm	La ppm	Cr %	Mg ppm	Ba %	Ti ppm	Al %	Na %
Average RPD values	4.72	6.37	3.70	2.7	7.1	7.0	4.31	2.6	2.32	7.5	6.69	65.92	3.64	5.4	16.18	5.21	2.73	3.3	4.65	6.59	4.64	4.0	2.34	4.9	2.91	2.01	4.93
Count of RPD values	21	21	21	21	21	21	21	21	21	21	21	16	21	21	21	21	21	21	21	21	21	21	21	21	21	21	21
CHROR4059	1.00	9.30	17.60	119.0	74.0	21.0	14.10	276.0	4.68	46.9	1.70	0.50	5.30	65.4	0.03	1.50	0.22	228.0	0.35	0.05	16.40	37.1	0.33	627.9	0.16	3.02	0.13
RE CHROR4059	1.10	9.50	17.40	116.0	71.0	26.0	14.80	268.0	4.58	46.6	1.80	0.90	5.30	68.3	0.03	1.40	0.22	236.0	0.34	0.05	17.50	38.4	0.33	658.9	0.16	3.00	0.13
SROR4076	2.10	23.70	46.90	311.0	70.0	57.0	34.10	188.0	9.55	61.2	4.00	0.80	10.30	82.6	0.08	2.60	0.55	700.0	0.22	0.09	33.60	69.1	0.59	807.2	0.33	6.03	0.27
RE SROR4076	2.00	22.40	47.20	318.0	64.0	55.0	33.30	190.0	9.66	59.7	4.00	0.70	10.00	79.8	0.08	2.50	0.54	685.0	0.22	0.09	33.00	69.1	0.60	788.7	0.33	6.03	0.26
CHROR4016	10.60	7.10	50.30	540.0	35.0	83.0	51.90	1097.0	42.64	222.7	5.80	<2	12.00	137.1	0.03	8.50	0.97	1480.0	1.49	0.65	29.70	154.5	0.81	472.4	0.09	2.53	0.05
RE CHROR4016	10.30	6.50	50.80	537.0	47.0	88.0	52.30	1092.0	42.49	242.8	5.60	<2	12.10	144.3	0.03	8.70	0.97	1505.0	1.47	0.66	29.70	155.6	0.81	493.4	0.09	2.49	0.05
SROR4012	8.40	9.80	30.80	375.0	88.0	142.0	54.90	1295.0	15.81	180.6	2.30	0.30	7.50	138.7	0.71	3.70	0.38	488.0	2.34	0.34	28.80	56.6	0.54	577.8	0.14	2.75	0.12
RE SROR4012	8.40	9.40	28.40	363.0	89.0	151.0	55.30	1273.0	15.48	178.8	2.50	<2	7.60	142.7	0.73	3.90	0.37	499.0	2.28	0.32	30.30	57.0	0.53	596.9	0.13	2.70	0.11
SROR4036	9.80	7.00	45.80	523.0	28.0	84.0	54.90	911.0	37.33	231.1	4.60	<2	12.90	151.4	0.02	6.80	0.95	1387.0	3.17	0.58	29.30	149.3	0.90	396.1	0.09	2.27	0.23
RE SROR4036	10.40	6.50	49.10	541.0	27.0	86.0	53.00	938.0	38.24	230.9	4.20	0.20	13.70	152.3	0.03	7.40	0.99	1416.0	3.17	0.59	29.30	157.7	0.91	374.6	0.09	2.42	0.24
SROR4073	3.30	13.40	42.00	501.0	69.0	76.0	51.80	511.0	25.32	199.5	4.60	0.60	12.00	224.3	0.06	7.10	0.81	1063.0	3.15	0.70	38.20	124.3	1.26	647.6	0.18	3.97	0.22
RE SROR4073	3.10	11.50	42.30	493.0	66.0	84.0	54.90	508.0	24.94	200.8	4.60	<2	11.90	233.1	0.08	6.60	0.82	1092.0	3.12	0.69	39.60	125.3	1.25	618.1	0.18	3.91	0.20
SRROP5019	1.30	22.50	15.30	140.0	113.0	44.0	12.70	146.0	3.20	15.0	3.60	0.50	4.70	122.4	0.10	1.00	0.21	187.0	0.41	0.09	33.00	20.9	0.59	922.6	0.43	6.31	0.38
RE SRROP5019	1.30	24.80	15.90	144.0	112.0	41.0	13.10	146.0	3.21	14.4	3.50	0.30	4.50	121.6	0.10	0.90	0.20	196.0	0.41	0.09	35.20	19.3	0.59	955.0	0.42	6.43	0.40
CHROR5003A	4.30	9.00	55.60	443.0	52.0	121.0	29.20	1455.0	27.58	109.1	3.40	1.80	5.20	207.1	0.19	2.70	0.44	203.0	11.38	0.91	23.80	23.4	0.47	605.1	0.10	2.06	0.06
CHROR5003B	4.40	9.40	53.00	440.0	53.0	102.0	34.10	1402.0	27.52	125.5	4.10	2.20	5.30	231.2	0.17	2.90	0.45	213.0	10.84	1.09	25.00	25.0	0.48	633.0	0.10	2.04	0.06
CHROR5006	0.70	19.20	45.90	278.0	143.0	58.0	20.70	184.0	8.70	48.5	3.80	1.30	8.30	110.1	0.18	1.50	0.36	269.0	0.76	0.15	38.60	35.2	0.53	642.7	0.30	5.42	0.21
RE CHROR5006	0.70	19.60	46.10	282.0	136.0	57.0	20.20	175.0	8.20	45.6	4.00	1.20	7.80	107.8	0.16	1.50	0.34	261.0	0.73	0.15	36.60	32.3	0.50	637.5	0.29	5.31	0.21
CHROR5021A	13.30	8.30	46.70	653.0	54.0	86.0	55.10	1202.0	37.74	254.8	6.30	2.00	10.70	152.5	0.04	10.50	0.72	1224.0	1.53	0.79	33.40	128.3	0.43	791.3	0.09	2.61	0.04
CHROR5021B	12.80	10.10	46.70	642.0	54.0	87.0	54.80	1145.0	36.93	252.0	6.60	1.90	9.90	157.0	0.02	10.30	0.67	1252.0	1.45	0.80	35.30	124.2	0.42	939.9	0.08	2.56	0.04
6ROSRR016	4.40	15.60	53.30	388.0	96.0	66.0	48.70	499.0	12.97	47.1	3.40	0.80	12.70	160.2	0.10	4.00	0.71	851.0	1.23	0.36	31.60	89.5	0.95	741.5	0.25	4.78	0.20
RE 6ROSRR016	4.30	15.30	51.20	382.0	93.0	66.0	50.10	481.0	12.58	47.4	3.20	1.00	12.10	163.9	0.11	4.00	0.71	888.0	1.18	0.35	31.90	87.3	0.93	795.0	0.23	4.72	0.20
6ROCR007	11.70	8.30	22.40	235.0	97.0	30.0	27.50	361.0	14.25	56.4	4.60	<2	6.10	116.9	0.09	3.20	0.34	463.0	2.34	0.25	17.60	43.2	0.39	750.8	0.09	2.30	0.07
RE 6ROCR007	11.40	8.00	23.30	226.0	98.0	32.0	27.40	354.0	13.81	56.5	4.30	<2	6.10	120.0	0.07	3.20	0.33	481.0	2.29	0.25	16.90	42.4	0.38	742.5	0.09	2.26	0.07
6ROCR037	10.10	11.40	44.00	550.0	57.0	61.0	54.20	1276.0	32.99	318.6	5.90	0.70	10.70	158.6	0.07	8.50	0.80	1208.0	1.33	0.59	27.10	123.0	0.62	399.9	0.09	2.71	0.05
RE 6ROCR037	9.60	10.00	41.00	516.0	56.0	60.0	51.60	1258.0	32.20	320.1	6.20	0.50	10.40	161.2	0.08	7.90	0.77	1236.0	1.28	0.56	29.20	121.4	0.61	397.3	0.09	2.64	0.05
7ROSRR001	5.90	6.50	20.20	156.0	38.0	41.0	19.70	1373.0	32.09	16.5	2.60	0.60	3.60	175.3	0.06	2.10	0.20	391.0	4.12	0.32	18.10	22.2	2.32	621.4	0.13	2.28	0.15
RE 7ROSRR001	5.60	6.70	19.70	165.0	40.0	35.0	20.10	1308.0	31.92	16.9	2.50	1.30	3.70	174.2	0.06	2.00	0.20	391.0	3.97	0.32	18.20	23.6	2.22	623.9	0.13	2.27	0.15
CHROR4016	10.45	6.80	50.55	538.5	41.0	85.5	52.10	1094.5	42.57	232.8	5.70	0.10	12.05	140.7	0.03	8.60	0.97	1492.5	1.48	0.66	29.70	155.1	0.81	482.9	0.09	2.51	0.05
CHROR4017(Duplicate)	9.30	6.70	52.50	540.0	33.0	83.0	57.00	1125.0	44.09	166.6	5.20	0.20	11.90	127.7	0.02	8.70	0.95	1498.0	1.41	0.61	27.60	148.7	0.82	466.6	0.09	2.56	0.05
CHROR4037	5.00	9.90	48.20	516.0	79.0	82.0	51.40	627.0	27.76	227.0	5.70	0.10	14.00	188.1	0.05	8.40	1.05	1244.0	2.28	0.68	30.20	163.3	0.53	758.1	0.10	2.82	0.06
CHROR4038(Duplicate)	5.30	10.00	48.50	520.0	72.0	93.0	52.70	630.0	28.37	181.5	4.90	0.20	14.30	143.8	0.05	7.50	1.04	1281.0	1.69	0.49	27.10	166.3	0.51	698.8	0.10	2.79	0.05
CHROR4054	5.50	8.80	55.00	627.0	47.0	90.0	58.30	1059.0	39.03	233.2	5.00	1.80	14.20	170.8	0.03	6.20	1.11	1717.0	2.85	0.67	35.10	182.8	0.93	528.0	0.10	2.69	0.04
CHROR4061(Duplicate)	5.20	9.50	57.20	639.0	40.0	83.0	60.70	1117.0	40.40	241.0	5.10	0.10	13.20	173.4	0.03	6.40	1.07	1660.0	3.01	0.73	37.00	170.6	0.96	528.0	0.11	2.71	0.04
SROR4019	10.60	9.70	54.60	785.0	41.0	159.0	71.70	1563.0	44.75	302.9	4.80	0.10	15.70	145.4	0.57	8.60	1.08	1536.0	1.28	0.74	44.70	185.1	0.47	417.4	0.10	2.67	0.14
SROR4081(Duplicate)	9.70	8.60	57.30	770.0	38.0	170.0	77.50	1573.0	42.55	282.7	5.10	0.50	15.30	155.3	0.62	8.50	1.10	1664.0	1								

	K	W	Zr	Ce	Sn	Y	Nb	Ta	Be	Sc	Li	S	Rb	Hf	B	Tl	Hg	Se	Te	Ga	Cs	Ge	In	Re	SiO2	Al2O3	
Unit	%	ppm	ppm	ppm	ppm	ppm	ppm	ppm	ppm	ppm	ppm	%	ppm	ppm	ppm	ppm	ppb	ppm	ppm	ppm	ppm	ppm	ppm	ppm	ppb	%	%
Average RPD	3.16	6.98	7.4	4.64	9.99	3.83	3.97	11.35	11.31	2.93	4.82	3.63	3.2	7.56	4.76	11.55	15.4	14.7	12.3	4.25	8.48	5.13	3.42	25.87	1.38	1.18	
Count of RPD values	21	21	21	21	21	21	21	21	21	21	21	18	21	21	21	20	20	21	21	21	21	12	14	11	21	21	
CHROR4059	0.93	0.80	161.9	33.30	1.10	17.50	5.40	0.40	1.00	5.00	30.10	<.01	45.7	4.50	7.00	0.10	35.0	0.6	0.2	6.90	2.70	<.1	0.07	1.00	80.78	5.57	
RE CHROR4059	0.92	0.60	177.8	35.90	1.00	17.70	5.80	0.40	1.00	5.00	27.40	0.01	45.7	4.70	7.00	0.10	32.0	0.5	0.2	7.00	2.60	<.1	0.07	<1	80.72	5.57	
SROR4076	1.50	2.10	201.3	66.60	1.10	30.30	13.40	0.80	3.00	13.00	79.00	0.28	95.5	6.20	22.00	0.08	59.0	0.8	0.4	15.80	6.00	0.10	0.12	1.00	61.36	11.49	
RE SROR4076	1.50	2.20	196.4	66.30	1.80	29.00	13.10	0.80	3.00	13.00	76.70	0.27	93.7	5.50	20.00	0.07	53.0	0.8	0.5	14.80	5.50	<.1	0.12	1.00	61.51	11.53	
CHROR4016	0.29	7.30	90.8	58.90	1.30	75.50	6.50	0.30	4.00	15.00	12.80	<.01	19.0	1.90	47.00	0.02	<5	0.5	0.7	8.70	1.20	0.20	0.28	<1	13.21	5.40	
RE CHROR4016	0.30	7.10	101.0	59.30	1.40	77.90	6.30	0.30	5.00	15.00	13.80	<.01	19.3	2.10	51.00	0.03	<5	0.6	0.8	8.50	1.30	0.20	0.26	<1	13.29	5.39	
SROR4012	0.73	0.70	102.2	58.50	0.70	78.70	5.90	0.30	2.00	8.00	60.70	0.66	37.9	3.00	41.00	0.12	27.0	1.2	0.4	6.60	2.20	0.40	0.11	5.00	56.94	5.20	
RE SROR4012	0.73	0.70	125.9	61.90	0.90	80.50	5.90	0.30	2.00	8.00	62.60	0.64	38.9	3.30	40.00	0.11	27.0	1.3	0.4	7.00	2.50	0.40	0.12	4.00	57.33	5.32	
SROR4036	0.25	10.20	96.3	55.10	1.10	72.40	7.10	0.20	5.00	14.00	9.20	0.37	17.1	2.00	55.00	0.02	20.0	0.6	0.7	9.00	1.30	0.20	0.26	2.00	12.62	5.07	
RE SROR4036	0.26	10.20	101.3	54.90	1.20	71.70	7.00	0.20	4.00	13.00	10.10	0.38	17.7	2.20	59.00	0.02	12.0	0.7	0.6	8.30	1.20	0.20	0.27	3.00	12.56	5.11	
SROR4073	0.80	3.00	112.6	72.90	1.40	63.20	9.20	0.40	3.00	15.00	38.60	0.52	49.4	2.80	47.00	0.13	37.0	1.5	0.8	12.00	3.30	0.10	0.20	5.00	28.99	8.35	
RE SROR4073	0.80	3.00	115.7	78.30	1.60	65.50	9.40	0.40	3.00	15.00	37.20	0.51	52.6	3.00	41.00	0.12	44.0	1.4	0.7	11.50	3.40	0.10	0.20	5.00	29.14	8.40	
SRROP5019	2.06	1.90	241.2	61.60	1.80	28.10	14.00	1.00	1.00	12.00	73.90	0.88	104.6	6.70	14.00	0.07	70.0	0.6	0.1	15.00	6.80	NA	NA	NA	70.62	12.19	
RE SRROP5019	1.96	1.80	251.5	64.80	2.10	28.40	14.20	1.10	1.00	11.00	75.00	0.87	107.2	7.10	14.00	0.07	71.0	0.7	0.0	15.00	7.10	NA	NA	NA	71.42	11.92	
CHROR5003A	0.44	0.50	87.3	56.70	0.60	67.90	4.00	0.20	3.00	12.00	19.70	3.72	26.1	2.20	13.00	0.10	56.0	0.3	0.3	3.40	1.80	NA	NA	NA	14.94	4.37	
CHROR5003B	0.45	0.40	82.5	57.80	0.60	72.80	4.30	0.30	4.00	13.00	20.30	3.51	27.5	2.20	13.00	0.11	53.0	0.2	0.3	4.40	2.00	NA	NA	NA	15.63	4.41	
CHROR5006	1.46	1.20	280.5	85.20	1.50	49.60	12.60	0.80	2.00	15.00	44.60	0.14	79.4	7.40	13.00	0.12	82.0	0.3	0.2	12.80	5.30	NA	NA	NA	66.18	9.67	
RE CHROR5006	1.40	1.40	262.5	78.30	1.60	48.90	11.80	0.90	2.00	15.00	44.90	0.14	76.3	7.40	12.00	0.10	73.0	0.3	0.1	12.60	5.10	NA	NA	NA	66.58	9.74	
CHROR5021A	0.33	5.10	73.9	63.70	1.20	64.10	5.60	0.30	5.00	13.00	12.20	<.01	18.1	1.50	30.00	0.02	5.0	<.1	0.4	8.60	1.20	NA	NA	NA	22.42	4.77	
CHROR5021B	0.30	4.50	74.3	66.10	1.10	67.10	5.80	0.30	4.00	13.00	12.50	<.01	18.3	1.60	30.00	0.02	<5	<.1	0.4	8.80	1.40	NA	NA	NA	22.74	4.74	
6ROSRR016	1.22	1.90	156.0	68.50	1.70	41.80	10.30	0.60	2.00	12.00	49.10	0.24	66.9	4.00	28.00	0.12	31.0	0.7	0.7	11.10	4.20	NA	NA	NA	56.83	9.17	
RE 6ROSRR016	1.16	1.80	150.8	70.00	1.50	41.40	10.30	0.60	2.00	13.00	47.30	0.24	67.1	4.10	25.00	0.11	42.0	1.0	0.6	11.90	4.40	NA	NA	NA	56.49	9.21	
6ROCHR007	0.69	0.80	80.0	37.50	0.80	27.60	5.00	0.30	2.00	7.00	24.20	0.03	32.2	2.20	12.00	0.08	14.0	1.4	0.4	6.00	1.90	NA	NA	NA	61.08	4.39	
RE 6ROCHR007	0.67	0.90	83.8	37.20	0.80	26.30	4.80	0.30	2.00	7.00	23.80	0.03	33.4	2.30	11.00	0.08	11.0	1.4	0.3	6.20	1.90	NA	NA	NA	60.76	4.45	
6ROCHR037	0.39	4.00	88.9	55.60	1.20	55.60	6.40	0.30	5.00	11.00	15.10	0.03	23.8	2.00	47.00	0.04	6.0	0.4	0.8	8.50	1.70	NA	NA	NA	26.45	5.12	
RE 6ROCHR037	0.36	4.10	78.1	57.30	1.10	56.10	5.80	0.30	4.00	11.00	14.00	0.03	23.8	1.90	47.00	0.04	7.0	0.3	0.7	8.70	1.70	NA	NA	NA	26.53	5.14	
7ROSRR001	0.55	1.10	89.3	39.10	0.90	34.60	5.60	0.30	4.00	10.00	33.80	0.29	30.9	2.20	37.00	0.07	19.0	0.5	0.2	6.20	2.00	0.10	0.05	<1	18.97	4.45	
RE 7ROSRR001	0.53	1.10	87.2	38.50	0.80	33.50	5.90	0.20	4.00	9.00	33.40	0.29	30.8	2.30	38.00	0.06	17.0	0.4	0.2	6.00	1.90	0.20	0.05	<1	19.05	4.41	
CHROR4016	0.30	7.20	95.9	59.10	1.35	76.70	6.40	0.30	4.50	15.00	13.30	0.01	19.2	2.00	49.00	0.03	2.5	0.6	0.7	8.60	1.25	0.20	0.27	0.50	13.25	5.40	
CHROR4017(Duplicate)	0.30	7.20	93.3	53.20	1.30	73.70	6.40	0.20	6.00	15.00	12.60	0.01	19.9	2.20	51.00	0.02	2.5	0.5	0.6	8.90	1.30	0.20	0.25	0.50	13.05	5.41	
CHROR4037	0.49	6.50	83.5	63.80	1.30	70.30	6.90	0.30	4.00	14.00	21.10	0.01	25.4	2.00	26.00	0.06	16.0	1.0	0.9	8.70	1.40	0.10	0.29	1.00	34.78	5.61	
CHROR4038(Duplicate)	0.49	7.40	101.6	55.50	1.20	68.00	7.00	0.30	4.00	14.00	20.80	0.01	25.9	2.00	28.00	0.05	9.0	1.1	0.9	9.00	1.60	0.10	0.30	2.00	34.32	5.61	
CHROR4054	0.29	8.80	89.9	64.40	1.30	80.40	9.00	0.30	6.00	16.00	20.00	0.17	21.2	1.90	41.00	0.04	217.0	1.0	1.1	10.00	1.30	0.20	0.27	0.50	13.37	6.01	
CHROR4061(Duplicate)	0.30	8.70	104.1	65.00	1.30	82.60	8.30	0.30	6.00	16.00	21.00	0.16	22.3	2.40	42.00	0.05	223.0	1.0	1.0	9.90	1.70	0.20	0.27	1.00	13.11	5.96	
SROR4019	0.30	8.60	92.6	86.90	1.40	135.10	7.70	0.30	6.00	15.00	31.70	0.16	18.2	1.90	66.00	0.04	35.0	0.8	0.8	9.00	1.40	0.20	0.27	2.00	14.67	5.66	
SROR4081(Duplicate)	0.32	8.50	95.1	87.70	1.50	148.70	7.80	0.20	5.00	17.00	33.90	0.14	19.5	2.00	60.00	0.04	46.0	0.8	0.9	9.40	1.20	0.20	0.29	2.00	15.12	5.98	
SROR4031	0.26	9.50	95.1	64.90	1.20	81.40	7.80	0.30	7.00	15.00	13.10	0.15	17.4	2.10	58.00	0.03	11.0	0.5	0.4	8.80	1.20	0.20	0.24	0.50	12.24	5.23	
SROR4082(Duplicate)	0.26	8.80	90.6	60.60	1.40	82.60	7.60	0.30	5.00	16.00	15.30	0.13	16.9	1.80	61.00	0.02	12.0	0.3	0.6	8.80	1.00	0.20	0.25	0.50	11.51	5.41	
SROR4072	0.62	4.50	84.2	46.50	1.30	51.30	7.60	0.30	3.00	13.00	25.90	0.16	40.7	2.10	45.00	0.08	58.0	1.1	0.8	9.30	2.40	0.10	0.17	6.00	24.22	6.67	
SROR4084(Duplicate)	0.62	5.00	98.8	52.60	1.30	57.80	7.80	0.40	3.00	13.00	26.70	0.17	43.1	2.30	45.00	0.08	59.0	1.3	0.7	9.10	2.60	0.10					

	Fe2O3	MgO	CaO	Na2O	K2O	TiO2	P2O5	MnO	Cr2O3	LOI	Pr	Nd	Sm	Eu	Gd	Tb	Dy	Ho	Er	Tm	Yb	Lu
Unit	%	%	%	%	%	%	%	%	%	%	ppm	ppm	ppm	ppm	ppm	ppm	ppm	ppm	ppm	ppm	ppm	ppm
Average RPD	1.10	1.55	3.67	4.26	1.24	1.88	5.60	0.58	5.02	2.05	4.14	4.75	5.02	4.08	3.93	4.35	3.57	3.20	3.83	3.55	4.56	4.76
Count of RPD values	21	21	21	21	21	21	21	21	21	21	21	21	21	21	21	21	21	21	21	21	21	21
CHROR4059	6.03	0.80	0.43	0.16	1.03	0.25	0.10	0.03	0.01	4.30	4.17	16.20	3.90	0.89	3.49	0.54	3.12	0.62	1.73	0.26	1.66	0.27
RE CHROR4059	6.23	0.79	0.43	0.16	1.02	0.25	0.10	0.03	0.01	4.30	4.36	18.90	4.00	0.90	3.54	0.57	3.06	0.62	1.73	0.26	1.60	0.26
SROR4076	13.31	1.03	0.31	0.32	1.76	0.57	0.21	0.02	0.02	9.10	8.61	38.00	7.30	1.66	6.60	1.07	5.74	1.07	2.93	0.46	3.34	0.43
RE SROR4076	13.35	1.06	0.31	0.32	1.78	0.57	0.22	0.02	0.02	8.80	8.38	36.50	7.20	1.65	6.18	1.06	5.54	1.07	2.97	0.46	3.24	0.38
CHROR4016	57.05	1.59	2.19	0.07	0.39	0.13	1.72	0.13	0.02	17.70	9.42	45.10	13.50	3.58	16.10	2.63	14.39	2.43	6.33	0.88	5.43	0.70
RE CHROR4016	57.03	1.58	2.16	0.07	0.38	0.13	1.71	0.13	0.03	17.70	9.43	44.70	14.00	3.56	16.15	2.68	14.06	2.46	6.34	0.86	5.24	0.75
SROR4012	20.56	0.99	3.08	0.15	0.83	0.22	0.73	0.14	0.01	10.60	8.86	42.90	11.50	2.99	15.14	2.21	12.19	2.20	5.63	0.70	4.02	0.56
RE SROR4012	20.51	0.99	3.12	0.15	0.83	0.23	0.74	0.14	0.01	10.20	9.24	47.20	12.30	3.14	15.99	2.38	12.55	2.29	5.88	0.77	4.17	0.56
SROR4036	52.89	1.81	4.85	0.34	0.33	0.14	1.67	0.11	0.03	20.00	8.76	43.80	12.80	3.23	14.70	2.64	13.15	2.24	6.05	0.78	5.16	0.68
RE SROR4036	52.75	1.82	4.80	0.34	0.33	0.14	1.67	0.11	0.03	20.20	8.72	43.80	12.70	3.23	14.44	2.50	13.30	2.25	6.02	0.77	5.14	0.65
SROR4073	34.58	2.46	4.69	0.27	0.94	0.31	1.70	0.06	0.02	17.40	10.72	49.00	12.30	3.29	13.44	2.35	12.08	2.11	5.16	0.72	4.45	0.61
RE SROR4073	34.46	2.47	4.68	0.27	0.95	0.31	1.70	0.06	0.02	17.30	11.10	51.30	12.80	3.35	13.96	2.34	12.39	2.21	5.34	0.78	4.75	0.60
SRROP5019	4.21	1.17	0.53	0.50	2.45	0.70	0.20	0.02	0.01	7.20	7.53	27.10	5.00	1.10	4.91	0.71	4.36	0.88	2.67	0.43	2.88	0.43
RE SRROP5019	4.12	1.12	0.52	0.50	2.41	0.68	0.19	0.02	0.01	6.90	7.68	27.20	5.40	1.13	4.51	0.85	4.56	0.87	2.72	0.43	2.86	0.41
CHROR5003A	41.15	0.94	16.44	0.08	0.60	0.20	2.14	0.19	0.01	18.80	8.17	37.60	10.50	2.49	12.21	2.15	11.50	2.08	5.53	0.78	4.51	0.64
CHROR5003B	41.05	0.94	15.82	0.10	0.61	0.21	2.46	0.19	0.01	18.40	8.61	40.30	10.10	2.87	12.39	2.26	12.00	2.23	5.93	0.84	4.82	0.64
CHROR5006	11.29	0.85	0.95	0.27	1.71	0.56	0.32	0.02	0.01	8.10	10.59	44.20	10.10	2.16	9.40	1.60	8.50	1.60	4.18	0.61	3.82	0.55
RE CHROR5006	11.25	0.85	0.97	0.28	1.73	0.55	0.33	0.02	0.01	7.60	9.81	43.10	9.60	2.15	9.52	1.68	8.77	1.56	4.21	0.58	3.57	0.53
CHROR5021A	50.42	0.75	1.95	0.05	0.38	0.14	1.62	0.14	0.03	17.00	10.00	45.90	12.80	3.00	13.76	2.45	12.91	2.12	5.21	0.77	4.20	0.56
CHROR5021B	50.17	0.75	1.92	0.06	0.38	0.14	1.61	0.14	0.02	17.00	10.39	46.00	13.80	3.19	14.20	2.56	13.29	2.30	6.03	0.84	4.53	0.61
6ROSRR016	17.88	1.80	1.65	0.27	1.46	0.44	0.85	0.06	0.02	9.30	9.48	39.60	9.30	2.18	9.82	1.75	9.04	1.44	4.09	0.53	3.29	0.48
RE 6ROSRR016	18.15	1.76	1.64	0.28	1.53	0.43	0.83	0.06	0.02	9.50	9.70	41.00	10.00	2.19	9.99	1.74	9.16	1.45	3.95	0.54	3.35	0.47
6ROCHR007	18.88	0.68	3.09	0.09	0.87	0.19	0.59	0.04	0.01	9.90	5.44	23.30	5.80	1.35	5.91	1.09	5.40	0.92	2.48	0.29	1.97	0.28
RE 6ROCHR007	19.01	0.68	3.11	0.09	0.88	0.19	0.58	0.04	0.01	10.00	5.27	23.50	5.60	1.31	5.94	1.08	5.35	0.94	2.35	0.29	2.07	0.29
6ROCHR037	45.32	1.11	1.86	0.06	0.46	0.17	1.38	0.15	0.02	17.60	8.94	40.20	10.10	2.64	12.02	2.19	10.75	1.84	4.75	0.62	3.79	0.53
RE 6ROCHR037	45.46	1.11	1.84	0.06	0.46	0.16	1.41	0.15	0.02	17.40	9.11	40.10	10.90	2.68	12.21	2.25	10.82	1.83	4.71	0.66	3.98	0.55
7ROSRR001	38.68	3.99	5.81	0.21	0.72	0.24	0.68	0.16	0.01	25.90	5.18	22.00	5.35	1.29	6.10	1.11	5.17	0.99	2.79	0.40	2.42	0.34
RE 7ROSRR001	38.80	3.84	5.79	0.19	0.70	0.24	0.66	0.15	0.01	26.00	5.03	23.00	5.29	1.20	5.87	1.10	5.34	0.96	2.76	0.38	2.41	0.37
CHROR4016	57.04	1.59	2.18	0.07	0.39	0.13	1.72	0.13	0.03	17.70	9.43	44.90	13.75	3.57	16.13	2.66	14.23	2.45	6.34	0.87	5.34	0.73
CHROR4017(Duplicate)	57.87	1.59	2.04	0.07	0.38	0.13	1.61	0.13	0.02	17.30	8.74	42.00	12.80	3.36	15.13	2.46	13.21	2.32	6.09	0.87	5.16	0.68
CHROR4037	38.18	0.98	3.16	0.08	0.59	0.17	1.64	0.07	0.02	14.20	9.08	42.90	13.00	3.47	15.03	2.44	13.29	2.22	6.08	0.86	5.33	0.74
CHROR4038(Duplicate)	39.39	0.95	2.36	0.07	0.59	0.16	1.21	0.07	0.02	14.60	8.19	39.70	12.40	3.34	14.42	2.37	12.88	2.20	5.88	0.84	4.90	0.72
CHROR4054	53.95	1.94	4.24	0.06	0.40	0.16	1.85	0.13	0.03	17.50	10.27	49.70	15.10	3.59	16.55	2.78	15.10	2.59	6.81	0.97	5.82	0.75
CHROR4061(Duplicate)	54.00	1.96	4.42	0.06	0.40	0.16	2.00	0.13	0.03	17.40	10.56	51.80	15.70	3.76	17.92	2.82	15.91	2.77	7.18	0.96	5.84	0.75
SROR4019	57.50	0.83	1.80	0.20	0.37	0.14	1.84	0.18	0.03	16.40	15.07	73.30	21.90	5.50	26.95	4.37	22.85	4.12	10.46	1.35	7.69	1.04
SROR4081(Duplicate)	55.71	0.92	2.06	0.20	0.37	0.15	2.04	0.17	0.03	16.90	14.60	73.00	20.40	5.76	26.85	4.50	23.26	4.20	10.46	1.37	7.63	1.03
SROR4031	58.17	1.22	2.47	0.12	0.32	0.14	1.86	0.13	0.03	17.90	10.21	51.30	14.40	3.64	16.74	2.94	15.34	2.59	6.88	0.87	5.86	0.80
SROR4082(Duplicate)	59.29	1.22	2.34	0.13	0.31	0.14	1.91	0.13	0.03	17.30	9.59	47.80	13.60	3.75	16.13	2.86	14.69	2.67	6.60	0.92	5.60	0.72
SROR4072	37.25	1.67	8.88	0.19	0.78	0.24	0.88	0.08	0.02	18.90	6.89	31.70	8.80	2.37	10.11	1.74	9.60	1.72	4.34	0.66	3.74	0.47
SROR4084(Duplicate)	37.79	1.66	8.77	0.19	0.76	0.25	1.05	0.08	0.02	18.20	7.51	35.40	9.40	2.64	11.27	1.95	10.73	1.91	4.90	0.70	4.56	0.52
SROR4059	42.81	1.97	2.69	0.09	0.63	0.21	1.22	0.11	0.02	17.90	7.88	37.40	10.10	2.73	11.95	2.19	11.03	2.06	5.04	0.72	4.61	0.56
SROR4083(Duplicate)	42.25	1.99	2.65	0.10	0.63	0.21	1.17	0.11	0.02	17.70	8.20	41.00	10.90	2.96	12.91	2.27	11.79	2.13	5.40	0.74	4.80	0.59

APPENDIX IV: COMPARATIVE RESULTS FOR CANMET STANDARD SAMPLES

Element	Cu	Pb	Zn	Ni	Co	Mn	U	Th	Sr	V	La	Cr	Ba	Zr	Ce	Y	Nb	Ta	Be	Sc	Li	Rb	Hf	Ga	Cs
Unit	ppm	ppm	ppm	ppm	ppm	ppm	ppm	ppm	ppm	ppm	ppm	ppm	ppm	ppm	ppm	ppm	ppm	ppm	ppm	ppm	ppm	ppm	ppm	ppm	ppm
Analytical method	1EX	1EX	1EX	4A	4B	1EX	4B	1F	4B	4B	4B	1F	4B	4B	4B	4B	4B	4B	4B	4A	1EX	4B	4B	4B	4B
CHROR4001B(PULP)	4.6	9.3	91	20	2.5	856	0.8	1	1295	8	58.7	9.2	356.6	587.7	140.5	142.3	14	0.8	3	1	33.2	57.5	12.2	37.7	1.7
CHROR4022B(PULP)	5.5	9.4	93	20	2.2	868	1.2	1.1	1184	6	52.8	10	325.9	533.5	123.5	126.6	13.7	0.7	3	1	38.5	54	11	33.2	1.5
CHROR4052B(PULP)	5.6	9.5	96	20	2	879	1	1	1300	7	62.8	9.1	342.6	563.2	135.2	136.4	14.2	0.8	1	1	36.3	57.4	11.3	38.2	1.6
SROR4014B(PULP)	4.5	10	102	20	2.7	913	0.9	1.1	1223	6	61.6	9.9	340.2	495.3	129.4	128.9	13.7	0.8	4	1	39.5	55.3	10.5	38.2	1.7
SROR4033B(PULP)	5.4	10.5	102	20	2.2	884	1	1	1224	<5	60.9	9.7	329.8	522.4	130.5	131.3	13.8	0.7	4	1	40.4	54.3	10.8	34.7	1.6
SROR4059B(PULP)	5.1	8.8	100	20	2.5	834	1.1	0.9	1171	7	58.1	8.8	327.6	528.7	127.9	131.5	13.6	0.7	2	1	38.4	56.4	11.3	35.5	1.6
SROR4084B(PULP)	5.1	8.6	100	20	2.3	858	1	1.1	1201	<5	60.3	9.6	359.3	548.9	129.5	133	14.3	0.8	3	1	36	58.6	11.2	35.2	1.6
SRROP5039(PULP)	4.9	9.4	94	11	2.2	858	1	1	1190	8	58	9.4	352.6	519.8	133.9	121.8	12.6	0.8	3	1	39.9	52.1	10.6	34.6	1.6
CHROR5014(PULP)	5.6	9.6	90	10	3.3	868	1	1.1	1278	5	63.4	9.2	368	577.8	142.9	131.2	13.7	0.9	3	1	38.8	55.8	12.6	36.4	1.7
6ROSRR002P(PULP)	8.1	10.6	111	12	2.4	855	0.8	1.1	1222	7	52.9	8.3	367.3	597.6	119.9	116.4	13.7	0.8	3	<1	39.5	53	12.2	35.3	1.5
6ROSRR042P(PULP)	4.8	9.7	100	<5	2	883	0.9	1	1308	6	52.9	8.5	334.4	565	120.8	120.2	13.5	0.8	3	1	40.5	52.9	11.4	36.5	1.5
6ROCHR052P (PULP)	2.6	10.1	99	6	2.3	908	0.9	1	1286	5	51.8	8.2	331	552.6	138.3	121.9	13.4	0.8	3	1	40.5	53	11.8	37.3	1.6
7ROSRR022 (PULP)	4.4	10.4	81	<5	2.7	882	0.8	1.1	1299	7	55.4	8.5	343.7	617.4	129.7	142	14.4	0.8	3	1	41.4	53.5	11.5	35.4	1.6
Mean	5.09	9.68	96.85	16.27	2.41	872.8	0.95	1.04	1244.5	6.55	57.66	9.11	344.5	554.6	130.9	129.5	13.74	0.78	2.92	1.00	38.68	54.9	11.42	36.02	1.60
SY-4 Certified Values	7.00	10.0	93.00	9.00	2.80	819.0	0.80	1.40	1191.0	8.00	58.00	12.0	340.0	517.0	122.0	119.0	13.0	0.90	2.60	1.10	37.00	55.0	10.6	35.00	1.50
Percentage Recovery	72.7	96.8	104.1	180.8	86.0	106.6	119.2	74.2	104.5	81.8	99.4	75.9	101.3	107.3	107.3	108.8	105.7	87.2	112.4	90.9	104.6	99.8	107.7	102.9	106.7

Element	SiO2	Al2O3	Fe2O3	MgO	CaO	Na2O	K2O	TiO2	P2O5	MnO	Cr2O3	LOI	Pr	Nd	Sm	Eu	Gd	Tb	Dy	Ho	Er	Tm	Yb	Lu
Unit	%	%	%	%	%	%	%	%	%	%	%	ppm	ppm	ppm	ppm	ppm	ppm	ppm	ppm	ppm	ppm	ppm	ppm	ppm
Analytical method	4A	4A	4A	4A	4A	4A	4A	4A	4A	4A	4A	4B	4B	4B	4B	4B	4B	4B	4B	4B	4B	4B	4B	4B
CHROR4001B(PULP)	50.04	20.84	5.98	0.51	8.03	7.12	1.54	0.27	0.14	0.1	8E-04	4.9	15.15	62.3	14	2.13	15.54	2.95	19.55	4.51	15.07	2.5	16.32	2.12
CHROR4022B(PULP)	49.68	20.92	6.22	0.51	7.88	6.93	1.53	0.27	0.12	0.1	0.002	5.3	13.73	56.3	12.6	2.04	13.6	2.59	18.15	4.07	13.75	2.38	14.77	2.14
CHROR4052B(PULP)	49.81	20.78	5.91	0.51	8.04	6.78	1.57	0.28	0.13	0.1	0.002	5.6	15.12	63.4	14.5	2.1	14.68	2.92	19.99	4.7	15.01	2.52	15.9	2.14
SROR4014B(PULP)	50.08	21	6.09	0.52	8.16	7.05	1.59	0.28	0.13	0.1	0.002	4.5	15.08	62.2	13.5	2.07	14.37	2.81	19.9	4.5	14.86	2.45	15.22	2.04
SROR4033B(PULP)	49.23	20.54	5.73	0.51	7.97	6.75	1.48	0.27	0.12	0.1	0.001	6.9	14.67	62.7	13.1	2.06	14.36	2.95	19.25	4.27	14.79	2.29	15.71	2.18
SROR4059B(PULP)	48.85	20.86	5.72	0.51	8.03	6.85	1.54	0.27	0.13	0.09	0.001	6.8	14.18	59.4	12.3	2.09	13.54	2.89	18.34	4.39	14.16	2.36	15.53	1.94
SROR4084B(PULP)	50.27	20.99	5.81	0.51	7.99	7.06	1.53	0.27	0.12	0.09	0.001	5	14.63	62.5	12.8	2.09	13.95	2.84	19.72	4.55	14.59	2.44	15.55	2.05
SRROP5039(PULP)	50.17	20.8	6.35	0.51	8.11	7.02	1.72	0.3	0.13	0.1	0.002	4.6	14.47	58.5	12.8	1.89	12.94	2.86	19.82	4.66	14.45	2.44	14.24	2.14
CHROR5014(PULP)	50.14	20.89	6.25	0.51	8.15	7.09	1.73	0.3	0.13	0.1	0.002	4.5	16.1	62.7	13.9	1.97	14.31	2.95	20.11	4.74	15.24	2.49	15.45	2.22
6ROSRR002P(PULP)	49.04	21.5	6.26	0.53	8.05	7.13	1.69	0.29	0.13	0.11	0.002	5.1	14.51	57.1	12	1.73	12.7	2.83	18.86	4.04	13.78	2.14	14.17	2.07
6ROSRR042P (PULP)	49.62	20.96	6.23	0.52	8.2	7.09	1.74	0.29	0.13	0.1	0.001	4.8	14.9	59.7	12.3	1.83	13.26	2.98	18.67	4.36	13.87	2.09	14.28	2.03
6ROCHR052P (PULP)	50.12	20.98	6.15	0.52	8.09	7.07	1.7	0.29	0.12	0.1	<0.001	4.5	14.85	58.9	12	1.83	13.2	2.95	18	4.02	13.55	2.19	13.71	2
7ROSRR022 (PULP)	49.99	21.05	6.04	0.51	8.08	7.16	1.68	0.29	0.11	0.1	0.001	4.7	15.56	61.8	12.85	1.85	14.15	3.1	17.42	4.2	13.91	2.26	14.35	2.05
Mean	49.77	20.93	6.06	0.51	8.06	7.01	1.62	0.28	0.13	0.10	0.00	5.17	14.84	60.58	12.97	1.98	13.89	2.89	19.06	4.39	14.39	2.35	15.02	2.09
SY-4 Certified Values	49.90	20.69	6.21	0.54	8.05	7.10	1.66	0.29	0.13	0.11	0.00	4.56	15.00	57.00	12.70	2.00	14.00	2.60	18.20	4.30	14.20	2.30	14.80	2.10
Percentage Recovery	99.7	101.2	97.5	95.2	100.1	98.7	97.5	98.4	96.3	91.9	118.8	113.4	98.9	106.3	102.2	98.8	99.2	111.3	104.7	102.0	101.3	102.2	101.5	99.3